LIGAND BINDING AND SIGNALLING BY THE T CELL ANTIGEN RECEPTOR AND CD28

HONG-SHENG LIM
SIR WILLIAM DUNN SCHOOL OF PATHOLOGY
AND
LINCOLN COLLEGE
UNIVERSITY OF OXFORD

A THESIS SUBMITTED FOR THE DEGREE OF
DOCTOR OF PHILOSOPHY
HILARY TERM 2014

This thesis is dedicated in loving memory of

Lee Siew Yen, 1958 - 2010

Siew Yen ice-walking on the Patagonia Glacier on one of her solo trips to Argentina.

Born to a humble family in the village of Segamat in the heartland of the Hakka community in Johor Malaysia, Siew Yen was the first of seven siblings in her family. Life was far from a piece of cake, and she shared the burden of raising her siblings; in-charge of kitchen responsibilities from an early age. Fortunately, her insatiable passion for culinary arts from the beginning would prove to be a life-long valuable asset.

Her family eventually relocated to Penang, where she'd meet and marry my father. The rebellious Siew Yen was never content with fulfilling the stereotypical role of a housewife and together with my dad and their first-born, they came to the southern city of Johor Bahru in pursuit of her dreams.

The couple operated a catering business from home and before long they were able to afford a food stall in the then-trending shopping mall. Hard work and perseverance saw the gradual expansion of a single food stall to five adjacent stalls, and from one restaurant to a chain of vegetarian restaurants. She eventually achieved her dream of establishing a concept café serving vegetarian fusion food from all around the world.

Siew Yen was a workaholic and a keen experimentalist; I cannot help but think that with those qualities, she'll make a great PI. It is not uncommon for her to return home from a gruelling 12 hour-day in the kitchen to doze off amongst the pile of culinary recipes and cookbooks with a pen in her palm. She would then emerge from the kitchen with new creations to the delight of her customers. Indeed, some

seemingly weird food combination proved to be a hit, and some even made it to the national newspaper (such as mushroom, pumpkin and mozzarella soup).

Food and travelling goes hand-in-hand. In her life, Siew Yen had travelled to no less than 28 countries, often with the aim of researching fresh recipes. Her out-going and adventurous nature also meant that she had no problem with solo travelling, often armed with zero command of the local language (see picture above).

Life grinded to a sudden halt in the summer of 2009, within a month of her return from Scandinavia, when she was diagnosed with Acute Lymphoblastic Leukaemia (ALL). Unfortunately, statistics had taught us a tough lesson when none of her many siblings were HLA-matched. To make matters worse, cytogenetics testing had revealed that the cancerous pre-B cells were Philadelphia chromosome-positive, often associated with a poorer disease prognosis. The Philadelphia translocation between chromosomes 9 and 22 results in the creation of a chimeric BCR-ABL protein, that is associated with uncontrolled activity of the ABL tyrosine kinase (Daley et al., 1990). Initial treatment with the 'frontline' tyrosine kinase inhibitor Imatinib (Glivec, Novartis) contributed to remission, but the relapse soon followed with the development of Imatinib-resistance within months. She was subsequently placed on Dasatinib, a newer ABL kinase inhibitor that can bind to both active and inactive conformations of the ABL kinase domain (Talpaz et al., 2006). Various nervous and neurological complications ensued, eventually ending with the build-up of drug resistance within months.

The family took turns throughout the treatment periods to keep her company around the clock in the hospital. That, rather shamefully, was when I truly learnt who she was: her character, her life, her beliefs and her favourite band in the 70's. She never gave up cooking and she'd rather spend a large part of her time during remission breaks conjuring dishes, even though she was wheel chair-bound by that time and would often run into exhaustion.

With the failure of Dasatinib, the physicians had run out of options. Siew Yen eventually succumbed to ALL-related septicaemia on the 5th of June 2010 at home in the comfort and company of her close friends and family.

"*Let your future children know that they have a grandmother that loves them. Tell them my story…*" This thesis is dedicated to your life and your legacy, Mummy.

Acknowledgements

I would like to express my sincerest gratitude to my DPhil supervisor Anton van der Merwe, without whom this entire project would have been impossible. I am especially grateful for the research freedom he has granted me throughout this journey, not to mention the guidance, encouragements, the engaging conversations and the many hours spent proofreading this thesis.

I would also like to thank the members of both van der Merwe and Dushek labs and Marion Brown for their support, company and insightful conversations, including some of the most bizarre topics on earth. Thank you for tolerating my random, ad hoc experiments, such as "*The comparative antibacterial properties of capsaisin and garlic*" and "*Effectiveness of carbonated-Phosphate Buffered Saline*". And so, to Shaun-Paul Cordoba, Jesse Goyette, Omer Dushek, Marcus Bridge, Eleanor Denham, Hao Zhang, Ben de Wet, Rachel Paterson, Melissa Lever, Himadri Mukhopadhyay, Hannah Johnston, Adrian Yemm, Ann Tivey and Shiqiu Xiong, thank you for being my surrogate family whilst at Oxford.

It has been an amazing time working at the Sir William Dunn School of Pathology, the staffs and colleagues have always been extremely friendly and accommodating. I thank Marcus Bridge, Nigel Rust, John Marriot and Alan Wainman for their technical assistance throughout the years in the Surface Plasmon Resonance, Flowcytometry, IT and Microscope facilities respectively. In addition, I would like to extend my gratitude to members of the Pathology Service Building for their invaluable service.

My time at Oxford would not have been possible without the generous funding from the Sir William Dunn School of Pathology Edward Penley Abraham Trust Scholarship and the Clarendon Fund. Thank you for giving me the wonderful opportunity to embark on this fruitful journey in Oxford.

I would also like to thank my friends from Lincoln College, the Clarendon Scholarship Association and the Global Scholars Network for all the inspiring conversations and for all the glasses and pints of intoxicating beverages we've shared. You have broadened my horizon to the world I never thought I'd be interested in. And most importantly, you have help shaped my personal vision and purpose in life.

I am indebted to members of the Bayer House: Dmitri Balzer, Annabelle Guillermo and Abigail Guillermo as well as UCL library services for accommodating me in London for the duration of my thesis write-up.

Most importantly, I would like to thank my family members, especially my parents Lim Hun Kok and Lee Siew Yen, and my uncle Lim Hun Hooi for their unyielding support and believe in me.

ABSTRACT

LIGAND BINDING AND SIGNALLING BY THE T CELL ANTIGEN RECEPTOR AND CD28
Hong-Sheng Lim
Sir William Dunn School of Pathology and Lincoln College
A Thesis Submitted for the Degree of Doctor of Philosophy

Successful T cell activation depends on the recognition of antigenic peptides in the context of a Major Histocompatibility Complex molecule (pMHC) by the T cell antigen receptor (TCR), together with additional signals from co-stimulatory receptors such as CD28. Despite their importance, a thorough understanding of how TCR-pMHC binding properties relate to T cell functional responses remains unclear. In addition, there are no consensuses to the exact mechanism leading to CD28 receptor triggering.

Activation of CD28 is dependent on the phosphorylation of key tyrosine residues within its cytoplasmic domain by Src family kinases. Just like the TCRs, CD28 receptors are susceptible to perturbations of the local kinase: phosphatase ratio. The K-S model postulates that upon ligand engagement, large RPTPs such as CD45 are segregated from the area of close contact, resulting in increased relative kinase concentration and CD28 receptor triggering. This hypothesis was tested in chapter 3, where elongated forms of CD80 were examined for their ability to costimulate primary T cells. CD28 costimulation was indeed diminished and there was reduced CD45 segregation from the elongated CD80 molecules. Additionally, CD28 habouring key Y170F tyrosine mutations were less susceptible to CD28 signal abrogation by elongated CD80 molecules. Interestingly, elongated CD80 molecules remained much less effective in mediating costimulation even when pMHC molecules were also elongated, suggesting that TCR-pMHC and CD28-CD80 size matching is not critical for costimulation.

Despite the well-documented MHC-restriction requirement for TCR recognition, the relative energetic contributions of peptide versus MHC in TCR-pMHC interactions remain elusive. To address this question, the energetic footprints of four TCRs (1G4, JM22, A6 and G10) to HLA-A2 were determined via systematic alanine scanning mutagenesis on the HLA-A2 heavy chain in chapter 4. By targeting exclusive TCR contacting residues on the MHC, we conservatively estimate the contribution of MHCs for the four TCRs to range from 15% to over 70%.

Several models have been formulated in an attempt to relate TCR-pMHC binding properties to T cell activation. Validity of the models was tested in chapter 5 using a supra-physiological TCR. By mutating key residues within the cognate pMHC, we generated a panel of TCR-pMHC with affinities that varies up to 10^5-fold. These reagents were used to stimulate Jurkat and primary T cells transduced with the supra-physiological TCR. Results in the Jurkat T cell system demonstrated the presence of an optimal off-rate (k_{off}) for TCR-pMHC interaction at low concentrations of pMHC concentration. The results argue against affinity models and the basic kinetic proofreading model for T cell activation.

LIST OF ABBREVIATIONS

2D	2-Dimensional
3D	3-Dimensional
AP-1	Activator Protein 1
APC	Antigen Presenting Cell
Arp2/3	Actin-Related Protein-2/3
AUC	Area Under Curve
Bcl10	B cell leukemia/lymphoma 10
BRR	Basic Rich Region
BTLA	B- and T-lymphocyte attenuator
Cabin1	Calcineurin-binding protein
CAR	Chimeric Antigen Receptor
CARMA1	CARD- containing MAGUK protein 1
Cat. No.	Catalogue Number
CCR	Chimeric Costimulatory Receptor
CD28RE	CD28 Response Element
CDK	Cyclin Dependent Kinase
CDR	Complementary Determining Region
CHO	Chinese Hamster Ovary
CMV	Cytomegalovirus
CRAC	Calcium Released Activated Calcium Channels
Csk	C-Src Kinase
CTLA-4	Cytotoxic T-Lymphocyte Antigen 4
DAG	Diacylglycerol
DAMP	Danger Associated Molecular Pattern
DC	Dendritic cells
DRE	Downstream regulatory element
DREAM	Downstream Regulatory Element Antagonistic Modulator
EAE	Experimental Autoimmune Encephalomyelitis
EBV	Epstein-Barr Virus
EM	Electron-Microscopy
Erk	Extracellular signal-Regulated Kinase
FACS	Fluorescence-Activated Cell Sorting
FITC	Fluorescein Isothiocyanate
FLNa	Filamin A
Fyn	Tyrosine protein kinase Fyn
Gads	GRB2-related adapter protein 2
GEF	Guanine Exchange Factor
Glut1	Glucose transporter 1
GPCR	G-Protein Coupled Receptor
Grb2	Growth factor receptor-bound protein 2
GSK3	Glycogen synthase kinase 3
H2	Histocompatibility 2
HIV	Human Immuno-deficiency Virus
HLA	Human Leukocyte Antigen
hsPALM	High Speed Photoactivated Localisation Microscopy
ICOS	Inducible T cell Costimulator
ICOSL	Inducible T cell costimulator Ligand
IDO	Indoleamine 2,3-dioxygenase
Ig	Immunoglobulin
IgSF	Immunoglobulin Super Family
IKK	IκB kinase
IL	Interleukin
IP_3	Inositol triphosphate
ITAM	Immunoreceptor Tyrosine based-Activatory Motif
ITC	Isothermal Titration Calorimetry
ITIM	Immunoreceptor Tyrosine based-Inhibitory Motif

Itk	Interleukin-2-inducible T-cell Kinase
ITSM	Immunoreceptor tyrosine based-switch motif
JNK	c-Jun N-terminal kinase
KIR	Killer-cell Immunoglobulin-like Receptor
KS	Kinetic Segregation
LAT	Linker for Activation of T cells
Lck	Lymphocyte-specific protein tyrosine Kinase
LILR	Leukocyte Immunoglobulin-like Receptors
MALT1	Mucosa associated lymphoid tissue lymphoma translocation gene 1
MAPK	Mitogen-Activated Protein Kinase
MEF2	Myocyte enhancer factor-2
Nck	Non-Catalytic region of tyrosine Kinase adaptor
NFAT	Nuclear Factor of Activated T-cells
NFκB	Nuclear Factor kappa-light-chain-enhancer of activated B cells
NK	Natural Killer
NOD	Non-Obese Diabetic
NTR	Non-catalytic Tyrosine-phosphorylated Receptors
PAMP	Pathogen Associated Molecular Pattern
PBMC	Peripheral Blood Mononuclear Cell
PD-1	Programmed cell death protein 1
PDK1	Phosphoinositide-Dependent Kinase-1
PH	Phosphatidylinositol 3,4,5- triphosphate
PIP2	Phosphatidylinositol 3,4-biphosphate
PIP3	Phosphatidylinositol 3,4,5- triphosphate
PKB/ AKT	Protein kinase B
PKCθ	Protein Kinase C Theta
PLCγ1	Phospholipase C Gamma 1
pMHC	peptide-Major Histocompatibility Complex
PP2A	Protein Phosphatase 2A
PTEN	Phosphatase and Tensin homolog
PTPN11 or Shp2	Tyrosine-protein phosphatase non-receptor type 11
RPTP	Receptor Protein Tyrosine Phosphatase
SCD	Single Chain Dimer
scFv	Single-Chain Variable Fragment
SCID	Severe Combined Immunodeficiency Syndrome
SHIP-1	SH2 domain-containing Inositol 5'-Phosphatase 1
Shp-1	Src Homology region 2 domain-containing Phosphatase-1
SIRS	Systemic inflammatory response syndrome
SLP-76	SH2 domain-containing Leukocyte Protein of 76kD
SMAC	Supra-Molecular Adhesion Complex
SNX9	Sorting Nexin 9
Sos1	Sons of Sevenless 1
SPR	Surface Plasmon Resonance
Syk	Spleen tyrosine kinase
TCR	T Cell Receptor
TEM	Transmission Electron Microscopy
T_H	T-Helper
TILs	Tumour Infiltrating Lymphocytes
TIM3	T-cell immunoglobulin domain and mucin domain 3
TIRF	Total Internal Reflection Fluorescence
TRAF6	TNF receptor-associated factor 6
Treg	Regulatory T cells
Vav	Vav 1 guanine nucleotide exchange factor
WASp	Wiskott-Aldrich Syndrome protein
ZAP70	Zeta-chain-Associated Protein kinase 70

TABLE OF CONTENTS

CHAPTER 3: IMPORTANCE OF RECEPTOR/ LIGAND DIMENSIONS IN T CELL CO-STIMULATION

CHAPTER 4: ENERGETIC CONTRIBUTIONS OF MHC CONTACTS TO THE AFFINITY OF TCR-pMHC INTERACTIONS

CHAPTER 5: BINDING PARAMETERS AND FUNCTIONAL CHARACTERISATION OF A SUPRA-PHYSIOLOGICAL TCR

CHAPTER 1:

T Cell Activation

1.1 Introduction

The immune system has evolved to protect biological organisms against infectious and cancerous diseases. Physical and chemical barriers such as the skin, mucosal layers and antimicrobial peptide secretions represent the first major barrier to most pathogens. Once in the body, effective clearance of pathogen and restoration of normal conditions are dependent on both innate and adaptive immune system for the following functions (Murphy, 2012):

(i) Immune recognition of infectious organisms or abnormal cells

(ii) Effector functions to clear pathogens or abnormal cells

(iii) Immune regulation to prevent immune overdrive and autoimmunity

(iv) Establishment of long-term memory to prevent re-infection

Activation of the innate immune system is mediated by the recognition of pathogen-derived molecules termed the pathogen associated molecular patterns (PAMPs) as well as host cell-derived molecules termed damage-associated molecular patterns (DAMPs) that are released during cell damage (Ausubel, 2005, Matzinger, 2002). Effector functions of the innate immune system aim to contain and clear the infection at an early stage and do so in a relatively non-specific manner. Long-term immunity to specific pathogens is achieved by the subsequent activation of the adaptive immune system, which can be subdivided into the humoral or cellular-mediated responses mediated by B cells and T cells respectively.

T cells are unique in that they typically recognise foreign antigenic peptides in the context of a peptide-Major Histocompatibility Complex molecule (pMHC) on an antigen presenting cell (APC). The evolution of T cells is a direct consequence of the

'immunological big bang' which saw the introduction of somatic gene rearrangement for the creation of a diverse T cell receptor repertoire. This enables T cells to recognise virtually any antigen in complex with MHC. Central to the outcome of infection or autoimmunity is the process of antigen recognition and T cell activation, which forms the basis of much of this thesis and this chapter review.

1.2 Mechanisms of T Cell Receptor Triggering

The T cell receptor (TCR) is one of the most complex and intensively studied receptors in any biological system. While there are many unanswered questions around TCR biology (see chapter 5 introduction), perhaps the most baffling question of all is the mechanism by which TCR transduce its signals across the plasma membrane, a process known as TCR triggering.

The TCR is a heterodimer of αβ or γδ subunits that lack intrinsic enzymatic activities in their cytoplasmic tails (Dushek et al., 2012). Instead, they contain positively charged arginine and lysine residues within their trans-membrane domain that associates with the negative aspartic acid and glutamic acid residues in three signalling-competent CD3 dimers CD3γε, CD3δε and CD3ζζ, forming the TCR signalling complex (Cosson et al., 1991, Call et al., 2002).

Signal transduction is mediated by a series of conserved amino acid motifs (YxxL/I-X6-8-YXXL/I) known as the immunoreceptor tyrosine-based activation motifs (ITAMs). Reversible phosphorylation of ITAMs by Src family kinases such as lymphocyte-specific protein tyrosine kinase (Lck) and Tyrosine protein kinase Fyn (Fyn) represents the first well-established biochemical event upon ligand engagement by the TCR. Dephosphorylation is mediated by both cytosolic and

membrane-bound receptor tyrosine phosphatases such as Src homology region 2 domain-containing phosphatase 1 (Shp-1) and CD45. While ITAMs are commonly found in leukocyte receptors, with ten ITAMs (one for each CD3δ, ε, and γ chain; three for each ζ chain), the TCR complex has by far the largest number of these motifs. Such abundance of ITAMs is thought to contribute to TCR signal amplification and ultrasensitivity, which would help prevent any potential spurious activation (Mukhopadhyay et al., 2013). While the subsequent biochemical signal transduction following ITAM phosphorylation has been extensively clarified, the exact mechanism by which TCR ligation leads to the initial increase in ITAM phosphorylation remains controversial. There are three main groups of non-mutually exclusive theories: conformational change, aggregation and segregation (van der Merwe and Dushek, 2011).

Conformational Change

The idea of conformational change represents an elegant solution to the problem of signal transduction across the plasma membrane. Such thoughts were no doubt inspired by existing G-protein coupled receptor (GPCR) and hormone receptor systems where ligand binding induces a conserved and constant conformational change to induce intracellular signal transduction (Bissantz, 2003, Greenfield et al., 1989). The TCR however is unlike any other receptor systems in the body. TCRs represent one of the most polymorphic proteins with enormous structural variation in its ligand binding site (Rudolph et al., 2006). This makes it hard to envisage the presence of a consistent conformational change across the repertoire of TCRs. Crystal structures of bound and unbound versions of TCRs have yielded no evidence

for the presence of a large scale conserved allosteric conformational change (Rudolph et al., 2006). However, technological limitations in crystallising membrane-bound proteins meant that no structural data is available for the full TCR/CD3 complexes. Therefore existing structural data do not rule out binding induced conformational changes.

Indications of a subtle conformational change in the membrane proximal AB loop of the TCRα constant domain were identified by Rossjohn and McCluskey (Kjer-Nielsen et al., 2003). The finding was later verified for an alternative TCR system using a different technique, highlighting the propensity of TCRα constant conformational change. Moreover, mutation of residues within the AB loop abrogated TCR antigen recognition (Beddoe et al., 2009). Fascinatingly, the same conformational change was not observed in an antagonistic TCR-pMHC complex, providing a tempting explanation to the molecular basis for antagonism (Beddoe et al., 2009).

Molecular dynamic simulations by Martinez-Martin et al also suggested a potential conformational change in the stalk of CD3ε (Martinez-Martin et al., 2009). Indeed, mutation of a conserved CXXC region within the CD3ε stalk abrogated TCR signalling and T cell development in a dominant negative way (Wang et al., 2009).

Taken together, experimental evidence for a conserved allosteric conformational change within the TCR extracellular region upon ligand binding remains weak. Given the huge structural variation at the TCR-pMHC binding interface this is not surprising. However other types of conformational change mechanism are consistent with existing structural data. One such mechanism is TCR conformational change induced by mechanical pulling or shearing. This stems from the fact that T cells are

constantly subjected to all forms of mechanical force throughout their life cycle [reviewed in (Chen and Zhu, 2013)]. Within an immune activation scenario, TCR-pMHC bonds can be subjected to mechanical stress as the T cell moves along an antigen-presenting cell. This could also happen to TCRs tethered to the moving actin cytoskeleton within the immunological synapse. Additionally, the exclusion of large phosphatases from the active signalling zone can also contribute to the mechanical stress experienced by the TCR as they try to diffuse back into the signalling zone. Ligand discrimination can thus be achieved with the duration of applied mechanical force (i.e. strong enough affinity).

In support for this model, Li et al demonstrated that an artificial shear force on the TCR induced by micropipette suction could induce Ca^{2+} signalling (Li et al., 2010). Furthermore, elongated CD3 molecules were signalling-incompetent unless an external force was applied to it, consistent with the suggestion that compression of large ectodomains may contribute to the mechanical stress (Li et al., 2010). In a separate report, Ca^{2+} signals were also observed with the application of a tangential force on the TCR using optical tweezers (Kim et al., 2009). Despite these, there is still a gap in understanding how mechanical force may be transduced into the cytoplasm. Reinherz and colleagues postulated that any mechanical force can be transduced by the FG loop of TCR Cβ domain, which is in contact with the rigid-rod like structure of CD3εγ, inducing a 'piston-like movement' of the CD3 cytoplasmic tails relative to the plasma membrane (Sun et al., 2001, Ghendler et al., 1998, Kim et al., 2010).

Any conformation change in the extracellular regions of the TCR/CD3 complex need to be transduced across the membrane to the cytoplasmic domains. A number of

studies have focused on identifying such conformational changes. Additional evidence of TCR conformational change has been reported in studies of the cytoplasmic tails of CD3 molecules. Alarcon and colleagues reported the exposure of a proline-rich region and subsequent recruitment of adaptor protein non-catalytic region of tyrosine kinase adaptor protein 1 (Nck) in CD3ε upon ligand binding (Gil et al., 2002, Gil et al., 2005). Importantly, the conformational change was independent of CD3ε and CD3ζ phosphorylation (Gil et al., 2002, Gil et al., 2005). Later studies however revealed that the proline-rich motif was not required for triggering but might be important for regulating TCR expression levels in thymocytes (Szymczak et al., 2005, Mingueneau et al., 2008).

Other indication of conformational change is based on the observations that basic residue rich (BRR) regions in CD3ε and CD3ζ cytoplasmic tails associate with acidic or negatively charged phospholipid of the plasma membrane in such a way that might prevent CD3-ITAM phosphorylation (Aivazian and Stern, 2000, Xu et al., 2008). This led to the 'safety catch' model, postulating that, in the resting state, BRR mediated interactions with the acidic membrane phospholipid result in the tyrosine residues in CD3 ITAMs being sequestered in the plasma membrane and protected from phosphorylation. According to the model ligand engagement induces a conformational change in the intracellular tail exposing the ITAM tyrosine residues for phosphorylation and signal transduction (Kuhns and Davis, 2008). The model predicts that BRRs mutation should disrupt CD3-plasma membrane interaction and enhance CD3-ITAM phosphorylation and TCR triggering. However, the opposite effects were observed in CD3ε and CD3ζ BRR mutants instead (Deford-Watts et al., 2009, Fernandes et al., 2010, Zhang et al., 2011). One explanation for the reduced

ITAM phosphorylation is the possible disruption of Lck recruitment in CD3 molecules with BRR mutation; while this was observed for CD3ε, it wasn't the case in CD3ζ (Gagnon et al., 2010, Zhang et al., 2011). Moreover, dissociation of CD3ζ from the plasma membrane was a consequence of and required ITAM phosphorylation (Zhang et al., 2011). These data do not support the 'safety catch' model, and the significance of CD3 cytoplasmic dissociation from the plasma membrane upon TCR ligation remains unclear.

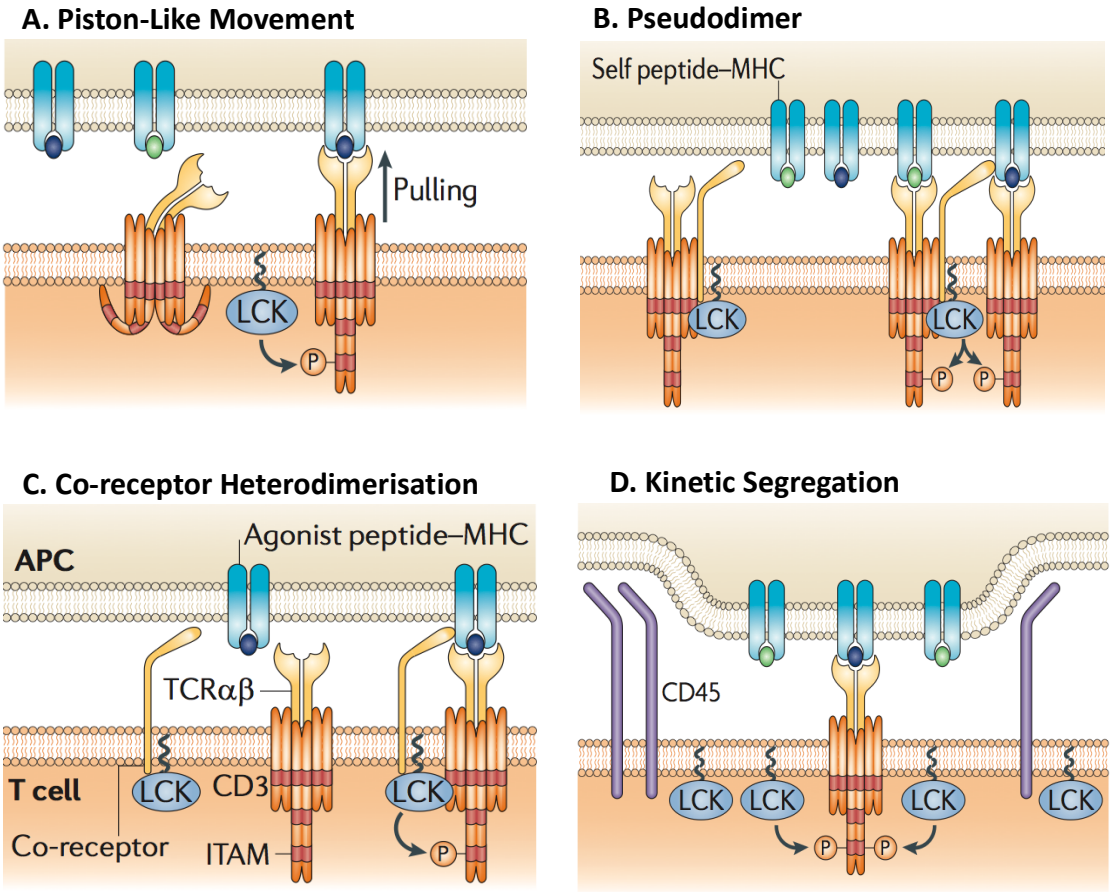

Figure 1.1 Mechanisms of TCR triggering

TCR triggering mechanisms can be broadly categorised into conformational change, aggregation and segregation models. (a) Ligand binding might induce a mechanical force (pulling) on the TCR and the associated CD3 in a 'piston-like' movement. This induces conformational change on the CD3-ITAM, allowing phosphorylation. (b) The pseudodimer model suggests that the co-receptor of a self-pMHC (green) could engage the agonist-pMHC (blue) to form a pseudodimer. Dimerisation of the TCR enhances biochemical-signalling events. (c) The co-receptor heterodimerisation model suggests that recruitment of Lck-associated co-receptors to the TCRs could lead to CD3-ITAM phosphorylation and initiation of TCR triggering. (d) The kinetic segregation model postulates that the segregation of large receptor protein tyrosine phosphatases (RPTPs) such as CD45 during TCR-pMHC engagement results in the re-balance of kinase: phosphatase ratio in favour of the former, thereby leading to ITAM phosphorylation and initiation of TCR signal transduction. Figures are adapted from van der Merwe and Dushek (van der Merwe and Dushek, 2011).

Aggregation

The concept of TCR aggregation as a mechanism for TCR triggering was informed by multiple observations that soluble multivalent pMHCs but not monovalent pMHC can trigger TCR activation (Boniface et al., 1998). Aggregation of TCR complexes could lead to triggering by enhancing trans-phosphorylation of CD3-ITAMs by closely associated Lck molecules and/or by enhancing trans-autophosphorylation of the Lck molecules, which increases their catalytic activity.

Electro-microscopy after label-fracture (in the absence of any detergent-induced artefacts) of intact T cells revealed the presence of TCR nano-clusters during the resting state (Schamel et al., 2005). The presence of pre-assembled TCR nano-clusters was subsequently confirmed using high-speed photoactivated localisation microscopy (hsPALM) (Sherman et al., 2011). Pre-assembled Linker for Activation of T cells (LAT) nanoclusters were also observed in the same study although the functional significance of this is unclear (Sherman et al., 2011, Williamson et al., 2011). However, one conflicting report refuting the presence of pre-assembled TCR oligomers came from the absence of two-coloured-coincidental-detection of TCRs labelled with different dyes (James et al., 2007).

One model that provides a solution to the low pMHC surface density problem is the pseudo-dimer model, which postulates that the co-receptor of a self pMHC-TCR complex can engage the agonist pMHC-TCR complex, thereby forming a pseudo-dimer (Krogsgaard et al., 2005). This model was initially informed by observations that as much as 20% of the pMHCs accumulated into the immunological synapse were endogenous null pMHC (Irvine et al., 2002). Direct support for this model was

demonstrated by Davis and colleagues who showed that certain combinations of covalent soluble heterodimers containing agonist and endogenous pMHC ligands could stimulate T cells. While this is well established in $C4^+$ T cells, corresponding data on $CD8^+$ T cells have been conflicting [reviewed in (Krogsgaard et al., 2007)].

The co-receptor heterodimerisation model also attempts to address the problem of low agonistic pMHC density on surface of APCs. In this model, signalling is enabled with the heterodimerisation of TCR and Lck-associated co-receptors; phosphorylation of CD3-ITAM by the Lck in proximity would lead to subsequent signal transduction. Despite their low affinities to MHC molecules, additional engagement of CD4 or CD8 could also improve the avidity of the interaction in theory. This was supported by the fact that co-receptor engagement could significantly enhance T cell activation (Holler and Kranz, 2003). Importantly though, TCR triggering can still occur in the absence of any co-receptor (Schilham et al., 1993), suggesting that if this were to be a credible model, it may only be applicable or necessary for TCR-pMHC interactions with weaker affinities.

Segregation

The notion of segregation contributing to T cell activation was first suggested by Springer who predicted that the exclusion of bulky glycocalyx elements such as CD45 (~45nm) could affect signalling, which is largely mediated by smaller (~15nm) signalling complexes (Springer, 1990). This concept, and the observation that inhibition of tyrosine phosphatases was sufficient to induce TCR triggering, provides the basis for the kinetic segregation (K-S) model as a potential mechanism for TCR triggering (Davis and van der Merwe, 1996).

The model proposes that large receptor protein tyrosine phosphatases (RPTPs), such as CD45 and CD148, are segregated from active signalling zones as a result of size incompatibility. Hence, tyrosine phosphorylation by Src kinases such as Lck, which will not be excluded, is strongly favoured in the absence of inhibitory RPTPs, leading to stable CD3-ITAM phosphorylation and enabling subsequent signalling events. Discrimination of ligands is achieved by TCR-pMHC interaction with sufficient duration. As such, careful balance of the kinase: phosphatase ratio at the site of signalling lies at the heart of the model; and any perturbation to the ratio in favour of the kinase would lead to T cell activation. Indeed, most evidence supporting this model was obtained by observing the effects of direct or indirect perturbation of kinase: phosphatase balance.

Firstly and crudely, T cell activation can be elicited with the treatment of tyrosine phosphatase inhibitor pervanadate (Secrist et al., 1993). Perturbation of the kinase: phosphatase balance was more elegantly achieved with the selective inhibition of c-Src tyrosine kinase (Csk; a Src kinase inhibitor) by Weiss and colleagues. Such event led to the spontaneous activation of Jurkat T cells and primary thymocytes (Schoenborn et al., 2011, Tan et al., 2014).

Additional evidences came from the microscopic observation of CD45 and CD148 exclusion from areas of TCR triggering; truncation of the ectodomains of these molecules abrogated this segregation as well as T cell signalling (Varma et al., 2006, Lin and Weiss, 2003, Cordoba et al., 2013). Similarly, elongation of pMHC molecules also abrogated CD45 segregation and TCR signalling (Choudhuri et al., 2005). Recently, Vale and colleagues demonstrated in reconstituted conditions that TCR

and CD3 were maintained in a dephosphorylated state at physiological concentrations of CD45. Additionally, CD45 segregation was demonstrated to be a passive event as a consequence of TCR-pMHC ligation without the need for any downstream signalling (James and Vale, 2012).

These experiments highlight the importance of receptor/ ligand dimensions in the preservation of kinase: phosphatase balance in the T cell, a concept that will be further investigated in chapter 3. Moreover, there has been a long standing observation that surface bound ligands (including antibodies) are much more effective than the soluble versions (Ma et al., 2008). These experiments therefore demonstrate that perturbation of kinase: phosphatase ratio (in favour of the former) as a pre-requisite for TCR triggering. Under physiological conditions, this is mediated by the passive exclusion of large inhibitory phosphatase from active signalling zones.

Kinetic segregation as a mechanism for triggering is not restricted to the TCR. The same concept is applicable to a larger family group of up to a hundred non-catalytic tyrosine-phosphorylated receptors (NTRs) including co-stimulatory receptors CD28, inducible costimulator (ICOS) and natural killer (NK) cell receptor family Leukocyte immunoglobulin-like receptors (LILR) and killer cell immunoglobulin-like receptors (KIRs) among others (Dushek et al., 2012). Like the TCRs, NTRs possess small extracellular domains (<20nm) and contain no intrinsic kinase activity. Instead, signal initiation is dependent on the phosphorylation and dephosphorylation of key cytoplasmic tyrosine residues by Src family kinases and RPTPs respectively. In addition, NTR ligands are generally surface-anchored and ligation can lead to the segregation of large RPTPs to re-balance the local kinase: phosphatase ratio in favour

of the former, thereby contributing to receptor triggering. Indeed, evidence that the K-S mechanism contributes to triggering by receptors apart from the TCR is growing (Dushek et al., 2012).

It is important to note that while the mechanisms discussed above are described separately, they are not mutually exclusive. In fact, all mechanism may come into play, as proposed in the integrated model of TCR triggering by van der Merwe and Dushek (van der Merwe and Dushek, 2011).

1.3 T cell receptor signalling pathway

ITAM phosphorylation by Src kinases

Phosphorylation of CD3 associated ITAM represents the first step in TCR signal transduction pathway. This was initially demonstrated by generating chimeras containing intracellular domains of CD3 molecules in T cells lacking TCRs where mutation or alterations of ITAM residues would inhibit T cell activation (Letourneur and Klausner, 1992, Irving and Weiss, 1991). As mentioned previously, such events are dependent on the careful balance of kinase: phosphatase ratio in the local environment.

Initial phosphorylation of ITAM is mediated by Src family kinases including Lck and Fyn [reviewed in (Palacios and Weiss, 2004)]. Both molecules contain a N-C architecture of *SH3-SH2-Kinase* domains. Membrane association of the kinases is mediated by myristoylation and palmitoylation of the N-terminal domain as well as its association with co-receptors CD4 and CD8 (Barber et al., 1989). The activity of Lck is dependent on the phosphorylation status of two tyrosine residues at positions 394 and 505. Phosphorylation of the inhibitory C-terminal Y505 residue by Csk

promotes intra-molecular interaction between pY505 and the SH2 domain, which occludes the kinase domain and locks Lck in an inactive state. Y505 dephosphorylation by CD45 relieves the autoinhibitory conformation and releases Lck in a 'primed' state. Finally, Lck is fully activated with the trans-autophosphorylation of activatory Y394 (Palacios and Weiss, 2004). Interestingly, a report by Acuto and colleagues demonstrated that up to 40% of Lck are constitutively active at the cell membrane during resting state (Nika et al., 2010). Such observation is consistent with the finding that ITAMs can be constitutively phosphorylated in resting T cells (van Oers et al., 1994). Aberrant over-phosphorylation of ITAMs in this case is held in check by the high densities of CD45 (Davis and van der Merwe, 2011).

Recruitment of ZAP-70

Phosphorylated tyrosine residues on an ITAM serve as a docking site for the recruitment of Syk kinase family member Zeta-chain-associated protein kinase 70 (ZAP-70) (Chan et al., 1992). The importance of ZAP-70 is highlighted by the arrest of T cell development during the positive selection stage in ZAP-70-deficient mice (Negishi et al., 1995). Additionally, patients deficient in ZAP-70 have no peripheral T cells and suffer from severe combined immunodeficiency (SCID) syndrome (Elder et al., 1994).

ZAP-70 is composed of two N-terminal tandem SH2 domains and a C-terminal kinase domain. Under resting conditions, ZAP-70 adopts an autoinhibitory conformation (Folmer et al., 2002). Binding of ZAP-70 tandem SH2 domains to phosphorylated ITAM is thought to release ZAP-70 from its autoinhibitory conformation and exposes

Y315 and Y319 residues for Lck phosphorylation by Lck. Phosphorylation of Y315 and Y319, which lie in the inter-SH2-kinase domain loop, destabilises the autoinhibitory conformation and promotes the phosphorylation of tyrosine residues Y492 and Y493 in the activation loop of the kinase domain by Lck and/or trans auto-phosphorylation by ZAP-70 [reviewed in (Wang et al., 2010)].

Therefore, recruitment of ZAP-70 to phosphorylated ITAM is mandatory for full activation of ZAP-70. Fully activated ZAP-70 in turn phosphorylates the adaptor molecules LAT and SLP-76 (Zhang et al., 1998a, Bubeck Wardenburg et al., 1996). Recent modelling studies have suggested an explanation for the long-standing observation that ZAP-70 binds with differing affinities to different ITAMs, arguing that this, when combined with sequential phosphorylation of ITAMs, could contribute to TCR ultrasensitivity (Mukhopadhyay et al., 2013, Isakov et al., 1995).

LAT is the nucleating site for initiation of multiple downstream signalling pathways

LAT is a type-III transmembrane protein with a short (four amino acids) extracellular domain and an intracellular tail with two cysteine and nine tyrosine residues. Post-translational modification of LAT is central to its localisation and function as the intracellular nucleating site for multiple signalling proteins [reviewed in (Balagopalan et al., 2010)]. The two cysteine residues at the membrane proximal region of the intracellular tail are involved in LAT palmitoylation and membrane localisation (Zhang et al., 1998b, Lin et al., 1999), absence of which can lead to LAT degradation (Hundt et al., 2009, Hundt et al., 2006).

The tyrosine residues are rapidly phosphorylated by tyrosine kinases including ZAP-70 upon T cell activation (Zhang et al., 1998a). Growth factor receptor-bound protein

2 (Grb2) family of adaptor proteins (Grb2, Gads and Grap) are recruited to LAT via their SH2 domains to phospho-Y171, Y191 and Y226 residues (Wange, 2000). Grb2 associates constitutively with Sons of sevenless-1 (Sos1), a guanine nucleotide exchange factor (GEF) that promotes the activation of Ras, which in turn initiates the MAP kinase pathway (Houtman et al., 2006). The MAP kinase pathway consists of a series of serine/ threonine kinases Raf➔Mek➔Erk forming a relay that phosphorylates the next member in the series. Active Extracellular signal-regulated kinases (Erk) phosphorylates transcription factor Elk, which initiates the transcription of c-fos, a component subunit of activator protein-1 (AP-1), yet another transcription factor that plays a major role in cell proliferation and cytokine secretion (Chang et al., 2003). In addition to activating the MAP kinase pathway, Grb2 was thought to facilitate LAT oligomerisation on the basis that both LAT and Sos1 could potentially bind two Grb2 at once. This allows both Grb2 and Sos1 to act as a bridge between multiple LAT molecules. The potential association was verified using isothermal calorimetry (ITC) and confocal microscopy (Houtman et al., 2006). The importance of LAT oligomerisation may be to concentrate and encourage inter-molecular phosphorylation to favour downstream signalling (Balagopalan et al., 2010).

Binding of GRB2-related adapter protein 2 (Gads), another member of the Grb2 family, to LAT facilitates the recruitment of SH2 domain- containing leukocyte protein of 76kD (SLP-76) to the TCR signalling complex (Liu et al., 1999). Like LAT, SLP-76 is an adaptor protein with three tyrosine residues that, upon phosphorylation by local tyrosine kinases, recruits further downstream signalling molecules including vav 1 guanine nucleotide exchange factor (Vav), Nck and IL-2 inducible T cell kinase (Itk). Vav is a GEF that activates the Rho family of G-proteins (including Rac1, RhoA

and Cdc42) necessary for the reversal of Wiskott-Aldrich syndrome protein (WASp) auto-inhibition. Activated WASp initiates downstream actin polymerisation and cytoskeletal changes by interacting with the actin related protein 2/3 (Arp2/3) complex (Hornstein et al., 2004). Nck was also shown to interact with WASp and is thought to regulate WASp mediated actin cytoskeletal rearrangement in the signalling complex (Rohatgi et al., 2001). Itk is a member of the Tec kinase family known to phosphorylate and activate Phospholipase C- γ1 (PLC-γ1). Mutation of Y145 on SLP-76 that mediates Itk association diminishes PLC-γ1 phosphorylation and function, highlighting the importance of Itk in TCR transduction pathway (Jordan et al., 2008).

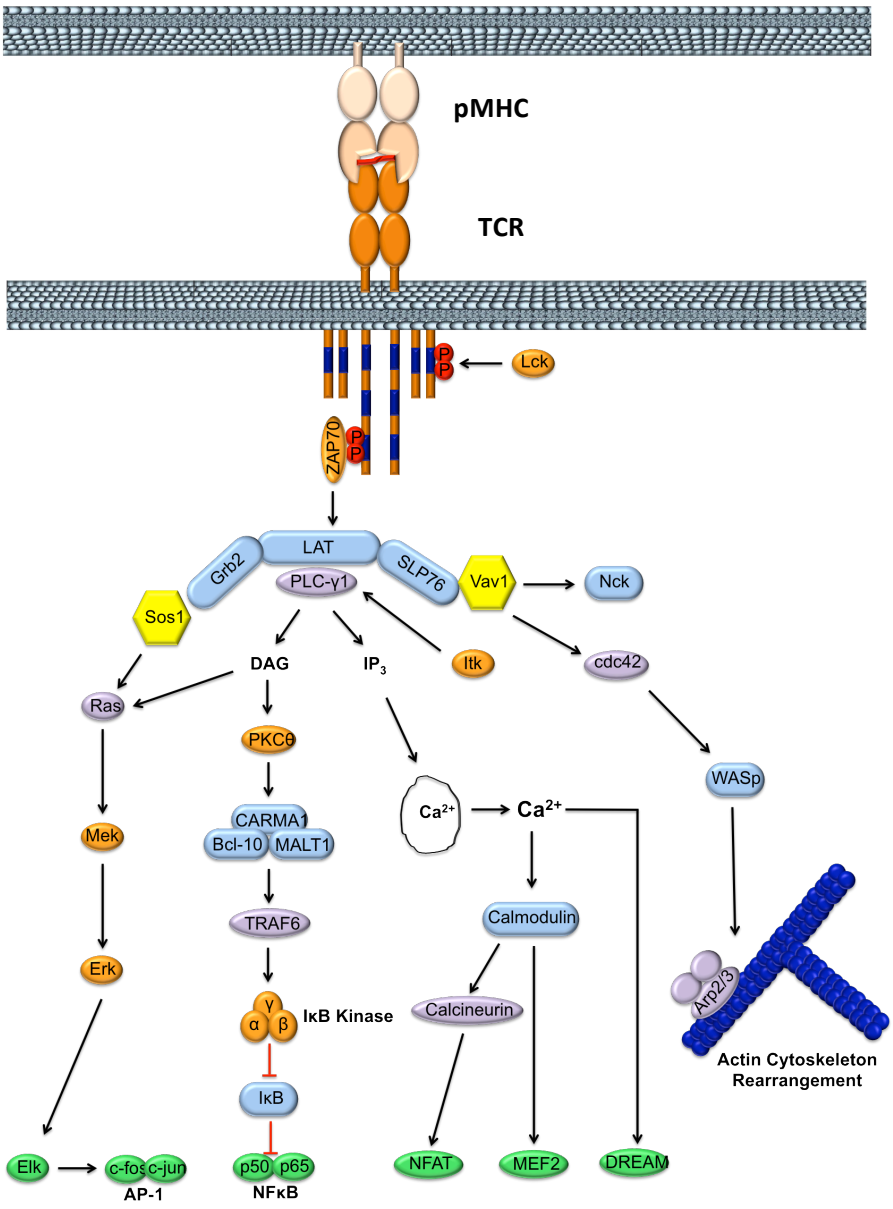

Figure 1.2 TCR signal transduction pathway

The TCR signal transduction pathway begins with Src kinase (Lck) phosphorylation of CD3 ITAM tyrosine residues. ZAP70 recruitment to the ITAMs facilitates LAT phosphorylation and the recruitment of other adaptor molecules including Grb2, SLP76 and PLCγ1. Grb 2 recruits Sos1 to initiate the MAP kinase pathway, ultimately culminating in the activation of transcription factor AP-1. PLCγ1 catalyses the formation of DAG and IP_3. DAG activation results in the activation of MAP kinase and PKCθ mediated pathways while IP_3 initiates the calcium signalling pathways. SLP76 recruitment to the TCR facilitates actin cytoskeletal rearrangement via Vav1 and WASp.

PLC-γ1 on the other hand, is recruited to the signalling complex via high affinity interaction between its SH2 domain interactions with LAT pY132 (Paz et al., 2001). At the plasma membrane, Itk activated PLC-γ1 hydrolyses membrane lipid PIP_2 to produce second messengers diacylglycerol (DAG) and Inositol trisphosphate (IP_3).

DAG activates MAP Kinase- and PKCθ-mediated signalling pathways

Activation of DAG by PLC-γ1 also results in the activation of the MAP kinase pathway involving Ras, culminating in the production of transcription factor AP-1 as mentioned previously. In addition, DAG activates a second major signalling pathway involving protein kinase C θ (PKCθ). PKCθ initiates a series of steps that ultimately lead to the activation of Nuclear-Factor κB (NFκB) by phosphorylating scaffold protein CARD- containing MAGUK protein 1 (CARMA1). Phosphorylated CARMA1 oligomerises and association with Bcl10. Mucosa associated lymphoid tissue lymphoma translocation gene 1 (MALT1) binds to B cell leukemia/lymphoma 10 (Bcl10) to form a trimolecular CARMA1/Bcl10/MALT1 complex that contributes to the activation of TNF receptor-associated factor 6 (TRAF6). TRAF6 activates a complex of serine kinase IκB kinase (IKK), which phosphorylates IκB, targeting it for ubiquitylation and degradation. Degradation of IκB relieves its inhibition of transcription factor NFκB, allowing its translocation into the nucleus (Smith-Garvin et al., 2009). PKCθ can also activate c-Jun N-terminal kinase (JNK), and may be able to activate AP-1 by this route (Moller et al., 2001). Activation of DAG therefore provides independent mechanisms for the activation of AP-1 and NFκB.

IP_3 and calcium mediated signalling pathways

IP_3, generated as a result of PIP_2 hydrolysis by PLC-γ1, binds to IP_3-Ca^{2+} ion channel receptors on endoplasmic reticulum membrane leading to the release of stored intracellular Ca^{2+}. The spike in intracellular Ca^{2+} triggers a sustained influx of Ca^{2+} from by activating plasma membrane Ca^{2+} released activated Ca^{2+} (CRAC) channels (Oh-hora and Rao, 2008). Ca^{2+} is well established as efficient intracellular secondary messenger. In the case of TCR signalling, intracellular Ca^{2+} binds calmodulin and induces a conformational change in the latter, enabling the binding and activation of additional downstream signalling molecules. One of them is calcineurin, a phosphatase that dephosphorylates and allows nuclear factor of activated T-cells (NFAT) nuclear translocation (Savignac et al., 2007). In the nucleus, NFAT can cooperate with other unrelated transcription factors such as AP-1, thereby serving as a point of signal integration between different signalling pathways. For example, NFAT/ AP-1 cooperation is important in transcription of IL-2, while activity of NFAT alone in the absence of AP-1 induces T cell anergy (Macian et al., 2002). In addition, such cooperation is also implicated in T cell lineage development. Synergistic activity between NFAT and Gata-3 favours IL-4 and IL-5 production for T_H2 lineage differentiation while association with Foxp3 displaces NFAT/AP-1 complex to promote regulatory T cell development [(Wu et al., 2006), reviewed in (Savignac et al., 2007)].

Myocyte enhancer factor-2 (MEF2) represents another family of transcription factor activated downstream of Ca^{2+} signalling in a calmodulin dependent pathway. Relevance of MEF2 in the T cell signalling pathway was demonstrated by investigating mice harbouring a partial calcineurin-binding protein (Cabin1) knockout. Cabin1 is a MEF2 transcriptional repressor that interacts with MEF2 and

calmodulin in a mutually exclusive way, interaction of the latter releases MEF2 from repression. Partial Cabin1 knockout highlighted a role for MEF2 in IL-2, IL-4, IL-9 and IL-13 upregulation following TCR stimulation (Esau et al., 2001).

Ca^{2+} signal also enhances the expression of immune-related genes by inhibiting transcriptional repressor downstream regulatory element antagonistic modulator (DREAM). DREAM is a Ca^{2+} binding protein that also binds downstream regulatory elements (DRE) of DNA. Increased Ca^{2+} concentration promotes Ca^{2+} binding to DREAM to release DREAM from the DRE thereby de-repressing DRE-dependent transcription (Savignac et al., 2007). Target sequences of DREAM include IL-2 and IFNγ (Savignac et al., 2005).

1.4 T cell co-stimulation

'*Paralysis and induction involve the recognition of one and two determinants on an antigen, respectively*' - **Bretscher and Cohn, 1970**

While the TCR is central to delineating the specificities of agonistic pMHCs, full T cell activation often requires the presence of a second, co-stimulatory signal. In the absence of the costimulatory signal TCR engagement can result in T cell unresponsiveness or anergy. This requirement was originally developed to explain B cells discrimination between self and foreign antigen, where it was known as the 'two signal' hypothesis (Lafferty and Cunningham, 1975), and was subsequently applied to T cells (Bretscher and Cohn, 1970a).

Evolution of the 'two signal' hypothesis

The original hypothesis has come a long way since the functional discovery of CD28, which remains to this day, the quintessential T cell co-stimulation receptor (June et

al., 1987). The input of secondary signals reveals the possibility of signal integration between receptors on the T cell surface, representing a natural modification of the original hypothesis. Whether co-stimulatory receptors represent a qualitative or quantitative enhancement of TCR signalling remains to be an area contentious debate (Acuto and Michel, 2003). CD28 signalling however, is known to reduce TCR signalling threshold by feeding into the main TCR signalling pathway as well as to transduce qualitatively unique signals (Lenschow et al., 1996b).

Subsequent discovery of CTLA-4 as an inhibitory 'co-stimulatory' molecule for T cells further extended the paradigm of co-stimulation to include negative regulatory pathways (Linsley et al., 1991). More recently, the discovery of bi-directional signalling, where costimulatory receptor ligands also transduce signal into antigen presenting has uncovered the dynamic two-way nature of co-stimulation (Munn et al., 2004, Eissner et al., 2004). This is perhaps best demonstrated by the induction of indoleamine 2,3-dioxygenase (IDO) by CTLA-4 engagement of its ligands CD80 or CD86 on dendritic cells (DCs) (Munn et al., 2004).

These developments, along with increasing appreciation of the importance of spatial-temporal regulation of co-stimulatory have prompted a re-evaluation of T cell co-stimulation, as reviewed by Chen and Flies (Chen and Flies, 2013).

The CD28 group of co-stimulating receptors

CD28 family, which includes CD28, Cytotoxic T-Lymphocyte Antigen 4 (CTLA-4), ICOS and programmed cell death protein 1 (PD-1), is the best-characterised group of co-stimulatory receptors. Members have a single extracellular Ig V-like domain, and interact with cell-surface proteins in the CD80 family, which have two Ig domains. As

functions of CD28 will be thoroughly reviewed in chapter 3, this section will focus on selected members of the CD28 superfamily.

Inducible co-stimulator (ICOS) is upregulated on T cell surfaces upon ICOS ligand (ICOSL) binding. Intracellular tail of the disulphide-linked Ig-V homodimer contains two tyrosine residues. Tyrosine phosphorylation of the YMFM motif results in PI3-kinase recruitment via p85-SH2 domain association (Gigoux et al., 2009). As such, ICOS delivers a co-stimulatory signal akin to CD28 in part via the cell survival effects of AKT activation downstream of PI3-kinase (see Chapter 3 introduction). Indeed, defects observed in CD28 knockout mice can be rectified by crossing the animals with mice expressing ICOS constitutively (Linterman et al., 2009). ICOS signalling can contribute to TH1 and TH2 lineage differentiation by inducing IL-4, IL-5, IL-10, IFNγ and TNFα secretion [reviewed in ((Simpson et al., 2010)]. In addition, the role of ICOS in maintaining memory T effector cells was highlighted by reduced $CD44^+$ and $CD62L^+$ T cells in ICOS deficient mice (Burmeister et al., 2008).

CTLA-4 represents the prototypical inhibitory 'co-stimulatory' receptor. Importance of this receptor was demonstrated by severe autoimmunity characterised by lymphadenopathy, splenomegaly and multiple organ failure in CTLA-4 deficient mice (Tivol et al., 1995, Waterhouse et al., 1995). CTLA-4 is a homologue of CD28 (~30% sequence identity) and they share the same ligands CD80 and CD86 by virtue of their MYPPPY binding motif (Teft et al., 2006). Molecular mechanisms of CTLA-4 inhibition have traditionally been distinguished between its ability to affect T cells that express it or (cell intrinsic) or its ability to mediate its effects through other cells (cell extrinsic) [reviewed in (Walker and Sansom, 2011)]. One cell intrinsic mechanism is

transduction of an inhibitory signal: CTLA-4's ability to recruit tyrosine phosphatases Protein phosphatase 2A (PP2A) and Tyrosine-protein phosphatase non-receptor type 11 (PTPN11 or SHP2) could antagonise tyrosine-phosphorylation-dependent signalling by TCR and CD28 (Teft et al., 2006). A second cell intrinsic mechanism is competition for ligand: the fact that CTLA-4 and CD28 shared the same ligands suggested that both receptors could in theory compete for ligand engagement (Thompson and Allison, 1997). Such views were exceptionally attractive as CTLA-4 binds its ligands with greater affinity and avidity than CD28 does (van der Merwe et al., 1997). Effective sequestrations of ligands however would require high levels of CTLA-4 expressions relative to CD28, which is a rare phenomenon in conventional T cells since CTLA-4 are only inducible upon T cell activation.

Several cell-extrinsic mechanisms have been proposed. Sansom and colleagues have demonstrated that CTLA-4 can mediate trans-endocytosis of CD80 and CD86 ligands on APCs. Ligands 'snatched off' the surface of the APC then undergo lysosome-mediated degradation (Qureshi et al., 2011), abrogating the ability of the APC to costimulate other T cells. Other cell extrinsic mechanisms of CTLA-4 function include the induction of inhibitory cytokines and enzymes by regulatory T cells and APCs respectively, as well as the production of soluble CTLA-4 molecules [reviewed in (Walker and Sansom, 2011)].

PD-1 is another well-established inhibitory co-stimulatory receptor on T cells. The inhibitory function of PD-1 is mediated by its intracellular immunoreceptor tyrosine based-inhibitory motif (ITIM) and immunoreceptor tyrosine based-switch motif (ITSM) (Ishida et al., 1992). Expression of PD-1 is inducible upon T cell activation and

its downstream signalling event involves the recruitment of a number of phosphatases including SHP2 and phosphatase and tensin homolog (PTEN), which can reverse the phosphorylation events of Lck and PI3-kinase respectively (Parry et al., 2005, Yamazaki et al., 2002). PD-1 expression is also enhanced on exhausted T cells like other inhibitory IgSF members including CTLA-4, B- and T-lymphocyte attenuator (BTLA) and T-cell immunoglobulin domain and mucin domain 3 (TIM3). Exhausted T cells exhibit progressive loss of T cell function as a result of chronic antigen exposure in persistent infections or cancer (Wherry, 2011). Therapeutic significance of PD-1 is stressed by the reversal T cell exhaustion to reduce viral load upon PD-1 blockade in several infection models (Velu et al., 2009, Barber et al., 2006).

CHAPTER 2:

Methods and Materials

2.1 Plasmid Constructs

Elongating CD80

SacII and BspEI restriction sites were first introduced into the region of the CD80 cDNA encoding the linker between the ectodomain and transmembrane domain by overlapping Polymerase Chain Reaction (PCR) mutagenesis using primer sets 1 and 2 (see Table 2.1; restriction enzyme sequences are underlined). To elongate CD80, DNA encoding spacer fragments of human CD2 or CD4 were inserted in between the SacII and BspEI sites. The CD2 and CD4 spacer fragments were cloned from human CD2 and CD4 cDNA using primer sets 3 and 4 respectively. For expression, the CD80 constructs were cloned into pcDNA^{TM}3.1^{+}/Hygro (Invitrogen^{TM}) expression vector between the HindIII and NotI enzymatic sites. HindIII and Not I enzymatic sites were introduced at the 5' and 3' end of CD80-WT, CD80CD2 or CD80CD4 DNA by PCR using primer set 5. The elongated constructs were verified by DNA sequencing.

Elongating H2K^{b} Single Chain Dimer (SCD)

PKG5-SCD vector was a gift from Dr Keith Gould of Imperial College London, UK. To elongate SCD, a SalI enzymatic site was introduced into the stalk region of H2k^{b} heavy chain by PCR overlapping mutagenesis using the primer set 6. SalI enzymatic sites were introduced at the 5' and 3' end of the CD2 and CD4 spacer fragment using primer sets 7 and 8 respectively. These spacer fragments were then ligated into SalI-containing stalk region of H2K^{b} to elongate the molecule. Incorporation of the spacer fragments was confirmed by DNA sequencing.

Table 2.1 List of primers used

Primer Set	Primer Names	Primer Sequence
Set 1	SACII-CD80 Forward	ACGTGTCCGCGGATTTCACCTGGG
	SACII-CD80 Reverse	AATCCGCGG ACACGTGAGCATCT
Set 2	BspEI-CD80 Forward	GGGAAAAACCTCCGGAAGACC
	BspEI-CD80 Reverse	GGTCTTCCGGAGGTTTTTCCC
Set 3	SACII-CD2 Forward	ATGATGCCGCGGATTTCACCTGGGAGATTACGAATGCCTTGG
	BspEI-CD2 Reverse	ATCATCTCCGGAGGTTTTTCTTTCTCTGGACAGCTGACAGGCT
Set 4	SACII-CD4 Forward	ATGATGCCGCGGATTTCACCTGGAAAGTGGTACTGGGCAAA
	BspEI-CD4 Reverse	ATCATCTCCGGAGGTTTT TCTGTGGGCAGAACCTTGATGTTGG
Set 5	HindIII-CD80 Forward	ATGATGAAGCTTATGGCTTGCAATTGTCAG
	NotI-CD80 Reverse	ATGATGGCGGCCGCCTAAAGGAAGACGGTCTG
Set 6	SalI SCD Forward	AGCCTCCTCCGTCGACTGTCT
	SalI-SCD Reverse	AGACAGTCGACGGAGGAGGCT
Set 7	SalI-CD2 Forward	TAGTAGGTCGACTGAGATTACGAATGCCTTGG
	SalI-CD2 Reverse	TAGTAGGTCGACGGTTTCTCTGGACAGCTGACAGGCT
Set 8	SalI-CD4 Forward	TAGTAGGTCGACTAAAGTGGTACTGGGCAAA
	SalI-CD4 Reverse	TAGTAGGTCGACGGTGTGGGCAGAACCTTGATGTTGG
Set 9	HindIII-CD80 Forward	ATGATGAAGCTTATGGCTTGCAATTGTCAG
	NotI-CD80 nonstop Reverse	TACTACGCGGCCGCCAAGGAAGACGGTCTGTTCA
Set 10	NotI-GFP Forward	TAGTAGGCGGCCGCATGGTGAGCAAGGGCGAGGA
	XhoI-GFP Reverse	TAGTAGCTCGAGCTACTTGTACAGC
Set 11	PKG5-XhoI-SCD Forward	TTTTGCAAAAAGCTCTCGAG
	BamHI-SCD nonstop Reverse	TAGTAGGGATCCCGCTAGAGAATGAGGGTCATGAACCA
Set 12	BamHI-DsRed Forward	TAGTAGGGATCCATGGACAACACCGAGGACGTCAT
	HindIII-DsRed Reverse	TAGTAGAAGCTTCTACTGGGAGCCGGAGTGGCG

CD80-GFP Fusion

Stop codons of CD80, CD80CD2 and CD80CD4 were mutated by PCR using primer set 9. 'Non-stop' mutants of CD80, CD80CD2 or CD80CD4 were ligated back into pcDNA^{TM}3.1^{+}/Hygro (Invitrogen^{TM}) expression vector between the HindIII and NotI enzymatic sites. DNA encoding GFP was ligated in between NotI and XhoI enzymatic site immediately downstream of the 'non-stop mutants'. NotI and XhoI sites were cloned into the 5' and 3' end of GFP respectively, by PCR using primer set 10.

SCD-DsRed Fusion

Stop codons of SCD, SCDCD2 and SCDCD4 were mutated by PCR using primer set 11. 'Non-stop' mutants of SCD, SCDCD2 or SCDCD4 were ligated back into the PKG5 expression vector in between the XhoI and BamHI restriction sites. DNA encoding DsRed was ligated in between the BamHI and HindIII restriction sites immediately downstream of the 'non-stop' mutants. BamHI and HindIII sites were cloned into the 5' and 3' end of DsRed respectively, by PCR using primer set 12.

HLA-A2 mutants

Amino acid substitutions were introduced by mutating HLA-A2-encoding plasmids using a combination of overlapping PCR mutagenesis and QuickChange site directed mutagenesis (Strategene Cat. No. 200523). Mutations were verified by DNA sequencing.

TCR Constructs

Five TCR were used in this thesis: 1G4, 1G4c58/c61, A6, JM22 and G10. 1G4, JM22 and G10 TCR constructs were obtained respectively from Professors Vincenzo Cerundolo and Yvonne Jones, and Dr Guillaume Stewart-Jones from the University of Oxford, UK. The A6 TCR was provided by Professor Brian Baker from the University of Notre Dame, USA. The 1G4c58/c61 TCR was provided by Immunocore Limited, UK.

2.2 Cells

CHO Cell-lines

IE^K or SCD expressing CHO cell lines were maintained by culturing in RPMI-10% FCS medium containing 100U/ml penicillin/streptomycin and 0.5mg/ml G418. CD80

expression was maintained by adding 0.3mg/ml hygromycin in the relevant cell culture medium.

Mouse Primary T Cells

To prepare primary T cells, spleens from A1 TCR transgenic $Rag1^{-/-}$ x CBAc/a mice, OT1 TCR transgenic C57BL/6 mice or CD28-Y170F DO11.10 TCR transgenic mice were harvested into single cell suspensions and lysed with 5ml RBC lysis buffer (150mM NH_4Cl, 1mM $KHCO_3$, 20mM EDTA). $CD4^+$ or $CD8^+$ T cells were purified using Dynal® mouse CD4 or CD8 cell negative selection kit (Life Technologies Ltd Cat. no. 11415D/ 11417D). CD28-WT and CD28-Y170F DO11.10 TCR transgenic mice were kindly provided by Professor Christopher Rudd, University of Cambridge, UK with permission from Dr Jonathan Green, Washington University School of Medicine, USA.

Human Primary T cells

Blood obtained from HLA-$A2^+$ or HLA-$A2^-$ donors were directly dispensed into sterile heparinized vacutainer tubes (BD Biosciences Cat. No. 368480), diluted 1:2 in PBS and laid carefully onto 10ml of Ficoll (GE Healthcare Cat. No. 17-1440-02). Following 30 mins centrifugation at 1600RPM without brakes, peripheral blood mononucleated cells (PBMC) were gently pipetted and washed 2 times in PBS. $CD8^+$ T cells were purified using magnetic beads negative isolation as described in the manufacturer's protocol (Life Technologies Ltd Cat. no. 11348D). Human primary T cells were maintained in DMEM-10% FCS medium containing 100U/ml penicillin/streptomycin and 50U/ml IL-2 (Peprotech Cat. No. 200-02).

T cell lines

Human Jurkat and Mouse 2B4 and B3Z T cell hybridomas were cultured in RPMI-10% FCS and 100U/ml penicillin/streptomycin. Human Jurkat T cell lines were cultured in DMEM-10% FCS and 100U/ml penicillin/streptomycin. E6.1 Jurkat T cells expressing NFAT-Luciferase construct were obtained from Professor Oreste Acuto, University of Oxford, UK.

2.3 Protein Purification, Refolding and Biotinylation

HLA-A2 Molecules

HLA-A2 heavy chains containing a C-terminal BirA tag and β2-microglobulin were expressed as inclusion bodies in *E.coli*, refolded *in vitro* with the indicated peptide and purified using size-exclusion chromatography (Madden et al., 1993). Purified pMHC was biotinylated according to the manufacturer's protocol (Avidity).

T Cell receptors

Separate TCR α and β subunits were expressed as inclusion bodies in *E.coli*, refolded *in vitro* and purified first using anion exchange chromatography before using size-exclusion chromatography [as described in (Boulter et al., 2003)].

2.4 Peptides

The peptides used in this thesis were purchased at >95% purity. A list of peptides used and their source can be found in Table 2.2.

Table 2.2 List of peptides used

Peptide Name	Sequence	Source
NYES0-4A	SLLAWITQV	GenScript Co. USA (Customised)
NYES0-5F	SLLMFITQV	
NYES0-5P	SLLMPITQV	
NYES0-8K	SLLMWITKV	
NYES0-8S	SLLMWITSV	
NYES0-9V	SLLMWITQV	
Dby	REEALHQFRSGRKPI	Courtesy of Dr Dominika Misztela
$OVA_{257-264}$	SIINFEKL	Sigma Aldrich (Cat No. S7951)

2.5 Cell Transfection and Transduction

CHO cell transfection

2µg of the respective DNA constructs were transfected into 50% confluent CHO cell lines using LONZA transfection kit according to the manufacturer's protocol (Amaxa® Cell line Nucleofector Kit T; Lonza Cat. no. VCA-1002).

Lentiviral Transduction

293T cells were co-transfected with the relevant lentiviral vector along with the pre-mixed packaging mix (18µg of pRSV-REV and pMDLg/p-RRE vectors, 7µg of pVSV-G vector) using X-tremeGENE 9 DNA Transfection Reagent (Roche Applied Science Cat. No. 06365787001). Viruses were harvested and 22µm-filtered after 24 hours and concentrated using Lentipac™ Lentivirus concentrator (Genecopoeia Cat. No. LPR-LCS-01) according to the manufacturer's protocol. Purified human T cells were pre-stimulated 24 hours before viral transduction using CD3/CD28-antibody coated microbeads (Life Technologies Dynabeads® Human T cell Activator Cat. No. 111.31D)

at a 1:1 ratio. 1ml of fresh, concentrated lentivirus were added onto equal-volume of 10^6 T cells in culture media supplemented with 50U/ml IL-2. Fresh IL-2 supplemented media were replaced every 2-3 days after viral transduction and the magnetic beads removed on day 5 after viral transduction.

2.6 T Cell Stimulation Assays and Statistical Analysis

Mouse primary T cells – Transgenic A1, OT1 and DO11.10 TCR mice

5 x 10^4 CD80-expressing CHO-IE^K or CHO-SCD cells were pulsed with titrating concentrations of deadbox gene Dby peptide (REEALHQFRSGRKPI) or Ovalbumin $OVA_{257-264}$ (SIINFEKL) peptide, which are recognized by A1 and OT1 TCRs respectively. 5 x 10^4 $CD4^+$ A1 $Rag1^{-/-}$ x CBAc/a T cells or $CD8^+$ OTI C57BL/6 T cells were added to the pulsed CHO cells in RPMI-10 medium for 48 hours. For trans-costimulation assays, 5 x 10^4 IE^K expressing CHO cells were pulsed with 5µM of Dby peptide and incubated with A1 $Rag1^{-/-}$ x CBAc/a T cells at a 1:1 ratio, together with the indicated number of unpulsed, CD80-expressing co-stimulatory CHO cells. In assays comparing CD28-WT versus CD28-Y170F DO11.10 TCR transgenic mice, TCR activation was provided by immobilising 5µg/ml anti-CD3 (Clone 2C11) antibodies on streptavidin-coated plates (Sigma Aldrich Cat. No. S6940) instead. Supernatants were harvested after 48 hours and assayed for IL-2 by ELISA.

To analyse the data from CD28-WT of CD28-Y170F DO11.10 TCR transgenic mice, the dose response curves were fitted with a Gaussian function on log scale and the area under curve (AUC) calculated as a measure of IL-2 secretion. In this analysis, data from both CD80CD2 and CD80CD4 were collated and the degree of IL-2 secretion impairment as a result of CD80 elongation was quantified by calculating the ratios of

elongated CD80 AUC: CD80-WT AUC. Paired T test analysis was used to determine if IL-2 secretion from elongated CD80 in CD28-WT T cells was significantly different from T cells with CD28-Y170F.

1G4^{hi}-expressing Jurkat T cell lines

Refolded biotinylated pMHC molecules were serially diluted (20µg/ml - 2.7ng/ml) and transferred onto 96-well streptavidin coated plates (ThermoScientific Cat. No. 15500) for 90 mins at 4°C. Two plates were prepared for every experiment; the first used for the stimulation assay and the second was used to determine the levels of correctly folded plate-immobilised pMHC.

Levels of active plate-immobilised pMHC were measured using mouse anti-human HLA class I antibody (clone W6/32; eBioscience Cat. No. 14-9983) in combination with fluorescent secondary goat anti-mouse IgG IRDye 800CW antibodies (LI-COR Cat. no. 926-32210). Fluorescence measurement were performed with LI-COR Odyssey® Imaging System and plotted as a function of the initial pMHC concentration on Prism 6 (Graphpad Prism Software, Inc.). EC_{50} values for pMHC immobilisation were obtained by fitting a sigmoid-dose response model to the data. Levels of pMHC immobilisation were normalised to an index pMHC (WT/ 4A) using the following formula:

$$\text{Normalised Log [pMHC]} = \text{Log [pMHC]} + (\text{LogEC}_{50\ \text{Index pMHC}} - \text{LogEC}_{50\ \text{pMHC}})$$

For stimulation, 5 x 10^4 1G4^{hi}-expressing Jurkat T cells were incubated overnight at 37°C and the concentration of released IL-8 were measured by ELISA (eBiosciences Cat. No. 88-8086). To measure the amount of NFAT expression, the cells were lysed using ONE-Glo^{TM} Luciferase substrate (Promega Cat. No. E6110) and analysed using

plate reader (Pherastar^{Plus}, BMG Lab Tech). IL-8 secretion and NFAT-Luciferase expression were plotted against the normalised pMHC concentrations and fitted using a Gaussian function on a log scale.

For correlation analysis, the K_D and k_{off} values were plotted against the ascending EC_{50} and amplitude values derived from the Gaussian curve. A linear regression was performed to determine the degree of correlation. EC_{50} values were extracted from the Gaussian curve using the following formula:

$$EC_{50} = \mu \pm SD.(\sqrt{\ln 2})$$

where μ is the mean derived from the Gaussian curve and SD refers to the Standard deviation of the Gaussian curve.

The same curves were fitted with a Lowess curve to extract normalized pMHC concentrations for the plots described in Figure 5.14.

1G4^{hi}-expressing primary human T cells

pMHC were immobilised onto streptavidin-coated plates as described previously. For stimulation, 5 x 10^4 T cells were added onto the pMHC-immobilised plates and their supernatant harvested after 4 hours and 48 hours for IFNγ and IL-2 ELISA respectively (eBioscience Cat. nos. 88-7316-88 and 88-7025-88).

2.7 CD28 binding assay

To measure CD28 binding to CD80 expressing CHO cells, 120μl of protein A coated fluorescent beads (Spherotech, Inc., Libertyville Cat. No. PAFP-0556-5) were incubated with 5.2μg of CD28 recombinant protein fused to the Fc portion of human IgG_1 (R&D Systems Cat. No. 483CD/CF) at 37°C for 1 hour. The resultant mixture was

then serially diluted 12 fold before incubation with 10^6 CHO cells at each concentration for 45 mins in a staining volume of 50µl. T cells were then washed at low speed before analysis by flow cytometry.

2.8 $H2K^b$ Loading Assay

Wild type and elongated SCDs were incubated with titrating concentrations of pOVA-SIINFEKL peptide for 2 hours at 37°C. The cells were then washed before staining for $H2K^b$-SIINFEKL complex using anti-mouse pOVA-SIINFEKL peptide bound to $H2K^b$ antibodies (eBiosciences, clone 25-D1.16). Stained cells were washed at low speed before fixation and analysis by flow cytometry.

2.9 Confocal Microscopy and Image Analysis

Slide preparation

Mouse primary $CD8^+$ OT1 TCR T cells were incubated with 5µM pOVA-SIINFEKL-pulsed or unpulsed CHO-SCD cells expressing the various lengths of CD80-GFP constructs. The cell mixtures were gently dispensed onto 22mm round glass slide that had been pre-washed in 1M Hydrochloric acid and pre-incubated with Poly-L-Lysine. Cells on the glass slides were gently centrifuged at 400rpm for 2 minutes at 4°C before incubation at 37°C for 10 minutes to allow conjugate formation. The cells were then fixed in 4% methanol-free paraformaldehyde for 30 minutes, permeabilised with 0.1% Saponin for 30 minutes and stained for CD45 (Clone HI30, Biolegend Cat. No. 304020) for 45 minutes on ice. Cells on the glass slides were washed 3 times gently in 0.1% Saponin, mounted and analysed immediately.

Confocal Image Acquisition and 3D Image Re-construction

Images were taken with the Inverted Olympus FV1000 Confocal system at X resolution (512µm x 512µm) under ×60 UPlanSApo Olympus objective with a numerical aperture of 1.35. Image stacks consisted of 15–20 planes spaced by ~3-4µm. Three-Dimensional (3D) reconstruction of the CHO cell - T cell conjugate was generated using the Imaris software (Bitplane). Only conjugates whose contact areas were oriented properly to be contained in a rectangular volume for an en face projection were taken into consideration. Detailed flow chart of the 3D image analysis is described in Figure 3.14.

Statistical Analysis

Enface snapshots of the conjugate interface were analysed for CD45-Alexa647 and CD80-GFP correlations using Image J (PSC colocalisation plugin). A step-by-step protocol description is provided in (French et al., 2008). The plugin also calculates Pearson correlation coefficient values on the enface images to determine the degree of CD45-Alexa647 and CD80-GFP pixel overlap. Individual data set were tested for normality (D'Agostino & Pearson normality test) using Prism 6 (Graphpad Prism Software, Inc). One-way ANOVA was used to determine if the Pearson's correlation coefficient were sufficiently different between CD80-WT, CD80CD2 and CD80CD4.

2.10 Surface Plasmon Resonance

All SPR measurements were performed on Biacore 3000 (GE Healthcare) at 25°C using a flow rate of 10µL/ minute in HBS-EP buffer (0.01M pH 7.4 HEPES, 0.15M NaCl, 0.005% P20) unless otherwise stated. CM5 sensor chips (GE Healthcare) were activated with 1-ethyl-3-(3-dimethylaminopropyl) carbodiimide (EDC) and N-hydroxysuccinimide (NHS). EDC couples NHS to carboxymethylated dextran matrix

on the chip, resulting in the formation of a NHS ester. This allowed covalent linking of streptavidin to the chip surface via primary amines. Biotinylated pMHC were then immobilised onto flow-cells 2,3 and 4 of the sensor chips at various levels (~1200 RU for equilibrium binding analysis and ~120 RU for kinetic analysis). Flow-cell 1 was either left empty or coated with an irrelevant antibody as negative control.

Equilibrium Binding Analysis

The relevant TCRs were injected over the pMHC-immobilised chip for 120 seconds before the chip surface was flushed with HBS-EP running buffer for 5 minutes for TCR dissociation. This procedure was repeated for 7 ascending concentrations of serially diluted TCRs. The reaction was immediately repeated using the same TCR but in reverse descending concentration to demonstrate protein stability and robustness of the assay. K_D values were obtained by non-linear curve fitting using GraphPad Prism® (GraphPad Software) to the Langmuir binding isotherm:

$$\text{Bound} = C^A \times \text{Max} \,.\, (C^A + K_D)$$

where "bound" is the equilibrium binding in RU at injected TCR concentration C^A, and Max is the maximum binding (RU).

Single-Cycle Kinetics Analysis

Single-cycle kinetics analysis was used to measure TCR-pMHC interactions with supra-physiological affinities. A single concentration of (supra-physiologic) TCR was injected onto pMHC immobilised sensor chips for 400 seconds and flushed with HBS-EP buffer for 21600 seconds (6 hours) for TCR dissociation. Association curves and dissociation curves for the same pMHC were compiled across different experiments

and fitted globally in Prism 6 (Graphpad Prism, Inc) using the 'one-phase exponential decay function':

$$RU = (Max\text{-}NS) \cdot e^{-Koff.time} + NS$$

where Max and NS represent maximal and background binding in RU, respectively.

The obtained k_{off} values were used to fit the association phases of the corresponding pMHC using the association kinetics function on Prism 6:

$$RU = Max \cdot (1 - e^{-kob.time})$$

where Max represent maximal binding in RU and $k_{obs} = k_{on} \cdot [TCR] + k_{off}$

CHAPTER 3:

Importance of Receptor/ Ligand Dimensions in CD28 Costimulation

3.1.1 CD28 as a Costimulatory receptor

Successful T cell responses rely on the recognition of antigenic peptides by the T cell receptor complex in the context of a major histocompatibility complex presented by the antigen-presenting cell. The TCR complex alone however, is insufficient for optimal T cell activation and engagement of a second class of costimulatory receptors is needed to amplify the signal as proposed in the '2 signal hypothesis' of T cell activation (Bretscher and Cohn, 1970b).

CD28 is arguably the most potent and best characterised costimulatory receptor. Expressed on both $CD4^+$ and $CD8^+$ T cells, the importance of CD28 was highlighted with the generation of CD28 deficient mice (Shahinian et al., 1993). These mice were immuno-compromised with reduced T cell responses to antigen, impaired germinal centre formation, immunoglobulin isotype class switching (Borriello et al., 1997) and expression of T_H2 cytokines (Andres et al., 2004, King et al., 1995). CD28 was shown to promote cell cycle progression via the up-regulation of cyclin D/ cyclin dependent kinases (CDK) 4 and 6 as well as the degradation of CDK inhibitor $p27^{KIP}$(Boonen et al., 1999, Kovalev et al., 2001, Appleman et al., 2002). Moreover, CD28 activation promotes cell survival through the up-regulation of anti-apoptotic proteins Bcl-X_L and Bcl-2 in a protein kinase B (PKB/AKT) dependent pathway (Boise et al., 1995, Khoshnan et al., 2000). Through the same pathway, PKB inactivates glycogen synthase kinase 3 (GSK3) α and β which prevents the nuclear export of NFAT, thereby stabilising IL-2 mRNA transcript. CD28 serves to provide and amplify signals that modify the activation threshold of T cells.

Despite its clear role in the provision of costimulatory signals to T cells, the involvement of CD28 in different T cell subsets and their development can vary. For example, CD4 and CD8 thymocyte development in CD28-deficient mice appeared normal whilst $CD4^+CD25^+$ regulatory T cell development and homeostasis were dramatically reduced in CD80/CD86 or CD28 deficient mice (Shahinian et al., 1993, Salomon et al., 2000, Lohr et al., 2003). Indeed, in vivo mutagenesis studies by Singer and colleagues identified the specific Lck binding motif in the CD28 cytoplasmic tail that is crucial for Treg development (Tai et al., 2005). In addition, there seem to be a differential requirement of CD28 in T-helper cell 1 (T_H1) versus T_H2 development. In vitro experiments showed that CD28 costimulation preferentially induces T_H2 cytokines (IL-4, IL-5 and IL-10) while T_H1 cytokine production (IFNγ) was not affected in its absence (Schweitzer and Sharpe, 1998, Rulifson et al., 1997). Consistent with the cytokine data, CD28 costimulation favors T_H2 skewing and disease resolution in a non-obese diabetic (NOD) mouse model of T_H1-mediated autoimmune disease (Lenschow et al., 1996a).

To better understand CD28 and its role in mediating T cell activation, differentiation, homeostasis and disease modulation, it is useful to appreciate the molecular structure, interaction and signalling events following CD28 ligation.

3.1.2 CD28 Structure

Full length CD28 is a 44kDa, type-1 trans-membrane protein that exists as disulphide-linked homodimers with a single immunoglobulin variable (Ig-V) like extracellular domain. Early models of CD28 were based on the structure of CTLA-4, showing the core extracellular structure of CD28 consists of 2 β-sheets of the Ig fold

(DEBA and A'GFCC'C'' β-strands) and this was indeed confirmed by the crystal structure of CD28 (Evans et al., 2005). Despite the highly conserved ligand binding domain, geometric and electrostatic similarities in the ligand binding face between CD28 and CTLA-4, there are notable differences that would account for the different ligand affinities and binding valencies between CD28 and CTLA-4 (see Section 3.1.3 below).

The only CD28 crystal structure that was solved was a complex between CD28 and the Fab fragment of the human mitogenic CD28 antibody. These antibodies differ from conventional antibodies with the ability to activate primary resting cells without TCR ligation. Cryo electron microscopy (EM) images and mutational studies by Luhder et al mapped the binding site of mitogenic antibodies to the laterally exposed C''D loop of the Ig domain, in contrast to the MYPPPY binding site of conventional antibodies and CD80 and CD86 (Luhder et al., 2003, Evans et al., 2005).

3.1.3 CD28 interaction with CD80 and CD86

CD80 and CD86 (also collectively known as B7 molecules) represent the main ligands engaged by CD28 and Cytotoxic T Lymphocyte Antigen-4 (CTLA-4) on the APC. CD80 and CD86 exists as 45-60kDa surface proteins (Freeman et al., 1991) with a single membrane distal immunoglobulin (Ig) V and a membrane proximal Ig constant C-like domain. Expression profiles of these molecules vary with the activation state of the APC: CD80 is induced slowly upon activation while CD86 expression is constitutive. Surface Plasmon Resonance studies revealed that relative to CTLA-4 binding affinity, CD86 binds CD28 two-three fold more effectively than CD80 (van der Merwe et al.,

1997). Conversely, CTLA-4 binding is favoured towards CD80, providing an explanation for the delayed expression of both CD80 and CTLA-4 upon activation.

CD80 forms weak (K_D 20-50μM) non-covalent homodimers in solution and in crystalline state (Ikemizu et al., 2000, Stamper et al., 2001). Despite its dimeric form, CD80 engages CD28 in a monovalent fashion, in contrast to the bivalent binding to CTLA-4 (van der Merwe et al., 1997). Explanation for the phenomena would later be uncovered in the crystal structure of CD28: the shorter CC' loop in CD28 (as opposed to CTLA-4) led to a 'tighter', more closed CD28 homodimer on which the binding of one CD80 molecule sterically inhibits the binding of a second CD80 molecule (Evans et al., 2005). The importance of CD28 monovalency was investigated in a study where the monovalent CD28 ectodomain was switched to a bivalent ectodomain; whilst monovalent CD28 homodimers required a TCR signal to induce IL-2 secretion, bivalently ligated CD28 could induce IL-2 secretion alone (Dennehy et al., 2006).

3.1.4 CD28 Microclusters in the Immunological Synapse (IS)

Various groups have observed the formation of CD28 microclusters in the IS and their subsequent migration into the central supra-molecular adhesion complex (cSMAC). It is however unclear if such events have any implications in CD28 costimulation. Live T cell-DC imaging studies by Tseng et al demonstrated that CD80 microclusters co-localised with T cell CD28 and PKCθ microclusters and blockade of T cell signalling led to the rapid decline in CD80 microclusters; implying the possibility of TCR induced CD28 microcluster formation (Tseng et al., 2008). Using a lipid bi-layer system, CD28 microcluster formation was also shown to be highly dependent on the binding of CD80; fascinatingly, the truncation of CD28 cytoplasmic tail did not

prevent CD28 microclusters formation, hinting that this process is signal-independent (Yokosuka et al., 2008).

The exact mechanism mediating CD28 cluster patterning and movement is still unknown. Given the central role CD80 molecules play in CD28 clustering, it may be possible that we have to re-consider the nature of a 'passive' APC. Earlier studies have provided evidence that DC cytoskeleton polarisation is important for IS formation as well as T cell activation (Al-Alwan et al., 2001). The subsequent discovery of semaphorin receptor plexin-A1, in DC seems to account for DC cytoskeletal changes in T cell activation and IS formation. Plexin-A1 mediates cytoskeletal rearrangement by interaction with Rho family GTPases and shRNA knockdown in DC resulted in a near ablation of T cell activation (Eun et al., 2006). Furthermore, it has been demonstrated that the level of B7 molecules on resting and activated B cells correlates with the amount of TCR aggregation in the IS (Jackman et al., 2007). Given the ability of CD28 to induce stimulatory signals into DC via CD80/ CD86 molecules (Orabona et al., 2004), it is not surprising that 'reverse signalling' events in APC may also induce cytoskeletal changes. Indeed, this is highlighted by the finding of actin-modulating and signalling $PI(4,5)P_2$ clusters in DC IS; efficient killing of DC by cytotoxic T cells is dependent on these PIP_2 clusters (Fooksman et al., 2009).

To date, PKCθ is the only known signalling molecule described to associate with CD28 in the CD28 microclusters (Bhatia et al., 2010, Yokosuka et al., 2008, Tseng et al., 2008, Sanchez-Lockhart et al., 2008). Most other signalling molecules implicated in the CD28 costimulatory signalling pathway either associate transiently or do not

seem to co-localise with CD28 microclusters at all. Recruitment of PKCθ into the CD28 microclusters is dependent on an intact CD28 cytoplasmic tail and PKCθ V3 domain (Kong et al., 2011). Interestingly, these CD28-PKCθ clusters also co-localised with TCR microclusters early in the formation of IS, but later associate in regions of low TCR density in the cSMAC (Yokosuka et al., 2008, Tseng et al., 2008). Saito and colleagues then postulated the possibility of both positive and negative regulatory functions in the cSMAC based on the strength of antigen stimulation leading to the differential spatial organisation of TCR and CD28-PKCθ microclusters (Yokosuka and Saito, 2009). More recently, it was revealed that TCR regions of high density in the cSMAC might not be microclusters but extracellular or intracellular vesicles containing TCRs instead (Choudhuri et al., 2014).

Due to the characteristic pattern formation in the IS, many spatiotemporal studies of CD3 and CD28 microclusters have been done with special emphasis on their cSMAC localisation properties. It is therefore very tempting to suggest the importance of cSMAC formation in successful T cell activation. A study found that a CD28 mutation that disrupts PKCθ and CD28 cSMAC localisation also correlated with diminished NFκB nuclear translocation (Sanchez-Lockhart et al., 2008). This brings us to an interesting question, whether it is the impaired signalling that led to a defective cSMAC localisation or it is the other way round? The former is likely to be true. The phenomenon of cSMAC formation surrounded by a peripheral-SMAC (pSMAC) in a 'bull's eye' pattern is mainly observed in bi-layer studies and its occurrence in cell-cell systems may be rare (Tseng et al., 2008). The relevance of cSMAC in a physiological cell-cell interaction was addressed by Dustin and colleagues with the description of ‘kinapse’. Unlike the highly stable structure of the symmetrical IS, the

asymmetric kinapse is caused by the absence of symmetrical radial actin structures giving rise to a leading lamellipodium, an intermediate lamella and a trailing uropod (analogous to dSMAC, pSMAC and cSMAC in an IS) towards a chemotactic gradient. This meant that the kinapse is a moving junction that allows its TCR to scan and sample surrounding pMHC complexes and costimulatory ligands (Dustin, 2009, Dustin, 2007).

3.1.5 Cytoplasmic motifs in CD28 costimulation

CD28 has a short 41 amino acid conserved intracellular cytoplasmic tail with no intrinsic enzymatic activity. Signalling capacity is instead mediated by the recruitment of adaptor or signalling molecules to the cytoplasmic motifs of CD28 including four tyrosine residues, four serine and 2 threonine residues, two proline-rich motifs and two lysine residues (Boomer and Green, 2010, Rudd et al., 2009).

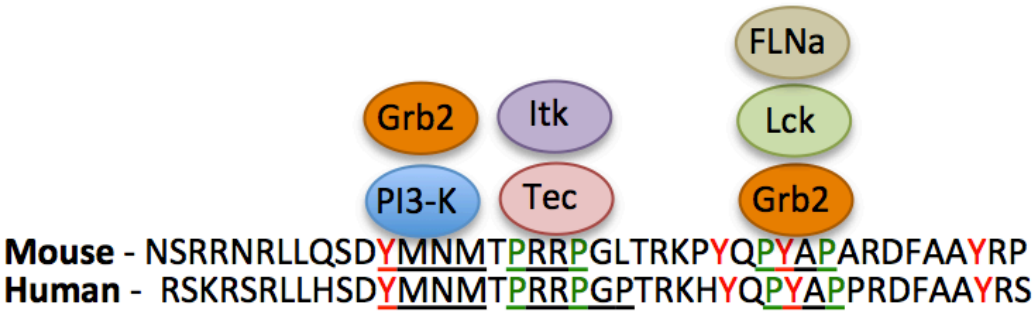

Figure 3.1 Cytoplasmic sequence of CD28

The amino acid sequence of mouse and human CD28 is shown. Phosphorylated tyrosine residues of the YMNM motif recruit PI3K and Grb2. Two proline rich regions exists downstream of the YMNM motif. Itk and Tec were reported to bind the PRRP motif while the PYAP is heavily implicated with the function of CD28 mediated co-stimulation via the recruitment of Lck, Grb2 and Filamin A. Signaling motifs are underlined with phosphorylated tyrosine residues highlighted in red and proline residues in green.

Membrane proximal YxxM motif is highly conserved between members of the CD28 superfamily (members including CTLA-4, ICOS) and is responsible for the recruitment of PI3K via the SH2 domain of its p85 subunit (Pages et al., 1994, Prasad et al., 1994, August and Dupont, 1994). The same YMNM motif in CD28 confers an additional binding site for Grb2 and GADS binding by virtue of the YxNx motif, which is absent in CTLA-4 and ICOS. Further downstream of the YMNM motif, CD28 has two proline rich regions PRRPGP, which was reported to bind ITK and Tyrosine-protein kinase (Tec) (August and Dupont, 1994, Holdorf et al., 1999, Yang et al., 1999) and PYAP, which recruits Lck, Grb2 and Filament A (Holdorf et al., 1999, Okkenhaug and Rottapel, 1998, Tavano et al., 2006).

YMNM and PI3K

CD28 YMNM motif is perhaps the best studied of all CD28 cytoplasmic motifs. CD28 crosslinking leads to rapid YMNM phosphorylation by Src Family kinases such as Lck and Fyn (Raab et al., 1995). pYMNM recruits the SH2 domain of the p85 subunit of PI3K, facilitating the localisation of the other p110 catalytic subunit of PI3K to the plasma membrane. There, PI3K catalyses the formation of phosphatidylinositol 3,4-biphosphate (PIP_2) and phosphatidylinositol 3,4,5- triphosphate (PIP_3). These D3-lipids then recruit proteins containing the pleckstrin homology (PH) domain such as PDK1 and PKB. PDK1 phosphorylates and activates PKB at T308, in turn leading to a diverse array of signalling pathways.

Activation of PKB would lead to cell survival and cell proliferation as a result of enhancing pro-survival proteins Bcl-X_L (Khoshnan et al., 2000) and down-modulating CDK inhibitors $p18^{INK}$ ad $p21^{KIP}$ function (Boonen et al., 1999, Kovalev et al., 2001)

respectively. Importantly, PKB mediated activation of serine/ threonine kinase IκB Kinase targets IκB for degradation through ubiquitination. IκB degradation reveals the nuclear localisation signal of transcription factor NFκB and promotes its migration into the nucleus, mediating IL-2 upregulation (Kane et al., 1999). In a separate pathway, activated PKB can also inhibit GSK3, the kinase that inhibits calcineurin, a calcium dependent serine/threonine phosphatase which dephosphorylates NFAT and promotes its translocation into the nucleus, in turn upregulating IL-2 secretion (Cantrell, 2002). In addition, PKB activation would improve cell metabolism by upregulating glucose transporter 1 (Glut1) expression in a PI3K dependent manner (Frauwirth et al., 2002).

Despite the apparent importance of PI3K in CD28 mediated costimulation, numerous groups have produced conflicting reports on the dispensability of PI3K in the context of IL-2 secretion and T cell proliferation. Mutation of the tyrosine residue in YNMN, which abolishes PI3K association, abrogates IL-2 secretion in T cell hybridomas while the same mutation has no or little effect in in vivo responses (Dodson et al., 2009, Cefai et al., 1998, Harada et al., 2001). Discrepancies in the data over the years can be partly explained by the heterogeneity of experimental settings such as the utilisation of tumour cell lines, which lack phosphatases PTEN and SHIP-1; as well as the usage of artificial stimuli in the form of antibodies. Intriguingly, a recent report noted a clear disparity in cell proliferation between $CD44^{low}$ naïve T cells and unfractionated T cells (which included effector and memory T cells) harbouring the YMNM mutation, suggesting that the reliance of PI3 kinase may be different in different T cell types (Ogawa et al., 2013). Furthermore, the discovery that CD28 promotion of PIP_3 production is independent of the YMNM motif may also explain

the confusion in the literature (Garcon et al., 2008). In addition, data from Andres et al's study suggests that signals generated from various motifs within CD28 cytoplasmic tail act in a redundant way where each pathway can compensate for the absence of others (Andres et al., 2004).

YMNM and Grb2

Grb2 contains an SH2 domain that binds to CD28 YMNM by virtue of the YnXn motif. Two SH3 domains on Grb2 can also bind to CD28 PYAP motif. Grb2 adaptor is involved in Ras and MAP kinase pathway activation mainly by association with the GEF Sos1. Sos1 activates $p21^{ras}$, which then sets off the MAP kinase pathway leading to activation of transcription factor c-Jun that combines with c-fos to form AP-1 transcription complex. Grb2 also associates with Vav (Ye and Baltimore, 1994, Schneider and Rudd, 2008), which activates Rac and cdc42. Apart from the initiation of MAPK pathway leading to the eventual formation of AP-1, Rac and cdc42 has also been implicated in actin cytoskeletal remodelling, an event needed for TCR clustering (Kaga et al., 1998, Fischer et al., 1998). Indeed, Vav-1 deficient mice had T cells that were defective in TCR-induced actin polymerisation, integrin activation and MTOC reorientation (Penninger and Crabtree, 1999, Krawczyk et al., 2002, Ardouin et al., 2003). Vav is also shown to have induced PKCθ membrane translocation and effector functions in a CD28 dependent manner (Villalba et al., 2000).

The importance of Grb2 in CD28 mediated costimulation can be demonstrated by mutating the asparagine (N) residue within the YxNx motif. Loss of Grb2 binding led to a loss of CD28 mediated phosphorylation of Vav and subsequent activation of c-Jun kinase (Kim et al., 1998). Interestingly, the introduction of the YxNx motif via a

single amino acid alternation in ICOS permitted Grb2 recruitment and IL-2 promoter activation that is otherwise absent in ICOS mediated costimulation (Harada et al., 2003).

Proline rich sequence in CD28 cytoplasmic tail

Two proline rich regions exist further downstream of the YMNM motif. The N-terminal PRRP motif was shown to interact with Itk and Tec kinases (*29, 31, 32*). Early studies indicated a negative role for Itk in CD28 mediated costimulation (Liao et al., 1997), in contrast to the traditional stimulatory role of Itk downstream of CD3 signalling. Recent studies by Jain et al however, revealed the exacerbating role of CD28 derived Itk signalling in enhancing autoreactive T cell infiltration in CTLA-$4^{-/-}$ mice. CD28-Itk signals, on the other hand, were dispensable for T cell infiltration in various parasite and viral infection model (Jain et al., 2013). The conflicting results warrants a more systemic approach to decipher the exact role of Itk in CD28-mediated costimulation, taking into account the various cell types and experimental scenarios (in vitro versus in vivo; autoimmune versus infection).

The C-terminal PYAP motif is more heavily implicated in the function of CD28. Mutation of the proline residues to AYAA in an in vivo mouse model led to impaired CD28-dependent functions including proliferation, IL-2 secretion and other adaptive immune system defects, with particular impact on the generation of regulatory T cells (Dodson et al., 2009, Friend et al., 2006, Tai et al., 2005). In addition to Grb2 binding, Lck was shown to be recruited to the PYAP motif via its SH2 domain to the phosphorylated tyrosine or its SH3 domain to the proline rich motif (Holdorf et al., 1999). Lck recruited in this manner was speculated to bridge PKCθ forming a CD28-

Lck-PKCθ tripartite complex, required for mediating CD28-PKCθ recruitment into the immunological synapse (Kong et al., 2011). Indeed, PYAP mutation would abolish CD28 recruitment into the immunological synapse (Yokosuka et al., 2008).

In addition to Lck, filamin A (FLNa), an actin-binding scaffolding protein was reported to bind to the PYAP motif where it colocalises with PKCθ. Knockdown of FLNa too prevented CD28-mediated raft accumulation at the immunological synapse (Tavano et al., 2006). It was also demonstrated that FLNa was required for PKCθ activity (Hayashi and Altman, 2006). It is currently unclear if selective or competitive molecule recruitment to CD28 PYAP motif would mediate any differential functional output.

3.1.6 Actin involvement in CD28 function

Mechanisms for the formation of the IS and the segregation of different microclusters (such as CD3 and CD28 microclusters) has been the subject of extensive investigation. The inhibition of microclusters translocation by latrunculin-A suggested the role of actin-based transport in cSMAC localisation of microclusters (Varma et al., 2006). Kaizuka et al further demonstrated the wave-like movement of filamentous actin from the periphery which does not extend into the actin-poor cSMAC (Kaizuka et al., 2007). TCR and CD28 microclusters may therefore exploit different sets of actin linkers which underlie their differential clustering patterns. Nck in particular, was found to mediate TCR localisation via WASp activation while similar events were mediated by sorting nexin-9 (SNX9) in the case of CD28 (Barda-Saad et al., 2005, Badour et al., 2007). Hence, the observed clustering pattern may be explained by the recruitment of WASp through different adaptor proteins.

Actin cytoskeleton is not only responsible for migratory patterns of CD28 microclusters; studies have elucidated their involvement in NFAT activation. Actin polymerisation in response to CD28 stimulation is required for maintaining Ca^{2+} flux to induce NFAT mediated c-rel transcription and subsequent activation of the CD28 Response Element (CD28RE) (Nolz et al., 2007). Over-expression of SNX9 also triggered NFAT activation (Badour et al., 2007) strongly implicating SNX9 in Ca^{2+} regulation. While the exact mechanism by which actin cytoskeleton regulates Ca^{2+} remains elusive, Nolz et al argued against the involvement of ARP2/3 and instead suggested the role of CRAC channels in this process (Nolz et al., 2007).

More recently, elegant studies by Weiss and colleagues have highlighted the potential role of CD28-mediated actin cytoskeleton polarisation in costimulation. By inhibiting Csk function using drugs specific to the analogue sensitive version of the kinase, Csk^{AS}, the authors were able to spontaneously trigger TCR signalling, but only at the proximal level, until phosphorylation of PLCγ1. Either disruption of the actin cytoskeleton or engagement of CD28 were necessary for downstream signalling such as increased Ca^{2+} and Erk phosphorylation and full T cell activation. Accordingly, the authors propose a model whereby CD28 induces actin-remodelling signals that enables PLCγ1 activated by TCR signals to access its substrate in the otherwise actin-occluded plasma membrane (Tan et al., 2014, Dustin and Davis, 2014), rekindling a decade long feud on the qualitative versus quantitative signalling nature of CD28 costimulation (Acuto and Michel, 2003). This study is reminiscent of earlier observations of actin remodelling in mediating B cell activation, although signals from BCR alone seems to be sufficient for mediating actin-cytoskeletal rearrangements (Treanor et al., 2010).

In addition to its contribution to CD28 localisation and costimulation, the actin cytoskeleton is also involved in CD28 endocytosis. CD28 down-regulation occurred in a clathrin-mediated pathway that is dependent on intact PI3K signalling (Cefai et al., 1998, Badour et al., 2007) and the mutation of SNX9 markedly reduces CD28 internalisation, implicating the role of actin cytoskeleton in CD28 down-regulation (Badour et al., 2007).

3.1.7 CD28 Superagonistic antibodies

CD28 mitogenic or superagonistic antibodies fully activate T cells without the need for TCR ligation. The first CD28 superagonistic antibodies were discovered in rats and later in mouse and human. Aptly named, a single intra-peritoneal dose of the CD28 superagonistic antibodies led to potent T cell activations in vivo to induce lymphadenopathy and splenomegaly (Tacke et al., 1997). However, the antibody was later shown to preferentially stimulate rat $CD4^{+}CD25^{+}$ regulatory T cells and low doses of the antibody would reverse autoimmune conditions in rat models of experimental autoimmune encephalomyelitis (EAE) (Lin and Hunig, 2003, Beyersdorf et al., 2005). This highlighted the therapeutic potential of CD28 superagonistic antibodies in a wide range of autoimmune and inflammatory diseases. A humanised version of the CD28 superagonistic antibody, TGN1412, was soon discovered and tested in primate and human peripheral blood mononuclear cells (PBMCs). No toxicities were observed in both primate and PBMC studies at doses as high as $50mg.kg^{-1}$ (Pallardy and Hunig, 2010).

Unexpectedly, intravenous infusion of TGN1412 at $0.1mg.kg^{-1}$ resulted in a life-threatening systemic inflammatory response syndrome (SIRS) characterised by

sudden and rapid release of pro-inflammatory cytokines in all 6 patients tested. The phase I clinical trial was ended abruptly and subsequent efforts were focused on understanding how existing studies have failed to predict the outcome of the disaster.

Firstly, studies by Stebbings and colleagues indicated that the cytokine storms observed in the volunteers were mediated by IFNγ and TNFα released by $CD4^+$ effector memory T (T_{EM}) cells (Eastwood et al., 2010); which were relatively rare in experimental mice bred under germ-free conditions. Secondly, the same study discovered that cynomolgus macaques $CD4^+$ T cells lose CD28 expression as they differentiate into T_{EM} cells, rendering the cells refractory to the high CD28 superagonist dosage. Thirdly, TGN1412 was later found to positively stimulate human PBMCs but only if they are present at a high enough density (Romer et al., 2011). More recently, TGN1412 (now known as TAB08) was shown to exhibit anti-inflammatory properties in a renewed clinical trial where a much lower dose of the antibody (0.1%-7% of the original dosed used in the 2006 trial) specifically stimulated Treg cells without the induction of pro-inflammatory cytokines from conventional T cells (Tabares et al., 2014). Phase II clinical trials of TAB08 are currently underway (TheraMAB, 2014).

Despite the number of studies published on the effects of CD28 superagonistic antibodies, the exact mechanism by which mitogenic antibody induces T cell activation remains elusive. Two opposing views stand out amongst the several proposed mechanisms (Linsley, 2005, Luhder et al., 2003). The first, championed by Hünig and Dennehy, hypothesised that CD28 superagonists have the unusual ability

to form stable CD28 lattices (Hunig and Dennehy, 2005). This based on their (unpublished) observation that CD28 superagonists contain twice as many epitopes on cells as a conventional CD28 antibody. In addition, bivalent ligation of CD28 (by fusing the extracellular domain of CD80 or CTLA-4 to CD28 intracellular tail) could induce T cell activation in the absence of TCR ligation (Dennehy et al., 2006). On the other hand, elucidation of the binding sites of CD28 superagonist antibodies have highlighted the possible role of the K-S model on the mechanism of CD28 superagonist antibody action (Evans et al., 2005, Luhder et al., 2003). Superagonist antibodies bind near the CD28 membrane proximal C''D loop, and when coupled to Fc-Receptors, they could lead to closer membrane approximation. This enhances the size-based segregation of large inhibitory RPTP such as CD45, thereby resulting in T cell signalling and activation (Figure 3.2). This is not observed for conventional antibodies, which bind CD28 near the MYPPPY motif 'on the top' of CD28. Such observations highlight the importance of receptor/ ligand dimensions in mediating receptor triggering, as postulated by the K-S model.

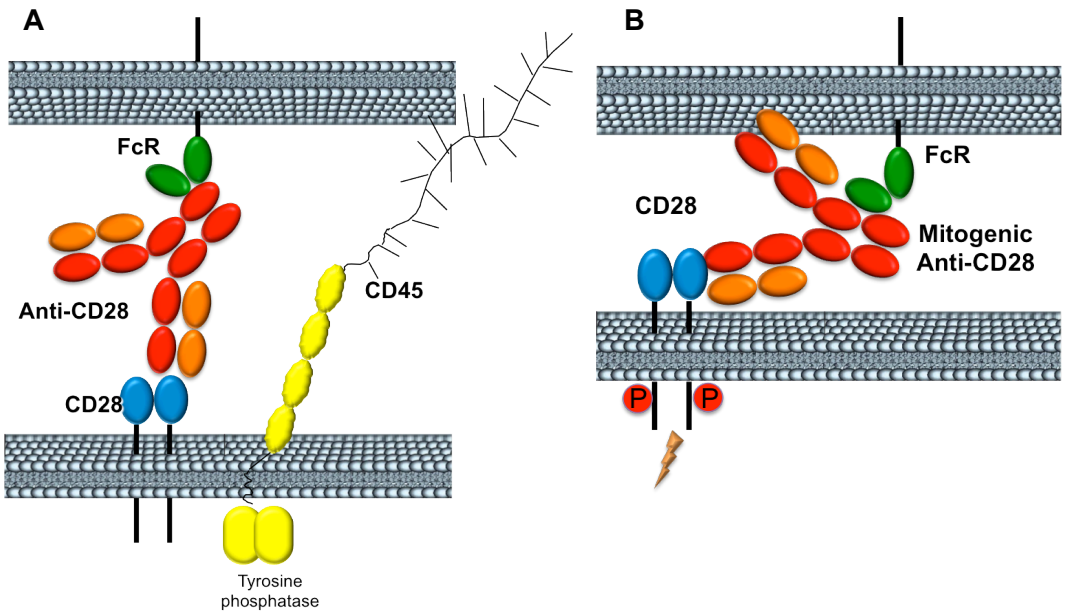

Figure 3.2 Possible mechanism of action for CD28 superagonist antibodies

Cartoon depicting the possible mechanism of action for CD28 superagonist antibodies. (a) Conventional CD28 antibodies coupled to Fc receptors in vivo bind near the MYPPPY motif at the 'top' of CD28. This results in an increased intermembrane distance permitting co-localisation with the high density of CD45 which keeps the conventional CD28 antibody from any aberrant activations. (b) Superagonist (or mitogenic) CD28 antibodies however, bind near the membrane proximal domain of CD28 and in doing so, pulls the two opposing membrane closer, leading to improved CD45 segregation. This leads to an increase in local kinase: phosphatase concentration resulting in CD28 phosphorylation and T cell activation.

3.2 Aims and Objectives

The TCR complex alone is insufficient to produce optimal signalling for T cell function. A second costimulatory signal is necessary to prevent T cell anergy and promote activation. The best-studied costimulatory receptor CD28, binds CD80 and CD86 on APCs. The exact mechanism of CD28 triggering is as yet unknown and several mechanisms have been discussed (Dennehy et al., 2006). With a small extracellular domain and no intrinsic enzymatic activity, CD28 relies on the recruitment of downstream signalling molecules after tyrosine phosphorylation by Src kinases. Thus, CD28 classifies as a NTR as described previously in chapter 1. The K-S model postulates that NTR triggering is critically dependent on the local kinase: phosphatase balance and the segregation of RPTP such as CD45 upon ligand ligation as postulated by the K-S mechanism. Receptor-ligand dimension therefore plays an important role in segregating RPTP for T cell activation. Although the crystal structure of CD28 and its natural ligand has yet to be solved, they are expected to span a length similar to that of TCR-pMHC at approximately 15nm, based on the crystal structure of the related CTLA-4/CD80 molecules (Stamper et al., 2001).

A key prediction of the K-S model states that the small dimensions of the ligand/ receptor complex is necessary to maintain optimal inter-membrane distance for the segregation of large inhibitory phosphatases. Indeed, disruption of the optimal inter-membrane distance between non-catalytic tyrosine-phosphorylated receptors led to the abrogation of receptor activation (James and Vale, 2012, Choudhuri et al., 2005, Kohler et al., 2010, Goodridge et al., 2011).

To test the hypothesis for CD28, the extracellular domain for CD80 was elongated and tested for its capability to costimulate CD28.

3.3.1 Elongating the Ectodomain of CD80

Insertion of Immuno-globulin Super Family (IgSF) domains to elongate extracellular molecules is well-established and have been demonstrated in a number of systems including CD2/ CD48 (Wild et al., 1999), TCR/ pMHC (Choudhuri et al., 2005), NKG2D/ MICA and KIR2DL1/ HLA-C (Kohler et al., 2010). The IgSF domains were typically inserted in the stalk region of the ectodomain, the structure-less region in between the membrane proximal domain and the transmembrane domain, to preserve maximum structural integrity. The successes of these experiments justify a similar approach to testing the CD28/ CD80 costimulatory system. CD80 elongation became the obvious option in favour of the technical complication of elongating CD28 in primary T cells.

To elongate CD80, spacer domains corresponding to the extracellular domain of human CD2 or CD4 were inserted into the mouse CD80 extracellular stalk region. The extracellular region of CD2 consists of a membrane distal V-type IgSF domain followed by a membrane proximal C2-type IgSF domain (Bodian et al., 1994). The extracellular domain of CD4 consists of 4 sets of IgSF domains: a membrane distal V-Type IgSF and a C2-type IgSF domains d1-d2 followed by a repeating set of V-Type and C2-Type IgSF domains d3-d4 (Garrett et al., 1993). The structure of soluble CD80 revealed that the two anti-parallel β sandwich IgSF domains joined by a short linker region stands at a height of approximately 9nm. Interestingly, the overall organisation and dimensions of soluble CD80 resemble that of extracellular hCD2 at

approximately 9nm (Ikemizu et al., 2000). Based on the low resolution X-ray diffraction derived structure of CD4 by Wu et al (Wu et al., 1997), as well as high-resolution CD4 crystal structures of d1-d2 and d3-d4, the extracellular domains of CD4 is predicted to be an extended structure of ~12nm. As such, insertion of human CD2 and CD4 would ideally elongate the CD80 molecule by approximately 9nm to 12nmn respectively.

Importantly, these inserts are deemed functionally inert, as the binding affinities of human CD2 and CD4 and their corresponding ligands in mouse are very low. In addition, inserting both CD2 and CD4 at the base of CD80 would have occluded the binding sites of the molecules, which resides on the top of their membrane distal domain end *(Li et al., 2013)*, thereby inhibiting any unintended cross-reactivity.

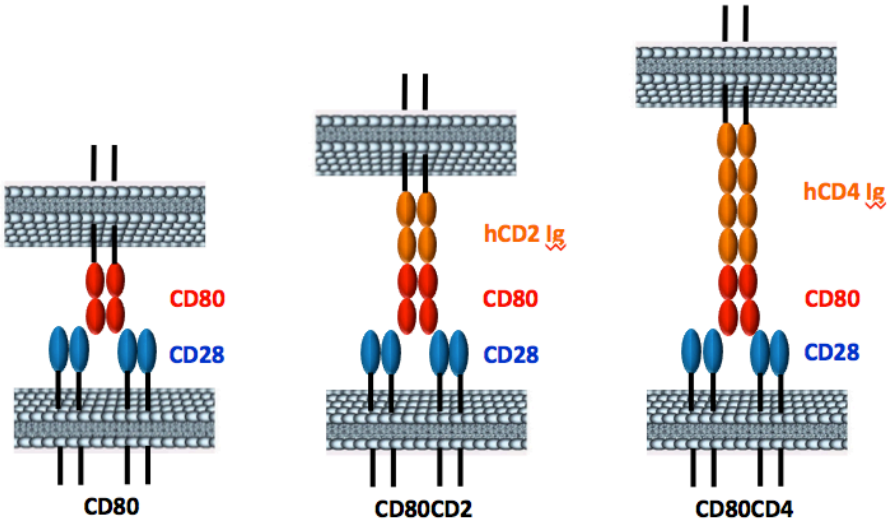

Figure 3.3 Elongating CD80 ectodomains

Cartoon depicting the elongation of CD80 extracellular domain. Human CD2 or CD4 extracellular domains (orange) were cloned into the stalk region of mouse CD80 ectodomain (red) to elongate the molecule by approximately 9 nm and 12 nm respectively. CD2 elongated CD80 is termed CD80CD2 and likewise, CD4 elongated CD80 is termed CD80CD4.

The introduction of a suitable restriction enzyme site for the insertion of spacer domains introduced an E230A mutation in the stalk region of CD80. A mutation in the unstructured stalk region is unlikely to have a significant effect of the structural stability of the molecule. In addition, as depicted in the diagram below, a series of 6 negatively charged residues are evenly distributed across the stalk region. The impact of a loss of one Glutamic Acid in this stretch of negatively charged residues will be minimal. Indeed, as indicated in figure 3.6, there are no observable differences between WT CD80 and CD80 harbouring the E230A mutation.

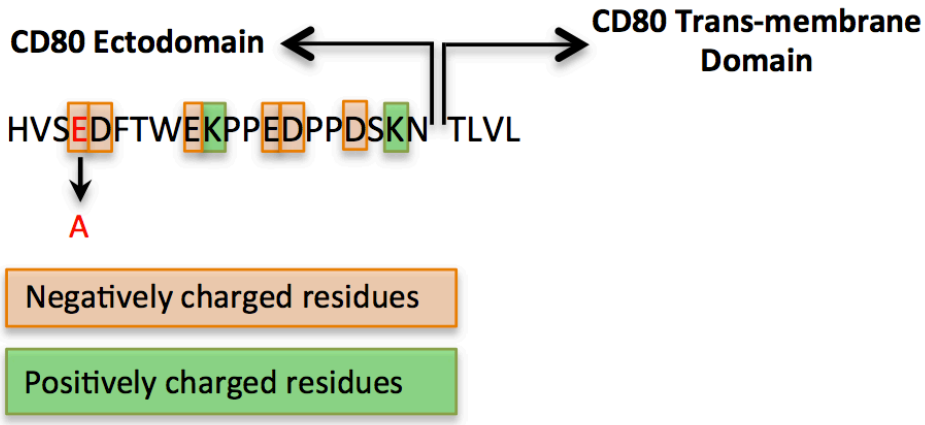

Figure 3.4 Mouse CD80 extracellular stalk region

The extracellular stalk region for mouse CD80 is depicted with a string of abundant negatively charged residues highlighted in orange and two positively charged residues highlighted in green. A mutation was introduced in the cloning process, leading to the replacement of a negatively charged glutamic acid with a neutral alanine residue.

The various CD80 or CD80CD2 or CD80CD4 constructs were then cloned into pcDNA3.1+ vector using overlapping PCR mutagenesis as described in the Materials and Methods section.

3.3.2 Expression of elongated forms of CD80

For expression, the constructs were transfected into Chinese Hamster Ovary (CHO) cells expressing mouse IE^K class II molecules which were used as antigen-presenting cells. Stable transfectants were selected using complete media supplemented with 300µg/ml Hygromycin and sorted for CD80 expression. Figure 3.5a shows the expression levels of CD80 and CD2 or CD4 by FACS analysis; note that the expression of CD80 correlates well with CD2 or CD4 expression in IE^K-CD80CD2 and IE^K-CD80CD4, as predicted in a fusion molecule. In addition to FACS analysis, the transfected cells were stained with antibodies for CD80 and CD2 or CD4 and imaged using confocal microscopy. Figure 3.5b showed that for both CHO-IE^K-CD80CD2 and CHO-IE^K-CD80CD4 cells, CD80 expression was restricted to the cell surface. Moreover, in agreement with the FACS data, CD80 (red) expression colocalised with CD2 or CD4 staining (green). In contrast, this correlation was not observed in CHO-SCDCD2, CD80 cells where CD80 was expressed as a single molecule in the same CHO cell expressing CD2 elongated SCD molecules. This experiment suggests that elongation does not disrupt the overall structural integrity of CD80, indicated by the preservation of mAb recognition for FACS and confocal analysis.

Levels of CD80 expression between WT and elongated CD80 were sorted before every experiment. Figure 3.5c represents a typical FACS plot depicting matched CD80 expressions between the various CHO cells. Hamster ICAM were shown to cross-react and costimulate mouse T cells (Gaglia et al., 2001), to ensure that this does not impact in any experiments described in this chapter, the levels of ICAM expressions between CHO cells expressing the different variants of CD80 were also assessed using mAB J5-3F9 (kindly provided by Professor Vijay Kuchroo, Harvard Medical School, USA; Figure 3.5d).

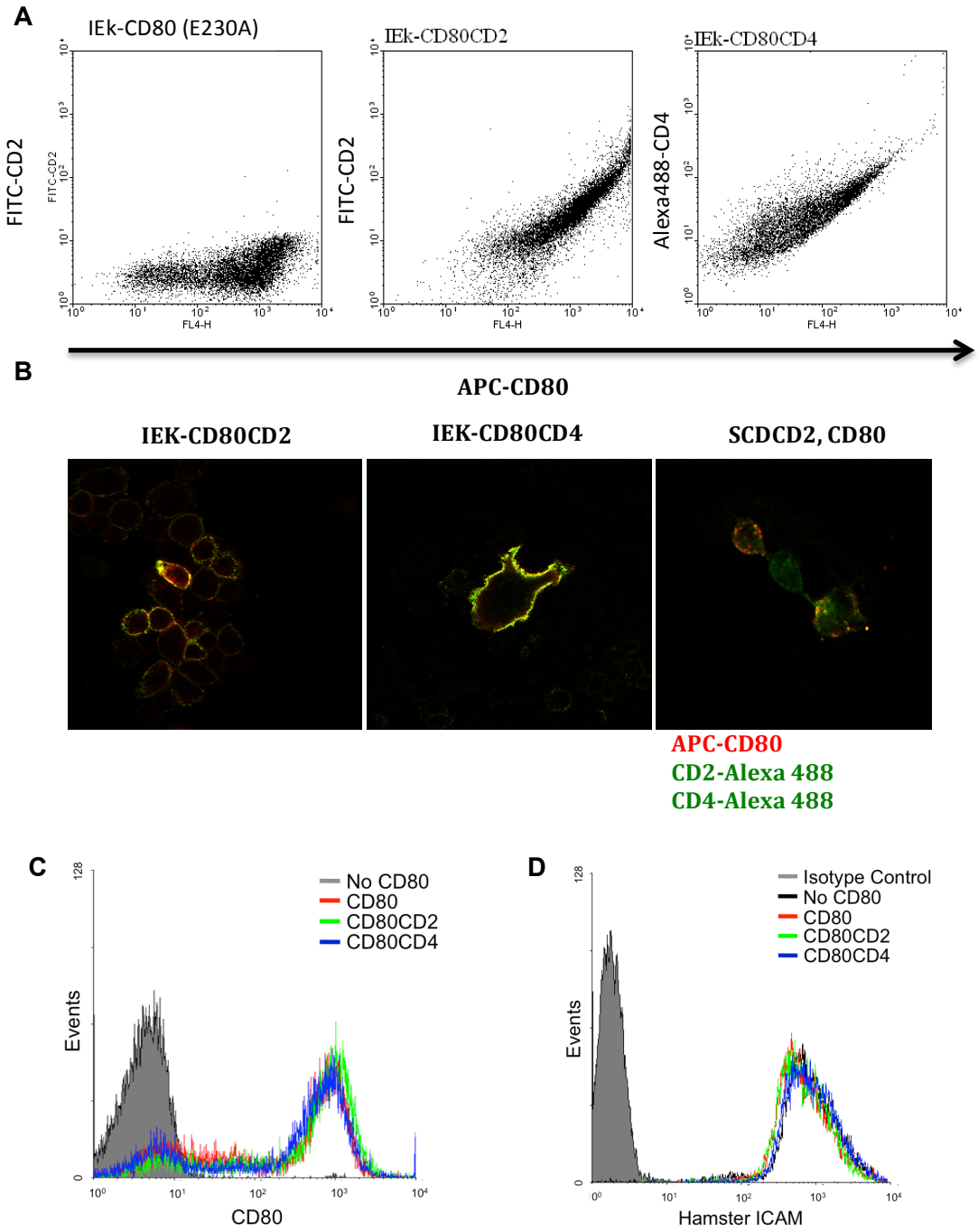

Figure 3.5 Expression of CD80 molecules in CHO-IE^K cells

CD80 constructs containing hCD2 or hCD4 inserts were transfected into CHO cells expressing IE^K MHCs. To assess the expression levels, the cells were stained with antibodies to mCD80, hCD2 or hCD4 directly conjugated with APC, FITC, and Alexa488, respectively, and analysed using (a) FACS analysis or (b) confocal microscopy. (c) CHO cells expressing the different variants of CD80 molecules were stained using CD80-APC and analysed by FACS. (d) Hamster ICAM levels between the different CHO cells were analysed using mAB J5-3F9 (Gaglia et al., 2001).

3.3.3 Binding of CD28 by elongated forms of CD80

CD80 elongation may lead to the abolishment of CD28 ligation. To investigate this possibility, CHO cells expressing varying lengths of CD80 were sorted for matching CD80 expression before assessment for CD28 bead binding (Figure 3.6). CD28 beads were prepared by incubating CD28 (dimer)-Fc molecules with fluorescently labeled, Protein A-coated beads. The mixture were then serially diluted in 12 concentrations and washed in PBS. CHO cells expressing different variants of CD80 were then incubated with the serially diluted CD28 labelled beads and binding levels analysed using FACS. All variants of CD80, including the E230A mutant bound similarly to CD28-beads. If anything CD28 beads bound better to CHO cells expressing elongated CD80. Elongation of CD80 therefore, does not lead to impaired CD28 engagement.

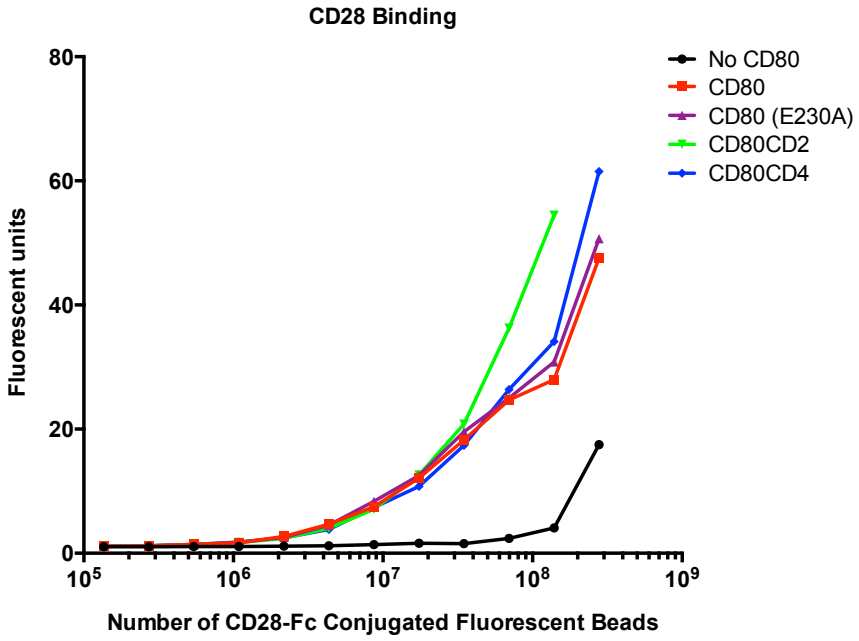

Figure 3.6 CD80 elongation does not impair CD28 binding

CD28-Fc fusion proteins were incubated with protein A conjugated fluorescent beads and serially diluted. The resulting CD28-Fc coated fluorescent beads were then washed and used to stain CHO cells expressing the indicated forms of CD80. Levels of binding were analysed by flow cytometry.

3.3.4 Elongation of CD80 reduces primary T cell costimulation

Upon activation, T cells undergo a drastic change in transcriptional profile and begin to express a number of activation markers on their cell surface. In addition to cell surface markers, T cells also begin to secrete a number of cytokines. Chief among these is IL-2, which is necessary for growth, proliferation and differentiation of naïve T cells into effector T cells. As discussed previously, CD28 mediated costimulatory signals are central to the regulation of IL-2 secretion by up-regulating IL-2 transcription through the CD28 response element and post-transcriptional mRNA stabilisation. To examine the effect of CD80 elongation on costimulation of T cells, CHO-IE^K cells expressing varying lengths of CD80 were tested for their ability to induce IL-2 secretion from T cells.

CHO-IE^K cells expressing the no or different variants of CD80 were sorted for CD80 expression and pulsed with indicated concentrations of the male antigen Dby peptide (REEALHQFRSGRKPI) for an hour. The pulsed APCs were then incubated with purified primary $CD4^+$ T cells isolated from the spleens of transgenic A1 TCR mice (Figure 3.7a). A1 TCR recognise Dby peptide in the context of IE^K, thereby providing specificity for the interaction. After 48 hours, the supernatant was harvested and analysed for IL-2 secretion by ELISA.

No IL-2 secretion was detected for T cells stimulated with negative control CHO-IE^K expressing no CD80 (Figure 3.7b). This does not come as a surprise as it is long known that TCR engagement in the absence of CD28 costimulation does not activate naïve T cell populations. Introduction of CD80 provides costimulation that led to IL-2 secretion plateauing between 1-2 μM of Dby peptide. Importantly, the IL-2 secretion

profile for WT CD80 and that harbouring the E230A mutation was largely similar, indicating that the mutation has minimal effect on the stimulatory capacity of CD80 E230A. As such, the mutant CD80 is referred from hereon as CD80-WT.

Elongation of CD80 on the other hand, led to a reduction of IL-2 secretion at all concentrations of Dby peptide (Figure 3.7b). Secretion of IL-2 by primary $CD4^+$ T cells correlated inversely with the dimension of CD80, with CHO-IE^K-CD80CD4 being a poorer co-stimulating APC than CHO-IE^K-CD80CD2. This result indicates that elongated forms of CD80 are less effective co-stimulatory ligands for T cell activation.

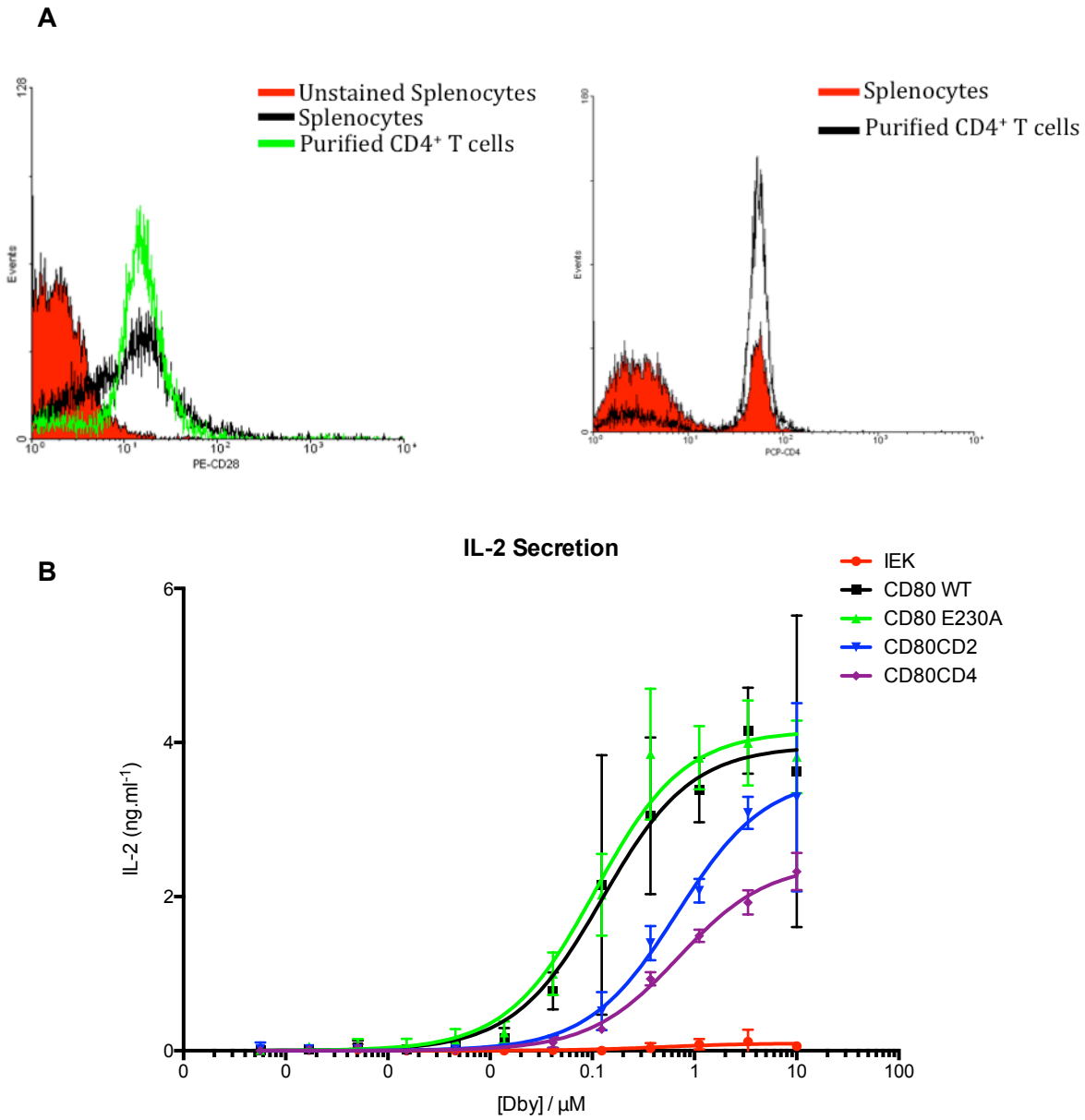

Figure 3.7 CD80 elongation reduces costimulation of primary CD4$^+$ T cells

(a) Spleens from A1 TCR transgenic mice specific to male antigen Dby were harvested and purified for CD4$^+$ T cells. The purified cells were stained for CD28 (left) and CD4 (right) expression. (b) CHO-IE^K cells expressing CD80-WT or elongated CD80s were pulsed with titrating concentrations of Dby peptides before incubation with the purified CD4$^+$ A1 TCR transgenic T cells for 48 hours. The supernatants were then harvested and analysed for IL-2 using ELISA. This is a representative plot from 3 separate experiments and the error bar represents SEM from 3 replicate data points.

3.3.5 Elongation of CD80 impairs CD28 signalling

Elongation of CD80 may reduce efficiency of CD28 co-stimulation by two possible mechanisms. Firstly, they may impair CD28 signal transduction as a result of increased inter-membrane distance, thereby allowing passive diffusion of large inhibitory phosphatases within CD28 signalling zone as postulated by the K-S model (Davis and van der Merwe, 2006). Secondly, elongation of CD80 may affect costimulation because of the resulting mismatch between the CD28-CD80 and TCR receptor-pMHC dimensions as depicted in the cartoon below (Figure. 3.8). Previous studies have suggested that such a mismatch between receptor/ ligand pairs could either disrupt TCR-pMHC engagement (Wild et al., 1999) and/or impair signal integration between TCR and CD28 (Kohler et al., 2010).

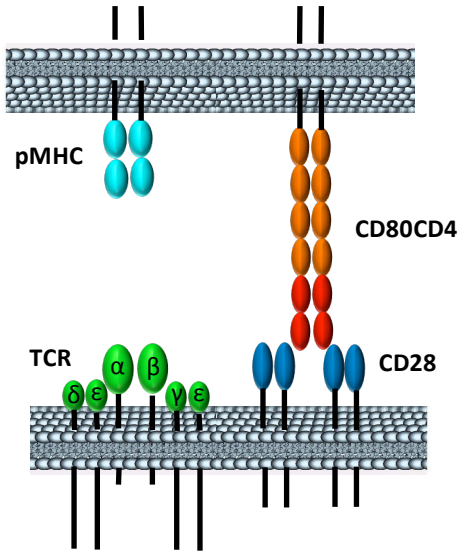

Figure 3.8 CD80 elongation may lead to a mismatch between the dimensions of the TCR-pMHC and CD28-CD80 complexes

Cartoon depicting how elongation of CD80 may disrupt antigen recognition of T cells. A mismatch between the dimensions of the TCR-pMHC and CD28-CD80 complexes may disrupt TCR binding to pMHC binding by positioning the membranes too far apart (left). Alternatively it may force engaged segregation of engaged TCR and CD28 at the T cell surface, leading to impaired TCR-CD28 signal integration [right see Dushek et at Figure 8b for suggested panel (Dushek et al., 2012)].

To distinguish between the two mechanisms, a trans co-stimulation assay was set up where T cells receive its TCR and CD28 signals from two separate APCs (i.e. *in trans*). Presentation of TCR and CD28 ligands into two APCs eliminates any complications that may arise from mismatches in the sizes of the TCR-pMHC and CD28-CD80 complexes. This allows the investigation of any potential CD28 signal transduction impairment due to increased inter-membrane distance (Figure 3.9).

CHO-IE^{K} cells were pulsed with 5µM (saturating levels) of Dby peptide for an hour. The pulsed APCs were then incubated with primary CD4^{+} T cells at a 1:1 ratio with the indicated-titrated numbers of CHO-CD80, CHO-CD80CD2 or CHO-CD80CD4 cells for 48 hours before their supernatants were harvested for IL-2 ELISA.

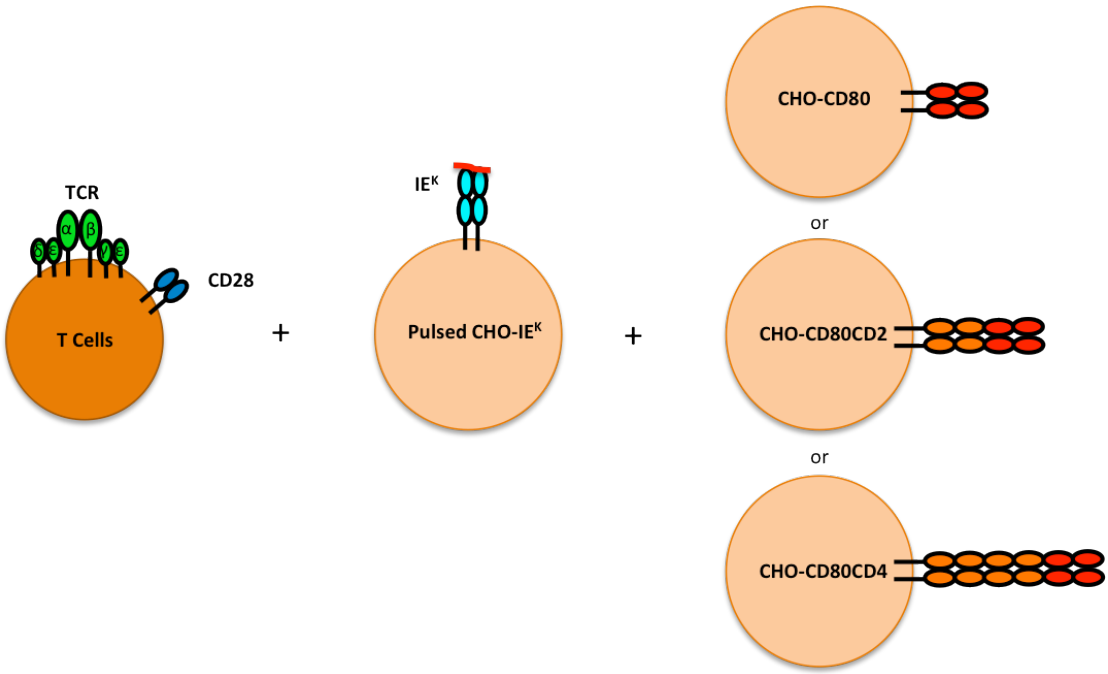

Figure 3.9 Trans-costimulation Assay

In the trans-costimulation assay, T cells were incubated with CHO-IE^{K} cells without CD80, pulsed with a fixed concentration of cognate Dby antigen. Co-stimulatory signals were provided in trans in the form of separate CHO cells expressing WT or elongated version of CD80 molecules. Strength of co-stimulatory signals were controlled by titrating the number of CHO-CD80 expressing cells. T cells were incubated for 48 hours before the supernatant were isolated for IL-2 analysis using FACS.

As before, in the absence of CD80 ligation, CHO-IE^K cells alone are poor stimulators of T cells. Provision of CD80 in trans markedly improves IL-2 secretion while CHO cells expressing CD80CD2 or CD80CD4 in trans were poor stimulators of IL-2 secretion (Figure 3.10). Thus, this suggests that elongated CD80 molecules less able to induce CD28 signal, which is consistent with predictions from the K-S model. Interestingly, it was noted that costimulation peaked at a starting ratio of CHO-CD80/T cells of just below 1. This is most probably an overcrowding artifact of the experimental condition at high cell density. Such an effect would be particularly obvious after an extended amount of time in culture (48 hours) during which time both cells would divide.

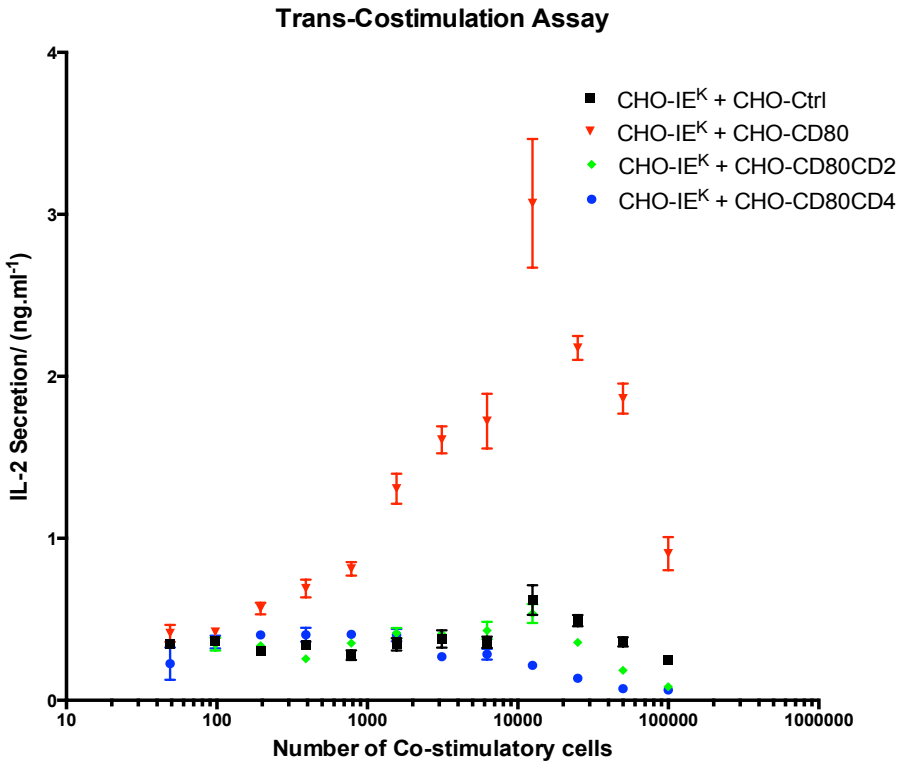

Figure 3.10 Elongation of CD80 abolishes CD28 signalling

5x10^4 primary CD4+ T cells were incubated 1:1 with pulsed (5μM Dby peptide) CHO-IE^K cells (with no CD80) or the indicated number of CHO-CD80 expressing cells in trans for 48 hours. The supernatant were then harvested for IL-2 ELISA. This is a representative plot from 3 separate experiments and the error bar represents SEM from 3 replicate data points.

3.3.6 Elongation of CD80 reduces CD45 segregation

Several groups have demonstrated the segregation of large membrane phosphatase like CD45 and CD148 from the site of TCR contacts areas during TCR triggering (Bunnell et al., 2002, Varma et al., 2006, James and Vale, 2012, Leupin et al., 2000, Johnson et al., 2000, He et al., 2002). Indeed, artificial elongation of several receptor/ ligand systems have led to the abrogation of receptor signal transduction, lending support to the importance of receptor/ ligand dimensions in receptor triggering (Choudhuri et al., 2005, Kohler et al., 2010, Brzostek et al., 2010). Elongation would realistically prevent large membrane phosphatases from segregating from the close inter-membrane signalling zone, leading to signal abrogation.

Imaging CD80, pMHC and CD45 at T Cell – APC contact interface

To determine if the reduction of segregation can explain the observed phenomenon, CD80 and CD45 molecules were imaged at the T cell – APC contact interface and analysed for any potential co-localisation using confocal microscopy. To do this, GFP was fused to the C-terminal end of the CD80 to create a CD80-GFP fusion protein for efficient protein tracking. Likewise, GFP was fused to the end of CD80CD2 and CD80CD4 to generate CD80CD2-GFP and CD80CD4-GFP fusion proteins. The various CD80-GFP constructs were then transfected into stable CHO cell lines expressing MHC class I Single Chain Dimers (SCD)-dsRed fusion molecules.

SCD are mouse MHC class I $H2K^b$ heavy chain fused to β2 microglobulin by a flexible glycine/ serine linker sequence (see Figure 3.20). Stably transfected CHO cells expressing SCD (CHO-SCD) presumably present endogenous peptides and exogenous

provision of cognate peptides such as the ovalbumin peptide 257-264 SIINFEKL should displace the endogenous peptide on the SCD. To demonstrate this, CHO-SCD cells were exogenously pulsed with the indicated concentration of SIINFEKL peptide. The cells were then stained with monoclonal antibody 25-D1.16 that reacts with SIINFEKL bound to $H2K^b$, but not unbound $H2K^b$ or $H2K^b$ bound to an irrelevant peptide. Figure 3.11 shows that increasing concentration of exogenous SIINFEKL improves its loading onto $H2K^b$. Thus, CHO-SCD expressing cells can be pulsed with SIINFEKL peptide can be utilised as APCs for OT1 TCR transgenic T cells recognising SIINFEKL-$H2K^b$ complex.

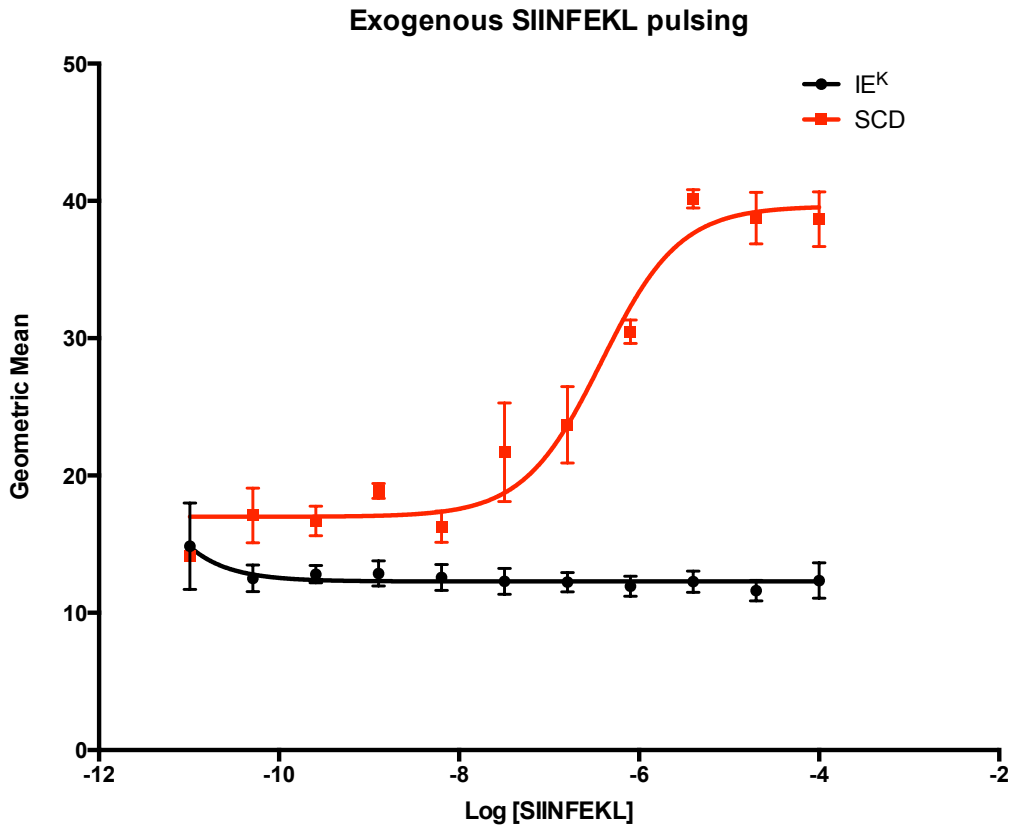

Figure 3.11 Exogenous SIINFEKL peptide pulsing of SCD molecules

CHO cells expressing $H2K^b$-β2 Microglobulin Single Chain Dimer (SCD) molecules were pulsed with the indicated concentration of SIINFEKL peptide. The degree of peptide loading was determined by FACS using monoclonal antibody 25-D1.16. As negative control, CHO cells expressing IE^K MHC class II molecules were pulsed with the same concentrations of SIINFEKL peptide. Error bars represent SEM from 3 replicate data points. This experiment was performed once.

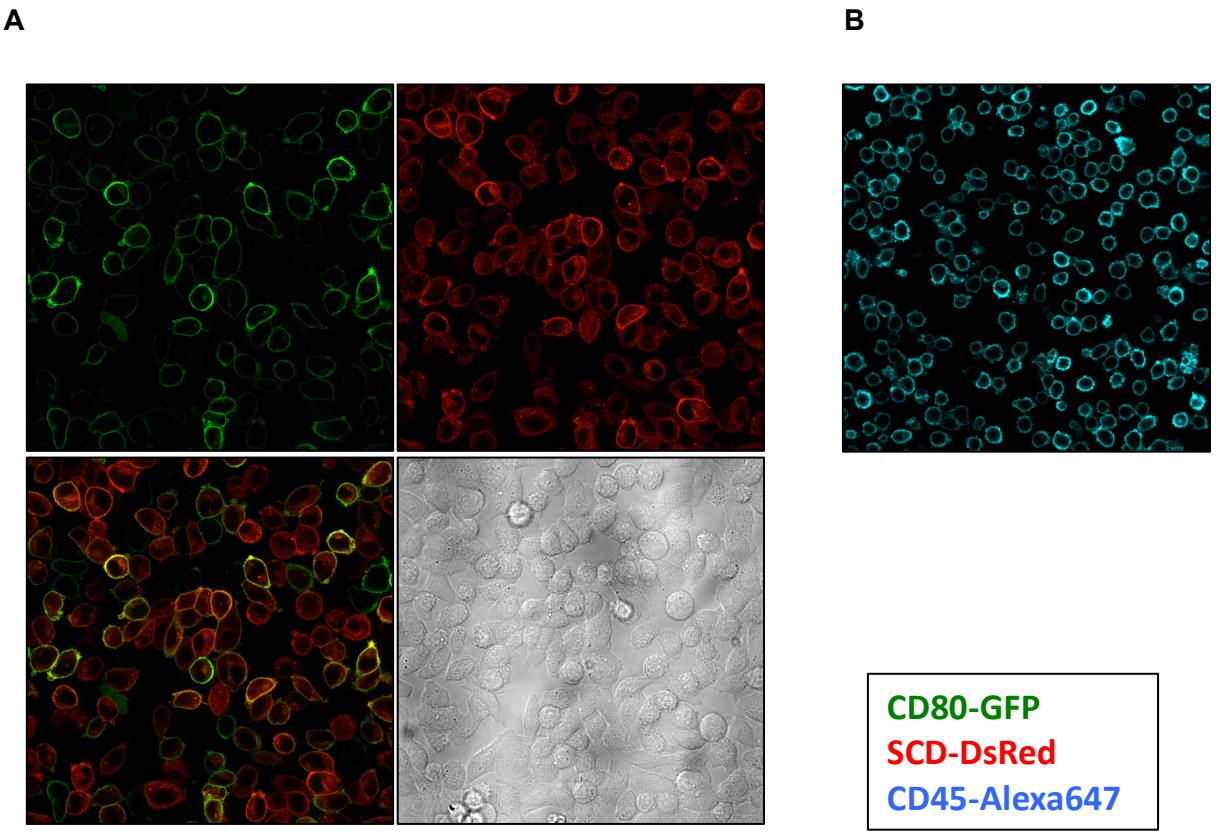

Figure 3.12 Imaging CD80-GFP, SCD-DsRed and CD45 molecules

(a) CHO cells expressing CD80-GFP and SCD-DsRed fusion molecules were fixed using 4% methanol-free Paraformaldehyde and imaged using the Olympus Fluoview FV1000 confocal microscope. (Top left: CD80-GFP expression; Top right: SCD-DsRed expression; Bottom left: CD80-GFP and SCD-DsRed overlay; Bottom right: DIC) (b) Primary mouse $CD4^+$ T cells were purified, fixed using 4% methanol free paraformaldehyde, permeailised using 0.1% Saponin, and stained using alexa647 conjugated anti-CD45 antibodies (Clone HI30).

Just like CD80-GFP, DsRed DNA sequence was added to the 3' end of SCD cDNA just before the end codon using overlapping PCR mutagenesis to create a construct expressing the SCD-DsRed fusion molecule. This enables the imaging of MHC in relation to the CD80-GFP molecules as depicted in figure 3.12a. CD80-GFP expression was largely restricted to the cell membrane while SCD expression was detected both intra-cellularly and on cell membrane.

To image T cells, we turn to $CD8^+$ T cells from OT1-TCR transgenic mice. As mentioned previously, these TCRs recognize OVA SIINFEKL peptide in the context of mouse $H2K^b$ MHC. The T cells were permeabilised and stained with monoclonal anti-CD45 antibodies (HI30) conjugated to Alexa-647 dye. As with CD80-GFP, CD45 expression was largely restricted on the cell surface.

3D image reconstruction and analysis

CD80-GFP, CD80CD2-GFP or CD80CD4-GFP expressing CHO-SCD-dsRed cells were incubated with purified transgenic mouse $CD8^+$ Primary OT1 TCR T cells in either pulsed or unpulsed condition for 10 minutes. The cells were gently spun down and pipetted onto Poly-L-Lysine coated cover slips to encourage conjugate formation. They were then fixed, permeabilised and stained for CD45 expression before analysis by confocal microscopy.

To image the relative positions of CD80-GFP and Alexa-647 stained CD45 in the CHO cell – T cell conjugate interface, it is necessary to first define what is meant by a conjugate. In this case, an apparent conjugate is defined as a CHO cell and a T cell in close proximity (i.e. in direct contact with each other). A striking observation from figure 3.13 shows that under unpulsed conditions, there is a clear lack of conjugate formation between the CHO cells and the T cells, in stark contrast to the pulsed samples. This can perhaps be attributed to the lack of TCR specific signal transduction to promote secondary integrin engagement that will improve conjugate formation.

Three-Dimensional (3D) reconstruction of the CHO cell - T cell conjugate was generated using the Imaris software. Only conjugates whose contact areas were

oriented properly to be contained in a rectangular volume for an en face projection were taken into consideration. Figure 3.14 demonstrates how conjugate pairs in the correct X, Y or Z orientation can be cropped enface and rotated to reveal the molecules present in the inter-membrane surface.

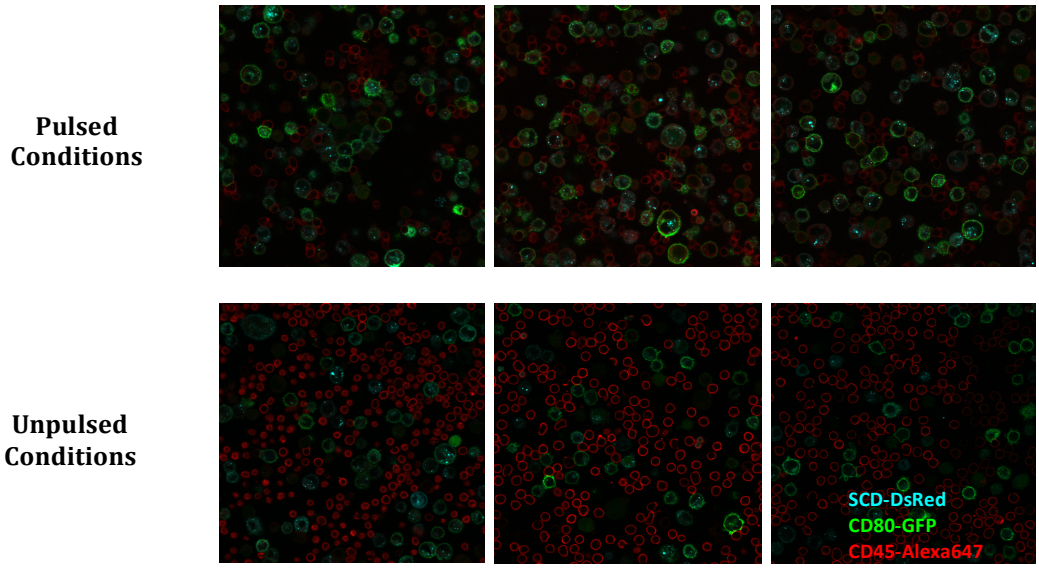

Figure 3.13 Conjugate formations vary under pulsed vs unpulsed conditions

CHO cells expressing CD80-GFP and SCD-DsRed were either pulsed with 5μM SIINFEKL peptide (top) or left untreated (bottom). They were then mixed with at a 1:1 ratio with purified $CD8^+$ T cells from transgenic OT1 TCR mice. The cells were gently spun down at 400rpm for 2 minutes to encourage conjugate formation before incubation at 37°C for 10 minutes. The cells were then allowed to rest on poly-L-lysine coated cover slips before fixation, permeabilisation and staining with anti-CD45 antibodies. Images were taken using the Olympus Fluoview FV1000 confocal microscope.

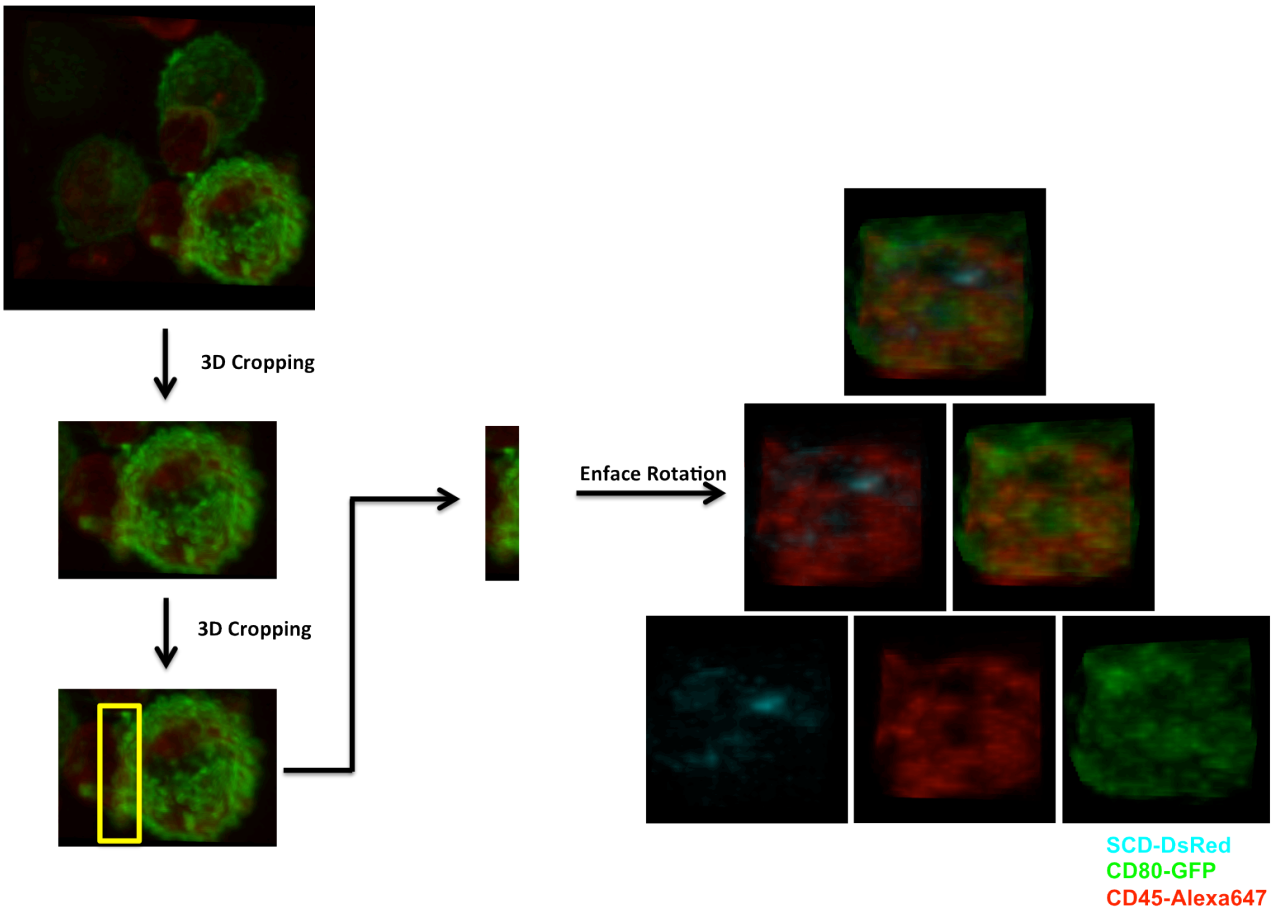

Figure 3.14 Three-dimensional analysis of CHO cell – T cell contact interface

This flow chart illustrates the steps taken to analyse the distribution of CD80-GFP (green), SCD-DsRed (cyan) as well as CD45 (red) molecules in the CHO cell – T cell contact interface. Three-dimensional re-construction of the confocal images was generated using Imaris software. Only conjugates that were oriented properly to be contained within a rectangular volume for en face projection were analysed. These conjugates were cropped to reveal only the close contact interface between the CHO cell and T cell. The interface was then rotated enface to reveal the distribution of the various proteins.

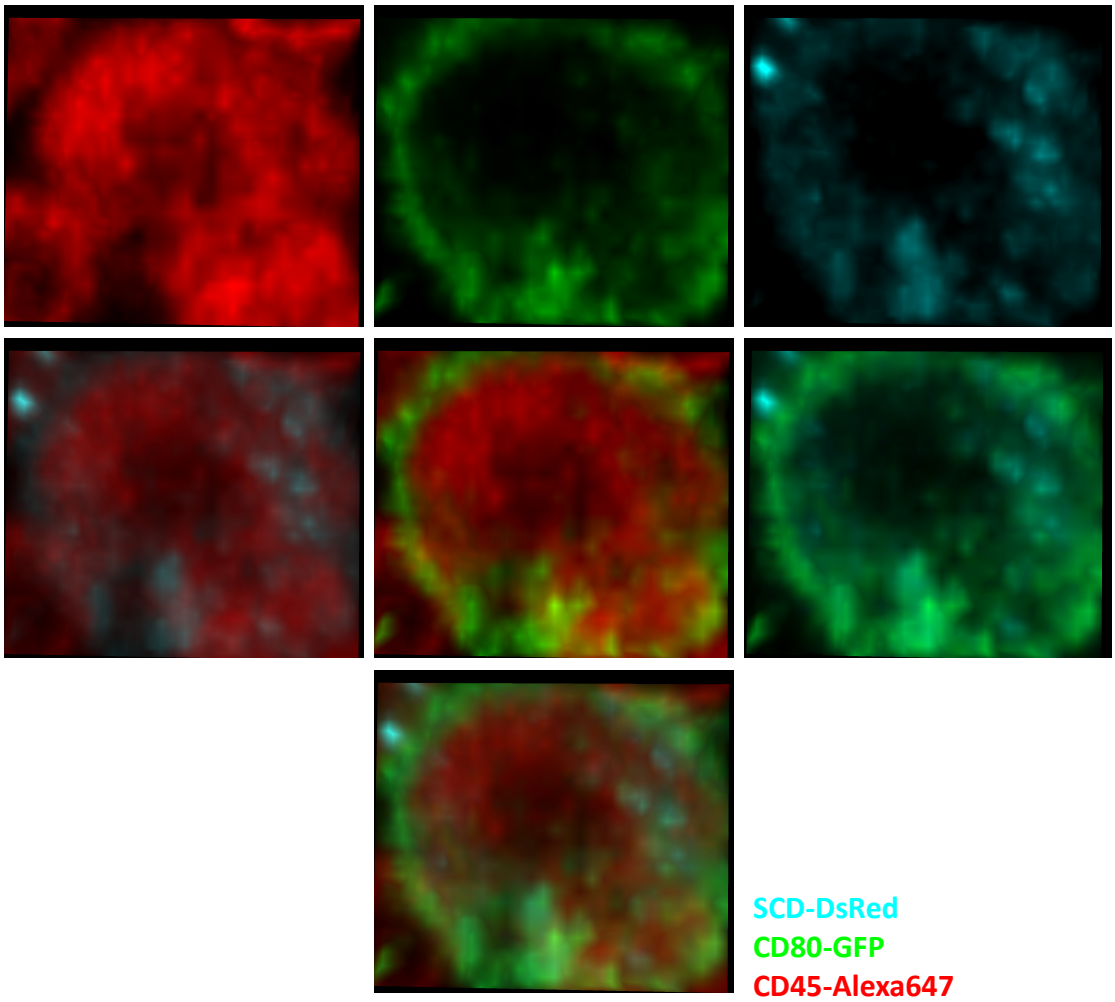

Figure 3.15 Apparent segregation of CD45 from CD80-GFP and SCD-DsRed

Representative image of a pulsed CHO cell – T cell interface. Peptide pulsed CHO cells expressing CD80-GFP and SCD-DsRed were incubated with primary transgenic $CD8^+$ OT1 T cells for 10 minutes. The resulting cell mixture were stained for CD45 as described in Figure 3.13 and analysed as described in Figure 3.14. The top row represents individual CD45 (red), CD80-GFP (green) or SCD-dsRed (cyan) channel. The colours were overlaid on top of each other; two at a time in the middle row and the bottom row represents an overlay of all three colours of the same image.

In addition to figure 3.14, figure 3.15 represents another the enface figure of the interface between a pulsed CHO cell and T cell. Manual inspection of the images revealed that there is very little mixing of CD45 (red) with CD80 (green) or SCD (cyan). Suggesting that there is an apparent segregation of both SCD and CD80 from CD45, as predicted by the K-S model. There are, however, many problems associated with manual observation of co-localisations. Manual observations are subjective and they are dependent on the quality of presentation and display of the information. Co-localisation may also not be apparent should the signal strength between of one dye dominate over the other.

Pearson's correlation coefficient (r) was used to determine the amount of co-localisation or segregation between CD80 and CD45 in the CHO cell – T cell interface. Pearson's correlation coefficient calculates the degree of overlap between two images by subtracting the average pixel intensity values from the original intensity values. This produces the correlation coefficient (r) ranging from -1 to 1, with a value of -1 representing complete segregation and 1 representing complete co-localisation.

Indeed, quantification of pulsed CHO-SCD cells expressing CD80 WT revealed a relative segregation between CD80 and CD45 as indicated by the negative Pearson's correlation coefficient (Figure 3.16a). Pulsed CHO cells expressing CD2 or CD4 elongated CD80 on the other hand demonstrated a reduced segregation of CD80 from CD45. The observed phenomenon however, could be attributed to secondary effects downstream of TCR signalling in the pulsed CHO cells. To investigate if this is the case, unpulsed CHO cells were incubated with the T cells and cell – cell interface

between apparent conjugates were analysed. Interestingly, CD80CD4 molecules were less segregated from CD45 molecules (Figure 3.16b), indicating that at resting states, CD80CD4 was more likely to be found in the vicinity of CD45 molecules. Difference in co-localisation between CD80 and CD80CD2 molecules on the other hand, did not appear to be significant. Taken together, these results suggest that when elongated, CD80 appears to segregate to a lesser extent from CD45 molecules. The mechanism mediating this process can be passive (unpulsed CHOs) or active, downstream of the TCR signalling. Reduced segregation or increased relative co-localisation of elongated CD80 with CD45 would provide a plausible explanation to the inability of these molecules to transduce CD28 mediated co-stimulation.

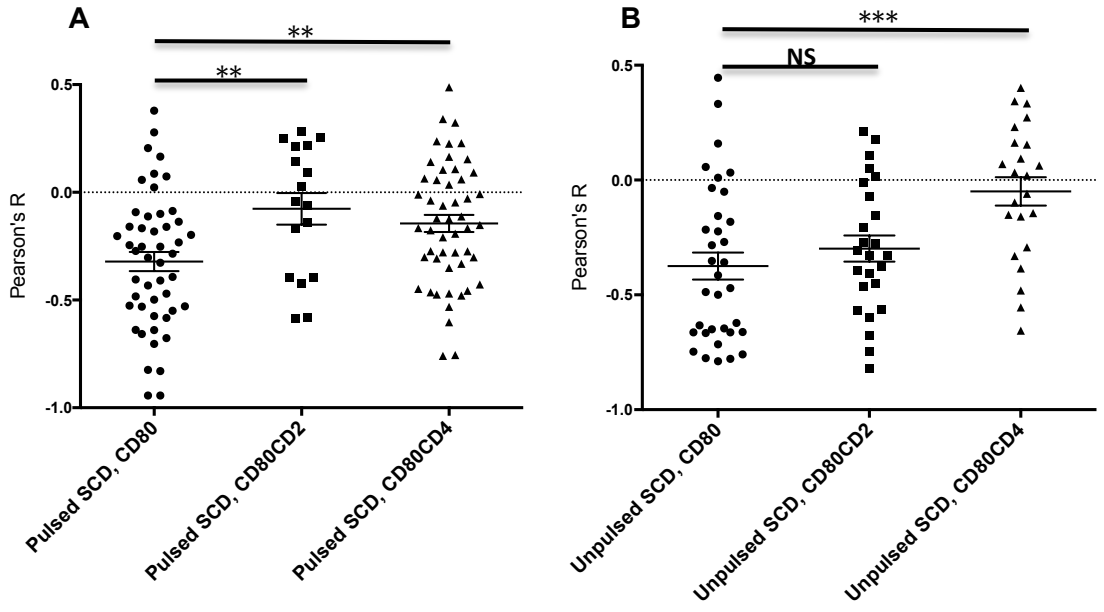

Figure 3.16 Reduced CD45 segregation from elongated CD80

(a) Peptide pulsed or (b) unpulsed CHO-SCD-DsRed cells expressing varying lengths of CD80-GFP were incubated with primary T cells and stained for CD45 as previously described in figures 3.12 and 3.13. The degree of co-localisation between CD80 and CD45 is represented by Pearson's correlation coefficient (R). Horizontal lines with error bars indicate mean with SEM. Statistical significance were determined using one way ANOVA (**p<0.01; ***p<0.001). Presented analysis represents one of two imaging studies.

3.3.7 Functional analysis of CD28 cytoplasmic tyrosine mutant

To further understand the role of CD45 regulation in CD28-mediated co-stimulation, we turn to the use of CD28 cytoplasmic mutants. CD28 contains 4 tyrosine residues in its cytoplasmic tail. The phosphorylatable Y170 residue within the YMNM motif is implicated in CD28 mediated costimulation because of its ability to recruit PI3K and Grb2. If large receptor protein tyrosine phosphatases (RPTPs) such as CD45 were indeed involved in the regulation of tyrosine phosphorylation state in a ligand dimension dependent manner, CD28-Y170F mutants should be refractory to the effects of CD80 elongation.

To test the hypothesis, we stimulate mouse primary $CD4^+$ T cells with or without the CD28 Y170F mutation using plate bound anti-CD3 antibodies (Clone 2C11). CD28 co-stimulation was provided using CD80 - expressing CHO cells. This allows CD28 co-stimulation to be provided in trans by CD80-WT or elongated CD80 molecules. As negative control, CHO cells expressing no CD80 molecules were used. Titrating the number of co-stimulatory CD80 expressing CHO cells controlled the levels of co-stimulation received by the T cells. CHO cells without CD80 (IE^K) were used as negative controls (Figure 3.17).

In the absence of CD80, wild-type T cells secreted a background level of IL-2 induced by the anti-CD3 antibodies only. Provision of CD80 in trans dramatically improved secretion, while elongation of CD80 abolished IL-2 secretion to background (no CD80 equivalent) levels (Figure 3.18). The results are consistent with other data presented in this study (Figures 3.7, 3.10, 3.24).

CD28-Y170F T cells when stimulated with CD80-WT in trans, secreted less IL-2 in comparison to wild-type T cells. However, the CD28 mutants were less affected by differences in CD80 dimensions (Figure 3.18b). To compile and quantify data from multiple experiments, we calculate the integrated IL-2 responses from T cells with WT CD28 or CD28-Y170F, when stimulated by WT or elongated CD80 molecules. To facilitate comparison, the integrated IL-2 responses were expressed as the ratio of the response with elongated CD80 versus normal length CD80. While elongated CD80 molecules stimulated less IL-2 response than CD80-WT by both CD28-WT and CD28-Y170F T cells (ratio < 1), the difference is significantly smaller with CD28-Y170F T cells (Figure 3.18c).

The fact that CD80 elongation still affected CD28-Y170F T cells suggests that additional tyrosine-containing motifs apart from YMNM are also sensitive to changes in CD80 dimensions.

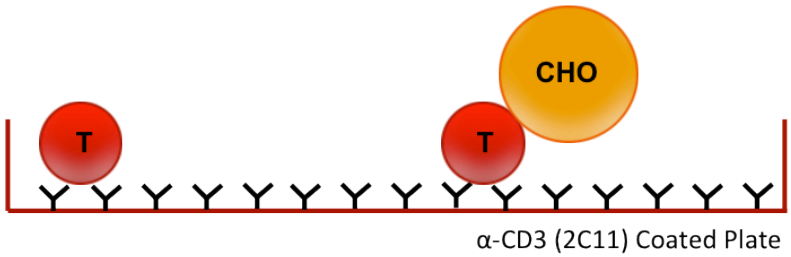

Figure 3.17 Functional analysis of CD28 tyrosine mutant

Cartoon depicting the experimental set up involving the CD28 Y170F mutant. T cells harbouring CD28 Y170F mutation in its YMNM motifs were stimulated using plate bound anti-CD3 antibodies. To provide costimulation, CHO cells expressing different variants of CD80 were added in trans. Number of CHO cells were titrated to alter the amount of CD28 co-stimulatory signals delivered. The cells were incubated for 48 hours before supernatants were harvested for IL-2 ELISA.

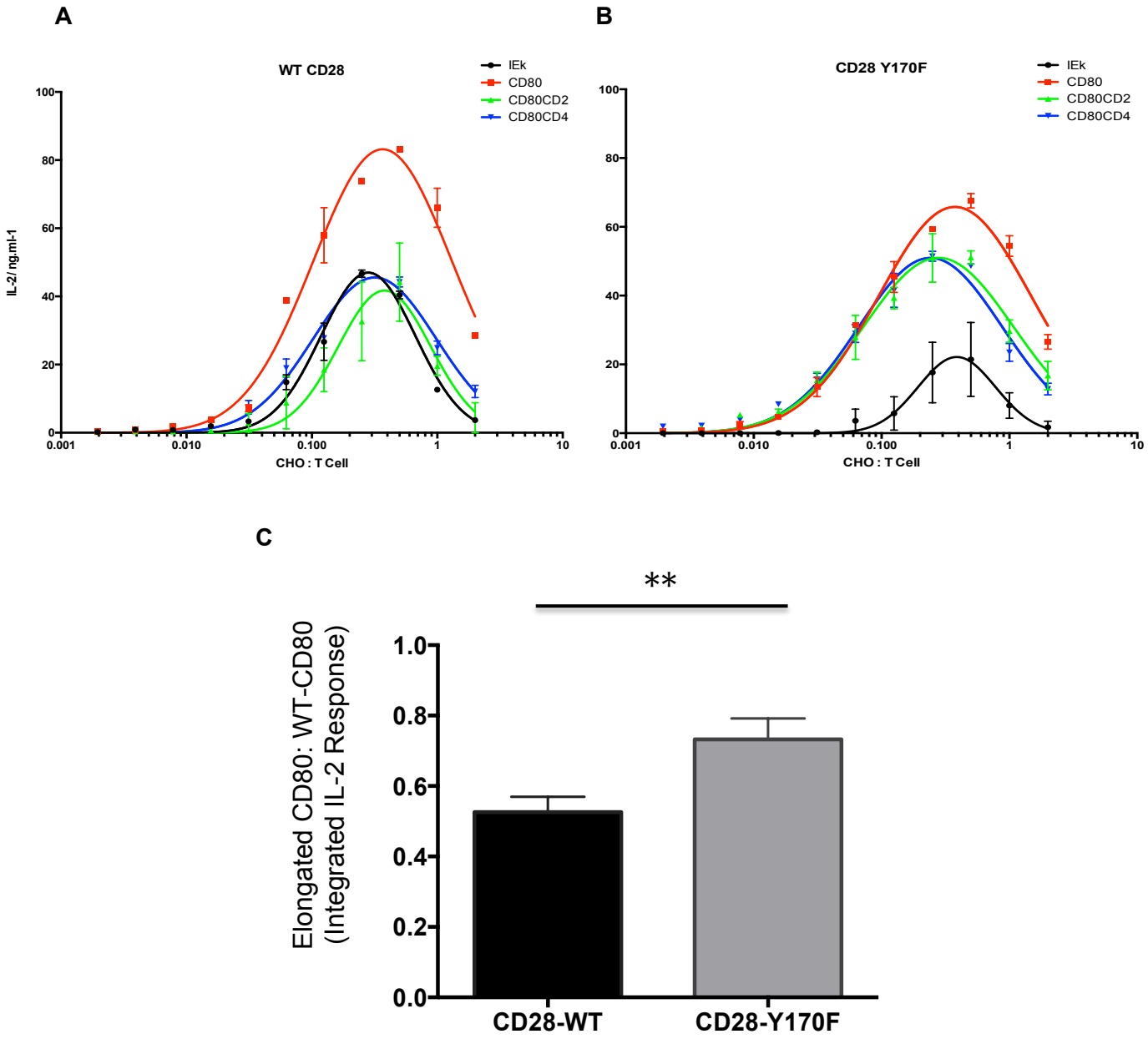

Figure 3.18 CD28-Y170F mutants less affected by changes in CD80 dimensions

(a) Wild type CD4 T cells or (b) CD4 T cells harbouring the CD28 Y170F mutant were stimulated using plate bound anti-CD3 antibodies and incubated with CHO cells expressing no CD80 (IE^K), wild type CD80, CD80CD2 or CD80CD4. This is a representative result from at least 3 experiments. Error bars represent the SEM of three replicates. (c) The integrated IL-2 response was calculated by measuring the area under curves such as those depicted in (a) and (b). The integrated IL-2 response for elongated CD80 molecules were then expressed as a ratio of the response to corresponding normal length (WT) CD80 molecules within the same experiment. Error bars represent the SEM from 5 repeat experiments. The data were analysed using paired T test; $p<0.01$ (**).

3.3.8 Requirement of match receptor/ ligand dimensions in CD28 co-stimulation

As mentioned previously, elongation of CD80 may reduce efficiency of CD28 co-stimulation by two possible mechanisms:

(i) Less effective segregration of engaged CD28 from CD45, leading to CD28 dephosphorylation and signal attenuation.

(ii) Mismatch between the dimensions of the CD28-CD80 and TCR-pMHC complexes which could disrupt ligand engagement and/or signal integration between TCR and CD28.

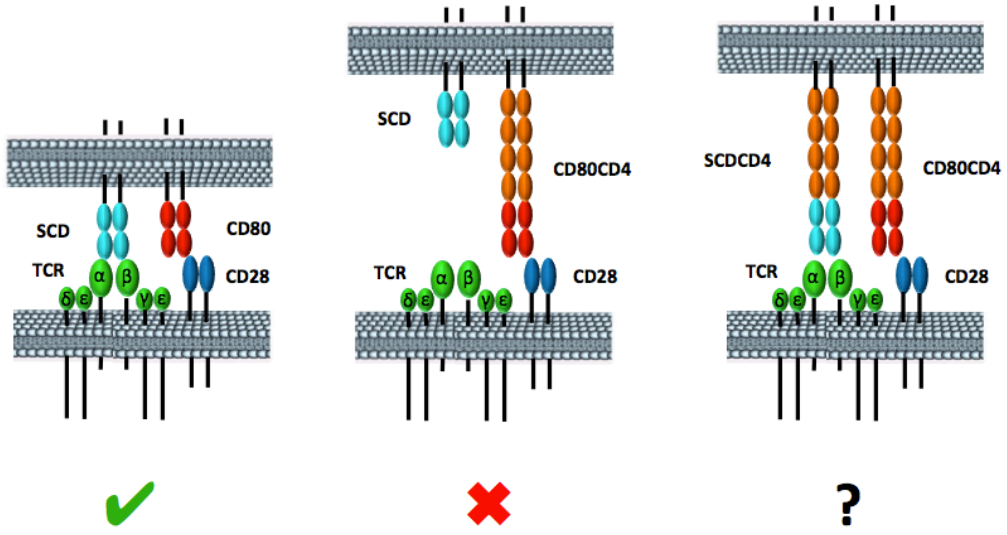

Figure 3.19 CD80 elongation may reduce efficiency of CD28 costimulation

This schematic cartoon demonstrates how CD80 elongation may reduce efficiency of CD28 costimulation by disrupting TCR/pMHC engagement and/or preventing potential TCR and CD28 signal integration (see Figure 3.8). The left panel shows an ideal scenario where matched ligand/ receptor dimensions can lead to efficient costimulatory signals. The middle panel illustrates how the mismatch in dimension following CD80 elongation could disrupt costimulation. The cartoon on the right depicts how elongation of the MHC (SCDCD4) to match the dimension of CD80CD4 may restore signalling capacity.

To investigate the importance of matched TCR and CD28 receptor/ligand dimension in T cell activation, the assay was switched to an MHC class I system using CHO-SCD cells as APCs. As described earlier, SCD comprises of a mouse $H2K^b$ heavy chain fused to β2 microglobulin by a flexible glycine/ serine linker sequence. A major advantage of using MHC class I system and in particular, SCDs is the ability to elongate the MHC molecule. To test if mismatched receptor/ ligand dimensions contributes to the reduction in costimulation observed when CD80 is elongated (Figure 3.7), we examined what happened when MHC molecules were extended in the same manner to match the elongation in CD80 molecules.

Elongating SCD for Mammalian Cell Expression

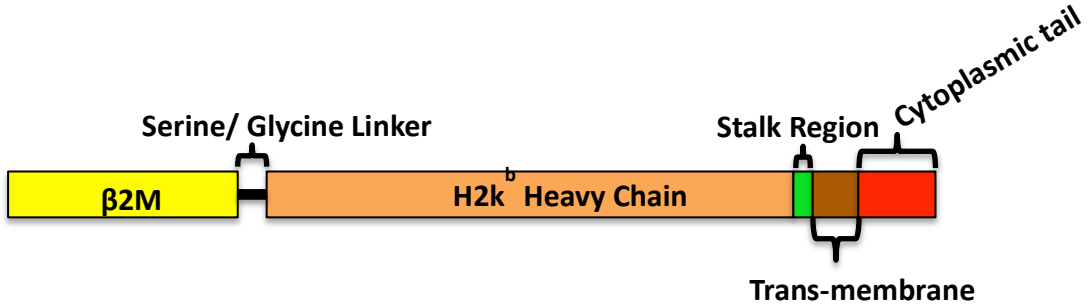

Figure 3.20 Schematic diagram of SCD

Single chain dimer (SCD) consists of $H2k^b$ heavy chain fused to β2 microglobulin by a flexible serine/ glycine linker. The various domains are depicted in scale. The 10 amino acid stalk region represents a suitable site for elongation.

Not dissimilar to CD80, SCD contains a short 10 amino acid stalk region that serves as a suitable site for insertion of spacers for elongation (Figure 3.20). The spacer acts as a natural separator between the $H2k^b$ heavy chain α3 domain and the trans-membrane domain of the MHC. Insertion of human CD2 or CD4 extracellular domain will elongate SCD to match the dimensions of CD80CD2 or CD80CD4 respectively.

Constructs containing elongated SCD were transfected into CHO cells and their expression levels confirmed by FACS analysis. Figure 3.21 shows the expression levels of SCD on transfected CHO cells. As negative control, CHO cells expressing IE^K molecules were stained with the same anti-$H2k^b$ antibodies (clone AF6-88.5; BD Biosciences Cat. No. 553570). Staining for $H2k^b$ and CD2 or CD4 correlated perfectly for SCDCD2 and SCDCD4, as they should do in a fusion molecule. Preservation of the AF6-88.5 antibody epitope on SCDCD2 and SCDCD4 also suggests that elongation of SCD molecules do not disrupt the overall structure of the $H2k^b$ molecules as it was known that the AF6-88.5-defined epitope depended on sequences in the α1 and α3 heavy chain regions (Kuhns and Pease, 1998).

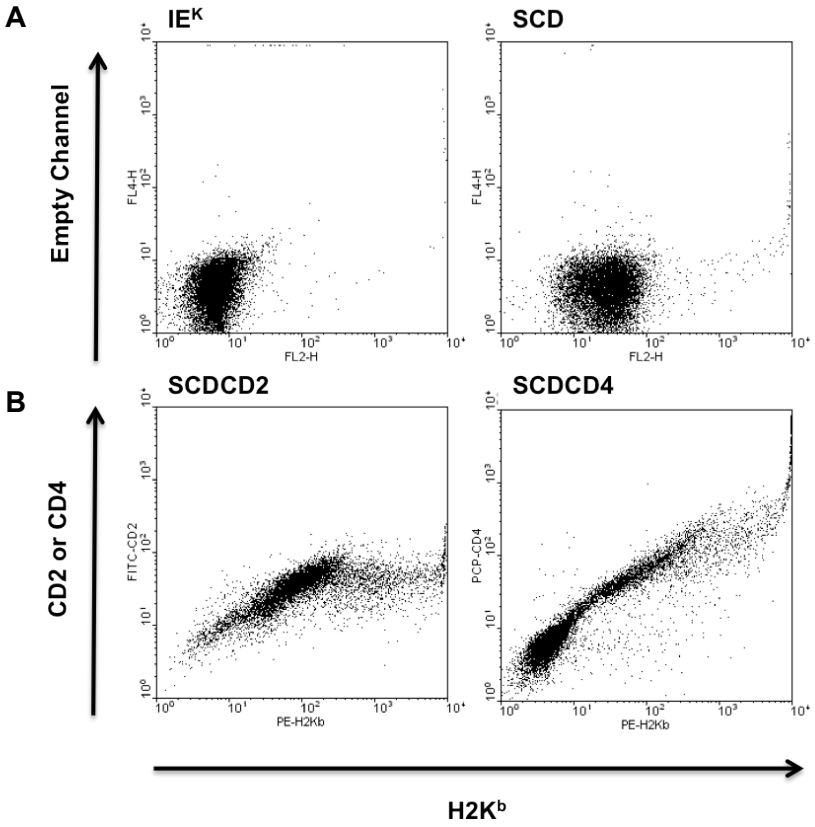

Figure 3.21 Expression of elongated SCD in CHO cells

SCD and elongated SCD (SCDCD2 or SCDCD4) were stably transfected into CHO cells. The cells were stained with (a) $H2K^b$ antibodies alone or (b) $H2K^b$ antibodies with CD2 or CD4 antibodies.

Elongation of SCD does not impair SIINFEKL peptide loading

While SCD elongation may not affect the overall conformation of the molecule, it may well impair the degree of peptide loading onto the MHC molecules. To probe this, CHO cells expressing SCD, SCDCD2 or SCDCD4 were pulsed with titrating concentrations of the cognate SIINFEKL peptide and the degree of peptide loading measured on the different SCD molecules using mAb 25-D1.16 specific to $H2K^b$-SIINFEKL complex by FACS analysis.

Figure 3.22 represents the presence of $H2k^b$-SIINFEKL level for SCD, SCDCD2 and SCDCD4 molecules on CHO cells across the working/ pulsing concentrations of the SIINFEKL peptide between 10^{-7} to $\sim 10^{-12}$ M. The graph indicates that for most concentrations of pulsed SIINFEKL, the levels of peptide loading appear to be similar between SCD, SCDCD2 and SCDCD4. Off course, the relative insensitivity of the assay may also occlude any observable differences.

Reduced OT1 $CD8^+$ T cell responses to elongated SCD

We next determined if elongation of SCD would impair T cell activation by incubating pulsed CHO-SCD or CHO-SCDCD4 with mouse $CD8^+$ primary OT1 T cells for 48 hours before collecting the supernatant for IL-2 ELISA. As negative controls, CHO cells expressing non-cognate MHC ($I\text{-}E^K$) were used. Unlike $CD4^+$ T cells, $CD8^+$ T cells were less sensitive to the requirement of CD28 co-stimulation and can be activated with high enough levels of TCR signals. When stimulated with CD4 elongated SCD molecules, the levels of IL-2 secretion was reduced, consistent with published data (Choudhuri et al., 2005).

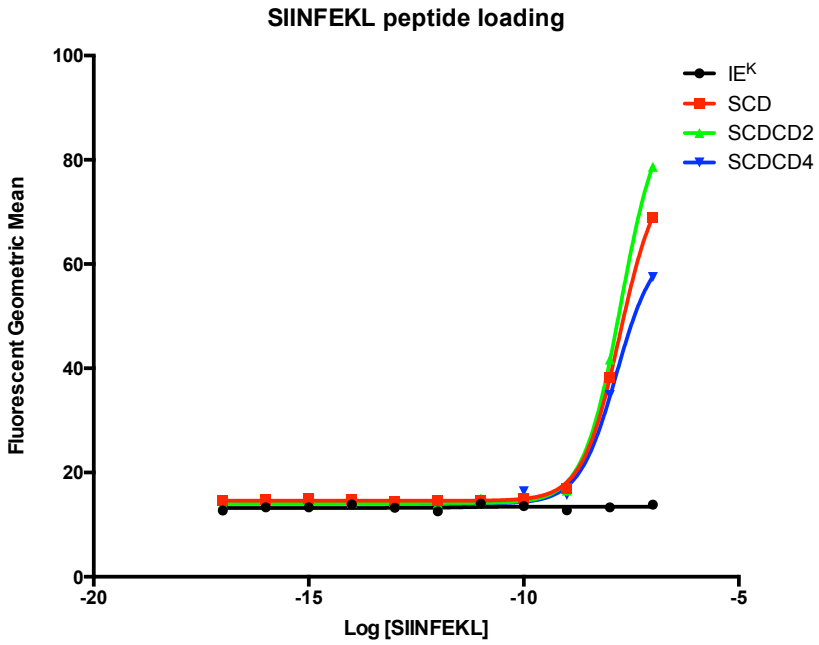

Figure 3.22 Peptide loading between SCD and elongated SCD

CHO cells expressing SCD or elongated SCD (SCDCD2 or SCDCD4) molecules were pulsed with the indicated concentrations of SIINFEKL peptide and analysed for SIINFEKL loading using antibody specific for $H2K^b$-SIINFEKL complex (25-D1.16). SIINFEKL concentrations were plotted against geometric mean values from flow cytometry analysis. This is a representative plot of 2 separate experiments.

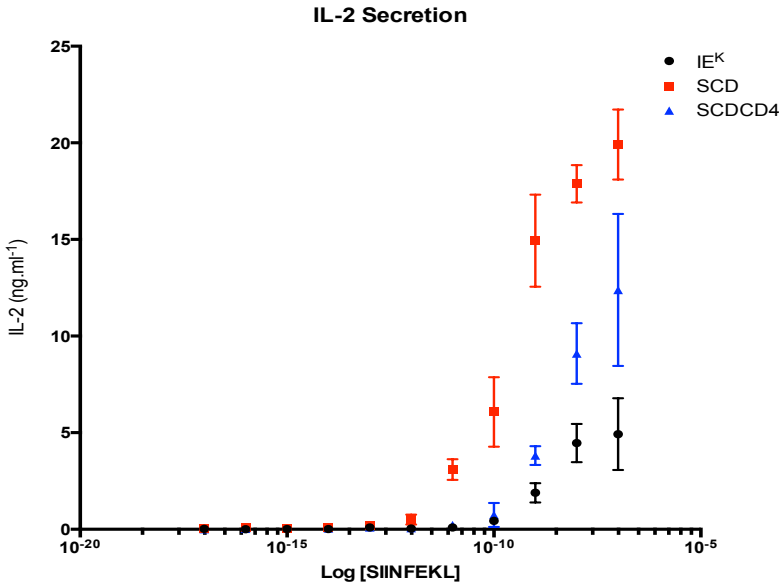

Figure 3.23 Impaired IL-2 secretion from elongated SCD molecules

CHO cells expressing SCD or elongated SCD (SCDCD2 or SCDCD4) molecules only were pulsed with the indicated concentrations of SIINFEKL peptide and used to stimulate transgenic mouse primary $CD8^+$ OT1-TCR T cells. Supernatents were collected after 48 hours and analysed for Il-2 secretion. Error bars represent SEM for 3 replicate points. This figure is a representative figure of at least 3 repeats.

SCD elongation reduces IL-2 secretion by OT1 primary T cells in a length dependent manner

Having determined the functionality of SCD and elongated SCD on primary OT1 T cells, we set off to examine the importance of CD80 dimensions in a MHC class I system. WT CD80, CD80CD2 or CD80CD4 were transfected into CHO cells expressing WT SCD. These cells were matched for CD80 and SCD expression, pulsed with SIINFEKL and presented to primary mouse $CD8^+$ OT1 cells for 48 hours. The supernatants were then harvested for IL-2 ELISA. Stimulation with pulsed SCD alone led to limited IL-2 secretion. Provision of CD28 signals in the form of CHO-SCD, CD80 dramatically improved IL-2 secretion and, as observed with the MHC class II system (Figure 3.7), elongation of CD80 abrogates IL-2 secretion (Figure 3.24). One notable difference is that some IL-2 secretion is observed in the absence of CD80, in line with the observations that CD8 T cells are less dependent than CD4 cells on CD28 engagement for activation.

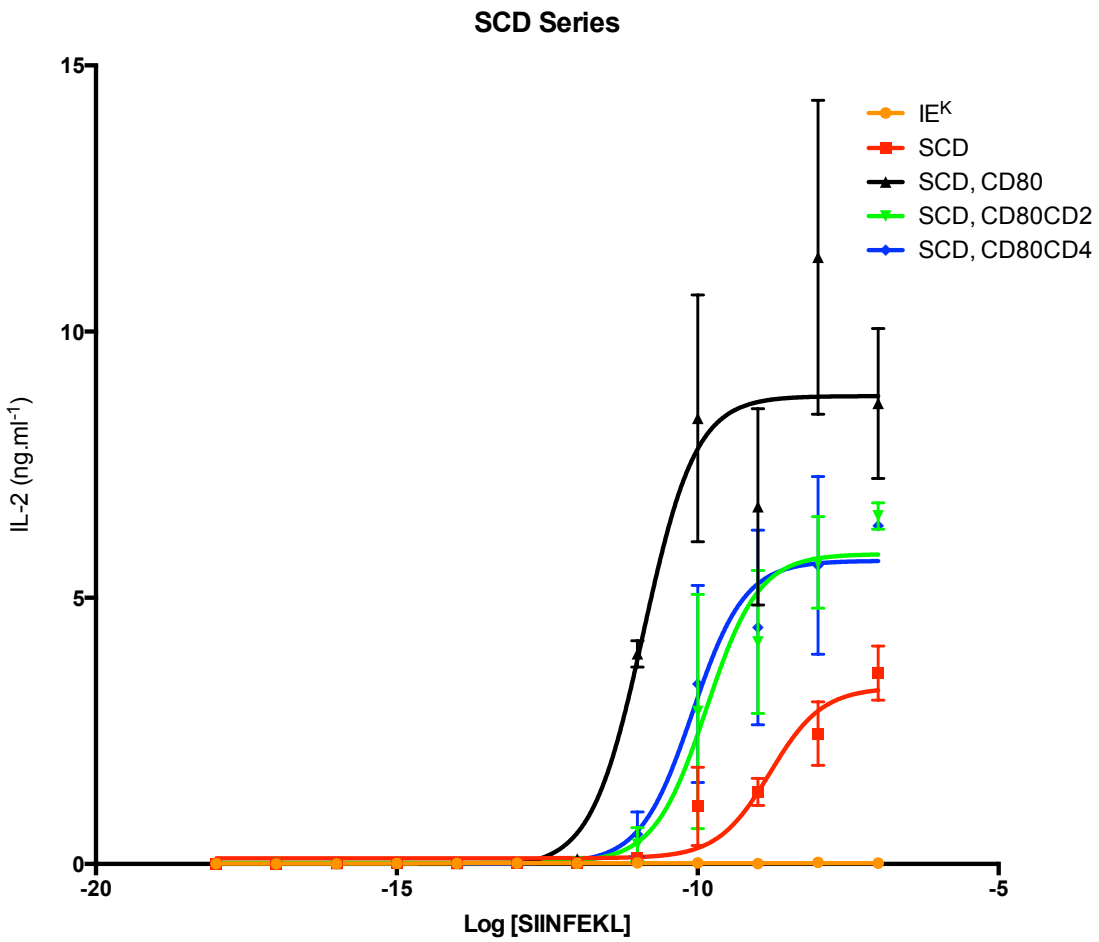

Figure 3.24 CD80 elongation reduces IL-2 secretion in primary CD8$^+$ T cells

CHO-SCD cells expressing CD80-WT or elongated CD80s were pulsed with titrating concentrations of SIINFEKL peptides before incubation with the CD8$^+$ OT1 T cells for 48 hours. The supernatants were then harvested for IL-2 ELISA after 48 hours. Error bars represent SEM for three replicate data points. This is a representative figure from 4 repeats.

No evidence for the requirement of matched CD28 and TCR ligand/ receptor dimensions in T cell co-stimulation

Finally, to investigate the importance of matched TCR-pMHC and CD28-CD80 dimensions in T cell co-stimulation, we compared the effectiveness of normal length (WT) and elongated CD80 in costimulation when the TCR ligand SCD was elongated to the same extent as the CD80CD4. If matched dimensions are critical for

costimulation the elongated CD80 should be better than WT CD80 at costimulating when the TCR ligand is also elongated.

To do this, CD80-WT, CD80CD2 or CD80CD4 were transfected into SCDCD4 expressing CHO cells. These CHO cells were then pulsed with titrating concentrations of SIINFEKL peptide and incubated with mouse primary $CD8^+$ OT1 T cells for 48 hours. The supernatant were collected for IL-2 ELISA. For comparison the effect of different forms of CD80 in costimulation by CHO expressing SCD was examined in the same assay (Figure 3.25).

Once again, expression of CD80 on the CHO-SCD cells only modestly improved IL-2 secretion by these CD8 cells and, as before, elongated forms of CD80 were less effective at mediating costimulation than WT CD80.

Peptide-pulsed CHO cells expressing the elongated SCDCD4 were able to induce IL-2 secretion from the T cells in the absence of CD80 expression, as observed with WT SCD, and expression of WT CD80 improved IL-2 secretion. Importantly, elongated forms of CD80 remained less effective that WT CD80 at enhancing IL-2 secretion, even though the TCR ligand was also elongated. This suggests that matching the dimensions of the TCR-pMHC and CD28-CD80 is not critical for effective costimulation.

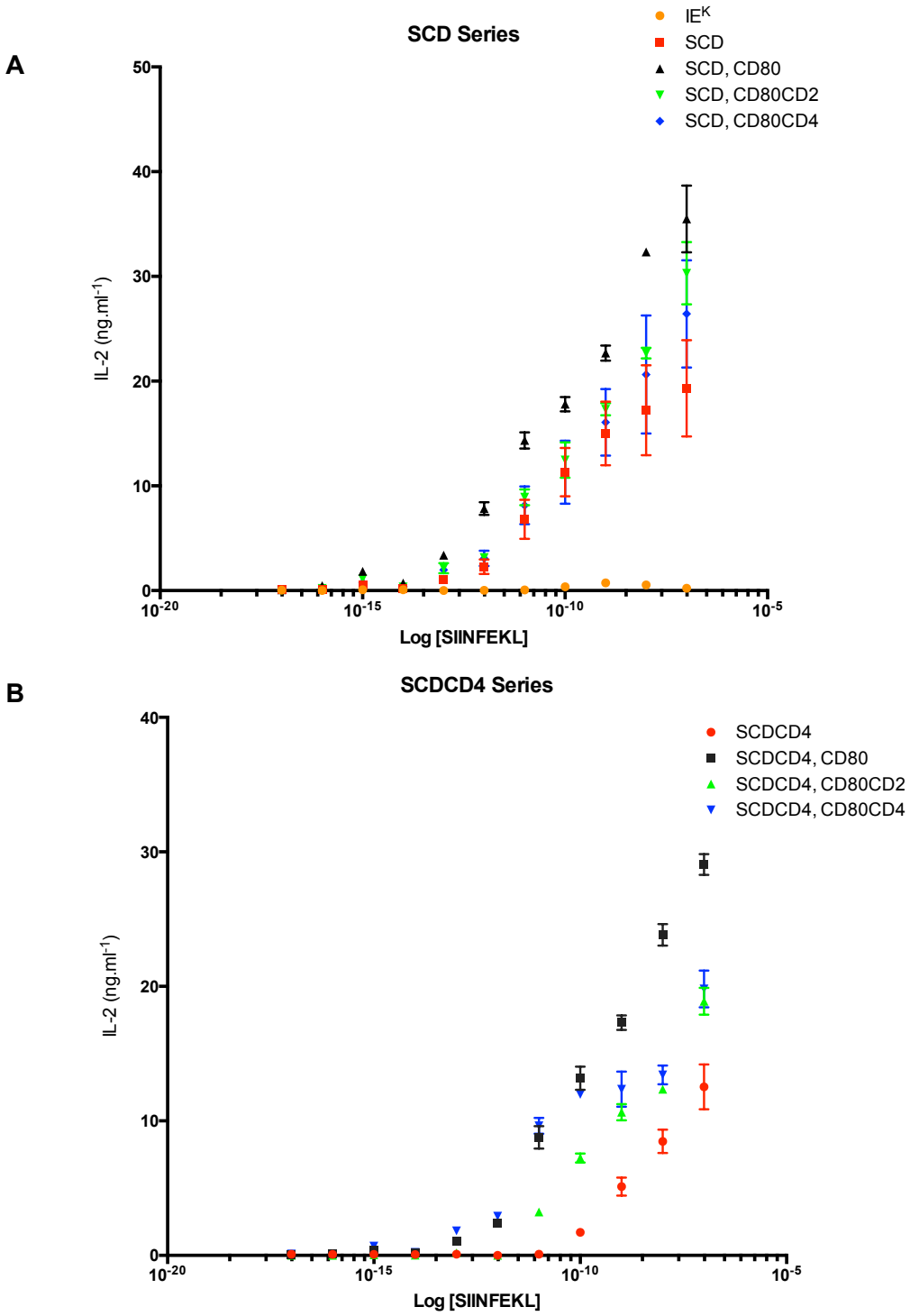

Figure 3.25 No evidence for the requirement of matched CD28 and TCR ligand/ receptor dimensions in T cell co-stimulation

Peptide pulsed (a) SCD or (b) SCDCD4- expressing CHO cells and with different variants of CD80 were used to stimulate mouse primary $CD8^+$ OT1 TCR transgenic T cells. The supernatant were collected after 48 hours and analysed for IL-2 secretion. CHO-IE^K cells not expressing any CD80 were used as negative controls. Error bars represent SEM for 3 replicate data points and this is a representative figure for 4 separate experiments.

3.4 Discussion

CD28 is arguably the best-characterised co-stimulatory receptor and yet, despite the relatively well-established biochemical pathways downstream of CD28 engagement, the exact mechanism by which CD28 triggers remains unclear. CD28 cytoplasmic tail has no intrinsic enzymatic activity and its signalling capability is dependent upon the recruitment of various signalling molecules or adaptor molecules to specific motifs. CD28 cytoplasmic tail contains 4 tyrosine residues and 2 out of 4 of which are known to be tyrosine-phosphorylated. This classifies CD28 as a non-catalytic tyrosine-phosphorylated receptor (NTR) that can be regulated in theory by changes in the local kinase and phosphatase concentrations (Dushek et al., 2012). Originally described for the TCR, the K-S mechanism postulates that differences in ectodomain dimensions between the TCR and large membrane phosphatases with would physically segregate large membrane receptor phosphatase away from the engaged TCR, leading to a net increase local kinase: phosphatase ratio, thereby leading to TCR triggering. This framework was further extended to include all NTRs (Dushek et al., 2012).

Work described in this chapter attempts to address the importance of CD28 receptor/ ligand dimension in mediating CD28 co-stimulation, directly testing the hypothesis that CD28 triggering would be susceptible to regulation via the K-S mechanism. To do this, CD28 ligand CD80 was elongated by inserting hCD2 or hCD4 molecules in its stalk region, corresponding to 2 or 4 Ig domains respectively.

The findings demonstrated that elongation of CD80 reduces CD28 co-stimulation efficiency in both purified $CD4^+$ and $CD8^+$ T cells. This effect is inversely proportional

to the length of the elongated CD80 molecules. The reduced co-stimulation was not a result of decreased binding to CD28 as elongated CD80 molecules bound as well as wild-type CD80 to CD28-Fc-Protein A-coated fluorescent beads. It is however, necessary to verify the results using a fixed concentration of fluorescent Protein A beads whilst titrating the CD28-Fc proteins. It is possible that elongated CD80 molecules have reduced their ability to form non-covalent dimers and that this might reduce CD28 triggering. This is unlikely to explain our results, for two reasons. Firstly, CD86 is monovalent and is nevertheless as effective as CD80 at inducing CD28 co-stimulation. Secondly, obligate disulphide-linked CD80 dimers were found to be worse costimulators than wild type CD80 molecules (Bhatia et al., 2010).

As noted previously, there are two possible, non-exclusive mechanisms by which elongation of CD80 could result in a reduced costimulation. Firstly, an increase in CD80 ectodomain membrane dimension could reduce CD28 triggering. Secondly, elongating CD80 would lead to a mismatch between the dimensions of the TCR-pMHC and CD28-CD80 complexes.

The trans-costimulation assay, by separating the pMHC and CD80 molecules onto different CHO cells, enabled the effects of elongated CD80 molecules to be investigated independently of any effects that might arise as a result of mismatching between the dimensions the CD28-CD80 and TCR-pMHC complexes. The strength of CD28 co-stimulatory signals provided in trans can be manipulated by titrating the number of CD80 expressing CHO cells. Crucially, elongated CD80 molecules were unable to provide co-stimulation in trans, as measured by the amount of IL-2 secretion, consistent with the notion that elongation disrupts CD28 triggering.

One likely mechanism by which elongation of CD80 disrupts triggering through CD28 is by reducing the segregation of CD28 from the inhibitory phosphatase CD45 upon ligand engagement. Indeed, confocal analysis of CHO cells expressing CD80CD4-GFP revealed a reduction in its segregation from CD45 as compared to wild-type CD80-GFP at the conjugate interface. Both elongated CD80 molecules demonstrated a negative Pearson's correlation with CD45, indicating segregation under all circumstances. This is not surprising as elongated CD80 molecules are still smaller than CD45 (predicted ~20nm for CD80CD4 versus ~45nm for CD45). Importantly, the elongated molecules were less well segregated than CD80-WT under both stimulatory and non-stimulatory conditions.

We were unable to detect direct phosphorylation of CD28 in our assays and so were unable to examine directly whether elongation of CD80 abrogated CD28 phosphorylation. We therefore used an alternative approach to investigate the role of phosphorylation. T cells from mice habouring Y170F mutations within the YMNM motif in its CD28 cytoplasmic tail were co-stimulated with wild-type or elongated CD80 molecules. If regulation of CD28 tyrosine phosphorylation were indeed mediated by RPTPs such as CD45 in a size dependent manner as postulated by the K-S model, CD28-Y170F mutant should be less sensitive to changes in the lengths of CD80.

Indeed, IL-2 secretion from CD28-Y170F T cells were less sensitive to the dimensions of CD80 as compared to wild-type T cells (Figure 3.18). The fact that IL-2 secretion by CD28-Y170F mutants were still impaired by CD80 elongation suggests that additional signalling motifs within the CD28 cytoplasmic tail were also affected by changes in

dimensions of CD80 molecules. One possibility is that one or more of the other tyrosine residues (such as Y188 within proline rich PYAP motif) is still susceptible to regulation from RPTPs (Sadra et al., 1999). It is also important to note that the cytoplasmic tail of CD28 also contains two proline-rich motifs known to recruit tyrosine kinases such as Itk and Lck via their SH3 domains (Holdorf et al., 1999, Raab et al., 1995). As such, it is possible that improved PTPRs co-localisation as a result of CD80 elongation may also negatively affect phosphorylation by these tyrosine kinases. Taken together, these results suggest that an optimal CD28-CD80 receptor/ ligand dimension is necessary to preserve PTPRs segregation during receptor engagement.

Another mechanism by which elongation of CD80 could disrupt costimulation is by generating a mismatch in the dimensions of the CD28-CD80 and TCR-pMHC complexes. As noted above, such a mismatch could either result in mutual disruption of binding (because of suboptimal position of the membranes) or disruption of signal integration. To investigate a contribution of size mismatching, we compared the relative effectiveness of WT and elongated CD80 when the TCR ligand pMHC was also elongated. Previously we have used a similar approach to demonstrate the importance of size-compatibility in signal integration between activatory and inhibitory NK cell receptors (Kohler et al., 2010). Elongated CD80 remained much less effective than CD80-WT in mediating costimulation when the TCR ligand was elongated. This indicates that size matching is not critical for costimulation. This is consistent with the fact that costimulatory and TCR ligands can be presented on different cells, as demonstrated by our transcostimulation experiments, and suggests that signal integration between the TCR and CD28 signalling pathways does

not have to occur close to the membrane. This contrasts with signal integration between TCR and PD-1 as well as activatory and inhibitory NK receptors, where signal integration occurs close to the membrane and therefore requires their close colocalisation (Kohler et al., 2010, Yokosuka et al., 2012b). Costimulation in trans by CD28 however, is much less effective than cis-costimulation under natural conditions. Taken together, this result suggests that CD28 is able to transduce independent signals separate from the TCR (qualitative); and when in proximity of TCR, able to integrate and amplify the antigen-specific signals (quantitative). Unlike signal integration between CD28 and the TCR, optimal signal integration between CD28 and CTLA-4 may depend on close colocalisation. It is increasingly clear that CTLA-4 exists to regulate CD28, as the autoimmune pathology observed in CTLA-4 deficient mice can be reversed by blocking CD80 and CD86 (Qureshi et al., 2011, Tivol et al., 1997, Walker and Sansom, 2011). Using total internal reflection (TIRF) microscopy, Saito and colleagues showed under physiological densities of CD80 that CTLA-4 prevents CD28 associated IL-2 secretion and PKCθ microcluster translocation to the cSMAC. Segregation of CTLA-4 by elongation reversed the effects (Yokosuka et al., 2010), implying the potential importance of signal integration between CD28 and CTLA-4.

Results in this chapter conclusively address the mechanism by which CD28 receptor triggers. Just like the TCR, several mechanisms non-mutually exclusive mechanisms can be considered for mediating CD28 triggering: conformational change, receptor aggregation and segregation.

Conformational change models postulate that ligand binding induces a conformational change. Evidence for such a change in the case of CD28 is lacking. Efforts at crystallising CD28-CD80 complex have been unsuccessful so far; the best CD28 crystal structure remains to be that solved by Davis and colleagues almost a decade ago (Evans et al., 2005). In the absence of the CD28-CD80 co-crystal, it is impossible to rule out the conformational change as a means of CD28 triggering. On the other hand, useful insights can be extrapolated from CTLA-4 – CD80 co-crystals: apart from small local changes restricted to the binding sites, no major conformational changes were observed between un-ligated and ligated CTLA-4 molecules (Stamper et al., 2001). Further evidence against a specific conformational change as a triggering mechanism is the observation that the ectodomain of CD28 can be replaced by the CTLA-4 or the CD80 ectodomain without compromising CD28 signalling (Dennehy et al., 2006).

Aggregation models require that CD28 binding to its ligands CD80 or CD86 leads to aggregation. Like many immune receptors, actively signalling CD28 microclusters can be detected seconds after T cell activation (Yokosuka et al., 2008). Clustering of receptors can improve trans auto-phosphorylation of CD28 cytoplasmic domains by bringing associated SFKs such as Lck in close proximity, thereby enhancing CD28 co-stimulatory effects. This relatively large scale clustering of CD28 microclusters however, does not necessary equate CD28 receptor aggregation at the molecular level. The key question is how ligand binding leads to CD28 aggregation. Crystal structures of CD28 by Evans et al along with other studies have demonstrated that although CD28 is a disulphide-linked homodimer it is functionally monomeric (Evans et al., 2005, Collins et al., 2002). The fact that CD80 is a non-covalent homodimer

and CD28 is also a homodimer raise the possibility that CD80 binding alone would induce dimerization of two CD28 homodimers. Interestingly, by swapping CD28 ectodomain for bivalently ligating CTLA-4 or CD80 ectodomains, CD28 fusion molecules were able to induce IL-2 secretion in the absence of TCR signals, supporting the role of aggregation in CD28 triggering (Dennehy et al., 2006). Indeed, the formation of bivalent CD28 molecules by swapping the extracellular domain of CD28 for CTLA-4 or CD80 ectodomains led to IL-2 secretions without the need for TCR co-ligation. However, while artificial receptor aggregation may induce CD28 triggering within such experimental settings, this may not be relevant under physiological conditions. Moreover, covalent CD80 dimer is less effective than wild type CD80 at providing a costimulatory signal (Bhatia et al., 2010). Taken together, these argue against the role of aggregation for CD28 triggering.

A third possible mechanism for CD28 triggering is binding induced segregation from inhibitory RPTP such as CD45, the primary basis and motivation for this study. The results described in this chapter, along with the observation the activity of CD28 superagonists (Figure 3.2) strongly support a role for segregation in mediating CD28 triggering.

Therefore, work described in this chapter provides conclusive evidence for the role of RPTP segregation in CD28 triggering, as postulated by the K-S model. While this study demonstrates the importance of receptor-ligand dimension in CD28 costimulation, we find no evidence for the requirement of TCR-CD28 size matching. Understanding the mechanisms behind NTR triggering will be important for the design of chimeric antigen receptors for therapeutic use (see chapter 6). Subsequent

verification of the K-S model across all NTR systems will require in-depth and systematic analyses.

CHAPTER 4:

Energetics Contribution of MHC contacts to the Affinity of TCR-pMHC Interactions

4.1.1 Introduction

Initiation and propagation of the adaptive immune system is conditional on TCR's recognition of antigenic peptides presented by class I or class II MHC molecules. The TCR-pMHC interaction represents a unique recognition system such that effector functions are extremely dependent on the specificity of the pMHC despite an inherent '*promiscuity*' of TCR for any pMHC (Mason, 1998a). The co-existing trait of specificity and cross-reactivity is one of many unique TCR characteristics, which have, and will continue to puzzle T cell biologists for the years to come.

Insights into the TCR-pMHC interactions have come from crystal structures of various TCR and peptide-MHC molecules [many of which were consolidated and reviewed by Rudolph et al (Rudolph et al., 2006)], careful thermodynamics (Armstrong et al., 2008), and mutagenesis studies (Manning et al., 1998, Ishizuka et al., 2008, Liu et al., 2012, Baker et al., 2001) which will form the basis for this chapter review. The important question of MHC restriction will also be addressed in light of recent evidences.

4.1.2 Structural insights into TCR-pMHC interactions

T cell receptors

T cell receptors were first identified using monoclonal antibodies to clonal T cell lines. Four distinct TCR polypeptides α, β, δ, γ have been identified and they form cell surface heterodimers of disulphide-linked α-β or δ-γ molecules. Early sequence comparison studies revealed a striking similarity of TCRs to the Fab fragment of antibodies (Davis and Bjorkman, 1988). This was confirmed by subsequent crystal structures of TCRs (Figure 4.1a). Just like antibodies, both chains of the TCR contain a

constant (C) region with a variable (V) region and a short stalk segment containing a cysteine residue that contributes to the inter-chain disulphide bond. Binding and recognition of pMHC is mediated predominantly by three complementarity determining regions (CDR) manifested as flexible end loops in each TCR polypeptide chain. TCR diversity arises as a result of somatic gene rearrangement of different V-, D- and J- segments or V- and J- segments. Further diversity results from the random addition/removal of P- and N- nucleotides between the V, D and the J gene segments. The CDR1 and 2 regions are encoded within germ-line derived V-segments and therefore show limited diversity. In contrast the CDR3 loops are encoded by the D- and J- segments and the junctions between V-, D- and J-segments, and therefore show enormous diversity. These loops are highlighted in colour in figure 4.1a.

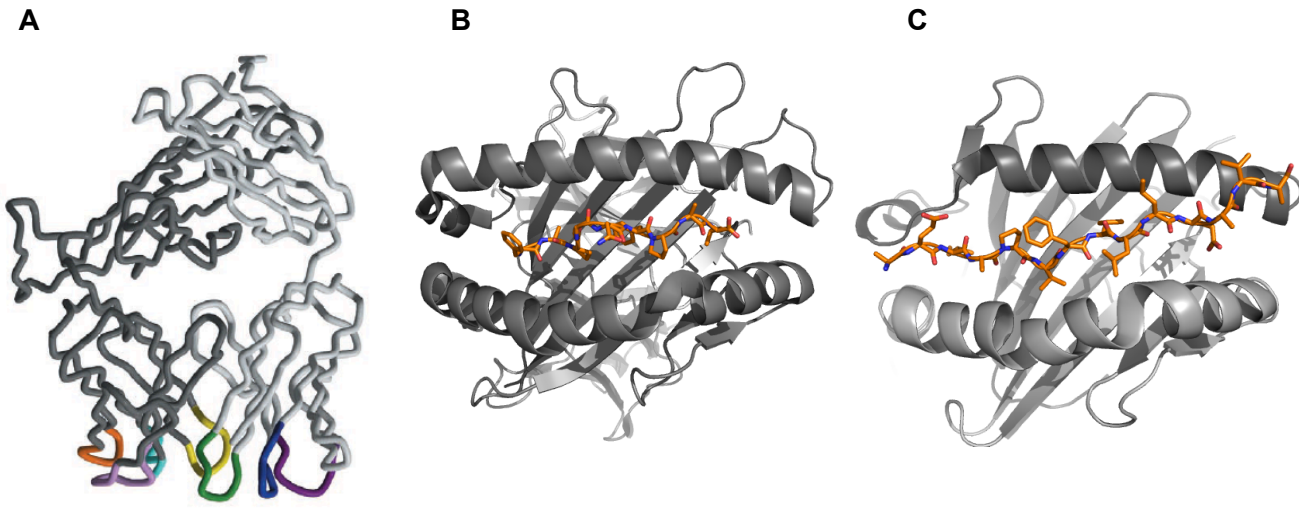

Figure 4.1 Crystal structures of TCR, Class I MHC and Class II MHC

(a) The TCR is composed of two (α and β) polypeptide chains, the pMHC contacting interface is composed of the complementarity determining regions (CDRs), highlighted in colour. (b) A top-down view of a class I MHC molecule (PDB:1FZK), which typically accommodates peptides with 8-10 residues as a result of it's 'closed' α-helices conformation. (c) Top-down view of a class II MHC molecule (PDB: 1ES0), which accommodates longer peptides as a result of the 'open' α-helices conformation. Note the α1-helix degeneration (α subunit, dark grey; β subunit, light grey)). These structures are adapted from Rudolph et al (Rudolph et al., 2006).

Class I and Class II Major Histocompatibility Complexes

MHC molecules were originally discovered for their role in facilitating transplant rejection between incompatible individuals. The cluster of genes responsible for the rejections were dubbed the H2 system (histocompatibility 2) in mice before their discovery in humans, where they are known as Human Leukocyte Antigens (HLA), a decade later (P. A. Gorer et al., 1948). MHC class I molecules consists of two polypeptide chains: the membrane spanning, polymorphic α heavy chain and the non-variant β2 microglobulin, while MHC class II molecules consists of two membrane-spanning α and β polymorphic chains. Both MHC class I and II molecules share the same overall structure with a peptide binding groove where a seven-stranded β-sheet floor is flanked by two α-helices (Figure 4.1b,c).

Class I MHCs often bind peptides of 8-10 residues long with most side chains pointing upward towards the TCR for recognition. Certain residues pointing downwards towards the MHC peptide binding groove and provide anchor points for stable peptide loading. MHC class II molecules typically accommodate longer peptides of approximately 13 residues as a result of the open groove conformation and the α1 helix degeneracy (Figure 4.1c).

T cell receptors and pMHC interactions

It is widely appreciated that TCRs have the potential to recognise virtually any antigen in the context of an MHC-like molecule (Godfrey et al., 2008, Wooldridge et al., 2012). The concept of 'MHC restriction' was conclusively demonstrated by the Nobel Prize-winning study of Zinkernagel and Doherty when cytotoxic T cells were

only effective against virally infected cells with the 'correct variant' of histocompatibility antigens, later revealed to be MHC molecules (Zinkernagel and Doherty, 1974). The need for more structural information was warranted by several crucial questions: What forms the molecular basis for the interaction between two structurally diverse TCR and MHC proteins? Can MHC restriction be explained by a universally conserved mode of binding?

These questions were partially addressed with the publication of two different TCR-pMHC crystals by independent laboratories (Garcia et al., 1996, Garboczi et al., 1996). Both studies and subsequent structures demonstrated several conserved features of the interactions (Garcia et al., 1998, Ding et al., 1999).

Firstly, all TCRs bind with a docking orientation that is roughly diagonal with regards to the path of the antigenic peptide, with the TCR Vα domain centred over N terminal half of the peptide and vice versa. While the docking angles may vary from as large as 120° (Garcia, 2012), no viable structures of the TCR positioned in a 180° rotation (i.e. Vα domain over C terminal half of the peptide and vice versa) have been observed. Indeed, there is one report suggesting that deviation from a conserved docking orientation would disrupt TCR triggering (Adams et al., 2011). Secondly, the germ-line encoded, less diverse CDR1 and CDR2 loops within TCR Vα and Vβ domain are usually positioned over the α helices of MHC molecules while the somatically-generated, more diverse CDR3 loops are largely positioned above the antigenic peptide. Finally, the buried surface areas for TCR interactions with both class I and class II MHC molecules are very similar, varying in the range of 1600Å^2 (Rudolph et al., 2006). Despite the large amounts of buried surface area, the

seemingly lack of optimal shape complementarity may account for the low affinity of these interactions, as opposed to other immune protein-protein recognition system such as the cytokine receptors (Garcia et al., 2009).

It is of significant research interest to understand why this conserved mode of TCR binding exists. Various hypotheses put out to describe this phenomenon have been the centre of intense debate in recent years and will be the focus of the following section.

4.1.3 TCR docking orientation: Germ-line selection or Thymic selection?

The VDJ gene recombinant process can yield up to 10^{15} different TCR variants, with the potential to bind virtually any pMHC. This, coupled with the conserved docking orientation of TCR-pMHC begs a conceptually important question: what are the mechanisms driving the conserved binding mode between the most structurally diverse proteins encoded within the genome?

The germ-line hypothesis provides an extremely logical and satisfactory explanation to the phenomenon. The theory proposes that the orientation is dictated by conserved amino acid contacts within the germ-line encoded regions of MHC and TCR as a result of receptor/ ligand co-evolution. This provides a clean explanation for the MHC- and peptide-centric nature of CDR1/2 and CDR3 binding respectively (Garcia et al., 2009, Garcia, 2012, Jerne, 1971).

The alternative hypothesis to germ-line selection revolves around the possibility that thymic selection can exclude non-MHC binding TCRs from surviving via co-receptor imposed restrictions (Van Laethem et al., 2012, Collins and Riddle, 2008, Garcia, 2012).

Germ-line selection: The evidences

Evidences for germ-line mediated selection have been informed by functional experiments (Dai et al., 2008, Huseby et al., 2005) and structural analysis of TCR-pMHC interactions (Feng et al., 2007, Adams et al., 2011). If TCR-pMHC interaction is a result of co-evolution, then there should be conserved amino acid residues on either side of the protein mediating binding in different context. To this end, Garcia and colleagues focused on the interactions of one particular germ-line $V_{\beta}8.2$ segment present in three separate TCRs, binding to the same I-A^{u}-MBP1-11 pMHC molecules. Intriguingly, the authors discovered a series of conserved residues contacts between the MHC class II-alpha helix and the $V_{\beta}8.2$ CDR1 and 2 loops, referred to as the '*MHC restriction codons*' (Feng et al., 2007). Similar pairwise amino acid contacts with $V_{\beta}8.2$-containing TCRs and I-A peptide complexes (I-A^{u}, I-A^{b}, I-A^{k}) were reported elsewhere (Dai et al., 2008, Stadinski et al., 2011). In addition, crystal structures of different yeast display-generated (CD4/ CD8 independent) variants of $V_{\beta}8.2$-containing 2C TCR also utilise conserved residues between CDR1/2 and H2-L^{d}-QL9 contacts (Colf et al., 2007, Jones et al., 2008).

As the many of the $V_{\beta}8.2$-containing TCRs mentioned above are already thymically selected, it remains possible that productive TCR-pMHC bindings may be a result of certain thymic-dependent, germ-line independent interactions. To address this issue, Marrack and Kappler engineered mice that express only a single pMHC (I-A^{b}-3K) that permits the escape of negative selection by TCRs in the absence of other selecting ligands (Huseby et al., 2005). The resulting TCR repertoire was particularly cross-reactive in a peptide independent manner (i.e. focused on the MHC). In a follow up

study, the authors looked at three V_β8.2-containing TCRs in complex with I-A^k-3K pMHC and found striking similarity between the V_β8.2/ I-A structural codons described by Garcia and colleagues (Dai et al., 2008). Thus, these results demonstrate the presence of a conserved germ-line encoded binding nature across several TCR-pMHC systems from both thymically selected and non-selected background. Importantly, the germ-line theory states that conserved contacts do tolerate 'wobble' or variations that maintain an overall docking convergence.

Additional evidences for germ-line selection can also be informed by the presence of immunodominant TCRs among different organisms of the same species sharing the same MHC alleles (Turner et al., 2006). This would suggest that certain TCRs variable regions are preferentially selected when presented with the same pMHC molecules. The use of particular TCR regions is particularly common in persistent infections such as Human Immuno-deficiency virus (HIV)(Pantaleo et al., 1994), Epstein-Barr Virus (EBV)(Argaet et al., 1994) and Cytomegalovirus (CMV)(Wills et al., 1996, Price et al., 2005). Outcome of these infections have further been linked to the complex of certain (preferential) TCR-pMHC pairs, providing a pathogen-driven evolutionary basis for the germ-line selection. Off course, such predominance of TCR can also be explained by post-thymic, peripheral-selection pressure during the course of an immune reaction (Turner et al., 2006).

Co-receptor imposed thymic-selection: The evidences

CD4 and CD8 co-receptors bind class II and class I MHC respectively. It has been long hypothesised that co-receptor interaction with MHC molecules serve a number of important functions: to enhance the effective affinity between the TCR complex and

the pMHC and to recruit associated Src-family kinase Lck to engaged TCRs. In the latter, co-receptor mediated delivery of Lck facilitates TCR-CD3ζ-ITAM and ZAP70 phosphorylation (Rudd et al., 1988), resulting in TCR proximal signalling, which is crucial for both thymic and peripheral functions (Van Laethem et al., 2013).

The requirement of co-receptor binding during thymic selection [reviewed in (Germain, 2002)] might impose a steric TCR-docking orientation. Structural evidence for this include the finding by Buslepp et al of a correlation between TCR-MHC docking orientation and CD8 dependence (Buslepp et al., 2003). This was supplemented by the groundbreaking crystallographic work by Yin et al who demonstrated just how co-receptors might impose steric requirement for TCRs to bind in a particular orientation to pMHC for productive CD4 and TCR co-ligation of the pMHC (Yin et al., 2012).

More recently, functional evidences for the co-receptor-imposed thymic-selection theory come from the elegant studies by Singer and colleagues. The authors investigated TCRs resulting from experimental mice with quadruple knockouts, lacking class I and II MHCs, CD4 and CD8 molecules altogether (Van Laethem et al., 2007). Surprisingly, the resulting TCRs (which have developed in the absence of MHC and co-receptors) exhibited reactivity to non-MHC ligands. In a follow up study, they identified CD155 as a high affinity target for one purified TCR, reminiscent of an antibody-antigen reaction (Tikhonova et al., 2012). Further antibody-like properties of TCRs can be demonstrated in a yeast proteome-array based screening study where a thymically-selected TCR is able to bind similar numbers of non-MHC antigens as an antibody (Bangham et al., 2005).

Such findings suggest that TCR-pMHC recognition is not intrinsic to germ-line encoded sequence in the TCR and/or pMHC. Under this argument, TCRs, like antibodies, can potentially recognise diverse ligands, not just MHC molecules. During normal circumstances, MHC-ligating CD4 or CD8 would sequester Lck away from non-MHC recognising TCRs preventing their selection. In the quadruple knockout, freely available Lck would enable the selection of all TCRs, MHC-ligating or not. Indeed, the generation of MHC-ligating TCRs depended only on two cysteine residues on Lck that mediate CD4 and CD8 binding (Van Laethem et al., 2013). Mutation of these residues led to co-receptor free Lck that preferentially promoted thymic selection of non-MHC ligating TCRs. Such an observation argues that TCRs are not inherently specific for MHC, at least in the thymus where T cells with TCR-pMHC interaction exist only because CD4 or CD8 compels them to.

This series of studies supports the notion that TCR's inherent reactivity for MHC is the result of a requirement for coreceptor-associated Lck during thymic selection.

A reconciling view of germ-line and thymic imposed selection?

In light of the additional evidences for co-receptor mediated TCR selection, Garcia offered a reconciling view of the two theories which he argues are not mutually exclusive, stating that: "*germ-line bias does not denote a negative bias toward non-MHC ligands but rather a positive bias for MHC*" (Garcia, 2012). TCRs would develop to bind any antigens in an environment devoid of MHC molecules, just like the antibodies, by virtue of the VDJ gene rearrangement process.

In this integrative model, the requirement of co-receptor engagement (or any other limiting extrinsic factors) would impose a conserved TCR-pMHC docking orientation

that is further enhanced over the years by co-evolution between specific TCR and MHC pairs. That coevolution would be expected to exclude sequences that preclude MHC recognition, creating a positive bias in favour of MHC binding. As recognition of non-MHC antigens are mediated by all CDR1, 2 and 3 loops, the presence of germ-line residues on its CDR 1 and 2 loops will not prevent TCRs from recognising non-MHC antigens. This would explain why both MHC- and non-MHC ligating TCRs are generated in MHC^{+} systems with freely available Lck (Van Laethem et al., 2013).

The integrative model for diagonal TCR binding is also consistent with an earlier proposal that accounts for the effects of both germ-line selection and co-receptor binding on TCR docking orientation (van der Merwe and Davis, 2003). A close examination of existing MHC class I structures reveal the presence of a conserved 'kink' on either end of the α-helices. This is exemplified by $H2K^{b}$ in Figure 4.2. Through their effects on the shape of the pMHC binding surface, these bumps may impose a diagonal binding requirement of TCRs while tolerating large variable docking angles of up to 120°.

Interestingly, such a 'kink' is only present in the α-helix of the β1 domain in MHC class II molecules as demonstrated by HLA-DR1 in Figure 4.2., and is absent from the α-helix contributed by the α1 domain. This is in line with observations that TCRs can adopt a close-to-perpendicular binding orientation to MHC class II molecules (Wang and Reinherz, 2002). The dual requirement of TCR and co-receptor binding during thymic selection on the other hand, may be incompatible with TCRs binding in a 180° rotation (i.e. Vα domain over C terminal half of the peptide and vice versa).

The road to interrogating the basis of MHC restriction has generated a series of fascinating and cleverly conducted experiments. It is probably true that TCR-pMHC recognition is driven both by co-receptors and conserved germ-line mediated interactions. Perhaps the concept of germ-line encoded interaction can be better appreciated with the notion of a 'permissive' structure where it is not the absolute presence of certain contacts that is required but rather the absence of any potentially disruptive structures/residue.

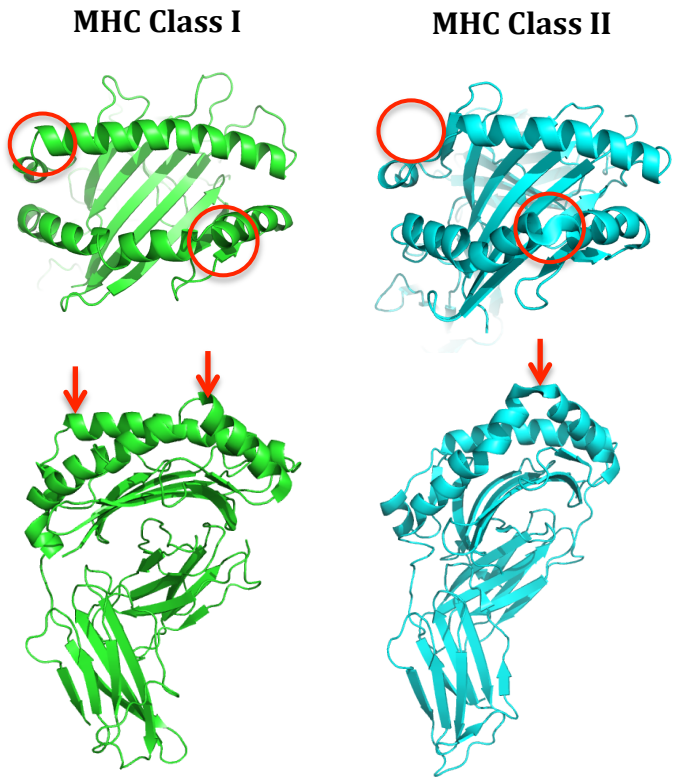

Figure 4.2 TCR binding orientation may be imposed by structural constraints in the MHC molecules

The presence of two 'kinks' on either end of the MHC class I α-helices may impose a diagonal binding requirement for TCRs (highlighted in red) in order to optimize surface-shape complementarity. For MHC class II molecules, the presence of only one 'kink' may permit a more perpendicular mode of binding by TCRs. MHC class I and class II molecules are exemplified by H2-K^b (PDB number: 2CKB) and HLA-DR (PDB number: 1FYT) respectively. Similar results were observed with other MHC class I molecules including HLA-B3, HLA-B8 and HLA-A2 [PDB numbers 2AK4, 1MI5 and 2BNR respectively] as well as MHC class II molecules I-A^K, I-A^{g7}, I-A^U, HLA-DR2a, HLA-DR2b and HLA-DR4 [PDB numbers 1IAK, IES0, 1U3H, 1ZGL, 1YMM and 1J8H respectively] (data not shown).

4.1.4 Thermodynamics of TCR-pMHC interaction

Methods for quantifying TCR-pMHC physical parameters

While crystal structures of TCR-pMHC interactions have yielded invaluable information on the structural basis of the interaction, it represents a 'frozen' shot of what is essentially a dynamic process of interaction (Ding et al., 1999). Furthermore, structural studies do not reveal which parts of the binding interface contribute to the binding energy, and so it is essential to combine them with measurements of thermodynamics and kinetics parameters. Two techniques stand out in particular as immunologists' favourite toolkits: Surface Plasmon Resonance (SPR) and Isothermal Titration Calorimetry (ITC).

SPR measures the changes in refractive index near a protein-tethered sensor surface that result from its binding of an injected protein. The overwhelming popularity of the SPR technique stems from its relative ease of affinity and kinetic data acquisition and the minute material requirement for proteins, even for low affinity interactions. Gibbs Free energy of the reaction can be derived directly from the measurement of the affinity: $\Delta G = -RT\ln K_A$ (where K_A = Affinity of the interaction = $1/K_D$ expressed in units M^{-1}). Reaction enthalpy (ΔH) and entropy (ΔS) values can also be derived indirectly using the van't Hoff plot which describes the dependency between affinity and temperature: $\ln K_A = -(\Delta H/RT) + (\Delta S/R)$, where R and T are the gas constant and temperature (in K), respectively. The major pitfalls of SPR revolves around the possibilities of protein aggregation, mass-transport limits and protein rebinding, which can lead to underestimation of the binding kinetics (van der Merwe and Barclay, 1996).

ITC represents a more direct measurement of the reaction enthalpy by measuring the absorption or release of heat (ΔH) as two molecules interact (Ladbury, 2004). This method negates the indirect calculation of ΔH using the van't Hoff-based method, which can be problematic over large temperature range as a result of changes in heat capacity (ΔC_p). Measuring the differences in enthalpy over a concentration of protein yields the reaction affinity from which the Gibbs free energy can be derived. With this, the reaction entropy (ΔS) can be calculated from the Gibbs-Helmholtz equation: $\Delta G = \Delta H - T\Delta S$. In addition, the change in constant pressure heat capacity (ΔC_p) can be determined from measurement of the ΔH over a range of temperatures since $\Delta C_p = d\Delta H/dT$. As such, this technique provides the possibility to acquire a full thermodynamic profile of the interaction (ΔH, ΔG, ΔS, ΔC_p). Despite these advantages, the major drawback for ITC remains the unsustainably high requirements of protein concentration for low affinity interactions. A comprehensive review of the various techniques was performed by Piepenbrink et al (Piepenbrink et al., 2009).

The hunt for a conserved thermodynamic signature

The affinity between TCRs and pMHC are low compared to conventional protein-protein interactions, in the range between 1 to 100μM (Rudolph et al., 2006). This can be attributed to both a fast dissociation rate (k_{off}) and slow association rate (k_{on}) between TCRs and its ligand (Willcox et al., 1999). The k_{on} between TCRs and pMHC ranges from 10^3 to 10^5 $M^{-1}s^{-1}$ and this is slow compared to the theoretical on rate of 10^5 to 10^9 $M^{-1}s^{-1}$, which takes into account random collisions and electrostatic interactions (Bridgeman et al., 2011). This time lag suggests the presence of a

structural rearrangement or conformational change of the TCR or pMHC during the association process. While large scale conformational changes were not observed between crystals of bound and unbound TCR (Garcia et al., 1996, Garcia et al., 1998, Degano et al., 2000), there are many examples of small-scale, local rearrangements in the CDR3 loops of the TCR upon binding to pMHC (Garcia et al., 1998, Reiser et al., 2003, Boniface et al., 1999). Local rearrangement of TCR and pMHC binding interface would provide an explanation for the inherent cross-reactivity of TCRs to pMHC molecules.

van der Merwe and colleagues first pursued this hypothesis from a thermodynamics perspective using both SPR and ITC techniques (Willcox et al., 1999). The results from two TCR systems revealed that the interactions are largely enthalpically driven with an entropically unfavourable profile, providing an explanation to the low affinity nature of TCR-pMHC interactions. This finding is in line with the conformational change at the TCR-pMHC interface, where the reduction of mobility or flexibility within binding interfaces would impose an entropic penalty. Alternatively, it could also reflect changes in the solvation of the molecules such as the incorporation of ordered water molecules that serves as molecular glue in between the binding interface (Ladbury, 1996). The latter was unlikely true given a net expulsion of water from the interacting surfaces (Cole et al., 2009). Similar findings echoing the results by van der Merwe and colleagues soon piled in with different TCR systems (Boniface et al., 1999, Garcia et al., 2001, Lee et al., 2004).

However, just as the concept of a particular thermodynamic signature (enthalpically favourable, entropically unfavourable) was gaining precedence within the

community, a string of TCRs with entropically favourable interactions were discovered (Ding et al., 1999, Ely et al., 2006). These receptors also demonstrated flexible conformational changes in their CDR3 loops, questioning the existence of a conserved thermodynamic signature for TCR-pMHC interactions.

An overwhelming number of thermodynamics studies were performed on class I MHC interactions. Interestingly, a recent crystallisation and thermodynamics study led by Cole and colleagues on class II MHC interactions defied existing trends. The authors described an entropically favourable interaction that is unaccompanied by significant CDR loop movements (Holland et al., 2012). This appears to be at odds with existing explanations for TCR cross-reactivity. As both class I and class II MHC binding involves the expulsion of ordered solvents in the interface (entropically favourable), the authors proposed that it is the extra need for CDR loop stabilisation that would contribute to the negative entropy in certain class I MHCs.

These discrepancies question the need for CDR loop rearrangement as a pre-requisite for TCR activation, and indeed the presence of a conserved thermodynamic signature at all. An in depth evaluation of the existing thermodynamic information by Baker and colleagues demonstrated a striking degree of enthalpy/ entropy compensation in TCR-pMHC binding data, where the Gibbs Free Energy spans only 3 kcal/mol (Armstrong et al., 2008). Therefore, it is safe to say that a productive TCR-pMHC interaction will proceed so long as it is energetically favourable, driven either by the enthalpy, entropy, or both.

4.2. Project Aims and Justification

Studies determining the energetic contribution of peptide versus MHC in a TCR-pMHC interaction are important as they provide insights into positive selection and autoimmunity. Positive selection occurs in the context of self-pMHC molecules while immune activation in the periphery involves the recognition of a foreign pMHC. If the MHC's energetic contribution to the TCR remains constant in both scenarios, the replacement of self- to antigenic-peptide might affect their relative energetic contributions.

Excessive recognition of the MHC may on the other hand, contribute to autoimmunity. This is exemplified by the discovery of an unusual binding bias of an autoimmune TCR over the MHC portion of self-pMHC (Hahn et al., 2005). All three CDR loops are predominantly centred on residues from the MHC helices for the autoimmune TCR, in stark contrast to normal TCR-pMHC interactions where it is usually mediated only by CDR1/2 loops. This implies a greater energetic contribution from MHC over the peptide, providing an interesting potential mechanism for escape from negative selection.

Structural studies are unable to map the energy footprint of TCR antigen recognition since buried surface areas do not always correlate with the energetic contributions of individual residues (Cunningham and Wells, 1989). To do so, it is necessary to combine them with mutagenesis studies. There have been relatively few studies of this question and their results have largely inconclusive. Studies with mutations on the TCR residues make it hard to estimate the contribution of the MHC as many TCR residues contact both

peptide and MHC residues (Lee et al., 2000, Manning et al., 1998). On the other hand, mutagenesis studies of peptide and MHC molecules did not always account for the possibility that MHC mutants may affect the peptide structure and its contacts to the TCR, complicating efforts to determine the exact energetic contributions of peptide and the MHC (Liu et al., 2012, Piepenbrink et al., 2013).

Work described in this chapter is built upon existing studies performed by previous members of the lab, where the energetic footprints of four TCRs (1G4, JM22, A6 and G10) to HLA-A2 were determined via systematic alanine scanning mutagenesis on the HLA-A2 molecule. The mutagenesis study is further coupled with structural data to determine exclusive TCR-contacting HLA-A2 residues for each TCR to conservatively quantify the relative energetics contribution of the peptide versus MHC in TCR-pMHC interaction.

4.3.1 A strategy to calculate energetic contribution of MHC to TCR-pMHC interaction

This work is based on the MHC Class I HLA-A2 system and its interaction with four different TCRs namely: 1G4, A6, JM22 and G10 TCRs. All residues on the A2 heavy chain within 6 Å of the TCR/ pMHC interface according to their respective complex structures were singly mutated [PDB IDs: 2BNR (1G4), 1AO7 (A6), 1OGA (JM22) and 2V2W (G10)], and systematically analysed for its resultant binding affinity and kinetics to all four TCRs. This mammoth task was undertaken, and successfully completed by a previous member of the laboratory (Zhang, 2010).

The change in Gibbs energy (ΔG) can be calculated for each single residue mutant using the following equation:

$$\Delta G = RT\ln K_D$$

where R = Gas Constant,

T = Temperature (K), and

K_D = Dissociation Constant (in units M)

As such the energetic contribution of the mutated residue can be calculated by subtracting the change in Gibbs Energy for the mutant (ΔG_{Mutant}) from that of the wild type, non-mutated HLA-A2 molecule complexed to the relevant peptide (ΔG_{WT}).

Difference of change in Free Gibbs Energy

$$\Delta\Delta G = \Delta G_{WT} - \Delta G_{Mutant}$$

In principle if all the residues contributed independently to the binding energy and the mutation only removed the contribution of that residue to the TCR binding then

$\Sigma\Delta\Delta G_{Mutants}$ would provide an estimate of the contribution of TCR-MHC interactions to the overall binding energy. However, this would include not only HLA-A2 residues mediating contacts with the TCR, but also residues mediating contacts with the peptide or both. Crystal structures of HLA-A2 in complex with 1G4, A6 and JM22 TCRs were scrutinised and amino acid residues within 6Å of the TCR-pMHC interface were categorised into four groups and presented in Table 4.1:

(i) Residues contacting TCR residues only (blue dots)

(ii) Residues contacting peptide residues only (orange dots)

(iii) Residues contacting both TCR and peptide residues (green dots)

(iv) Residues not contacting TCR or peptide residues (blank)

Contact residues in any case were defined as residues lying within 4 Å of each other.

Only HLA-A2 residues in contact with TCRs were considered, in order to make a conservative estimation of the contributions of TCR-MHC contacts to the binding energy of the TCR-pMHC interactions (Table 4.1, blue dots). As the HLA-A2/GAG/G10 TCR crystal is unavailable for the G10 TCR, we only considered HLA-A2 residues that were (i) not in contact with the GAG peptide and (ii) when mutated resulted in a more than 2-fold reduction in affinity, as shown in Table 4.1 (red dots), based on previous data generated in the lab (Zhang, 2010).

A straightforward and accurate way to measure the energetics contribution of all the TCR contacting residues would include the simultaneous mutations and subsequent analysis of affinity for the resulting HLA-A2 molecule. This approach however, will be limited by current SPR's sensitivity to detect molecular interaction, only in the range

of µM. Moreover, simultaneous mutations will most likely lead to pMHC destabilisation and complication of data analysis.

An alternative method to determine MHC's energetic contribution can be described by the following equation:

MHC's Energetic contribution to TCR-pMHC Interaction

$$\frac{\Sigma\Delta\Delta G_{\text{TCR Contacting Residues}}}{\Delta G_{WT}}$$

In this equation, the individual ΔΔG can be calculated for each TCR contacting HLA-A2 residues (blue dots) based on pre-existing affinity data, summed and divided by the ΔG for the non-mutated interaction with the respective TCRs. This will be the primary basis for investigating the relative energetic contribution of HLA-A2 molecules described in this chapter.

	1G4	A6	JM22	G10
E55	NA		NA	
E58				
Y59	NA		NA	
E63				
T64				
R65				
K66				
V67				
K68				
A69G				
H70				
Q72				
T73				
R75				
V76				
T80				
K146				
W147	NA			
A149G				
A150G				
H151				
V152				
E154				
Q155				
R157		NA	NA	
A158	NA			
Y159	NA		NA	
E161	NA	NA	NA	
T163				
E166	NA		NA	
W167	NA		NA	
R170	NA		NA	

Table 4.1 Characterisation of HLA-A2 binding residues

MHC residues within 6Å of the TCR/ pMHC interface are listed in the left column for each TCR. Residues are labelled "NA" if they do not fall within 6Å for that particular TCR. The residues are colour coded depending on the nature of their contact, blue to represent TCR contacts, orange for peptide contacts, green for both TCR and peptide contacts. Blank spaces indicate residues within 6Å of the interface with no TCR, peptide or MHC contacts. Due to the lack of TCR/ pMHC crystal structure for the G10 TCR, MHC residues were selected on the basis that they did not contact the GAG peptide, and whose mutation led to a more than 2-fold reduction in affinity. These residues are represented by red dots in the table. Adjacent residues that may interfere with the binding energy of each other are indicated by red or black connecting lines. Numbers located along the red line in between the spacing of the two blue dots indicate the reason(s) as to why that particular residue pairs are not considered clusters. Residues are not considered clusters if (1) their side chains are pointing in opposite directions, (2) TCR contacts are mediated by the peptide backbone and (3) if the residue does not contribute to the binding energetics (ΔΔG = 0)

4.3.2 Energetic contributions between independent residues are additive

The strategy described above for estimation to total contribution of TCR-MHC contacts to TCR-pMHC binding energy, is only valid if the single mutations only effect the contribution of the mutated residue, and that each residue contributes independently to binding. One way of validating this central assumption is to examine whether that differences in change in Gibbs Free Energy (ΔΔG) obtained for individual mutants are indeed additive.

To test if this is true, amino acid residues were distantly mutated in pairs, one each in the α1 and α2 chain and the resulting affinity to 1G4 or G10 TCR complex were determined by SPR on BIACore3000 (GE Healthcare) at 25°C. Figure 4.2 depicts a typical association and dissociation Biacore trace where 8 ascending concentrations of TCR were flowed onto chip-immobilised pMHC. The reaction was immediately repeated using the same TCR but in reverse descending concentration to demonstrate protein stability and robustness of the assay. As negative control, TCRs were flowed over anti-TNFα antibodies. The maximal response units (RU) for each concentration was plotted as a function of TCR concentration and curve fitted using the Langmuir Isotherm (Figure 4.2 inset). Affinity values were extracted from the curve and ΔG and ΔΔG of the interaction calculated as described earlier.

The tables in Figure 4.3 shows the ΔΔG of the TCR/ pMHC interaction when the residues were singly mutated, the theoretical ΔΔG if the two mutations are additive and the actual ΔΔG as measured by the resulting double mutants. Indeed, the results suggest that residues situated far apart contribute to the energetic composition of TCR/ pMHC interaction in an additive manner.

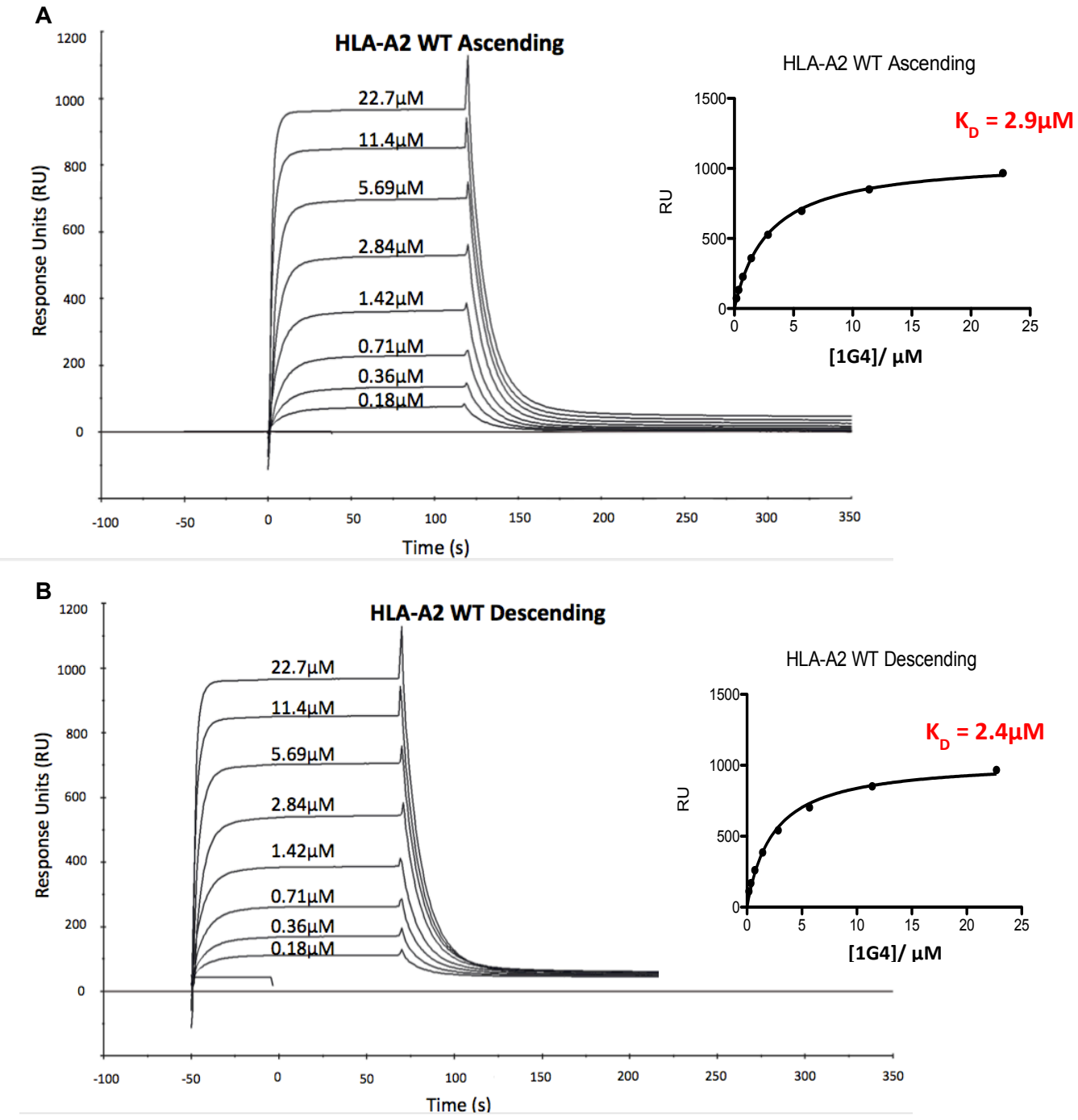

Figure 4.2 Representative Biacore binding data

(a) Eight serially diluted concentrations of TCR were flowed over pMHC-immobilised chips at ~1200 Response Units (RU). The maximal RU for each concentration was determined and plotted against the TCR concentration and curve fitted with the Langmuir Isotherm (inset). The dissociation constant is highlighted for each curve in red. (b) The same TCRs were immediately flowed over the same pMHC to demonstrate assay robustness.

A **1G4 TCR**

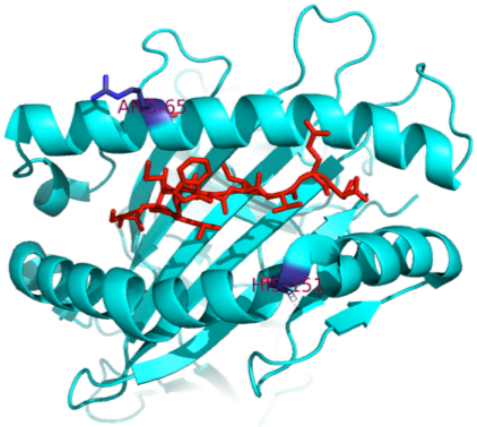

pMHC	ΔΔG (kcal.mol^{-1})
A69G	1.8 ±0.2
E154A	0 ± 0
Calculated	1.8
A69G, E154A	1.8 ± 0.04

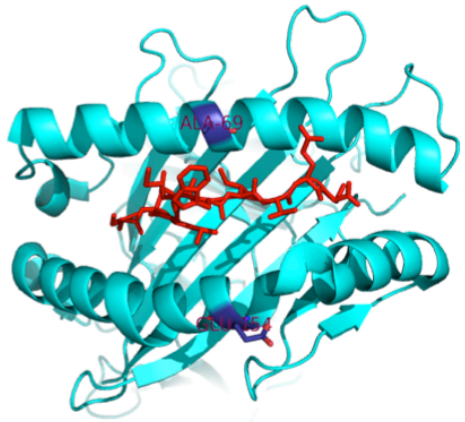

pMHC	ΔΔG (kcal.mol^{-1})
R65A	2.0 ± 0.05
H151A	0.5 ± 0.03
Calculated	2.5
R65A, H151A	2.5 ± 0.03

B **G10 TCR**

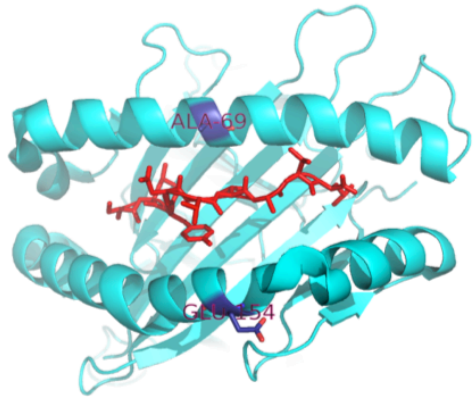

pMHC	ΔΔG (kcal.mol^{-1})
A69G	0.3
E154A	0.4 ± 0
Calculated	0.7
H151A, E154A	0.7

Figure 4.3 Residues situated far apart contribute independently to the TCR binding energy

Amino acids located on separate alpha strands of HLA-A2 were mutated singly or in unison (residues highlighted in purple) and their affinity were measured by Biacore 3000 at 25°C using a concentration series of the relevant TCR. Values in the table indicate mean ΔΔG (±SE) for at least three separate Biacore measurements. Calculated values indicate the theoretical ΔΔG values if mutated residues contribute independently to the binding energy. Residues located far apart in separate alpha chains contribute independently to TCR binding energy for both (A) 1G4 and (B) G10 TCR.

$\Delta\Delta G_{Mutant} = RT\ln(K_{D\text{-}WT}/K_{D\text{-}Mutant})$, where R = gas constant (1.98×10^{-3} kcal $K^{-1}mol^{-1}$), T = Temperature in Kelvin

4.3.3 Minimum binding energy contributed by HLA-A2 to different TCRs varies, ranging from 15-77%

The previous section demonstrated that residues located sufficiently far apart contribute independently to the energy of TCR/pMHC interaction, as might be expected. Residues located in close proximity, in clusters, are more likely to interact. In principle they may contribute to the binding energetics in the following manner:

(i) Independently

($\Delta\Delta G_{Double\ mutant} = \Delta\Delta G_{Single\ mutant\ 1} + \Delta\Delta G_{Single\ mutant\ 2}$)

(ii) Cooperate and enhance interaction

($\Delta\Delta G_{Double\ mutant} > \Delta\Delta G_{Single\ mutant\ 1} + \Delta\Delta G_{Single\ mutant\ 2}$)

(iii) Antagonise each other

($\Delta\Delta G_{Double\ mutant} < \Delta\Delta G_{Single\ mutant\ 1} + \Delta\Delta G_{Single\ mutant\ 2}$)

Given these possibilities, the most appropriate way to measure the contribution of clustered residues is to simultaneously mutate all the residues in the cluster and measure the overall change in binding energy.

To identify potential clusters (Table 4.1, blue dots), we analysed potential adjacent residues that preliminary analysis had suggested contributed to TCR binding (Zhang, 2010). These potential adjacent residue pairs, triplets (collectively known as clusters) are highlighted in Table 4.1 by connecting lines (both red and black). Residues were classified as potential clusters if:

(1) the residues side-chains were adjacent and pointing in the same direction.

(2) residue side chains made contact with the TCR

(3) mutation of the side chains resulted in a decrease in binding energy (ΔΔG <0)

Based on these criteria, no clusters were identified for the 1G4, JM22 or A6 TCRs. The provisionally-identified clusters are depicted as red connecting lines in Table 4.1, labelled by numbers 1,2 or 3 for the reasons why they are not classified as a cluster according to the above criteria. As such, we treat every single TCR contacting residues as residues contributing independently to the interaction.

Using similar criteria we identify three potential residue clusters: V76, T80; H151, E154; and T163, E166 in the case of G10 TCR, indicated by black connecting lines on the same table. These residues were mutated to alanine singly or in combination and their affinities for the G10 TCR determined; the results are presented in Table 4.5a. The cluster mutants exhibited variable cooperative effects, with V76A, T80A and T163A, E166A mutants demonstrating independent contributions to Gibbs free energy (ie additive effects). H151A, E154A mutants on the other hand resulted in a lesser, non-additive change in Gibbs free energy when combined indicating antagonism.

The difference in change of Gibbs Free Energy (ΔΔG) was compiled for TCR contacting HLA-A2 residues and presented in Figure 4.4 and 4.5 for the different TCRs. Also shown for each TCR are the sum of all the ΔΔG measured for each mutant (ΣΔΔG) and estimated contribution of TCR-MHC contacts to binding energy. We were unable to determine the affinity between A6 TCR and R65A mutant. To this end, we assume the affinity of the interaction to be lower than the lowest measurable affinities within our experimental system (K_D > 180μM), and the calculated ΔΔG value comes up to > 3.2 kcal/mol. This is in agreement with a recent study by

Piepenbrink et al who reported a similar value (3.3 kcal/mol) for the same interaction at 25°C (Piepenbrink et al., 2013).

Despite binding to the same HLA-A2 MHC, the minimum energetic contribution from MHC varies from one TCR to another, ranging from 15% (for JM22) to over 70% (for 1G4, A6 and G10).

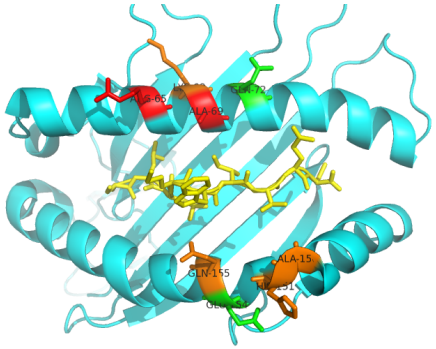

1G4 TCR

	K_D (μM)	ΔG (kcal/mol)	ΔΔG (kcal/mol)
WT	2.9	-7.5	NA
R65	81	-5.6	2.0
K68*	4.1	-7.4	0
A69	67	-5.7	1.8
Q72*	3.5	-7.4	-0.1
A150G	14	-6.6	0.8
H151	11	-6.8	0.5
E154	3	-7.5	0
Q155*	6.1	-7.1	0.3
		ΣΔΔG	**5.3**

HLA-A2/ 1G4 TCR Interaction:
Energetic contribution of HLA-A2 = 71%

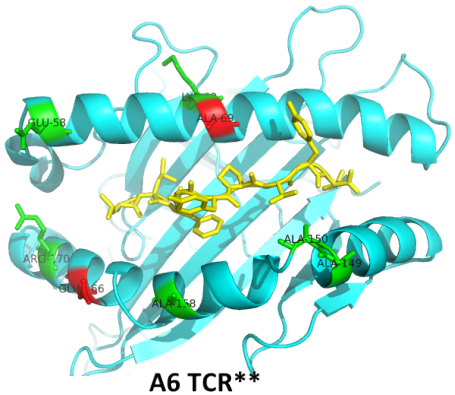

A6 TCR**

	K_D (μM)	ΔG (kcal/mol)	ΔΔG (kcal/mol)
WT	0.9	-8.3	NA
E58	0.6	-8.5	-0.3
R65	> 180	< -5.1	> 3.2
K68	1.2	-8.1	0.2
A69G	11.6	-6.7	1.5
A149G	0.7	-8.4	-0.2
A150G	1	-8.2	0.1
A158G	1.5	-8	0.3
E166	10.2	-6.8	1.5
R170	1.1	-8.2	0.1
		ΣΔΔG	**> 6.4**

HLA-A2/ A6 TCR Interaction:
Energetic contribution of HLA-A2 = >77%

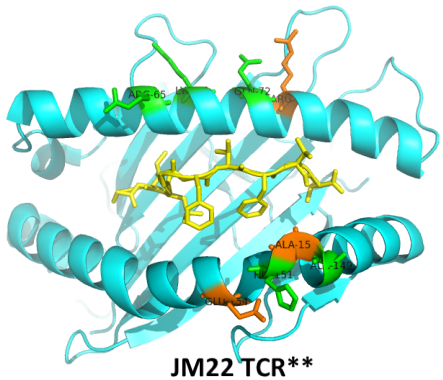

JM22 TCR**

	K_D (μM)	ΔG (kcal/mol)	ΔΔG (kcal/mol)
WT	5.3	-7.2	NA
R65	2.9	-7.6	-0.4
K68	8	-6.9	0.2
Q72	2.4	-7.7	-0.5
R75	18	-6.5	0.7
A149G	6.5	-7.1	0.1
A150G	11	-6.7	0.4
H151	5.3	-7.2	0
E154	15	-6.6	0.6
		ΣΔΔG	**1.1**

HLA-A2/ JM22 TCR Interaction:
Energetic contribution of HLA-A2 = 15%

Figure 4.4 MHC contributes 15% to 71% of the TCR binding energy

TCR contacting amino acids on HLA-A2 were mutated singly and their affinity, free energy and change in free energy relative to WT presented in table format. Mutated residues are presented for each HLA-A2 molecules and they are colour coded depending on the change in affinity; Red > 10 fold reduction in affinity; Orange 2-10 fold reduction in affinity; Green < 2 fold reduction in affinity. The energetic contribution of HLA-A2 for the respective TCR is presented in percentages under each table. Standard deviations (SD) for the ΔG and ΔΔG values lie within 10% for at least 3 separate Biacore measurements. Energetic contribution of MHC = $[(\Sigma\Delta\Delta G_{Mutants}) / \Delta G_{WT}] \times 100$

* / ** Values were derived from Zhang H (Zhang, 2010).

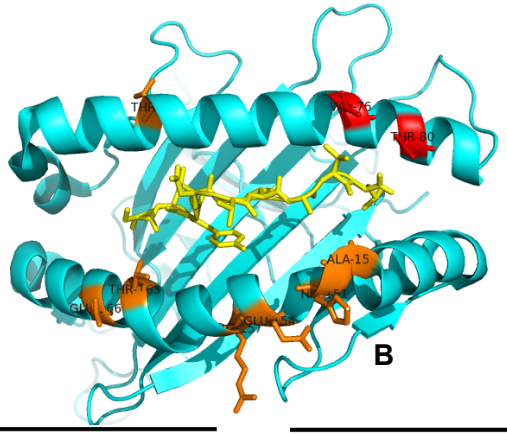

A

G10 TCR			
	K_D (μM)	ΔG (kcal/mol)	ΔΔG (kcal/mol)
V76	47	-5.9	1.1
T80	29	-6.2	0.8
V76, T80	222	-5	2
H151	34	-6.1	0.9
E154	14	-6.6	0.4
H151, E154	20	-6.4	0.6
T163	12	-6.7	0.3
E166	12	-6.7	0.3
T163, E166	21	-6.4	0.6

B

G10 TCR			
	K_D (μM)	ΔG (kcal/mol)	ΔΔG (kcal/mol)
WT	7.3	-7	NA
E55	22	-6.4	0.4
T64	33	-6.1	0.7
V76, T80	222	-5	2
A150G	24	-6.3	0.7
H151, E154	20	-6.4	0.6
R157	22	-6.4	0.4
T163, E166	21	-6.4	0.6
		ΣΔΔG	**5.4**

HLA-A2/ G10 TCR Interaction:

Energetic contribution of HLA-A2 = 77%

Figure 4.5 Energetic contributions of HLA-A2 for G10 TCR interaction

TCR contacting amino acids on HLA-A2 were mutated singly or in unison and their affinity, Free energy and change in Free Energy presented in table format. Mutated residues are presented for each HLA-A2 molecules and they are colour coded depending on the change in affinity; Red > 10 fold reduction in affinity; Orange 2-10 fold reduction in affinity. Change in Free Energy for singly and doubly mutated residues are presented in (A). The sum of change of Free Energy is calculated and presented in table (B). Standard deviations (SD) for all ΔG and ΔΔG values lie within 10% for at least 3 separate Biacore measurements.

Energetic contribution of MHC = $[(\Sigma\Delta\Delta G_{Mutants}) / \Delta G_{WT}] \times 100$

4.4 Discussion

The primary focus of the work presented in this chapter was to obtain estimates for the contribution of TCR/MHC contacts to the binding energy of the TCR/pMHC interaction. While there have been numerous studies delineating the structural footprint of the TCR on pMHC, only a handful of studies have attempted the more difficult task of defining the energetic footprint. These involved performing alanine scanning mutagenesis of the TCR (Lee et al., 2000, Manning et al., 1998), the peptide-MHC residues (Wu et al., 2002, Baker et al., 2001) or a combination of the two (Liu et al., 2012, Piepenbrink et al., 2013). A drawback of mutating the TCR is that many TCR residues contact both the peptide and MHC, making it difficult to estimate the contribution of the MHC. Previous studies did not always control for the possibility that MHC mutations could have long range effects, making interpretation difficult. Moreover, they did not account for the possibility that for MHC residue mutants may affect the peptide structure and its contacts with the TCR, making it difficult to decipher the exact energetic contributions of peptide and the MHC.

This study attempts to address these shortfalls by performing a thorough analysis of the contribution of the HLA-A2 class I molecule to the affinity of 4 different TCRs: 1G4, A6, JM22 and G10, informed by existing crystal structures of the interactions. MHC residues within 6Å of the TCR interface were systematically mutated to alanine residues (or glycine if they were alanine to begin with) and their affinities measured by a previous member of the lab (Zhang, 2010). Such mutation deletes all interactions made by atoms beyond the β carbon and provides an estimate of the

contribution to binding energy made by the missing portion of the side chain. Importantly, all of the mutants studied were able to bind with wild-type affinity to at least one of the 4 TCRs, ruling out the possibility that the mutation introduced long-range conformation changes in the pMHC binding surface.

Each single amino acid mutation may impact the TCR-pMHC binding affinity by three possible mechanisms: disrupting pre-existing contacts with TCR CDR loops exclusively, affecting peptide structure thereby influencing TCR binding indirectly, or a combination of both. The TCR-pMHC crystal for the various TCRs were further scrutinised and residues were categorised according to their contact patterns (Table 4.1). Contact residues were defined as residues within 4Å or each other; such is a conservative estimate as most non-covalent interactions fall within 4Å distance:

Non-Covalent Interactions	Distance (Å)
Ionic	2.5
Hydrogen Bond	3
van der Waal's Forces	3.5

Adapted from Molecular Biology of the cell, 5th edition

To determine the energetic contribution of MHC, only residues in contact with TCR only were selected. Since mutating peptide-contacting MHC residues may affect TCR-peptide contacts, observed changes in binding energy could be attributable to TCR-peptide rather than TCR-MHC contacts. As such, this approach allows a conservative, lower boundary estimation of the MHC's contribution to TCR-pMHC interaction, independent of the peptide's involvement.

To estimate the total contribution of MHC residues to the TCR-pMHC affinity we took advantage of the fact that within a protein/protein interface changes in binding energy observed following point mutation to Alanine are additive (Wells, 1990). However we first confimed that this additivity also applied to the pMHC complex by demonstrating that changes in free energies of binding following simulateous mutation of two residues not in contact was equal to the sum of change in binding energies observed when they were mutated individually.

Mutational effects of adjacent or 'clustered' residues may not be additive as they can influence each other. To investigate such effects, we reviewed potential clusters. Based on three criteria, we were able to rule out such effects for the 1G4, A6 and the JM22 TCRs. The first criteria, that residue side chains need to be truly adjacent and pointing in the same direction, assumes that the adjacent residue side chains are likely not going to influence each other if they are pointing in opposite directions. This is reasonable as the length of an amino acid (and by extension, distance between the side chains) is approximately 8-12Å long and this will most probably fall out of the reasonable length for any meaningful non-covalent interactions if the side chains are pointing away from each other. The rationale for the second criteria, that residues must contact the TCR via their side-chain rather than backbone atoms, follows that if a residue contacts the TCR exclusively via its peptide backbone, then side-chain interactions are unlikely to be relevant. Finally, if a residue, when mutated, does not alter the binding energy ($\Delta\Delta G = 0$), the residue is unlikely going to affect the contribution of neighbouring residues. Indeed, mutation of residues H151 ($\Delta\Delta G = 0.5$ kcal.mol^{-1}) and E154 ($\Delta\Delta G = 0$ kcal.mol^{-1}) in unison for the HLA-A2/ 1G4

complex yielded a molecule whose contribution to binding energy roughly equates that of H151 alone, $\Delta\Delta G = 0.4$ kcal.mol^{-1} (data not shown).

Whereas we were able to exclude any potentially non-additive mutants for 1G4, A6 or JM22 TCR interactions, several were identified for the G10 TCR interaction. In the absence of HLA-A2/ GAG/ G10 crystal structure, we chose non-peptide contacting residues in the HLA-A2 heavy chain that when mutated, had a >2 fold reduction in affinity. These clusters were investigated by examining the effect of single and double mutations on the binding energy. Of the three clusters two had residues that contributed independently of each other to the energetics of the interaction ($\Delta\Delta G$ were additive). The third cluster pair (H151, E154) when mutated together, resulted in a lesser, non-additive change in Gibbs free energy. Being oppositely charged these residues may screen each other such that mutation of H151 may increase an unfavourable negative potential associated with E154, and vice versa. Thus double mutation could remove an unfavourable electrostatic interaction introduced by the single mutation. Alternatively double mutation could induce local conformational changes that introduce additional TCR contacts.

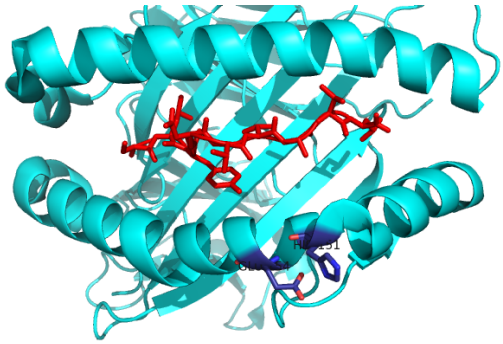

Figure 4.6 Close proximity between charged residues H151 and E154

The positively charged aromatic ring of H151 is situated in close proximity to the negative COO^- side chain of E154 (both highlighted in purple), providing the basis for potential residue interactions towards the same TCR contact.

The results suggest that the relative energetic contribution of MHC to TCR binding varies from one TCR to the other, ranging from 15% to over 70%. This range is consistent with studies performed on the 2C TCR systems using both alanine scanning mutagenesis for allogeneic 2C/ QL9/ L^D interactions (Manning et al., 1998) and tetramer studies for syngeneic 2C/ SIYR/ K^b systems (Lee et al., 2000). Both studies reported an approximately two-thirds of the energy attributable to interactions with MHC helices. In addition, comprehensive recent work by Piepenbrink et al also described a striking dominance of interaction (~60% of total binding energy) between A6 hypervariable CDR3α loop and the HLA-A2 α1 helix alone (Piepenbrink et al., 2013). Both our study and that by Pipenbrink et al identified R65 as the residue with the largest energetic contribution within the A6/ HLA-A2/ Tax interface.

Overall MHC contacts contributed ~70% of the binding energy. A similar contribution of MHC residues can be deduced from analysis of the single previous mutagenesis of a TCR/pMHC class II interaction (Wu et al., 2002). In this study of the cumulative energetic contribution of MHC II residues was between 55 and 75%. Substantial binding energy as a result of MHC contact has been interpreted as an evidence for MHC germ-line recognition where these contacts mediate inherent MHC reactivity by germ-line coded portions of the TCR (Manning et al., 1998). No such consistency was observed for the HLA-A2 system in study here, where the same MHC molecule was recognised to different extend by different TCRs. Although this does not preclude the fact that HLA-A2 molecules may have co-evolved with certain

TCR variable segment, as the TCRs investigated here were assembled from different germ-line encoded gene segments. The only shared segments are the TCR Vβ segments from the A6 and 1B4 TCR.

Variability of energetic contribution for the peptide or MHC can arise from two factors: length and flexibility of the associated CDR3 loops and the degree of peptide protrusion into the TCR CDR3 region or peptide "*flamboyancy*". TCRs with shorter CDR3 loops may be less able to contact the predominantly central peptide residues, leaving a higher proportion of interaction to CDR1/2 interaction with MHC alpha helices; such is the case for 2C TCR (Manning et al., 1998). On the other hand, TCR with longer CDR3 loops like LC13 span a larger surface area for contact with centrally located peptide residues (Borg et al., 2005). Likewise, the presence of a *flamboyant* peptide should encourage an increased role of peptide to the interaction. This is evident in a recent study involving HLA-B35 in complex with a 'super-bulged' peptide where approximately 55% of the energetic contributions can be traced back to the peptide molecule as a result of the lengthy, protruding peptide (Liu et al., 2012). Interestingly however, TCR-pMHC pair with the lowest MHC energetic contribution in this study came from JM22 TCR and its interaction with the virtually featureless MP peptide (Figure 4.7a). Not only was there a lack of prominent, protruding peptide, JM22 CDR3 loops are also the shortest among the TCRs under investigation, 21 residues for both CDR3 α and β as compared to 25 residues for both A6 and 1G4 TCR. Despite these features, MHC's energetic contribution remained low at 15%.

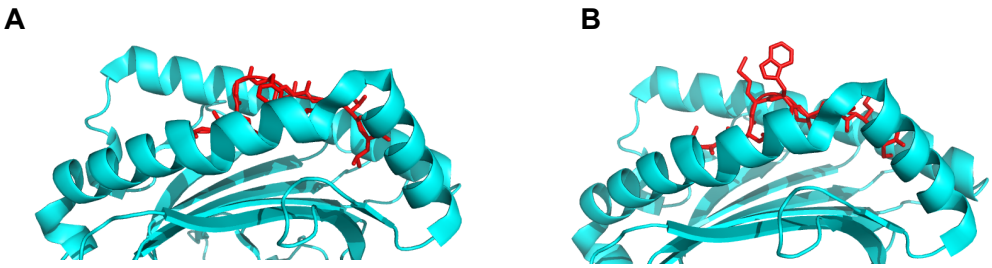

Figure 4.7 Featureless MP peptide versus the '*flamboyant*' OVA peptide

A side-on view of the peptide chain loaded onto HLA-A2 molecule. (A) The featureless MP peptide is derived from influenza virus matrix protein. (B) The ovalbumin peptide features a dominant methionine and tryptophan residue in its 4th and 5th position.

This is in stark contrast to the flamboyant peptide in display by the OVA peptide in the case of 1G4 TCR (Figure 4.7b) where over 70% of its energetic contribution can be attributed to the MHC alone. In fact, approximately 50% of the energetic footprint can be assigned to just two residues R65 and A69 on the MHC (Figure 4.4). This is reminiscent of a previous study identifying the same amino acid residues as hotspots for A6 TCR recognition (Baker et al., 2001). This shows that it is not possible to generalise the contribution of prominent peptide residues. One reason large peptide residues may not contribute to the binding energy is that there is a large entropic penalty associated with them binding as they lose flexibility. Nevertheless they can make an important contribution to specificity because they need to be accommodated by the TCR, even if they do not bind.

While alanine/ glycine scanning mutagenesis and double mutant cycles remain by far the most popular way to analyse protein energetics, a number of caveats exist. Firstly and perhaps most importantly, such techniques are often coupled with and advised by pre-existing crystallographic data that bears no representation of the

dynamic and plastic nature of the interacting surface. The cut off distance of 4Å for contacting residues may just be acceptable when it's based on crystal structures between 1.4-2.6Å resolutions in this study. Secondly, this method is unable to resolve energetic contributions for residues whose contacts are mediated by the peptide backbone and these may not be represented in the overall energy landscape. Thirdly, such approach may also lead to local or large-scale conformational change that would seriously impede binding and recognition. This was apparent for a triple HLA-A2 A149G, A150G, H151A mutation that abolished recognition by all the TCRs including a monoclonal anti HLA-class I (clone W6/32) antibody (data not shown).

Work described in this chapter featured the energetic contribution of HLA-A2 molecule to 4 different TCR systems. MHC's contribution can vary from as little as 15% for JM22 TCR to over 77% for A6 TCR, representing the range of percentages reported in other TCR systems including SB27, 2C and LC13 TCRs. While increased CDR3 lengths and protruding peptides in other receptor systems accounted for the improved relative peptide contribution; the reciprocal lack of lengthy CDR3 loops and protruding peptide did not result in an increased MHC contribution in the HLA-A2/ MP/ JM22 interaction. This suggests either that peptide contacts can sometimes play a dominant role in positive selection and/or that the contribution of MHC to TCR binding may be different for the positively selecting versus the antigenic peptide.

CHAPTER 5:

Binding Parameters and Functional Characterisation of a Supra-Physiological TCR

5.1.1 Introduction

Unlike its jawless counterparts, jawed vertebrates have evolved an elaborate adaptive immune system utilising T cell and B cell antigen receptors to provide durable protection against most pathogens. Conventional T cells are activated following the recognition of foreign peptide antigens by αβ T cell receptors (TCRs) in the context of cognate MHC molecules. Both self and foreign peptides are indiscriminately processed, loaded onto MHC molecules and presented to T cells, thereby 'delegating' the responsibility of ligand discrimination to T cells. Understanding the exact conditions leading to TCR triggering and activation have been an active field of research, the success of which would have implications to the design of therapies in diseases of autoimmune, infectious and cancerous origins.

The initial studies of this process focused on identifying and characterising the various molecules involved, including the signalling networks downstream of the TCR. Subsequent studies focused on using biophysical techniques to quantifying their interactions. Whilst these studies have provided crucial insights, a conceptual understanding of how and when the TCR would trigger remains unavailable. More recently mathematical modelling techniques have been introduced to provide a unifying framework for understanding existing biochemical and biophysical observations. To this end, accurately predicting how a T cell would respond under any stimulating conditions would be the goal for any T cell biologists.

This introduction outlines the unique challenges of antigen recognition by the TCR and reviews the studies that have been performed to date trying to understand the relationship between TCR-pMHC binding properties and T cell activation. It

concludes with a discussion of the use of TCRs with supra-physiological affinities, both as a tool to understand TCR recognition and for therapeutic purposes.

5.1.2 Modelling TCR- pMHC Interactions: How hard can this be?

The long lasting arms race against infectious organisms has warranted the evolution of a system in which a large, somatically-generated repertoire of TCRs is available that can recognize any potential pathogen, contributing to the clearance of most infections, as well as protection from a repeat infection. An important consequence of the way this TCR repertoire is generated is that all TCRs are able to bind, albeit at low affinity, to self peptides presented on MHC molecules. Features unique to TCR-pMHC interactions, exist to maximise efficiency of infection clearance while minimising any unnecessary collateral damage to self (Feinerman et al., 2008).

Specificity

Arguably the most important and intriguing aspect of TCR-pMHC interaction, the ability of TCRs to distinguish between foreign and self-peptide is a key feature of the adaptive immune system. Inappropriate activation of the TCR by self pMHC would lead to widespread and frequent events of autoimmunity, which is a relatively rare disease. Naturally, deciphering the mechanisms behind effective ligand discrimination has been the focus of many theoretical studies. The extent of TCR specificity can be appreciated in early studies and work described in this chapter where a single amino acid change on the pMHC is often sufficient to abolish TCR recognition (Sloan-Lancaster et al., 1993).

Sensitivity

Sensitivity to pathogen can be considered at a cellular/organismal or molecular level. T cells expressing TCRs specific for a novel pathogen are relatively rare in the primary T cell repertoire. In the event of an infection, foreign proteins are processed by resident professional antigen presenting cells such as dendritic cells and specially delivered to local lymph nodes via an efficient lymphatic system. This, together with continuous recirculation of naive T cells between lymph nodes, dramatically increases the likelihood of T cells coming into contact with their cognate pMHC. There, T cells would scan the surface of these APCs for the presence of any rare foreign peptides (in the range of tens to hundreds) in a 'sea' of irrelevant pMHC (~ 10^5-10^6). T cells with the cognate TCR would need to exercise great molecular sensitivity not only to ‘sniff out’ the low number of foreign pMHC, but also be fully activated when engaged. Indeed, calcium signals can be detected in the presence of only 1 cognate pMHC and this would scale linearly with calcium signals saturated at approximately 20 cognate pMHCs (Irvine et al., 2002, Purbhoo et al., 2004). Moreover, full cytotoxic functions were observed in the mere presence of 3 pMHCs (Purbhoo et al., 2004).

Speed

Speed is of the essence and can sometimes mean the difference between life and death in certain infections. Calcium signals are among the first measurable manifestations of a successful TCR signalling event, typically initiated between 0-5 minutes following APC – T cell contact (Wulfing et al., 1997). CD3ζ clustering followed shortly within 1 minute of calcium signalling with stable synapse formation established over the next 3-10 minutes (Krummel et al., 2000). Studies with

photoactivatable pMHC agonists revealed that an increase in Ca^{2+} is detected within 6s of TCR engagement (Huse et al., 2007).

Versatility

Another unique feature of TCR recognition is its ability to recognise different ligands and produce qualitatively distinct signals according to the affinity of the interaction (van der Merwe and Dushek, 2011). This is best demonstrated in the thymic selection of T cells during development where cells with TCRs that bind endogenous pMHC with a low affinity undergo positive selection. On the other hand, high affinity interactions with endogenous pMHC in the same environment will lead to T cell death by negative selection. How can the TCR differentiate between these two binding events?

Antagonism

A seemingly counterintuitive discovery about TCR-pMHC interaction is the fact that they can sometimes exhibit antagonistic behaviours where co-presentation of a second pMHC inhibits the activation of a T cell by a previously known agonistic pMHC. In one study as many as 40% of variants tested on an index peptide antagonized the response to the index peptide for certain TCR clones (Jameson et al., 1993). Early biochemical studies revealed the impairment of both proximal and downstream signalling pathways such as ZAP70 recruitment, inositol phospholipid hydrolysis and Erk phosphorylation as the molecular basis for ligand antagonism (Racioppi et al., 1996, Sloan-Lancaster et al., 1994). Two models have been put forward in an attempt to describe antagonism. Firstly, 'quantitative models' propose that antagonistic ligands out-compete agonistic ligands for TCR occupancy (Stotz et

al., 1999). On the other hand, 'qualitative models' suggest the transduction of negative signals by antagonistic ligands into T cells (Racioppi et al., 1996). One study suggested failure of an induced conformational change in the TCRα constant region when engaging an antagonistic pMHC (Beddoe et al., 2009).

Any satisfactory model relating TCR engagement of pMHC to signalling would need to account for the observed features of specificity, sensitivity, speed, versatility as well as antagonism. These unique requirements would indeed pose huge challenges in the attempt to model TCR-pMHC interactions.

5.1.3 Activation versus triggering models

A large number of different models have been described in relation to T cell antigen recognition. The focus in this section is to discuss models that try to explain the relationship between TCR-pMHC binding properties to T cell functional responses, hereafter termed T cell activation models. Arguably the most demanding requirement of these models is to account for the ability of the TCRs to recognise low densities of high affinity agonist or foreign pMHC in the 'sea' of irrelevant self-pMHC in events that happen in the range of seconds. T cell triggering models on the other hand (described in chapter 1) attempt to explain how signals are transduced across the cell membrane after a successful TCR-pMHC ligation event.

The oft-cited serial triggering model was first proposed to account for the observation that a relatively small number of agonist pMHC on an APC could lead to down-regulation of a far greater number of TCRs on the responding T cells (Valitutti et al., 1995, Valitutti and Lanzavecchia, 1997). The model proposes that a single pMHC can engage and trigger many TCRs in sequence, hence the term serial

engagement. This process is an inevitable consequence of the reversibility of the TCR-pMHC interactions and is implicit in all models described below.

5.1.4 T cell activation models

These models attempt to explain the relationship between TCR-pMHC binding properties and T cell response. The characterisations of TCR-pMHC binding parameters have largely been elucidated using the SPR technique using purified pMHC and TCR molecules. Since these are measured with one binding partner in solution they are often referred to a solution or 3D binding properties. Functionally relevant TCR-pMHC interactions however happen within a 2D contact interface. Direct measurements of 2D affinities reported large variations from the 3D measurements largely as a result of improved k_{on}, possibly due to signalling-induced receptor clustering (Huang et al., 2010, Huppa et al., 2010, Dushek and van der Merwe, 2014). Therefore, extra care is needed when correlating 3D to describe T cell functions.

Various reports have pointed to the importance of binding parameters, namely affinity and kinetics, in the ligand discrimination process [reviewed in (Stone et al., 2009)]. In its simplest format, the interaction can be described as:

$$\text{TCR} + \text{pMHC} \underset{k_{off}}{\overset{k_{on}}{\rightleftharpoons}} \text{TCR-pMHC}$$

Where k_{on} and k_{off} denotes the association and dissociation rates respectively. The Dissociation constant K_D, which is also the reciprocal of the affinity K_A can derived from its rate constant in the following relationship: $K_D = k_{off}/k_{on} = 1/K_A$. One key way to test a T cell activation model is to examine whether it can explain the relationship between solution TCR-pMHC binding properties and T cell activation. While many

studies have examined this relationship their findings have been somewhat contradictory (Tian et al., 2007, Holler and Kranz, 2003, Kalergis et al., 2001, Coombs et al., 2002). In some cases correlations are observed with k_{off} and in others with K_D, and there have been attempts to resolve these discrepancies (Aleksic et al., 2010).

Affinity model

The affinity model states that the number of TCR-pMHC bonds at equilibrium would determine the functional output of the interaction. In other words, T cell activation is related to the number of engaged TCR. This model predicts that ligands with a greater half-life will lead to greater number of TCR-pMHC bond formation and as a result, a greater degree of T cell activation (Figure 5.1a). However, the model also predicts that low affinity ligands (such as self pMHCs) would eventually produce T cell responses at high enough concentrations. Most studies supporting the affinity model typically do so by demonstrating a correlation between K_D and the EC_{50} (potency) of the interaction (Andersen et al., 2001b, Tian et al., 2007, Holler and Kranz, 2003). However such a correlation is also consistent with many other models (see below). One key prediction of the affinity model is the maximum response is independent of the k_{off}. Dushek et al showed that this is not the case, and that the maximum response instead correlated with the k_{off} ruling out the affinity model (Dushek et al., 2011).

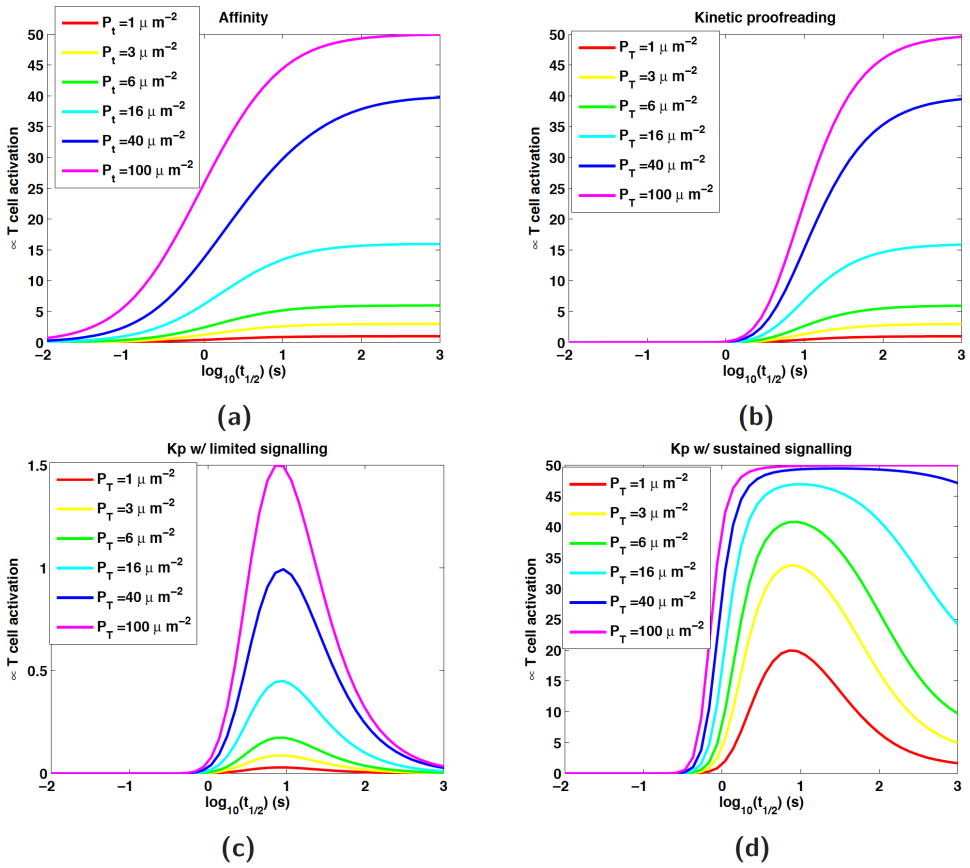

Figure 5.1 T cell activation as a function of pMHC half-life ($t_{1/2}$)

Mathematical predictions of T cell activation for different models with different values of half-life $t_{1/2}$ (and by extension k_{off}, since $t_{1/2}$ = ln2/ k_{off}). (a) The affinity model predicts greater T cell activation with extended half-life (or lower k_{off}) for all concentrations of surface ligands. T cell activation will therefore proceed for ligands with any half-life given sufficient surface concentrations (b) The basic kinetic proofreading model also predicts greater T cell activation with increasing half-life. Unlike the affinity model however, no T cell activation is observed below a critical half-life value even at high ligand concentrations. (c) The kinetic proofreading model with limited signalling [also known as the productive hit rate model in (Dushek et al., 2011)] extends McKeithan's kinetic proofreading model by postulating that an active TCR signals for a limited period even when TCR remains engaged to pMHC. The resulting model predicts an optimal half-life for maximal T cell activation at all concentrations of ligands. (d) The kinetic proofreading model with sustained signalling is based on Coombs et al (Coombs et al., 2002), where TCRs can remain in the signalling active state after pMHC dissociation. In this model, optimal half-life is only apparent at low concentrations of ligands.The modelling work described in this figure was performed by Melissa Lever (Dushek Group).

Basic Kinetic Proof reading model

The concept of kinetic proofreading to describe TCR specificity was first applied in 1995 by McKeithan (McKeithan, 1995). According to the model, ligation of a cognate pMHC to TCR would lead to an obligatory series of modifications, and signalling would only occur if the sequence of modification were complete. If the ligand dissociates at any time in the interval, the complex reverts to its original unmodified step (Figure 5.2). The kinetic proofreading model therefore provides a reasonable mechanism for a time lag separating ligand binding from receptor signalling and hence allowing a receptor to discriminate between ligands with small differences in off-rate (i.e. Specificity). This can also be visualized in Figure 5.1b where no amount of pMHC concentrations can induce TCR signaling for interactions with very high k_{off}.

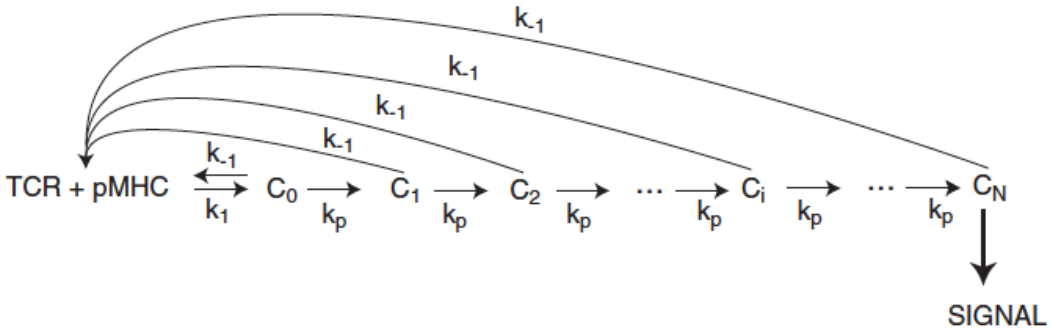

Figure 5.2 Schematic descriptions of the kinetic proofreading model

The original kinetic proofreading model as postulated by Mckeithan in 1995 (McKeithan, 1995). TCR binds pMHC with an association (k_{on}) rate of k_1 and a dissociation rate (k_{off}) of k_{-1}. Nascent complexes C_0 must undergo N modifications with a forward rate of k_p before a signaling competent complex C_N is generated. At every step, the TCR-pMHC complex may dissociate with rate k_{-1} where the reaction is completely aborted. In this way, the model provides a significant time lag with every step to allow discrimination between ligands with differences in their k_{off}. Figure adapted from Mckeithan (McKeithan, 1995).

In addition, the model proposes that TCR specificity would amplify in a non-linear way according to the number of proofreading steps involved. Our current

understanding of TCR signalling suggests multiple proofreading steps that could account for the delay. These include, for example, a need for sequential phosphorylation of TCR/CD3 ITAMs, ZAP-70 recruitment, ZAP-70 activation, phosphorylation of LAT by ZAP-70, and recruitment of effect enzymes (e.g. PLCγ1) and adaptor proteins to LAT. Why do longer TCR-pMHC engagements (before a productive signal) improve specificity? This can be better understood in the context of bound TCR-pMHC fractions. The fraction of bound TCR-pMHC decreases with time but this decreases more rapidly for TCR-pMHC interactions with lower half-life ($t_{1/2}$). As a result, an increase in threshold binding time for productive signalling magnifies small differences in dissociation times [see figure 1b in (Dushek and van der Merwe, 2014)].

Kinetic Proofreading with limited signalling

While the basic kinetic proofreading model offers an explanation for TCR discrimination, it alone is insufficient to describe some published findings. Most importantly the model cannot account for observations that in some systems there is an optimal ligand half-life, with increased half-life above the optimum leading to decreased T cell activation (Figure 5.1c) (Kalergis et al., 2001). One modification of the basic kinetic proofreading model was inspired by the aforementioned serial triggering model (Valitutti et al., 1995, Valitutti and Lanzavecchia, 1997). The key modification was to propose that the engaged TCR was only able to signal for a limited period, even if it remained engaged. This produced an optimal half-life because if the pMHC remained bound to TCR beyond this limited period it was unavailable to engage and serially trigger additional TCRs.

Kinetic Proofreading with sustained signalling

Another variation of this model by Coombs et al incorporates an additional state whereby the TCR continues to signal for an extended period of time even after ligand dissociation, before returning to its basal state via recycling of internalised TCRs (Coombs et al., 2002). Simulation of this model too predicts an optimum dwell time but only for low levels of ligand presentation (Figure 5.1d). At low or physiologically relevant concentrations of cognate pMHC, the requirements of serial triggering by the scarce ligands become a necessity, placing constraints on interactions with low k_{off} or long half-life (Valitutti et al., 1995, Valitutti and Lanzavecchia, 1997). At high cognate pMHC densities on the other hand, TCRs can be simultaneously engaged by abundant ligands, thus removing the need for serial triggering. Indeed, no impairment of T cell activation was observed experimentally at high concentrations of ligands with extended TCR-pMHC dwell times (Gonzalez et al., 2005).

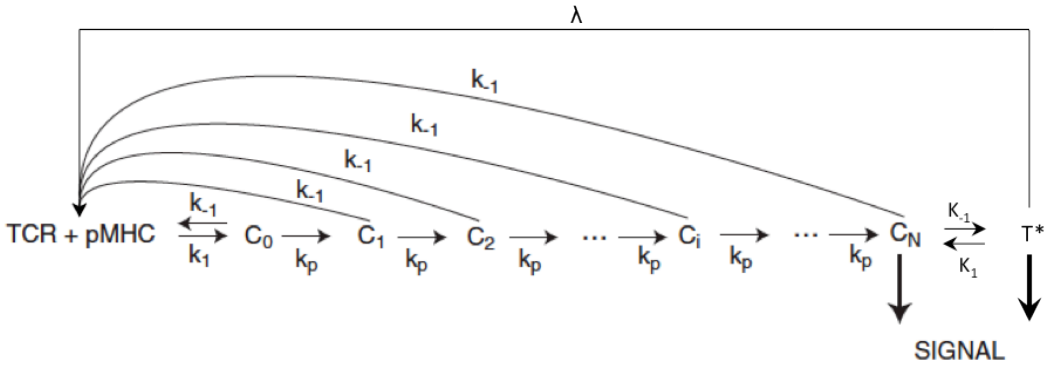

Figure 5.3 Schematic description of the kinetic proofreading model with sustained signalling

Initially proposed by Coombs et al (Coombs et al., 2002), the model suggests that productive signalling following TCR-pMHC binding necessitate the series of proofreading steps as described in the basic kinetic proofreading model described in Figure 5.1. Upon ligand dissociation, TCRs remain in the active signalling state T* before internalisation and recycled back onto the T cell surface at rate λ. This model predicts an optimal koff for T cell activation but only at low concentrations of cell surface ligands.

Additional modifications to the Kinetic Proofreading Model

More complex modifications to the kinetic proofreading model invoke additional mechanisms such as TCR signal integration as well as positive and negative feedback mechanisms. TCR signal integration can also cause neighbouring TCRs to be 'inhibited' or 'protected from ligand antagonism'. Such modification dramatically improves specificity of TCR responses at high ligand concentration albeit at a slight expense of receptor sensitivity (Chan et al., 2001).

Altan-Bonnet and Germain integrated receptor feedbacks mediated by Erk and SHP-1 within the kinetic proofreading framework. According to their model, TCR-pMHC ligation triggers Lck mediated ITAM phosphorylation as well as SHP-1 recruitment to Lck. SHP-1 would initiate negative feedback by dephosphorylating both Lck and ITAM residues. Positive feedback mechanism will only be initiated after digital activation of the MAPK pathway where Erk phosphorylates and prevents Lck from SHP-1 inhibition. This has been tested and verified in detailed experimental work (Stefanova et al., 2003).

More recently, Dushek and van der Merwe incorporated the concept of pMHC re-binding within the kinetic proofreading framework. pMHCs are likely to re-bind TCRs upon dissociation and the rate of re-binding increases with the formation and growth of TCR clusters. Induced rebinding was modeled by increasing the re-binding rate with each modification (step) in the proofreading scheme. Such modification greatly improves ligand specificity and sensitivity over the kinetic proofreading model (Dushek and van der Merwe, 2014).

Conclusion

The journey to describe the many unique characteristics of TCR signalling is challenging. T cell biologists have come a long way since the introduction of various models such as kinetic proofreading and serial triggering as a viable explanation for each of the unique TCR characteristics of specificity, sensitivity, speed and antagonism. In some cases very detailed models have been proposed with multiple parameters which produce a good description of the existing data. However, many such models could be compatible with the data and discriminating between them impossible but these are almost impossible to test. Powerful models instead rely on the integration of mathematical modelling and detailed experimentation.

5.1.5 Supra-physiological TCRs

An accurate model of how TCR-pMHC binding translates into T cell effector function will be invaluable in the rational design of therapeutic TCRs. While a fully functional model remains unavailable at present, there are some indications to suggest that TCR-pMHC interaction parameters can dictate the degree and extend to which T cell activates (Matsui et al., 1994). Moreover, TCRs with higher avidities* appears more efficient at clearing *in vivo* tumour and virally infected cells (Zeh et al., 1999, Alexander-Miller et al., 1996a, Soto et al., 2013). It is therefore of significant interest to generate TCRs with supra-physiological affinities beyond the normal range of 1-100μM as constrained by the requirements of thymic selection, and to study the tumorigenic or pathogenic effects of these TCRs in the context of T cell function and disease clearance.

*As it is not always possible to measure affinities for many TCR-pMHC interactions, the term avidity is used to describe the degree of TCR-pMHC association instead. Avidity described here is dependent on a number of variable parameters including affinity, receptor clustering and ligation of additional co-receptors or co-stimulatory receptors.

Generating Supra-Physiological TCRs

Stabilising TCRs for 'display' represents the major obstacle to generating supra-physiological TCRs. This is due to the reduced ability of TCRα and β chain to associate in the absence of mammalian chaperones. TCRs with enhanced affinities were first generated by Kranz and colleagues using yeast display techniques (Holler et al., 2000). This was done by expressing stabilised single-chain (V_β-linker-V_α) TCRs on the yeast surface as Aga-2-TCR fusion protein. The TCRs were first subjected to random mutations in the CDR3α chain using degenerate primers. Resulting PCR products were ligated into plasmid DNA and transformed into yeast, giving rise to a library of up to 10^5 or more clones. The TCR clones were then assessed and selected for their abilities to bind their respective ligands using flow cytometry. TCRs engineered for higher affinity using the yeast display system include the mouse 2C and 3.L2 TCRs, which represent class I- and class II- restricted TCRs respectively (Holler et al., 2000, Chlewicki et al., 2005, Holler et al., 2003).

An alternative system involves the use of phage display as a platform for directed evolution. TCRs of interests can be expressed on viral surfaces by fusion to the N-terminus of the viral coat protein. TCRs expressed this way were stabilised by a non-native disulphide bond between the α and β chain of the TCR (Boulter et al., 2003). Mutations were introduced using degenerate primers specific to CDR3α and β sequences. Enhanced-affinity TCRs were isolated by panning the phages through pMHC immobilised columns. Using this method, Boulter and Jakobsen managed to improve the affinity of a TCR specific for the tumour-associated NYESO-1-HLA-A2 pMHC by more than a million fold (Li et al., 2005).

A third display system was developed in mammalian cells, which involves the retroviral transduction of TCR α and β chains into TCR null hybridomas (Kessels et al., 2000). This system avoids the need for TCR stabilisation as the TCRs are fully refolded in their natural environment and assembled in their native conformation on the T cell surfaces. Mutations were again generated using degenerate PCR primers specific CDR3α, and affinity enhanced cells selected using FACS. Successful TCR maturation was described for the mouse 2C TCR in complex with the K^b/ SIY pMHC which saw a 15-fold improvement in affinity (Chervin et al., 2008).

Clinical Applications of Supra-Physiological TCRs

Generating TCRs with enhanced affinities represent a particularly attractive solution to the problem of cancer clearance where self-antigen affinities for cancer-specific TCRs are often too low. An advantage of this approach is that TCRs are able to recognize peptides derived from intracellular antigens, such as telomerase (Vonderheide, 2002) and survivin (Andersen et al., 2001a).

Supra-physiological TCRs can be introduced as therapeutic agents in several forms, the most promising of which involves the adoptive transfer of engineered T cells. Under such circumstances, T cells from a patient are isolated, retrovirally-transduced with the TCR of interest, and re-infused into the body. Early versions of adoptive T cell transfer only involved the re-introduction of non-transduced, ex vivo stimulated polyclonal lymphocytes (Rapoport et al., 2005). This generates a population of T cells with reduced activation threshold, facilitating the restoration of lymphocytes in the event of lymphopenia (e.g. leukaemia patients). Next came the selective infusion of autologous tumour-infiltrating lymphocytes (TILs – lymphocytes with anti-tumour

responses) with variable degrees (13% to 72%) of responsive rates (Morgan et al., 2006, Morgan et al., 2010). However, TILs may not always be available in every patient for every cancer. Such problems can be circumvented with the advent of genetics techniques that permitted the introduction of rationally designed TCRs that would represent effective TIL clones into autologous T cells isolated from patients. Such possibilities propel the realisation of the ultimate objectives of adoptive T cell therapy, which has been to recapitulate the end result of a successful T cell vaccine. This includes the robust maintenance of antigen-specific T cell functions and numbers in the event of a challenge (Kalos and June, 2013).

There has been extensive research into the use of supra-physiological TCRs in several human cancers targeting antigens such as MART-1 (melanoma), NYESO-1, MAGE-A3 (cancer testis) and WT1 (leukaemias) [reviewed in (Stone and Kranz, 2013)]. As TCRs are inherently restricted by MHC presentation, much attention has been focused on cancer antigens presented on HLA-A2, an allele expressed by ~40% of the Caucasian population. Indeed, all examples mentioned in this review and chapter study involve the HLA-A2 system.

MART-1, an antigen specific for the melanocyte lineage, exemplifies initial research attempts at improving efficacies of adoptive T cell transfers. The first T cell clone DMF4 with an affinity (K_D) of 170μM for the MART-1 antigen/HLA-A2 complex was isolated from a melanoma patient (Hughes et al., 2005). DMF4 achieved a modest 13% response rate following adoptive T cell transfer in lymphopenic metastatic melanoma patients (Morgan et al., 2006). A second generation T cell clone referred to as DMF5 with an improved affinity of K_D 40 μM achieved a more encouraging

response rate of 30%. However, patients infused with DMF5 also exhibited destruction of normal melanocytes in the eye, skin and ear (Johnson et al., 2009). These studies underscore the feasibility of adoptive T cell transfers as treatment therapies and also the importance of assessing valid T cell targets to avoid collateral on target/ off tumour effects.

Other potential consequences of in vivo use of affinity-enhanced TCRs can be highlighted by a recent MAGE-A3 cancer testis antigen study. High-avidity MAGE-A3 A118 TCR used in the adoptive T cell transfer study was generated by rational CDR3 loop mutations of TCRs derived from MAGE-A3 vaccination of HLA-A2 transgenic mice (Chinnasamy et al., 2011). While clinical regression was recorded in 5 of the 9 patients, unexpected neurological toxicities were observed in 3 patients, including 2 deaths. Subsequent autopsies revealed high levels of $CD8^+$ T cell infiltration with extensive gliosis and microglia activation (Morgan et al., 2013). Explanation for the phenomenon was pinned down to the cross-reactivity of A118 TCR with MAGE-A12 antigen, whose expression in human brain was unidentified until then (Morgan et al., 2013).

Despite the setbacks, studies on the adoptive transfer of supra-physiological 1G4-α95LY TCR (730nM) against testis cancer antigen NYESO-1 painted a positive outlook with low toxicities and high response rate of 45% and 67% in patients with metastatic synovial cell sarcoma and melanoma respectively (Robbins et al., 2011).

Nevertheless, cross- and auto-reactivity issues for supra-physiological TCRs still demand important considerations to be addressed for any adoptive T cell transfer therapies. Multiple studies have led to the appreciation of co-receptor involvement

in mediating supra-physiological TCR cross-reactivity prevalence (Zhao et al., 2007, Zhong et al., 2013, Holler and Kranz, 2003, Holler et al., 2003, Soto et al., 2013). Supra-physiological TCR cross-reactivity especially with self-pMHC, seems to depend on CD8 expression (Holler and Kranz, 2003, Holler et al., 2003, Zhao et al., 2007). This is probably a biased observation due to lack of sampling where almost all investigated supra-physiological TCRs are MHC class-I restricted. On the other hand, there is evidence that suggest a fundamental difference in the activation threshold of $CD4^+$ (~10 μM) T cells and $CD8^+$ (~300 μM) T cells for self-pMHCs as a result of co-receptor synergies (Stone and Kranz, 2013). Indeed, CD8 participation have been shown to further enhance the sensitivity of a TCR to its class-I MHC ligand by up to a million-fold (Holler and Kranz, 2003).

As such, there is a general consensus to preferentially transduce class-I specific supra-physiological TCRs into $CD4^+$ T cell. Apart from the higher affinity threshold for self-pMHC in $CD4^+$ T cells, $CD4^+$ T cells also regulate cytokines that elicit anti-tumour activities that can also promote the survival, proliferation and effector functions of $CD8^+$ cytotoxic T cells (Quezada et al., 2010, Antony et al., 2005). The heightened affinities of supra-physiological TCR would also relinquish any requirement for CD8 co-receptor binding, permitting CD4-specific T cell activities in vivo. Indeed, the only study resulting in the long term control of established tumours was performed with $CD4^+$ T cells transduced with a class-I specific supra-physiological (K_D) 30nM TCR (Soto et al., 2013). $CD8^+$ T cells transduced with this receptor were rapidly deleted *in vivo*, while $CD4^+$ T cells transduced with the high-affinity TCR exhibited superior tumour-control properties as compared to the WT TCR (K_D = 30μM). Interestingly, supra-physiological $CD8^+$ T cells were eventually deleted in vivo. It is important to

ensure that such effects are not an artefact of the experimental systems and can be reproducible in multiple systems.

To summarise, despite the successful anti-tumour effects of supra-physiological TCRs in vivo there are a number of serious caveats, particularly with TCR cross-reactivity and off-target activities. While limited successes were observed in certain TCR systems, there are increasing attempts to focus on adoptive T cell transfers of $CD4^+$ T cells alone. More work is necessary to decipher the value of synergistic or antagonistic receptor cross-talk between the supra-physiological TCR and various co-receptors and co-stimulatory receptors.

5.2 Project aims and objectives

An accurate understanding of the TCR-pMHC interaction is crucial, not just for the satisfaction of solving an age-old problem, but also for the rational design of effective therapeutic TCRs.

While a number of mathematical models have been formulated for the interaction, constraints on the availability of experimental tools have hindered the systematic analysis of the various mathematical models. For example, the limited affinity range of physiological TCRs (1-100μM) is insufficient for testing the validity of the various mathematical models. As represented in figure 5.2, clear discrimination between different models may require TCR-pMHC interactions whose $t_{1/2}$ ranges between 6 log values or a million-fold.

In addition, many published data that were suggestive of the mentioned T cell activation models were really only based on a limited number of data points for each

TCR that were not representative of a full stimulation curve [e.g. 3-5 pMHC concentrations in (Francois et al., 2013, Gonzalez et al., 2005)].

In order to resolve the difference between the various T cell activation models, we generate a panel of supra-physiological TCR-pMHC interactions with affinities that varies 10^5-fold by mutating key residues within the cognate pMHC. These reagents were tested for their ability to activate T cells transduced with the supra-physiological TCRs across a large range of concentrations. Results from these studies will help inform the validity of the various mathematical models presented in introduction.

5.3.1. Comprehensive Analysis of 1G4^{hi} TCR and HLA-A2/NYESO-1 contact

In this study, we utilise the 1G4 c58/c61 supra-physiologic TCR (hereby referred to as the 1G4^{hi} TCR) as a uniquely useful tool in the analysis and validation of TCR signalling models, since it is much easier to identify ligand variants with a reduced affinity than vica versa. Since 1G4^{hi} TCR has affinity of 70pM for the NYESO-1/9V index peptide (hereby referred to as 9V peptide; peptide residue number 9 + altered residue Valine), it is theoretically possible to generate a panel of pMHC ligands with a wide range of affinities, ranging from well above to below the usual affinities. Choice of the 9V peptide instead of the natural 9C ligand was informed by the improved stability and the stimulatory capacity of the 9V peptide (Bownds et al., 2001, Chen et al., 2000). Conserved mutations affecting MHC residues with limited contact with TCR residues would generate TCR-pMHC complexes with modest changes in the affinity. Changes to pMHC residues mediating close contacts with TCR residues on the other hand, would lead to a more drastic reduction in affinity.

The 1G4^{hi} TCR described in this work was first generated via phage display methods by Boulter and colleagues (Li et al., 2005). The co-crystal of the TCR and its cognate pMHC, HLA-A*0201/ SLLMWITQC was later crystallised (Sami et al., 2007) and unsurprisingly, differences between the wild type 1G4 TCR and the high affinity variant are largely centred on the CDR 2 and 3 region of the TCR (Figure 5.4).

The availability of the co-crystal offers a great vantage point for examining residues mediating close contacts between the 1G4^{hi} TCR and HLA-A2/9C. HLA-A2 residues within 6Å from the plane of the TCR-pMHC interface (based on the 1G4-WT crystal) were examined and their close contact residues on the 1G4^{hi} TCR molecules identified (Table 5.1). Close contacts in this case were defined as any TCR residues with atoms within 4Å of the selected 1G4^{hi} TCR residues. For comparison, the analysis was also performed on 1G4-WT TCRs, based on the structure described by Cerundolo and colleagues (Chen et al., 2005). Contact residues and distances between HLA-A2 and both the 1G4-WT or 1G4^{hi} TCR are largely similar. Similar proximity analysis of the peptides to the TCR was also performed and is presented in Table 5.2. Note the extensive TCR residue contacts by peptide residues 4M and 5W for both 1G4-WT and 1G4^{hi} TCR.

A

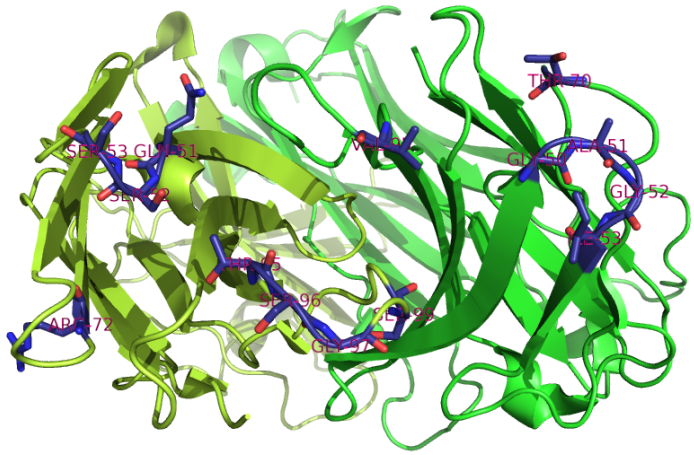

B

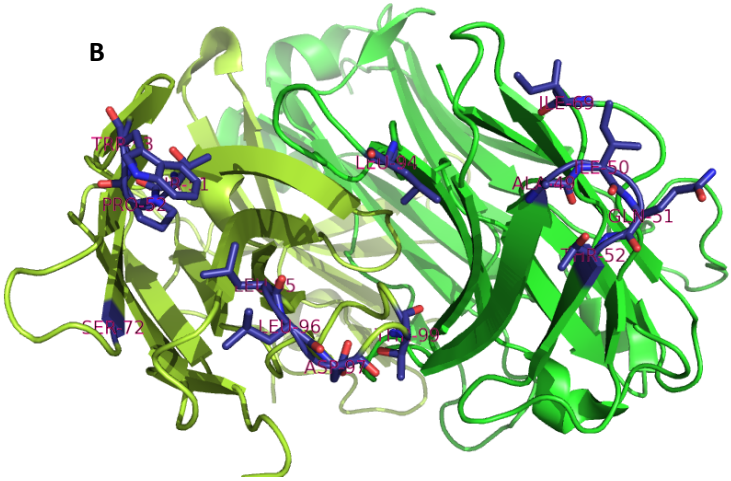

C

ALPHA			BETA		
WT		HI	WT		HI
Q	51	T	G	50	A
S	52	P	A	51	I
S	53	W	G	52	Q
R	72	S	I	53	T
T	95	L	T	69	I
S	96	L	V	95	L
G	97	D			
S	99	T			

Figure 5.4 Comparison of mutated residues between 1G4-WT and 1G4^{hi} TCRs

Difference in residues between (a) Wild-type 1G4 TCR and (b) 1G4^{hi} TCR are highlighted in purple. TCR alpha chain is denoted in light green while the beta chain is presented in a darker shade of green. (c) A list of the 14 amino acid residue changes is presented in table form. Residues in the table are colour coded depending on their respective CDR loop positions. Light green = CDR2α; Darker green = CDR3α; Light blue = CDR2β; Darker blue = CDR3β. The crystal structures are derived from Sammi et al for 1G4^{hi} [PDB:2P5E; (Sami et al., 2007)] and Chen et al for 1G4-WT [PDB: 2BNR (Chen et al., 2005)].

	1G4^{hi}		1G4-WT	
HLA-A2	**Nearest TCR Contact**	**Distance**	**Nearest TCR Contact**	**Distance**
R65	G98, T99 | Y46, V48, D54	2.8, 3.9 | 3.3, 3.8, 2.9	G98, S99, Y100 | Y47, D55, V49	2.9, 3.9, 4.5 | 3.3, 3.4, 3.6
K66	Y100	3.6	Y100, G98	3.6, 3.8
A69	Y100 | V48, L94	3.6 | 3.9, 3.8	Y101 | V49, V95, E29	3.6 | 4, 4.2, 4.7
Q72	E28, V48, A49, I50, I69	3.6, 4, 3.6, 2.9, 3.7	T70, A51, E29, G50, V49	2.9, 3, 3.4, 3.7, 3.9
T73	E28	2.7	E29, V95	2.8, 3.5
V76	N26, I69	4, 3.5	N27	4.1
A150	N96	3.3	Q51| N97	2.8 | 3.6
H151	W53	3.7	Q51, Q54, S53	3.4, 3.8, 4.2
E154	W53	3.5	S53, Q54	3.9, 4.7
Q155	Y31, W53 | N96	2.9, 3.7 | 3.5	Y31, T95	3.3, 3
T163	L96	3.7	S96	4.8

Table 5.1 Comprehensive analysis of distances between HLA-A2 residues and 1G4^{hi} or 1G4-WT TCR

HLA-A2 residues within 6Å of from the plane of the TCR-pMHC interface were examined and their close contact residues on the 1G4^{hi} TCR molecules were identified using the Pymol analysis software. Close contact resides were defined as residues within 4Å of each other. Black residues denote TCRα chain contact while red residues depict TCRβ chain contact. Residues are underlined if they represent altered residues between 1G4-WT and 1G4^{hi} TCR.

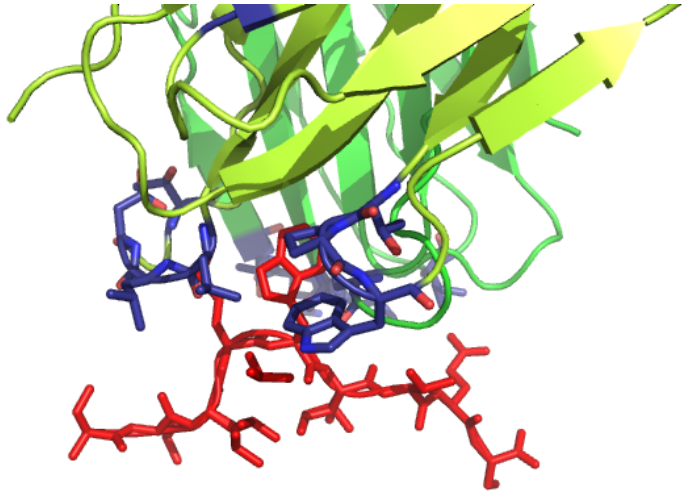

	1G4^{hi}		1G4-WT	
Peptide	Nearest TCR Contact	Distance	Nearest TCR Contact	Distance
S1	L96	6	G97	6.8
L2	L96	6.5	S96	6.9
L3	Y100	5	Y100	5
M4	P94, L95, L96, D97, G98, T99, Y100	3.5, 3.3, 3.7, 3.5, 3.3, 3.6, 2.5	Y100, G98, S96, P94, T95, G97, S99	2.7, 3.4, 3.4, 3.6, 3.7, 3.9, 3.9
W5	Y31, R93, P94, L95, Y100 | Y93, L94, L95	3.4, 3.9, 2.9, 3.8, 3.9 | 4, 3.5, 3.6	P94, Y31, T95, R93 | V95, G96, Y94	3, 3.4,3.6, 4 | 3.2, 3.6, 4
6I	E28, L94, L95, N96	4.6, 3.1, 3.5, 4.9	V95, G96	2.9, 3.5
7T	Y31, L94, L95, N96	4.4, 4.9, 3.7, 2.7	N97, G96	2.6, 3.8
8Q	M25, N26, E28, Y93	4.8, 2.9, 2.9, 3.5	N27, E29, Y94	2.9, 2.9, 3.6
9C	E28, Y93	7.7, 8.2	E29	7.7

Table 5.2 Comprehensive analysis of distances between NYESO-1$_{157-165}$ peptide SLLMWITQC and 1G4^{hi} or 1G4-WT TCR

TCR residues closest to individual peptide residues were systematically analysed using Pymol software and the closest distance recorded. Residues in black denote TCR α chain contact while red residues depict TCRβ chain contact. Residues are underlined if they represent altered residues between 1G4-WT and 1G4^{hi} TCR. A crystallographic structure shows the 1G4^{hi} TCR in contact with peptide (with HLA-A2 not shown). The crystal structures are derived from Sammi et al for 1G4^{hi} [PDB:2P5E; (Sami et al., 2007)].

5.3.2 Generating pMHC variants with 10^5-fold affinity range for $1G4^{hi}$ TCR

Three strategies were used in an attempt to reduce the affinity of pMHC for the $1G4^{hi}$ TCR back to the physiological range, based on the analysis from Tables 5.1 and 5.2.:

(i) Mutating residues on HLA-A2 α1 and α2 strands mediating TCR contacts;

(ii) Utilising altered peptide ligands;

(iii) Utilising altered peptide ligands in combination with mutated HLA-A2 molecules.

To disrupt $1G4^{hi}$ TCR binding, selected HLA-A2 residues were mutated to alanine (or glycine if they were alanine to begin with) and complexed with either the 9V index peptide or any other altered peptide ligands. HLA-A2 molecules were annotated in this study by their mutated residue numbers; followed by the position and amino acid of the altered peptide ligand (e.g. 72,75/ 5P denotes HLA-A2 molecules with alanine mutations in its 72^{th} and 75^{th} residue in complex with the SLLMPITQV peptide; while WT/5P denotes a wild type HLA-A2 molecule in complex with the SLLMPITQV peptide).

Soluble pMHC variants were generated via *in-vitro* refolding of bacterially produced HLA-A2 heavy chains, β2-microglobulin and the altered peptide ligands. The heavy chains also contain a BirA-tag for biotinylation using BirA enzymes and biotinylated pMHC variants were purified by gel-filtration.

Binding of the $1G4^{hi}$ TCR to pMHC variants were analysed by SPR on BIAcore 3000 (GE Healthcare) at 37°C. The association and dissociation phase were curve-fitted and their respective kinetic parameters (k_{on} and k_{off}) extracted. Figure 5.5a

demonstrates a typical association and dissociation curve from a single-cycle kinetics analysis between a high affinity TCR-pMHC interaction (WT/9V, K_D = 88 pM). Only one single concentration of TCR was used in this case as a result of the long experimental time where TCR dissociation occurs in the range of hours. Figure 5.5b depicts typical association and dissociation phases for multiple TCR concentrations with interaction towards the physiological range (WT/8K, K_D = 0.13 μM). The binding parameters are presented in orders of decreasing affinity in Table 5.3.

A five-order range of affinities was achieved for the various pMHC mutants. Reduction in affinity is mostly brought about by the increase in off rate, as k_{on} remains largely similar (ranging between 2 x 10^5/s to 1.88 x 10^6/s). Consistent with the data presented in the previous section, changes in peptide (using altered peptide ligands) generally resulted in a more drastic reduction of affinity, as compared to changes in HLA-A2 residues. As such, the use of certain altered peptide ligands (e.g. 4D, 5P) can function as a 'coarse tune' and the mutation of residues on HLA-A2 functioning as the 'fine tune' for changes in affinity.

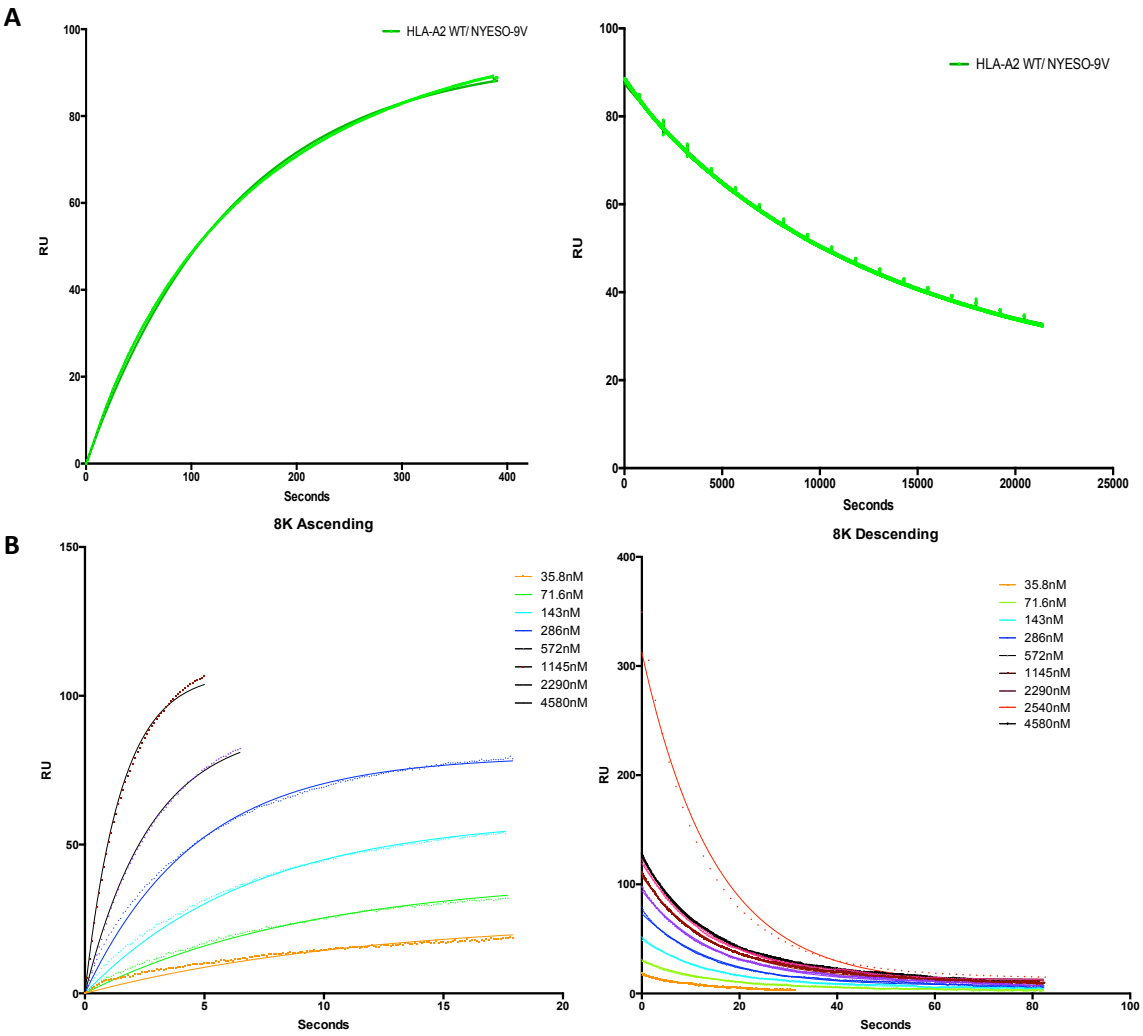

Figure 5.5 Kinetics measurements of pMHC variants to 1G4^{hi} or 1G4-WT TCRs

Representative SPR measurements of (a) a single injection of 1G4^{hi} TCR over an immobilized, high affinity ligand (~120 RU) represented by HLA-A2/ 9V complex in this case. (b) Multiple 1G4^{hi} concentration injections over immobilized, lower affinity ligands (~120 RU) represented by HLA-A2/ 8K. Note the difference in dissociation time between the high affinity interaction (~ hours) and the low affinity interaction (~ minutes). Both association and dissociation of 1G4^{hi} and the immobilized ligands were curve fitted for the derivation of k_{on} and k_{off} values (see Methods and Materials).

	k_{off}	k_{on}	K_D
72,75/9V	7.8E-05	1.9E+06	4.2E-11
WT/9V	8.7E-05	9.9E+05	8.8E-11
163, 166/ 9V	1.3E-04	1.0E+06	1.3E-10
151, 154/9V	1.5E-04	6.8E+05	2.3E-10
150, 151/ 9V	4.8E-04	6.7E+05	7.2E-10
72, 75/ 4A	1.1E-03	9.4E+05	1.1E-09
WT/4A	1.5E-03	1.2E+06	1.3E-09
76,80/ 9V	1.4E-03	8.6E+05	1.7E-09
WT/ 8S	5.9E-03	2.0E+06	3.0E-09
WT/ 5Y	4.5E-03	1.4E+06	3.3E-09
69, 154/ 4A	7.6E-03	8.2E+05	9.3E-09
69, 154/8S	8.6E-02	1.3E+06	6.6E-08
WT/ 4D	1.5E-02	1.7E+05	8.4E-08
WT/ 5F	1.2E-01	1.4E+06	8.8E-08
WT/6T	9.2E-02	9.5E+05	9.6E-08
76, 80/ 8S	6.4E-02	6.0E+05	1.1E-07
WT/8K	6.8E-02	5.1E+05	1.3E-07
69, 154/ 5P	1.8E-01	3.2E+05	5.7E-07
69, 154/ 8K	4.8E-01	6.8E+05	7.1E-07
WT/ 8E	2.8E-01	3.3E+05	8.4E-07
WT/ 5P	7.8E-01	9.1E+05	8.6E-07
69,154/ 5F	1.1E+00	9.2E+05	1.2E-06
72, 75/ 5P	3.6E-01	2.1E+05	1.7E-06

Table 5.3 Kinetics and affinity values of pMHC variants for 1G4^{hi} TCR

k_{on}, k_{off} and K_D values (in units $M^{-1}s^{-1}$, s^{-1}, and M, respectively) were determined by SPR and are arranged by ascending K_D. The values shown are the means of at least 3 separate measurements at 37°C. The SEMs were less than 2% of the respective k_{off} or k_{on} mean values with the following exceptions: SEMs for k_{on} determinations for 69,154/5F; WT/5Y; 69,154/8K and WT/8E were 3.51%, 2.14%, 4.04% and 2.28% of their means, respectively. The K_D measurements for 72,75/ 5P was derived from both kinetic and equilibrium binding analysis.

5.3.3 Jurkat T cell activations by pMHC variants

To investigate the relationship between the various binding parameters (k_{off}, K_D) and T cell activation, $1G4^{hi}$ TCR were stably transduced into Jurkat T cells expressing the CD8a co-receptors (Figure 5.6). These Jurkat T cells were also stably transfected with an NFAT-Luciferase reporter system, which allows effective monitoring of TCR signalling pathways associated with the activation of the NFAT transcription factor, notably increases in cytosolic calcium.

Biotinylated pMHC variants were titrated at a 1.5-fold dilution across streptavidin-coated 96 well plates. To control for the level of pMHC immobilisation onto the streptavidin-coated plates in every experiment, a control replica plate was prepared using the same batch of pMHC and the level of immobilisation verified using a conformationally sensitive anti-HLA-Class I monoclonal antibody W6/32 (Figure 5.7a). The immobilised levels were normalised against an index pMHC.

For stimulation, $1G4^{hi}$-expressing $hCD8a^{+}$ NFAT-Luciferase Jurkat T cells were added onto the test plates overnight and the levels of luciferase production as a result of downstream NFAT activation were assayed after coelentarazine-H substrate addition using a plate reader ($Pherastar^{Plus}$, BMG Lab Tech). The results are plotted on Figure 5.7b, where the normalised pMHC concentrations were plotted against the bioluminescence as a result of NFAT-Luciferase activity. The data were fitted using a standard Gaussian function on a log scale.

Unexpectedly, almost all pMHC variants tested displayed an optimal pMHC concentration with respect to NFAT-Luciferase expression. A Gaussian function was used to fit the data. pMHC concentrations inducing maximal luciferase activities

correlated with increasing affinities (lower K_D and k_{off}) of the TCR-pMHC interaction (Figure 5.11).

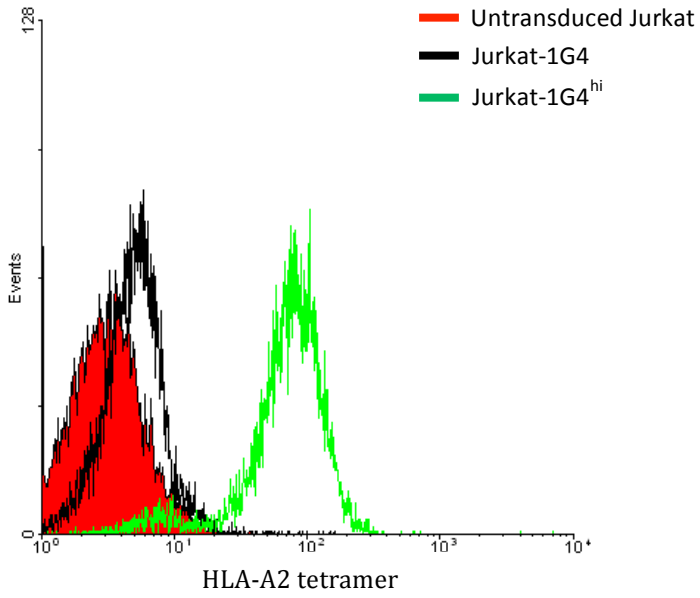

Figure 5.6 Lentiviral transduction of 1G4^{hi} into Jurkat T cells

Untransduced (red), 1G4-WT (black) or 1G4hi (green) TCR transduced T cells were stained for surface TCR expression using HLA-A2 tetramers conjugated with Phycoerythrin (PE) and analysed using FACS. The HLA-A2-PE tetramers were provided by Dr Annika Bruger and Professor Oreste Acuto, University of Oxford)

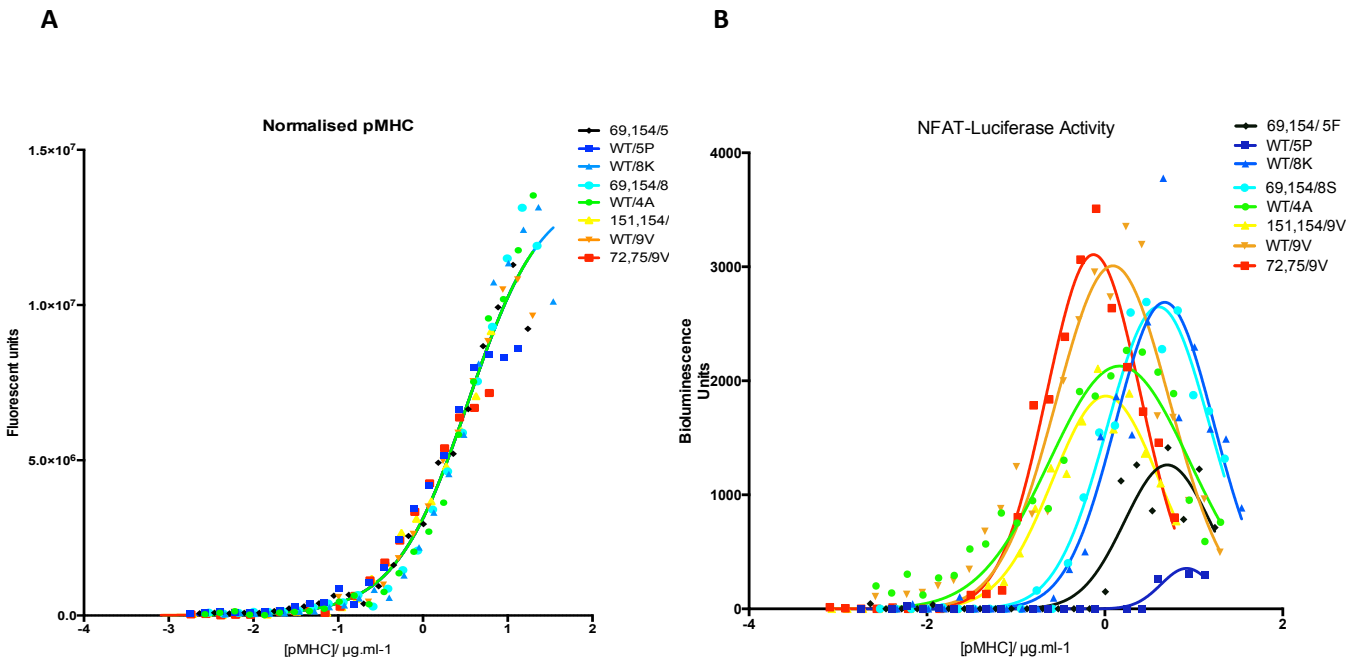

Figure 5.7 NFAT activation in Jurkat T cells

(a) Levels of biotinylated pMHC immobilisation were assessed on streptavidin-coated plates using mouse anti-HLA class-I antibody (clone W6/32) and an anti-mouse IRDye 800CW secondary antibody (LI-COR; Cat no. 926-32210). Immobilisation levels were analysed using the LI-COR Odyssey® Sa system and normalised against an index pMHC (WT/4A). (b) 5 x 10^4 Jurkat T cells were added per well and incubated for 16 hours before lysis and measurement of bioluminescence. NFAT luciferase expression were plotted as a function of the normalised pMHC levels in (a) and fitted using a Gaussian function. This is a representative figure of 3 separate experiments.

To verify these results, the assay was repeated in using IL-8 as an alternative readout. Barely detectable in resting condition, IL-8 is the founding member of the chemokine superfamily and is rapidly inducible in response to cellular stress factors induced by bacterial, viral or other pro-inflammatory cytokines such as IL-1 and TNF. IL-8 is regulated by the recruitment of transcription factors including NFκB and AP-1 to its promoter region (Hoffmann et al., 2002) and is hence a justifiable downstream readout for T cell activation.

T cells were subjected to identical stimulation conditions as described in Figure 5.7 but, instead of lysing the cell for assaying luciferase activity, the supernatant was isolated and assayed for IL-8 using ELISA. Just as the NFAT-Luciferase readout, pMHC concentration optimums were observed for almost every pMHC variants tested.

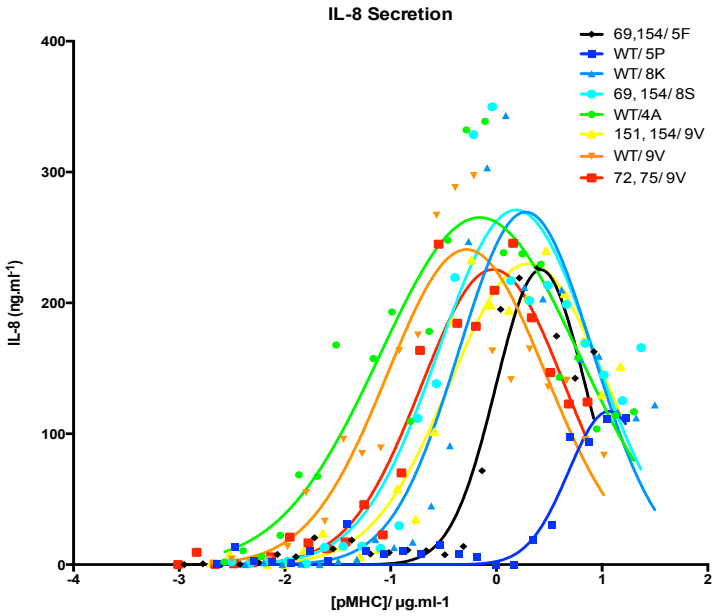

Figure 5.8 Measurement of IL-8 secretion from Jurkat T cells

Jurkat T cells expressing 1G4^{hi} TCR were subjected to identical experimental conditions to that described in Figure 5.8. Cell supernatant were harvested after 16 hours and analysed for IL-8 secretion by ELISA. As with figure 5.8, IL-8 secretions were plotted as a function of normalised pMHC levels and curve fitted using a Gaussian function. This is a representative figure of 2 separate experiments.

5.3.4 Primary T cell activations by pMHC variants

All results obtained thus far were derived from Jurkat T cell lines; to see if such trends are reproducible in a more physiological system, we sought to verify our results in primary T cells. To this end, $CD8^+$ T cells were isolated from HLA-A2 negative donors and the $1G4^{hi}$ TCRs were introduced into the cells using lentiviral transduction. Transduction efficiencies ranged between 50-60% and cell proliferation persists for up to 4 weeks in IL-2 supplemented media following transduction (Figure 5.9).

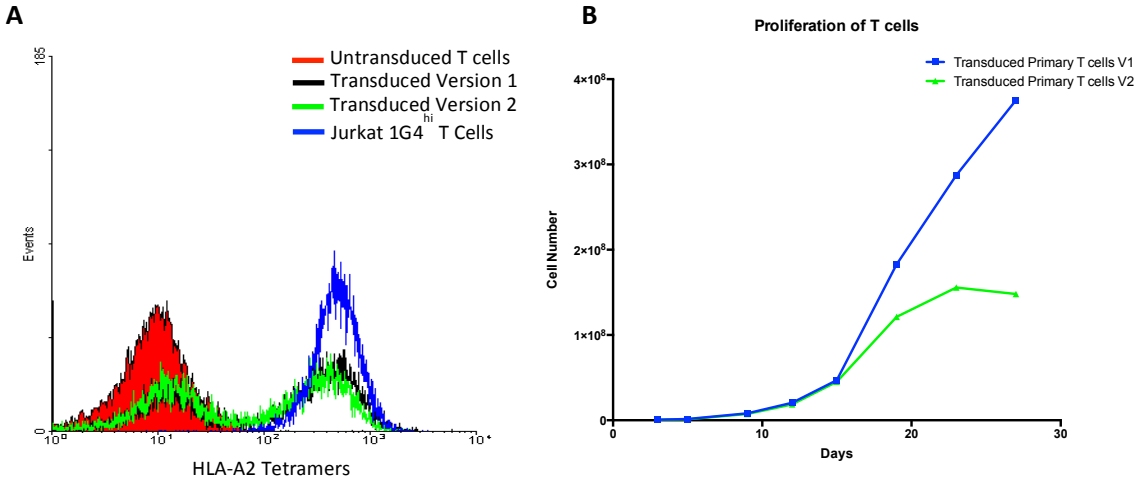

Figure 5.9 Lentiviral transduction and proliferation of primary human $CD8^+$ T cells

$CD8^+$ T cells were isolated from HLA-A2 negative PBMCs and transduced with concentrated $1G4^{hi}$ TCR lentiviral constructs. (a) Transduced T cells were verified by FACs using PE-conjugated HLA-A2/NYESO-9V tetramers. (b) Live cell count of $1G4^{hi}$- transduced primary T cells.

To determine if the observed optimal pMHC concentrations were also present in primary T cells, $1G4^{hi}$ TCR-expressing primary $CD8^+$ T cells were stimulated with 36 titrations of the index pMHC (WT/ 9V) for 4 or 48 hours, after which the IFNγ or IL-2 concentrations were measured respectively using ELISA. Unlike the Jurkat T cells, no

optimal pMHC concentration for T cell activation was observed (Figure 5.10). Interestingly, IL-2 secretion exhibited a 'switch-like' response whilst IFNγ secretion followed a more gradual pattern.

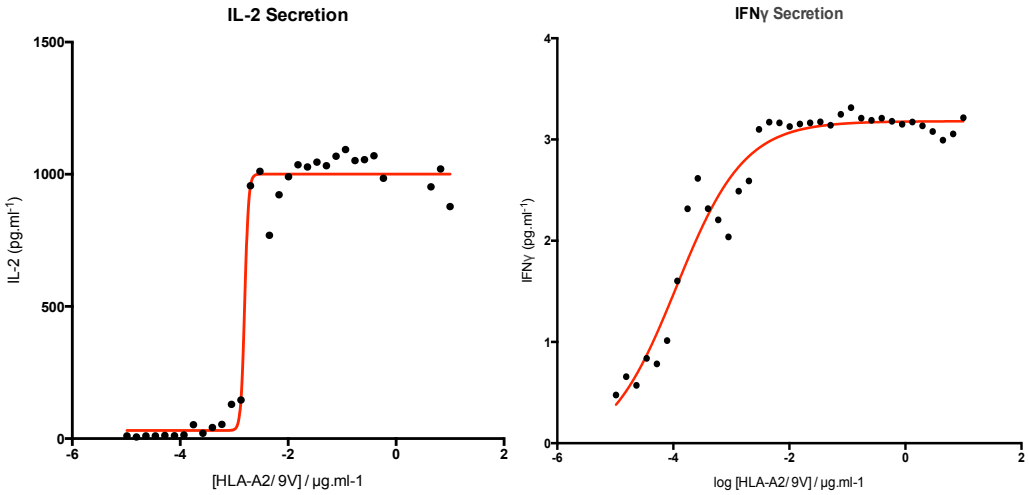

Figure 5.10 No optimum pMHC concentration observed for primary T cells

Transduced T cells were stimulated with the indicated concentrations of HLA-A2/ 9V pMHC and the supernatant were harvested after 4 and 48 hours for IFNγ and IL-2 analysis via ELISA respectively.

5.3.5 k_{off} and K_D correlates with EC_{50}

The kinetic proofreading model with limited signalling (also known as the productive hit rate model) predicts a correlation between K_D values and EC_{50} as well as a correlation between k_{off} and the E_{max}. Such predictions would not hold true for the affinity model, which only predicts only the former (Dushek et al., 2011).

To verify this within the high affinity TCR system, k_{off} and K_D were plotted against pMHC concentration and maximum amplitude values extracted from the Gaussian curve (Figure 5.11). The concentration producing maximal activation, also derived from the Gaussian fit, was used as a proxy for EC_{50}. A linear regression was performed on the data to test the degree of correlation.

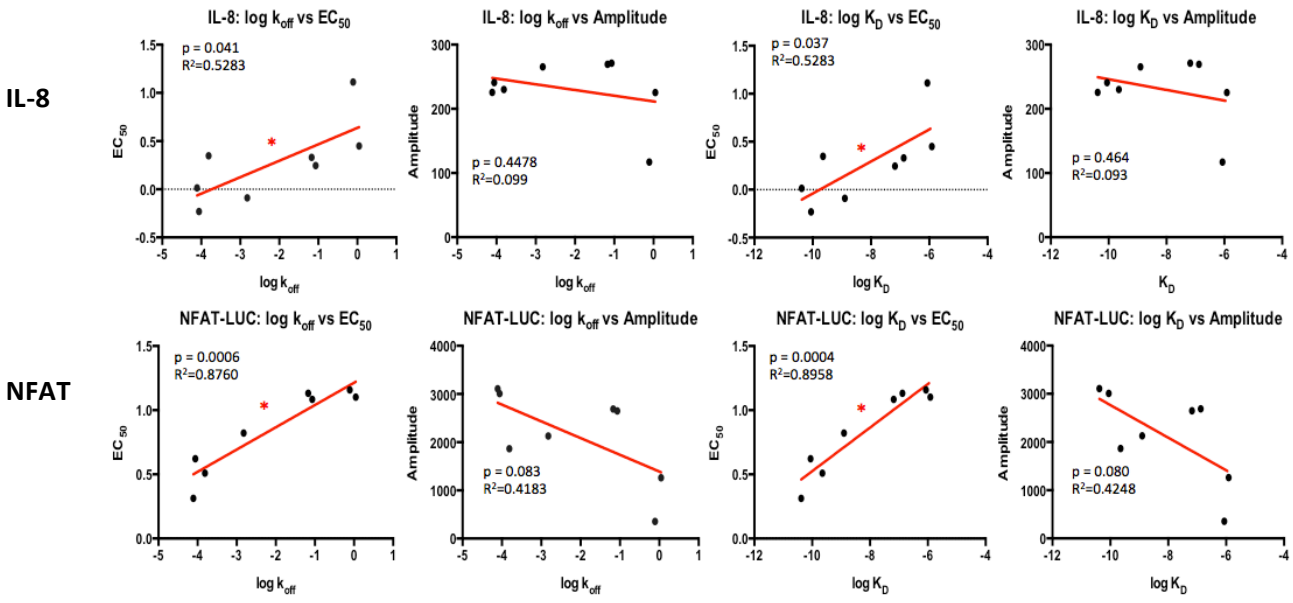

Figure 5.11 k_{off} values correlates with EC_{50}

k_{off} or K_D values were plotted against EC_{50} or amplitude values extracted from the Gaussian fit as described in Figures 5.9 and 5.10. A linear regression was performed to determine the degree of correlation.

Consistent with previous reports, there is a significant correlation between k_{off} and K_D with EC_{50} for both IL-8 secretion and NFAT expression. Although not statistically significant, K_D and k_{off} also correlated inversely with amplitude for NFAT expression. Maximal secretion of IL-8 however, appears to be similar across pMHC with differing kinetics. The tight correlation between K_D and k_{off} would explain their near-identical correlation pattern for EC_{50} and amplitude (Figure 5.12). These results echo the findings by Dushek et al and provide additional evidence against the affinity model and in favour of kinetic proofreading models (Dushek et al., 2011).

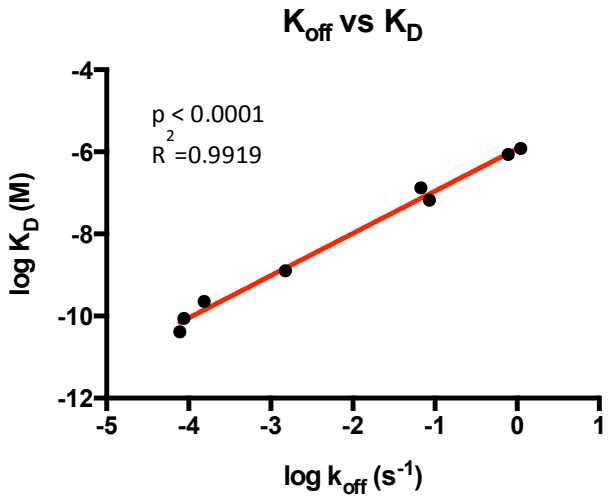

Figure 5.12 Near perfect correlation between k_{off} and K_D for pMHC variants

The k_{off} values for pMHC variants used in this study were plotted as a function of their respective K_D. There is a strong correlation between the two parameters, consistent with the data presented in Table 5.3.

5.3.6 An optimal dwell time is observed for low pMHC concentrations

Models of T cell activation that have been proposed (see introduction) can be distinguished on the basis of whether they do or do not predict an optimal k_{off} for T cell activation. Of the latter some models predict an optimal k_{off} at all pMHC concentrations whereas others predict that an optimal k_{off} will only be observed at low pMHC concentrations. To determine if there is an optimum kinetic exists for T cell activation within the $1G4^{hi}$ TCR system, k_{off} was plotted against NFAT expression or IL-8 secretion (data derived from Figures 5.7 and 5.8). The plot described in Figure 5.13 represents four separate concentrations of pMHC within a single experiment. An optimal k_{off} was observed for low pMHC concentrations, while no such optimum was observed for Jurkat T cells at higher pMHC concentration. The increased stimulatory capacity of lower-concentration peptides in Figure 5.13a is due to the presence of a pMHC optimum. Apart from the presence of an optimum pMHC concentration for T cell activation, the results described here is in agreement with existing mathematical studies (Gonzalez et al., 2005).

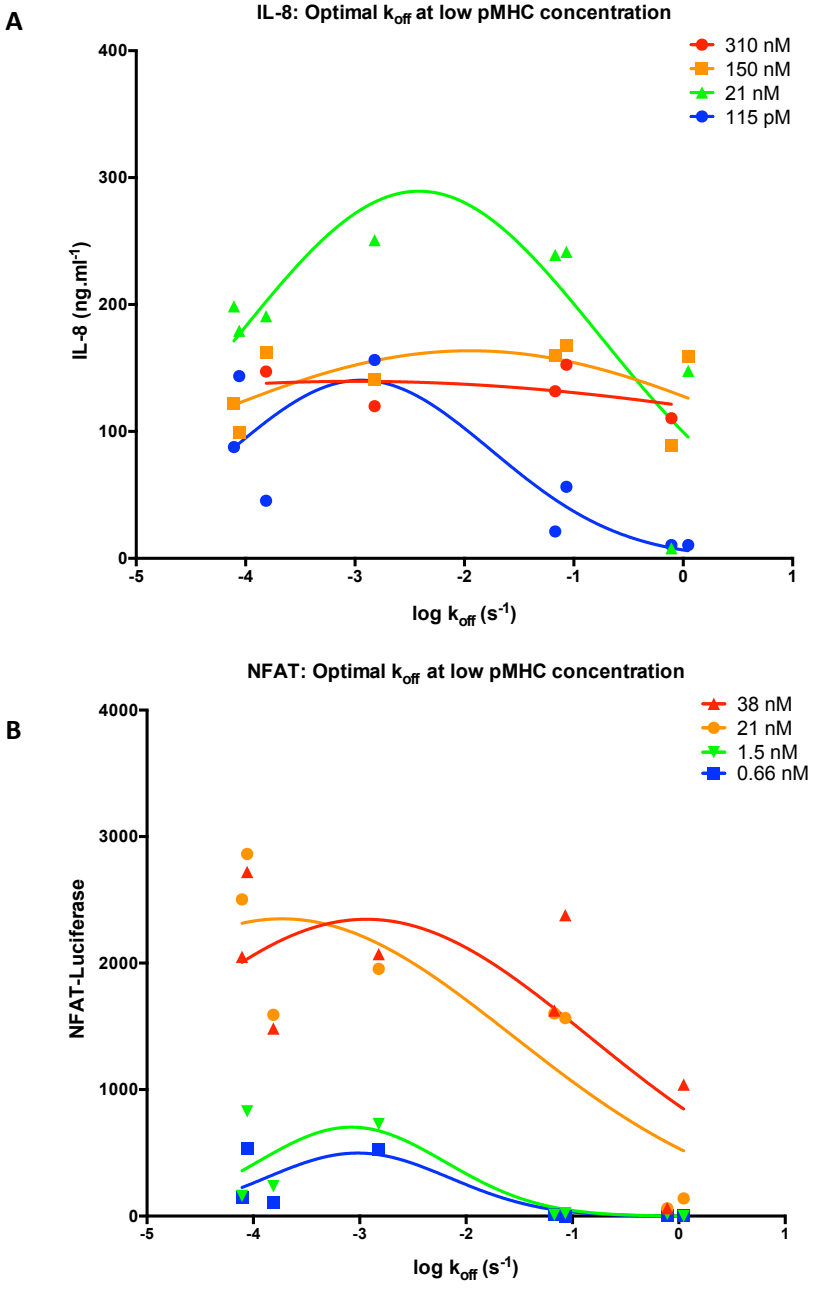

Figure 5.13 Exhibition of optimal k_{off} is dependent on pMHC concentrations

T cell activation in the form of (a) IL-8 secretion and (b) NFAT expression were plotted as a function of koff for the indicated concentrations of immobilized pMHC. Optimum k_{off} values were only observed at low pMHC concentrations, in agreement with previous studies. The disparity between high/ low concentration in (a) and (b) is a result of two independent data sets from two separate experiments, and they are not intended for direct comparisons.

5.4 Discussion

Affinities of normal TCR-pMHC interactions typically vary from 1-100μM, spanning a 100-fold range (Rudolph et al., 2006). Here we have generated and characterised TCR-pMHC interactions with up to 100,000-fold differences in range. This was made possible by the systematic mutation of both peptide and MHC residues that binds to the high affinity $1G4^{hi}$ (1G4 c58/c61) TCR with a 70pM affinity for the non-mutated index 9V peptide.

Mutations to the peptide residues by using altered peptide ligands had a larger impact on the affinity of the interaction in general. This was especially true for the 5^{th} residue of the peptide, a bulky tryptophan, described in the previous chapter as the *'flamboyant'* or prominent structural feature of the peptide. Decreases in affinities were mostly due to reductions in the k_{off} as opposed to differences in k_{on}.

The panel of pMHC ligands represent an excellent tool for the study of how affinities and rates may affect the output of TCR signalling. Representative pMHCs with a 100,000-fold range of affinities and rates were selected and used to stimulate T cell responses on a high throughput, plate-based assay.

A real surprise from this study came from the discovery of an optimum pMHC concentration for T cell activation as measured by NFAT expression and IL-8 secretion in Jurkat T cells (Figure 5.6, 5.7). This is may be a result of induced cell apoptosis under hyper-stimulatory conditions. The best-known example for this is negative selection of thymocytes displaying strong affinities to selecting self-pMHC molecules. Outside the thymus, apoptosis has been observed for mature peripheral $CD8^+$ T cells at high antigen doses (Alexander-Miller et al., 1996b). Indeed, work

performed in the lab has identified increased level of cell apoptosis by annexin V staining at higher pMHC concentrations (personal communication, Melissa Lever).

In a non-mutually exclusive way, hyper-stimulation can also lead to gradual impairment of T cell responsiveness, also known as anergy, which can be induced depending on both the duration and strength of the ligand (Yamamoto et al., 2007). A third possibility includes the induction of T cell exhaustion, which involves a gradual reduction of T cell effector function under hyper-stimulatory conditions. Chiu et al, who also noted the presence of an optimum pMHC concentration, recently elucidated the molecular basis by demonstrating increased levels of sprouty-2 (SPRY2) under hyper-stimulatory conditions (Chiu et al., 2014). SPRY2 functions as the negative regulator of MAPK/ Erk pathway. Unlike hyper-stimulation induced apoptosis or anergy however, T cell exhaustion is largely restricted to primary T cells. Nevertheless, the level of apoptosis, anergy or exhaustion (unlikely) is still a functional result of hyper-stimulation and therefore may be a reasonable readout of T cell activation.

It also remains possible that the observed pMHC optimum is an artefact of using cell lines even though it was verified using two independent IL-8 and NFAT readouts. To rule out the possibility conclusively, the experiment was repeated in transduced primary human HLA-A2 negative, $CD8^+$ T cells. HLA-A2 negative donors were recruited over the concern that transduction of $1G4^{hi}$ TCR into HLA-A2 positive T cell would lead to fratricidal killing as a result of cross-reactivity of the $1G4^{hi}$ TCR with self-peptide-HLA-A2 complexes (Holler et al., 2003, Zhao et al., 2007). Intriguingly, no pMHC optimum was observed for $1G4^{hi}$ expressing primary $CD8^+$ T cells, at least

for IL-2 and IFNγ responses (Figure 5.10). While it will be important to confirm these results using the same functional assays in primary T cells and Jurkat cells, this result raise doubts about the physiological relevance of the pMHC optimum observed in Jurkat T cell cells. These differences could be a reflection of the near homogenous expression of $1G4^{hi}$ in Jurkat T cells, as opposed to the 50-60% expression levels in primary T cells (Figures 5.6 and 5.9).

If it is assumed that events leading up to the optimum are independent of the events that led to the reduction of T cell activation after the optimum then parameters such as the ascending EC_{50} and amplitude remain valid for subsequent correlation studies. However it would be better to repeat these experiments under conditions in which additional process such as activation-induced apoptosis are not occurring. Our preliminary results with $1G4^{hi}$ TCR expressing primary T cells suggest that they would be suitable.

Experiments in primary T cells also revealed either switch-like or analogue responses of IL-2 and IFNγ secretion respectively, at the same peptide concentration (~2μM), consistent with findings reported by several groups (Itoh and Germain, 1997, Dushek et al., 2011). Early T cell antigen recognition is largely believed to involve a digital or switch-like response upon ligand engagement, as demonstrated by the all-or-nothing phosphorylation status of MAP kinase Erk (Altan-Bonnet and Germain, 2005, Das et al., 2009). How exactly can this be translated into an analogue response for certain cytokines (such as IFNγ) remains a mystery. It is also unclear if the epigenetical status of cytokine gene locus might have any bearing on the perception of intracellular signalling cascade to effect on subsequent gene transcription.

Work described in this chapter is in agreement with kinetic models of T cell signalling in general. A positive correlation between K_D and EC_{50} was observed for both IL-8 secretion and NFAT expression in Jurkat cells. Such correlations are mathematically predicted for both the affinity and kinetic models, and the distinguishing factor between the two models rest on the correlation between k_{off} and the maximal response or E_{max} of the interaction. The amplitude values of the fitted Gaussian curve was extracted and used as a proxy for EC_{50} described in Dushek et al (Dushek et al., 2011). Under this framework, a correlation between k_{off} and amplitude was observed for NFAT expression. Maximal IL-8 secretion however, seemed to be constant across the panel of ligands tested. This may stem from the additional dependency of IL-8 transcription and mRNA stabilisation on other cytokines such as IL-1 and TNF (Hoffmann et al., 2002). As such, maximal IL-8 secretion may not be entirely dependent on the rate of TCR-pMHC interaction. Nevertheless, the convergence of trends for multiple readout of TCR activation in different T cell systems provide compelling evidence in support of kinetic models and against simple affinity models. The natural step forward would be to repeat and confirm the results in transduced primary T cells.

Further insights from this study came from the analysis of how k_{off} impacts T cell activation under different pMHC concentrations. As described in the introduction, some kinetic models predict an optimal dwell time ($1/k_{off}$) for T cell activation. In these models (kinetic proof-reading with limited signalling, and kinetic proof reading with sustained signalling) a long enough dwell time is necessary for the completion of signalling cascade for productive signalling while too long a dwell time, however, would result in insufficient serial engagement of multiple TCRs by a few cognate

pMHC. The presence of an optimal dwell time was reported by several groups and has also been the focus of this study (Kalergis et al., 2001, Coombs et al., 2002).

By varying biotinylated-pMHC concentrations on streptavidin-coated plates, we observed an optimal k_{off} with Jurkat T cells but only at low concentrations of pMHC (Figure 5.13), consistent with the report by Gonzalez et al (Gonzalez et al., 2005) which is in turn based on the model by Coombs et al (Coombs et al., 2002) (kinetic model with sustained signalling, Figure 5.1d) While it is tempting to rule out the kinetic proofreading model with limited signalling (or productive hit rate model, Figure 5.1c) in favour of the sustained signalling model because of the absence of an optimal k_{off} at high pMHC concentrations, we cannot be sure if such observations are secondary to the effects of cell death at high peptide concentrations. Therefore, the outcome of this study only allows the definitive rejection of models that do not describe an optimum k_{off} with T cell activation (such as the affinity model and the basic kinetic proofreading model Figure 5.1a,b). Indeed, this finding was also verified by Allison and colleagues for *in vivo* T cell responses (Corse et al., 2010). Recently we have been able to identify more dramatic T cell responses from pMHCs with intermediate k_{off} values that would better demonstrate the presence of an optimal k_{off} (personal communication, Melissa Lever). As with the correlation studies, repeating the experiments in primary T cells represents the way forward to address the validity of each models for once and for all.

All experiments described here were performed on $CD8^+$ Jurkat and primary T cells. The presence of CD8 in particular has been shown to improve and facilitate high affinity TCR cross-reactivity, leading to a loss of antigen specificity (Zhao et al., 2007).

We have observed a similar phenomenon where TCR signalling as measured by NFAT activation was detected in $1G4^{hi}$ TCR expressing cells exposed to high concentrations of a HLA-A2 complexed with a peptide comprising only glycine residues (data not shown). It would be interesting to extend the experiments into $CD4^{+}$ primary T cells for comparison, where the potential effect of co-receptor enhanced avidity can be eliminated.

In summary, work described in this chapter represents a systematic investigation of the effect of TCR-pMHC binding k_{off} and K_D across a 10,000-fold range on T cell activation. Such investigation represents the first of its kind where earlier studies only characterised TCR-pMHC affinities with a range of ~100 fold. These results re-affirmed evidence that it is the kinetics, and not the affinity of TCR-pMHC binding that determines outcome of the interaction. The data also demonstrated an optimal dwell time for TCR-pMHC interactions in the Jurkat T cell system only at low pMHC concentrations, in agreement with previous studies. As a series of caveats may exist in the Jurkat T cell system (such as the discovery of an unexpected pMHC optimum), the data will have to be verified in primary T cell systems.

CHAPTER 6:

General Discussion

6.1 Summary of Experimental Findings

We have discussed the mechanism by which costimulatory receptor CD28 triggers and properties of TCR-pMHC binding in the previous three chapters.

In chapter 3, the importance of receptor-ligand dimension in CD28 costimulation was investigated by elongating its ligand. Artificial elongation of CD80 led to impaired CD28 costimulation. Control experiments and imaging were consistent with the hypothesis that this was the result of reduced CD45 segregation. Consistent with predictions from the K-S model, CD28 tyrosine mutants were also less sensitive to changes in CD80 dimensions. These illustrate the importance of RPTP segregation as a prerequisite for CD28 triggering. The natural step forward with this investigation is to test the validity of the K-S model across all NTR in a high throughput manner (Dushek et al., 2012). Interestingly, we found that size matching between TCR and CD28 ligand complexes was not critical for CD28 costimulation. This is consistent with the effectiveness of CD28 trans-costimulation, and suggests that close colocalisation of engaged CD28 and TCR is not critical for costimulation. These finding contrast with studies of the inhibitory receptors PD-1 and KIR2DL1, where close colocalisation with their respective activatory receptors, TCR and NKG2D, was necessary for their inhibitory effect (Kohler et al., 2010, Yokosuka et al., 2012a). This is consistent with the fact that CD28 and TCR signalling pathways integrate within the cytoplasm and nucleus (Diehn et al., 2002).

In chapter 4, we obtained estimates for the contribution of TCR-MHC contacts to the binding energy of the TCR-pMHC interaction. By analysing the TCR contacts between HLA-A2 to four different TCRs, we showed that MHC contributes ~70% of the TCR-

pMHC energetics with the exception of the JM22 TCR. This figure is similar to previous studies on both MHC class I and II molecules (Wu et al., 2002, Piepenbrink et al., 2013). This highlights the importance of MHC residues in mediating TCR-pMHC interactions, which may be particularly relevant during thymic selection. Presence of a basal affinity for the TCR that is contributed by the MHC alone may facilitate detection of a wide repertoire of foreign peptides by enabling the TCR to be promiscuous with respect to peptides. Given that the number of possible peptides presented on MHC molecules is several orders of magnitude larger than the number of unique TCRs in an individual, this is critical for ensuring that there are few or no 'holes' in the TCR repertoire (Mason, 1998b).

In chapter 5, we generated a panel of pMHC molecules with up to 10^5-fold variation in affinity for the $1G4^{hi}$ supra-physiological TCR. Eight pMHCs with varying affinities for the TCRs were titrated and tested for their ability to stimulate $1G4^{hi}$-transduced Jurkat T cells. Our results demonstrated the presence of an optimal k_{off} or dwell time for T cell activation at low concentrations of pMHC. While there is a need to repeat the experiments using primary T cells, the experimental finding allows us to definitively reject mathematical models of T cell activation that do not predict a k_{off} optimum.

6.2 Therapeutic implications

Chimeric Antigen Receptor Design

Chimeric antigen receptors (CAR) are recombinant receptors with the ability to redirect customised T cell responses to any targets. CAR typically consists of an extracellular single-chain variable fragment (scFv) derived from antibodies, a

transmembrane domain, and an intracellular signalling chain derived from the TCR and/or T cell co-stimulatory receptors (Chicaybam et al., 2011). As such, signalling events mediated by CARs will also be susceptible to regulations by the local kinase: phosphatase balance and can be classified as NTRs according to Dushek et al (Dushek et al., 2012). Our studies with the TCR (Choudhuri et al., 2005) and CD28 demonstrated the importance of receptor-ligand dimensions in mediating effective signal transduction. This has implications on the design of CAR target epitope. CARs specific to membrane proximal region of the target antigen would draw the two membrane on opposing cells closer together; thereby increasing the efficiently of signal transduction by the CAR in scenarios analogous to Figure 3.2. Indeed, there have been reports to suggest that this is the case (Hombach et al., 2007). Choosing the right target epitope for CARs may therefore offer improvement on CAR-T cells efficiency and survival. Conversely, extracellular dimensions of CARs are also important, and adjustment thereof could be used to modulate CAR signal strength. This could be useful to minimize cross-reactivity to tumour antigen expresses at low level on normal cells.

Studies from chapter 3 highlights the dispensability of size matching between TCR and CD28, which has direct implications on the design of chimeric costimulatory receptors (CCR). CCRs are a distinct type of receptor designed to provide costimulatory signals in CAR-expressing T cells. Under this scenario, stimulation of the CAR alone would not be sufficient to induce T cell activation, and co-ligation of a second CCR to another distinct epitope would be required for full T cell activation. This setup requires the co-ligation of two distinct epitopes and was designed to avoid ‘on-target, off-tumour’ effects of CARs (Hanada and Restifo, 2013). The fact

that CD28 can signal in trans meant that target epitope of CCR/ CAR containing CD28 cytoplasmic motifs do not have to be restricted on the same target cell, potentially limiting the usefulness of this approach.

CARs offer a great deal of flexibility in that it is possible to design CARs specific for any target and alter the receptor affinity for it. Yet, there has been little information on the effects of CAR affinities and functional outcome of the T cells. We expect affinities of existing CARs for its targets to be very similar to the corresponding antibody-antigen interaction (~nM). Hence, we may be able to infer the potential implications of changing CAR affinities on T cell activation from our findings with the supra-physiological TCR described in chapter 5: the observation of an optimal affinity for T cell activation at low ligand concentrations that may also hold true for CARs. This suggests that CARs with intermediate affinities may be most effective when its target epitope levels are low; although this may not be the case for existing CAR targets, as they tend to consist of overexpressed cancer-specific antigens (Sadelain et al., 2013). Nonetheless, this highlights the importance of considering the potential effects of epitope density when designing CARs (Sadelain et al., 2013). Adjusting CAR affinities may also help to minimize the risk of cytokine storms in some CAR-T cell therapies (Xu and Tang, 2014).

Caution is needed when extrapolating our data with a supra-physiological affinity TCR to CARs. The experiments described in chapter 5 were performed in the presence of CD8 co-receptor, which may confound the observations described. Secondly, signalling domains of TCRs and CARs can be quite different, with the latter often containing multiple signalling chains from different receptors in tandem. This

makes it difficult to make direct comparisons. Nevertheless, studies on T cell activation models will continue to provide invaluable insight into CAR design.

Engineering Therapeutic T Cell Receptors

The finding of an optimal TCR affinity at low ligand concentration will impact the design of therapeutic TCRs as just described for CARs. Unlike the CARs however, there have been a wealth of information on how TCR affinities could impact *in vivo* T cell responses. As mention in the introduction of chapter 5, TCRs with heightened affinities are generally better at controlling tumours *in vivo.* While informative, such studies only compared a limited number of affinities (Soto et al., 2013, Morgan et al., 2006, Robbins et al., 2011). Studies utilising greater numbers of TCRs with varying affinities have noted the presence of an optimal T cell affinities with regards to T cell responses in vivo (Corse et al., 2010) and tumour infiltration capabilities of transduced T cells (Chervin et al., 2013).

Our preliminary findings with 8 different TCR-pMHC affinities suggest that an optimum T cell affinity may only apply at low ligand concentrations. As mentioned above for CARs, ligand densities of the target antigen may need to be taken into considerations when designing therapeutic TCRs. This may be especially relevant for designing TCRs against highly abundant cancer antigens or dominant viral epitopes during chronic viral infections. A complication is the fact that the abundance of the antigen may drop during the disease process, either spontaneously or in response to immune responses targeting the antigen.

Work described in chapter 4 demonstrated that relative energetic contributions of MHC to TCR-pMHC interaction ranges from 15% to more than 70%. This cautions

against stabilising mutations within MHC-contacting CDR1/2 as means of enhancing TCR affinities for certain TCR-pMHC interactions. For example, enhancing MHC contacts in an interaction where the MHC already contributes to >70% of the energetic interaction may lead to indiscriminate recognition (auto-reactivity) of MHC regardless of the antigenic peptide. On the other hand, auto-reactivity may not be a problem for MHC-stabilising mutations in interactions where the MHCs have a reduced contribution to the energetics.

6.3 Closing Remark: The Danger of Generalisation

Studies into TCR-pMHC biology have often been guided, and perhaps restricted by measurable and quantifiable parameters of the interaction. These include structural information, thermodynamics data, as well as the affinity and kinetics of the interaction. It is tempting, when reporting such features, to explain TCR activation as a function of the unique structural binding footprint, thermodynamics footprint and/or the affinity and kinetic parameters of the interaction. This has frequently been the case with studies of TCR-pMHC system, However, in several cases subsequent studies of other TCRs revealed that these conclusions were premature. As described in chapter 5, it follows that there is no consistent structural binding and thermodynamics footprint in TCR-pMHC interactions. Quoting Brian Baker in his 2008 review, "*Energetically, biology does not care how you form the complex, just that you do*" in a response to whether TCR-pMHC interaction is driven by enthalpy or entropy (Armstrong et al., 2008).

Our findings in chapter 4 provide examples to the danger of generalising TCR-pMHC interaction based on limited studies. While length of TCR CDR3 loops and the degree

of peptide protrusion towards the TCR may explain the energetic dominance of peptide or MHC in several scenarios (Manning et al., 1998, Liu et al., 2012, Borg et al., 2005), it wasn't the case for JM22 and 1G4 TCR in our studies.

The only universal features of TCR-pMHC interaction that have withstood scrutiny are the roughly diagonal binding mode of TCRs on pMHCs and the fact that binding kinetics correlates with T cell activation. It has become increasingly apparent that many models described for T cell triggering and T cell activation are in fact non-mutually exclusive and the formulation of integrative models may be the way forward.

References

ACUTO, O. & MICHEL, F. 2003. CD28-mediated co-stimulation: a quantitative support for TCR signalling. *Nat Rev Immunol,* 3**,** 939-51.

ADAMS, J. J., NARAYANAN, S., LIU, B., BIRNBAUM, M. E., KRUSE, A. C., BOWERMAN, N. A., CHEN, W., LEVIN, A. M., CONNOLLY, J. M., ZHU, C., KRANZ, D. M. & GARCIA, K. C. 2011. T cell receptor signaling is limited by docking geometry to peptide-major histocompatibility complex. *Immunity,* 35**,** 681-93.

AIVAZIAN, D. & STERN, L. J. 2000. Phosphorylation of T cell receptor zeta is regulated by a lipid dependent folding transition. *Nature structural biology,* 7**,** 1023-6.

AL-ALWAN, M. M., ROWDEN, G., LEE, T. D. & WEST, K. A. 2001. The dendritic cell cytoskeleton is critical for the formation of the immunological synapse. *J Immunol,* 166**,** 1452-6.

ALEKSIC, M., DUSHEK, O., ZHANG, H., SHENDEROV, E., CHEN, J. L., CERUNDOLO, V., COOMBS, D. & VAN DER MERWE, P. A. 2010. Dependence of T cell antigen recognition on T cell receptor-peptide MHC confinement time. *Immunity,* 32**,** 163-74.

ALEXANDER-MILLER, M. A., LEGGATT, G. R. & BERZOFSKY, J. A. 1996a. Selective expansion of high- or low-avidity cytotoxic T lymphocytes and efficacy for adoptive immunotherapy. *Proceedings of the National Academy of Sciences of the United States of America,* 93**,** 4102-7.

ALEXANDER-MILLER, M. A., LEGGATT, G. R., SARIN, A. & BERZOFSKY, J. A. 1996b. Role of antigen, CD8, and cytotoxic T lymphocyte (CTL) avidity in high dose antigen induction of apoptosis of effector CTL. *The Journal of experimental medicine,* 184**,** 485-92.

ALTAN-BONNET, G. & GERMAIN, R. N. 2005. Modeling T cell antigen discrimination based on feedback control of digital ERK responses. *PLoS biology,* 3**,** e356.

ANDERSEN, M. H., PEDERSEN, L. O., CAPELLER, B., BROCKER, E. B., BECKER, J. C. & THOR STRATEN, P. 2001a. Spontaneous cytotoxic T-cell responses against survivin-derived MHC class I-restricted T-cell epitopes in situ as well as ex vivo in cancer patients. *Cancer research,* 61**,** 5964-8.

ANDERSEN, P. S., GEISLER, C., BUUS, S., MARIUZZA, R. A. & KARJALAINEN, K. 2001b. Role of the T cell receptor ligand affinity in T cell activation by bacterial superantigens. *The Journal of biological chemistry,* 276**,** 33452-7.

ANDRES, P. G., HOWLAND, K. C., NIRULA, A., KANE, L. P., BARRON, L., DRESNEK, D., SADRA, A., IMBODEN, J., WEISS, A. & ABBAS, A. K. 2004. Distinct regions in the CD28 cytoplasmic domain are required for T helper type 2 differentiation. *Nat Immunol,* 5**,** 435-42.

ANTONY, P. A., PICCIRILLO, C. A., AKPINARLI, A., FINKELSTEIN, S. E., SPEISS, P. J., SURMAN, D. R., PALMER, D. C., CHAN, C. C., KLEBANOFF, C. A., OVERWIJK, W. W., ROSENBERG, S. A. & RESTIFO, N. P. 2005. CD8+ T cell immunity against a tumor/self-antigen is augmented by CD4+ T helper cells and hindered by naturally occurring T regulatory cells. *Journal of immunology,* 174**,** 2591-601.

APPLEMAN, L. J., VAN PUIJENBROEK, A. A., SHU, K. M., NADLER, L. M. & BOUSSIOTIS, V. A. 2002. CD28 costimulation mediates down-regulation of p27kip1 and cell cycle progression by activation of the PI3K/PKB signaling pathway in primary human T cells. *Journal of immunology,* 168**,** 2729-36.

ARDOUIN, L., BRACKE, M., MATHIOT, A., PAGAKIS, S. N., NORTON, T., HOGG, N. & TYBULEWICZ, V. L. 2003. Vav1 transduces TCR signals required for

LFA-1 function and cell polarization at the immunological synapse. *European journal of immunology,* 33**,** 790-7.

ARGAET, V. P., SCHMIDT, C. W., BURROWS, S. R., SILINS, S. L., KURILLA, M. G., DOOLAN, D. L., SUHRBIER, A., MOSS, D. J., KIEFF, E., SCULLEY, T. B. & MISKO, I. S. 1994. Dominant selection of an invariant T cell antigen receptor in response to persistent infection by Epstein-Barr virus. *The Journal of experimental medicine,* 180**,** 2335-40.

ARMSTRONG, K. M., INSAIDOO, F. K. & BAKER, B. M. 2008. Thermodynamics of T-cell receptor-peptide/MHC interactions: progress and opportunities. *Journal of molecular recognition : JMR,* 21**,** 275-87.

AUGUST, A. & DUPONT, B. 1994. CD28 of T lymphocytes associates with phosphatidylinositol 3-kinase. *International immunology,* 6**,** 769-74.

AUSUBEL, F. M. 2005. Are innate immune signaling pathways in plants and animals conserved? *Nature immunology,* 6**,** 973-9.

BADOUR, K., MCGAVIN, M. K., ZHANG, J., FREEMAN, S., VIEIRA, C., FILIPP, D., JULIUS, M., MILLS, G. B. & SIMINOVITCH, K. A. 2007. Interaction of the Wiskott-Aldrich syndrome protein with sorting nexin 9 is required for CD28 endocytosis and cosignaling in T cells. *Proc Natl Acad Sci U S A,* 104**,** 1593-8.

BAKER, B. M., TURNER, R. V., GAGNON, S. J., WILEY, D. C. & BIDDISON, W. E. 2001. Identification of a crucial energetic footprint on the alpha1 helix of human histocompatibility leukocyte antigen (HLA)-A2 that provides functional interactions for recognition by tax peptide/HLA-A2-specific T cell receptors. *The Journal of experimental medicine,* 193**,** 551-62.

BALAGOPALAN, L., COUSSENS, N. P., SHERMAN, E., SAMELSON, L. E. & SOMMERS, C. L. 2010. The LAT story: a tale of cooperativity, coordination, and choreography. *Cold Spring Harb Perspect Biol,* 2**,** a005512.

BANGHAM, R., MICHAUD, G. A., SCHWEITZER, B. & PREDKI, P. F. 2005. Protein microarray-based screening of antibody specificity. *Methods in molecular medicine,* 114**,** 173-82.

BARBER, D. L., WHERRY, E. J., MASOPUST, D., ZHU, B., ALLISON, J. P., SHARPE, A. H., FREEMAN, G. J. & AHMED, R. 2006. Restoring function in exhausted CD8 T cells during chronic viral infection. *Nature,* 439**,** 682-7.

BARBER, E. K., DASGUPTA, J. D., SCHLOSSMAN, S. F., TREVILLYAN, J. M. & RUDD, C. E. 1989. The CD4 and CD8 antigens are coupled to a protein-tyrosine kinase (p56lck) that phosphorylates the CD3 complex. *Proceedings of the National Academy of Sciences of the United States of America,* 86**,** 3277-81.

BARDA-SAAD, M., BRAIMAN, A., TITERENCE, R., BUNNELL, S. C., BARR, V. A. & SAMELSON, L. E. 2005. Dynamic molecular interactions linking the T cell antigen receptor to the actin cytoskeleton. *Nat Immunol,* 6**,** 80-9.

BEDDOE, T., CHEN, Z., CLEMENTS, C. S., ELY, L. K., BUSHELL, S. R., VIVIAN, J. P., KJER-NIELSEN, L., PANG, S. S., DUNSTONE, M. A., LIU, Y. C., MACDONALD, W. A., PERUGINI, M. A., WILCE, M. C., BURROWS, S. R., PURCELL, A. W., TIGANIS, T., BOTTOMLEY, S. P., MCCLUSKEY, J. & ROSSJOHN, J. 2009. Antigen ligation triggers a conformational change within the constant domain of the alphabeta T cell receptor. *Immunity,* 30**,** 777-88.

BEYERSDORF, N., GAUPP, S., BALBACH, K., SCHMIDT, J., TOYKA, K. V., LIN, C. H., HANKE, T., HUNIG, T., KERKAU, T. & GOLD, R. 2005. Selective targeting of regulatory T cells with CD28 superagonists allows effective therapy of experimental autoimmune encephalomyelitis. *The Journal of experimental medicine,* 202**,** 445-55.

BHATIA, S., SUN, K., ALMO, S. C., NATHENSON, S. G. & HODES, R. J. 2010. Dynamic Equilibrium of B7-1 Dimers and Monomers Differentially Affects

Immunological Synapse Formation and T Cell Activation in Response to TCR/CD28 Stimulation. *J Immunol*.

BISSANTZ, C. 2003. Conformational changes of G protein-coupled receptors during their activation by agonist binding. *Journal of receptor and signal transduction research,* 23**,** 123-53.

BODIAN, D. L., JONES, E. Y., HARLOS, K., STUART, D. I. & DAVIS, S. J. 1994. Crystal structure of the extracellular region of the human cell adhesion molecule CD2 at 2.5 A resolution. *Structure,* 2**,** 755-66.

BOISE, L. H., MINN, A. J., NOEL, P. J., JUNE, C. H., ACCAVITTI, M. A., LINDSTEN, T. & THOMPSON, C. B. 1995. CD28 costimulation can promote T cell survival by enhancing the expression of Bcl-XL. *Immunity,* 3**,** 87-98.

BONIFACE, J. J., RABINOWITZ, J. D., WULFING, C., HAMPL, J., REICH, Z., ALTMAN, J. D., KANTOR, R. M., BEESON, C., MCCONNELL, H. M. & DAVIS, M. M. 1998. Initiation of signal transduction through the T cell receptor requires the multivalent engagement of peptide/MHC ligands [corrected]. *Immunity,* 9**,** 459-66.

BONIFACE, J. J., REICH, Z., LYONS, D. S. & DAVIS, M. M. 1999. Thermodynamics of T cell receptor binding to peptide-MHC: evidence for a general mechanism of molecular scanning. *Proceedings of the National Academy of Sciences of the United States of America,* 96**,** 11446-51.

BOOMER, J. S. & GREEN, J. M. 2010. An enigmatic tail of CD28 signaling. *Cold Spring Harb Perspect Biol,* 2**,** a002436.

BOONEN, G. J., VAN DIJK, A. M., VERDONCK, L. F., VAN LIER, R. A., RIJKSEN, G. & MEDEMA, R. H. 1999. CD28 induces cell cycle progression by IL-2-independent down-regulation of p27kip1 expression in human peripheral T lymphocytes. *European journal of immunology,* 29**,** 789-98.

BORG, N. A., ELY, L. K., BEDDOE, T., MACDONALD, W. A., REID, H. H., CLEMENTS, C. S., PURCELL, A. W., KJER-NIELSEN, L., MILES, J. J., BURROWS, S. R., MCCLUSKEY, J. & ROSSJOHN, J. 2005. The CDR3 regions of an immunodominant T cell receptor dictate the 'energetic landscape' of peptide-MHC recognition. *Nature immunology,* 6**,** 171-80.

BORRIELLO, F., SETHNA, M. P., BOYD, S. D., SCHWEITZER, A. N., TIVOL, E. A., JACOBY, D., STROM, T. B., SIMPSON, E. M., FREEMAN, G. J. & SHARPE, A. H. 1997. B7-1 and B7-2 have overlapping, critical roles in immunoglobulin class switching and germinal center formation. *Immunity,* 6**,** 303-13.

BOULTER, J. M., GLICK, M., TODOROV, P. T., BASTON, E., SAMI, M., RIZKALLAH, P. & JAKOBSEN, B. K. 2003. Stable, soluble T-cell receptor molecules for crystallization and therapeutics. *Protein engineering,* 16**,** 707-11.

BOWNDS, S., TONG-ON, P., ROSENBERG, S. A. & PARKHURST, M. 2001. Induction of tumor-reactive cytotoxic T-lymphocytes using a peptide from NY-ESO-1 modified at the carboxy-terminus to enhance HLA-A2.1 binding affinity and stability in solution. *Journal of immunotherapy,* 24**,** 1-9.

BRETSCHER, P. & COHN, M. 1970a. A theory of self-nonself discrimination. *Science,* 169**,** 1042-9.

BRETSCHER, P. & COHN, M. 1970b. A theory of self-nonself discrimination. *Science,* 169**,** 1042-9.

BRIDGEMAN, J., SEWELL, A., PRICE, D. & COLE, D. 2011. Structural and biophysical determinants of alpha beta T-cell antigen. *Immunology***,** 9-18.

BRZOSTEK, J., CHAI, J. G., GEBHARDT, F., BUSCH, D. H., ZHAO, R., VAN DER MERWE, P. A. & GOULD, K. G. 2010. Ligand dimensions are important in controlling NK-cell responses. *European journal of immunology,* 40**,** 2050-9.

BUBECK WARDENBURG, J., FU, C., JACKMAN, J. K., FLOTOW, H., WILKINSON, S. E., WILLIAMS, D. H., JOHNSON, R., KONG, G., CHAN, A. C. & FINDELL, P. R. 1996. Phosphorylation of SLP-76 by the ZAP-70 protein-tyrosine kinase

is required for T-cell receptor function. *The Journal of biological chemistry,* 271**,** 19641-4.

BUNNELL, S. C., HONG, D. I., KARDON, J. R., YAMAZAKI, T., MCGLADE, C. J., BARR, V. A. & SAMELSON, L. E. 2002. T cell receptor ligation induces the formation of dynamically regulated signaling assemblies. *The Journal of cell biology,* 158**,** 1263-75.

BURMEISTER, Y., LISCHKE, T., DAHLER, A. C., MAGES, H. W., LAM, K. P., COYLE, A. J., KROCZEK, R. A. & HUTLOFF, A. 2008. ICOS controls the pool size of effector-memory and regulatory T cells. *Journal of immunology,* 180**,** 774-82.

BUSLEPP, J., WANG, H., BIDDISON, W. E., APPELLA, E. & COLLINS, E. J. 2003. A correlation between TCR Valpha docking on MHC and CD8 dependence: implications for T cell selection. *Immunity,* 19**,** 595-606.

CALL, M. E., PYRDOL, J., WIEDMANN, M. & WUCHERPFENNIG, K. W. 2002. The organizing principle in the formation of the T cell receptor-CD3 complex. *Cell,* 111**,** 967-79.

CANTRELL, D. 2002. Protein kinase B (Akt) regulation and function in T lymphocytes. *Seminars in immunology,* 14**,** 19-26.

CEFAI, D., SCHNEIDER, H., MATANGKASOMBUT, O., KANG, H., BRODY, J. & RUDD, C. E. 1998. CD28 receptor endocytosis is targeted by mutations that disrupt phosphatidylinositol 3-kinase binding and costimulation. *J Immunol,* 160**,** 2223-30.

CHAN, A. C., IWASHIMA, M., TURCK, C. W. & WEISS, A. 1992. ZAP-70: a 70 kd protein-tyrosine kinase that associates with the TCR zeta chain. *Cell,* 71**,** 649-62.

CHAN, C., GEORGE, A. J. & STARK, J. 2001. Cooperative enhancement of specificity in a lattice of T cell receptors. *Proceedings of the National Academy of Sciences of the United States of America,* 98**,** 5758-63.

CHANG, F., STEELMAN, L. S., LEE, J. T., SHELTON, J. G., NAVOLANIC, P. M., BLALOCK, W. L., FRANKLIN, R. A. & MCCUBREY, J. A. 2003. Signal transduction mediated by the Ras/Raf/MEK/ERK pathway from cytokine receptors to transcription factors: potential targeting for therapeutic intervention. *Leukemia,* 17**,** 1263-93.

CHEN, J. L., DUNBAR, P. R., GILEADI, U., JAGER, E., GNJATIC, S., NAGATA, Y., STOCKERT, E., PANICALI, D. L., CHEN, Y. T., KNUTH, A., OLD, L. J. & CERUNDOLO, V. 2000. Identification of NY-ESO-1 peptide analogues capable of improved stimulation of tumor-reactive CTL. *Journal of immunology,* 165**,** 948-55.

CHEN, J. L., STEWART-JONES, G., BOSSI, G., LISSIN, N. M., WOOLDRIDGE, L., CHOI, E. M., HELD, G., DUNBAR, P. R., ESNOUF, R. M., SAMI, M., BOULTER, J. M., RIZKALLAH, P., RENNER, C., SEWELL, A., VAN DER MERWE, P. A., JAKOBSEN, B. K., GRIFFITHS, G., JONES, E. Y. & CERUNDOLO, V. 2005. Structural and kinetic basis for heightened immunogenicity of T cell vaccines. *The Journal of experimental medicine,* 201**,** 1243-55.

CHEN, L. & FLIES, D. B. 2013. Molecular mechanisms of T cell co-stimulation and co-inhibition. *Nature reviews. Immunology,* 13**,** 227-42.

CHEN, W. & ZHU, C. 2013. Mechanical regulation of T-cell functions. *Immunological reviews,* 256**,** 160-76.

CHERVIN, A. S., AGGEN, D. H., RASEMAN, J. M. & KRANZ, D. M. 2008. Engineering higher affinity T cell receptors using a T cell display system. *Journal of immunological methods,* 339**,** 175-84.

CHERVIN, A. S., STONE, J. D., SOTO, C. M., ENGELS, B., SCHREIBER, H., ROY, E. J. & KRANZ, D. M. 2013. Design of T-cell receptor libraries with diverse

binding properties to examine adoptive T-cell responses. *Gene therapy,* 20**,** 634-44.

CHICAYBAM, L., SODRE, A. L. & BONAMINO, M. 2011. Chimeric antigen receptors in cancer immuno-gene therapy: current status and future directions. *International reviews of immunology,* 30**,** 294-311.

CHINNASAMY, N., WARGO, J. A., YU, Z., RAO, M., FRANKEL, T. L., RILEY, J. P., HONG, J. J., PARKHURST, M. R., FELDMAN, S. A., SCHRUMP, D. S., RESTIFO, N. P., ROBBINS, P. F., ROSENBERG, S. A. & MORGAN, R. A. 2011. A TCR targeting the HLA-A*0201-restricted epitope of MAGE-A3 recognizes multiple epitopes of the MAGE-A antigen superfamily in several types of cancer. *Journal of immunology,* 186**,** 685-96.

CHIU, Y. L., SHAN, L., HUANG, H., HAUPT, C., BESSELL, C., CANADAY, D. H., ZHANG, H., HO, Y. C., POWELL, J. D., OELKE, M., MARGOLICK, J. B., BLANKSON, J. N., GRIFFIN, D. E. & SCHNECK, J. P. 2014. Sprouty-2 regulates HIV-specific T cell polyfunctionality. *The Journal of clinical investigation,* 124**,** 198-208.

CHLEWICKI, L. K., HOLLER, P. D., MONTI, B. C., CLUTTER, M. R. & KRANZ, D. M. 2005. High-affinity, peptide-specific T cell receptors can be generated by mutations in CDR1, CDR2 or CDR3. *Journal of molecular biology,* 346**,** 223-39.

CHOUDHURI, K., LLODRA, J., ROTH, E. W., TSAI, J., GORDO, S., WUCHERPFENNIG, K. W., KAM, L. C., STOKES, D. L. & DUSTIN, M. L. 2014. Polarized release of T-cell-receptor-enriched microvesicles at the immunological synapse. *Nature,* 507**,** 118-23.

CHOUDHURI, K., WISEMAN, D., BROWN, M. H., GOULD, K. & VAN DER MERWE, P. A. 2005. T-cell receptor triggering is critically dependent on the dimensions of its peptide-MHC ligand. *Nature,* 436**,** 578-82.

COLE, D. K., YUAN, F., RIZKALLAH, P. J., MILES, J. J., GOSTICK, E., PRICE, D. A., GAO, G. F., JAKOBSEN, B. K. & SEWELL, A. K. 2009. Germ line-governed recognition of a cancer epitope by an immunodominant human T-cell receptor. *The Journal of biological chemistry,* 284**,** 27281-9.

COLF, L. A., BANKOVICH, A. J., HANICK, N. A., BOWERMAN, N. A., JONES, L. L., KRANZ, D. M. & GARCIA, K. C. 2007. How a single T cell receptor recognizes both self and foreign MHC. *Cell,* 129**,** 135-46.

COLLINS, A. V., BRODIE, D. W., GILBERT, R. J., IABONI, A., MANSO-SANCHO, R., WALSE, B., STUART, D. I., VAN DER MERWE, P. A. & DAVIS, S. J. 2002. The interaction properties of costimulatory molecules revisited. *Immunity,* 17**,** 201-10.

COLLINS, E. J. & RIDDLE, D. S. 2008. TCR-MHC docking orientation: natural selection, or thymic selection? *Immunologic research,* 41**,** 267-94.

COOMBS, D., KALERGIS, A. M., NATHENSON, S. G., WOFSY, C. & GOLDSTEIN, B. 2002. Activated TCRs remain marked for internalization after dissociation from pMHC. *Nature immunology,* 3**,** 926-31.

CORDOBA, S. P., CHOUDHURI, K., ZHANG, H., BRIDGE, M., BASAT, A. B., DUSTIN, M. L. & VAN DER MERWE, P. A. 2013. The large ectodomains of CD45 and CD148 regulate their segregation from and inhibition of ligated T-cell receptor. *Blood,* 121**,** 4295-302.

CORSE, E., GOTTSCHALK, R. A., KROGSGAARD, M. & ALLISON, J. P. 2010. Attenuated T cell responses to a high-potency ligand in vivo. *PLoS biology,* 8.

COSSON, P., LANKFORD, S. P., BONIFACINO, J. S. & KLAUSNER, R. D. 1991. Membrane protein association by potential intramembrane charge pairs. *Nature,* 351**,** 414-6.

CUNNINGHAM, B. C. & WELLS, J. A. 1989. High-resolution epitope mapping of hGH-receptor interactions by alanine-scanning mutagenesis. *Science,* 244**,** 1081-5.

DAI, S., HUSEBY, E. S., RUBTSOVA, K., SCOTT-BROWNE, J., CRAWFORD, F., MACDONALD, W. A., MARRACK, P. & KAPPLER, J. W. 2008. Crossreactive T Cells spotlight the germline rules for alphabeta T cell-receptor interactions with MHC molecules. *Immunity,* 28**,** 324-34.

DALEY, G. Q., VAN ETTEN, R. A. & BALTIMORE, D. 1990. Induction of chronic myelogenous leukemia in mice by the P210bcr/abl gene of the Philadelphia chromosome. *Science,* 247**,** 824-30.

DAS, J., HO, M., ZIKHERMAN, J., GOVERN, C., YANG, M., WEISS, A., CHAKRABORTY, A. K. & ROOSE, J. P. 2009. Digital signaling and hysteresis characterize ras activation in lymphoid cells. *Cell,* 136**,** 337-51.

DAVIS, M. M. & BJORKMAN, P. J. 1988. T-cell antigen receptor genes and T-cell recognition. *Nature,* 334**,** 395-402.

DAVIS, S. J. & VAN DER MERWE, P. A. 1996. The structure and ligand interactions of CD2: implications for T-cell function. *Immunology today,* 17**,** 177-87.

DAVIS, S. J. & VAN DER MERWE, P. A. 2006. The kinetic-segregation model: TCR triggering and beyond. *Nature immunology,* 7**,** 803-9.

DAVIS, S. J. & VAN DER MERWE, P. A. 2011. Lck and the nature of the T cell receptor trigger. *Trends in immunology,* 32**,** 1-5.

DEFORD-WATTS, L. M., TASSIN, T. C., BECKER, A. M., MEDEIROS, J. J., ALBANESI, J. P., LOVE, P. E., WULFING, C. & VAN OERS, N. S. 2009. The cytoplasmic tail of the T cell receptor CD3 epsilon subunit contains a phospholipid-binding motif that regulates T cell functions. *Journal of immunology,* 183**,** 1055-64.

DEGANO, M., GARCIA, K. C., APOSTOLOPOULOS, V., RUDOLPH, M. G., TEYTON, L. & WILSON, I. A. 2000. A functional hot spot for antigen recognition in a superagonist TCR/MHC complex. *Immunity,* 12**,** 251-61.

DENNEHY, K. M., ELIAS, F., ZEDER-LUTZ, G., DING, X., ALTSCHUH, D., LUHDER, F. & HUNIG, T. 2006. Cutting edge: monovalency of CD28 maintains the antigen dependence of T cell costimulatory responses. *J Immunol,* 176**,** 5725-9.

DIEHN, M., ALIZADEH, A. A., RANDO, O. J., LIU, C. L., STANKUNAS, K., BOTSTEIN, D., CRABTREE, G. R. & BROWN, P. O. 2002. Genomic expression programs and the integration of the CD28 costimulatory signal in T cell activation. *Proc Natl Acad Sci U S A,* 99**,** 11796-801.

DING, Y. H., BAKER, B. M., GARBOCZI, D. N., BIDDISON, W. E. & WILEY, D. C. 1999. Four A6-TCR/peptide/HLA-A2 structures that generate very different T cell signals are nearly identical. *Immunity,* 11**,** 45-56.

DODSON, F. D., BOOMER, J. S., C.M, D., SHAH, D. D., SIM, J., BRICKER, T. L., RUSSELL, J. H. & J.M, G. 2009. Targeted Knock-in mice expressing mutations of CD28 reveal an essential pathway for costimulation. *Molecular and Cellular Biology***,** 3710-3721.

DUSHEK, O., ALEKSIC, M., WHEELER, R. J., ZHANG, H., CORDOBA, S. P., PENG, Y. C., CHEN, J. L., CERUNDOLO, V., DONG, T., COOMBS, D. & VAN DER MERWE, P. A. 2011. Antigen potency and maximal efficacy reveal a mechanism of efficient T cell activation. *Science signaling,* 4**,** ra39.

DUSHEK, O., GOYETTE, J. & VAN DER MERWE, P. A. 2012. Non-catalytic tyrosine-phosphorylated receptors. *Immunological reviews,* 250**,** 258-76.

DUSHEK, O. & VAN DER MERWE, P. A. 2014. An induced rebinding model of antigen discrimination. *Trends Immunol,* 35**,** 153-158.

DUSTIN, M. L. 2007. Cell adhesion molecules and actin cytoskeleton at immune synapses and kinapses. *Curr Opin Cell Biol,* 19**,** 529-33.

DUSTIN, M. L. 2009. Modular design of immunological synapses and kinapses. *Cold Spring Harb Perspect Biol,* 1**,** a002873.

DUSTIN, M. L. & DAVIS, S. J. 2014. TCR signaling: the barrier within. *Nature immunology,* 15**,** 136-7.

EASTWOOD, D., FINDLAY, L., POOLE, S., BIRD, C., WADHWA, M., MOORE, M., BURNS, C., THORPE, R. & STEBBINGS, R. 2010. Monoclonal antibody TGN1412 trial failure explained by species differences in CD28 expression on CD4+ effector memory T-cells. *British journal of pharmacology,* 161**,** 512-26.

EISSNER, G., KOLCH, W. & SCHEURICH, P. 2004. Ligands working as receptors: reverse signaling by members of the TNF superfamily enhance the plasticity of the immune system. *Cytokine & growth factor reviews,* 15**,** 353-66.

ELDER, M. E., LIN, D., CLEVER, J., CHAN, A. C., HOPE, T. J., WEISS, A. & PARSLOW, T. G. 1994. Human severe combined immunodeficiency due to a defect in ZAP-70, a T cell tyrosine kinase. *Science,* 264**,** 1596-9.

ELY, L. K., BEDDOE, T., CLEMENTS, C. S., MATTHEWS, J. M., PURCELL, A. W., KJER-NIELSEN, L., MCCLUSKEY, J. & ROSSJOHN, J. 2006. Disparate thermodynamics governing T cell receptor-MHC-I interactions implicate extrinsic factors in guiding MHC restriction. *Proceedings of the National Academy of Sciences of the United States of America,* 103**,** 6641-6.

ESAU, C., BOES, M., YOUN, H. D., TATTERSON, L., LIU, J. O. & CHEN, J. 2001. Deletion of calcineurin and myocyte enhancer factor 2 (MEF2) binding domain of Cabin1 results in enhanced cytokine gene expression in T cells. *The Journal of experimental medicine,* 194**,** 1449-59.

EUN, S. Y., O'CONNOR, B. P., WONG, A. W., VAN DEVENTER, H. W., TAXMAN, D. J., REED, W., LI, P., BLUM, J. S., MCKINNON, K. P. & TING, J. P. 2006. Cutting edge: rho activation and actin polarization are dependent on plexin-A1 in dendritic cells. *J Immunol,* 177**,** 4271-5.

EVANS, E. J., ESNOUF, R. M., MANSO-SANCHO, R., GILBERT, R. J., JAMES, J. R., YU, C., FENNELLY, J. A., VOWLES, C., HANKE, T., WALSE, B., HUNIG, T., SORENSEN, P., STUART, D. I. & DAVIS, S. J. 2005. Crystal structure of a soluble CD28-Fab complex. *Nat Immunol,* 6**,** 271-9.

FEINERMAN, O., GERMAIN, R. N. & ALTAN-BONNET, G. 2008. Quantitative challenges in understanding ligand discrimination by alphabeta T cells. *Molecular immunology,* 45**,** 619-31.

FENG, D., BOND, C. J., ELY, L. K., MAYNARD, J. & GARCIA, K. C. 2007. Structural evidence for a germline-encoded T cell receptor-major histocompatibility complex interaction 'codon'. *Nature immunology,* 8**,** 975-83.

FERNANDES, R. A., YU, C., CARMO, A. M., EVANS, E. J., VAN DER MERWE, P. A. & DAVIS, S. J. 2010. What controls T cell receptor phosphorylation? *Cell,* 142**,** 668-9.

FISCHER, K. D., KONG, Y. Y., NISHINA, H., TEDFORD, K., MARENGERE, L. E., KOZIERADZKI, I., SASAKI, T., STARR, M., CHAN, G., GARDENER, S., NGHIEM, M. P., BOUCHARD, D., BARBACID, M., BERNSTEIN, A. & PENNINGER, J. M. 1998. Vav is a regulator of cytoskeletal reorganization mediated by the T-cell receptor. *Current biology : CB,* 8**,** 554-62.

FOLMER, R. H., GESCHWINDNER, S. & XUE, Y. 2002. Crystal structure and NMR studies of the apo SH2 domains of ZAP-70: two bikes rather than a tandem. *Biochemistry,* 41**,** 14176-84.

FOOKSMAN, D. R., SHAIKH, S. R., BOYLE, S. & EDIDIN, M. 2009. Cutting edge: phosphatidylinositol 4,5-bisphosphate concentration at the APC side of the immunological synapse is required for effector T cell function. *J Immunol,* 182**,** 5179-82.

FRANCOIS, P., VOISINNE, G., SIGGIA, E. D., ALTAN-BONNET, G. & VERGASSOLA, M. 2013. Phenotypic model for early T-cell activation displaying sensitivity, specificity, and antagonism. *Proceedings of the National Academy of Sciences of the United States of America,* 110**,** E888-97.

FRAUWIRTH, K. A., RILEY, J. L., HARRIS, M. H., PARRY, R. V., RATHMELL, J. C., PLAS, D. R., ELSTROM, R. L., JUNE, C. H. & THOMPSON, C. B. 2002. The

CD28 signaling pathway regulates glucose metabolism. *Immunity,* 16**,** 769-77.

FREEMAN, G. J., GRAY, G. S., GIMMI, C. D., LOMBARD, D. B., ZHOU, L. J., WHITE, M., FINGEROTH, J. D., GRIBBEN, J. G. & NADLER, L. M. 1991. Structure, expression, and T cell costimulatory activity of the murine homologue of the human B lymphocyte activation antigen B7. *The Journal of experimental medicine,* 174**,** 625-31.

FRENCH, A. P., MILLS, S., SWARUP, R., BENNETT, M. J. & PRIDMORE, T. P. 2008. Colocalization of fluorescent markers in confocal microscope images of plant cells. *Nature protocols,* 3**,** 619-28.

FRIEND, L. D., SHAH, D. D., DEPPONG, C., LIN, J., BRICKER, T. L., JUEHNE, T. I., ROSE, C. M. & GREEN, J. M. 2006. A dose-dependent requirement for the proline motif of CD28 in cellular and humoral immunity revealed by a targeted knockin mutant. *J Exp Med,* 203**,** 2121-33.

GAGLIA, J. L., MATTOO, A., GREENFIELD, E. A., FREEMAN, G. J. & KUCHROO, V. K. 2001. Characterization of endogenous Chinese hamster ovary cell surface molecules that mediate T cell costimulation. *Cellular immunology,* 213**,** 83-93.

GAGNON, E., XU, C., YANG, W., CHU, H. H., CALL, M. E., CHOU, J. J. & WUCHERPFENNIG, K. W. 2010. Response multilayered control of T cell receptor phosphorylation. *Cell,* 142**,** 669-71.

GARBOCZI, D. N., GHOSH, P., UTZ, U., FAN, Q. R., BIDDISON, W. E. & WILEY, D. C. 1996. Structure of the complex between human T-cell receptor, viral peptide and HLA-A2. *Nature,* 384**,** 134-41.

GARCIA, K. C. 2012. Reconciling views on T cell receptor germline bias for MHC. *Trends in immunology,* 33**,** 429-36.

GARCIA, K. C., ADAMS, J. J., FENG, D. & ELY, L. K. 2009. The molecular basis of TCR germline bias for MHC is surprisingly simple. *Nature immunology,* 10**,** 143-7.

GARCIA, K. C., DEGANO, M., PEASE, L. R., HUANG, M., PETERSON, P. A., TEYTON, L. & WILSON, I. A. 1998. Structural basis of plasticity in T cell receptor recognition of a self peptide-MHC antigen. *Science,* 279**,** 1166-72.

GARCIA, K. C., DEGANO, M., STANFIELD, R. L., BRUNMARK, A., JACKSON, M. R., PETERSON, P. A., TEYTON, L. & WILSON, I. A. 1996. An alphabeta T cell receptor structure at 2.5 A and its orientation in the TCR-MHC complex. *Science,* 274**,** 209-19.

GARCIA, K. C., RADU, C. G., HO, J., OBER, R. J. & WARD, E. S. 2001. Kinetics and thermodynamics of T cell receptor- autoantigen interactions in murine experimental autoimmune encephalomyelitis. *Proceedings of the National Academy of Sciences of the United States of America,* 98**,** 6818-23.

GARCON, F., PATTON, D. T., EMERY, J. L., HIRSCH, E., ROTTAPEL, R., SASAKI, T. & OKKENHAUG, K. 2008. CD28 provides T-cell costimulation and enhances PI3K activity at the immune synapse independently of its capacity to interact with the p85/p110 heterodimer. *Blood,* 111**,** 1464-71.

GARRETT, T. P., WANG, J., YAN, Y., LIU, J. & HARRISON, S. C. 1993. Refinement and analysis of the structure of the first two domains of human CD4. *Journal of molecular biology,* 234**,** 763-78.

GERMAIN, R. N. 2002. T-cell development and the CD4-CD8 lineage decision. *Nature reviews. Immunology,* 2**,** 309-22.

GHENDLER, Y., SMOLYAR, A., CHANG, H. C. & REINHERZ, E. L. 1998. One of the CD3epsilon subunits within a T cell receptor complex lies in close proximity to the Cbeta FG loop. *The Journal of experimental medicine,* 187**,** 1529-36.

GIGOUX, M., SHANG, J., PAK, Y., XU, M., CHOE, J., MAK, T. W. & SUH, W. K. 2009. Inducible costimulator promotes helper T-cell differentiation through

phosphoinositide 3-kinase. *Proceedings of the National Academy of Sciences of the United States of America,* 106**,** 20371-6.

GIL, D., SCHAMEL, W. W., MONTOYA, M., SANCHEZ-MADRID, F. & ALARCON, B. 2002. Recruitment of Nck by CD3 epsilon reveals a ligand-induced conformational change essential for T cell receptor signaling and synapse formation. *Cell,* 109**,** 901-12.

GIL, D., SCHRUM, A. G., ALARCON, B. & PALMER, E. 2005. T cell receptor engagement by peptide-MHC ligands induces a conformational change in the CD3 complex of thymocytes. *The Journal of experimental medicine,* 201**,** 517-22.

GODFREY, D. I., ROSSJOHN, J. & MCCLUSKEY, J. 2008. The fidelity, occasional promiscuity, and versatility of T cell receptor recognition. *Immunity,* 28**,** 304-14.

GONZALEZ, P. A., CARRENO, L. J., COOMBS, D., MORA, J. E., PALMIERI, E., GOLDSTEIN, B., NATHENSON, S. G. & KALERGIS, A. M. 2005. T cell receptor binding kinetics required for T cell activation depend on the density of cognate ligand on the antigen-presenting cell. *Proceedings of the National Academy of Sciences of the United States of America,* 102**,** 4824-9.

GOODRIDGE, H. S., REYES, C. N., BECKER, C. A., KATSUMOTO, T. R., MA, J., WOLF, A. J., BOSE, N., CHAN, A. S., MAGEE, A. S., DANIELSON, M. E., WEISS, A., VASILAKOS, J. P. & UNDERHILL, D. M. 2011. Activation of the innate immune receptor Dectin-1 upon formation of a 'phagocytic synapse'. *Nature,* 472**,** 471-5.

GREENFIELD, C., HILES, I., WATERFIELD, M. D., FEDERWISCH, M., WOLLMER, A., BLUNDELL, T. L. & MCDONALD, N. 1989. Epidermal growth factor binding induces a conformational change in the external domain of its receptor. *The EMBO journal,* 8**,** 4115-23.

HAHN, M., NICHOLSON, M. J., PYRDOL, J. & WUCHERPFENNIG, K. W. 2005. Unconventional topology of self peptide-major histocompatibility complex binding by a human autoimmune T cell receptor. *Nature immunology,* 6**,** 490-6.

HANADA, K. & RESTIFO, N. P. 2013. Double or nothing on cancer immunotherapy. *Nature biotechnology,* 31**,** 33-4.

HARADA, Y., OHGAI, D., WATANABE, R., OKANO, K., KOIWAI, O., TANABE, K., TOMA, H., ALTMAN, A. & ABE, R. 2003. A single amino acid alteration in cytoplasmic domain determines IL-2 promoter activation by ligation of CD28 but not inducible costimulator (ICOS). *The Journal of experimental medicine,* 197**,** 257-62.

HARADA, Y., TOKUSHIMA, M., MATSUMOTO, Y., OGAWA, S., OTSUKA, M., HAYASHI, K., WEISS, B. D., JUNE, C. H. & ABE, R. 2001. Critical requirement for the membrane-proximal cytosolic tyrosine residue for CD28-mediated costimulation in vivo. *J Immunol,* 166**,** 3797-803.

HAYASHI, K. & ALTMAN, A. 2006. Filamin A is required for T cell activation mediated by protein kinase C-theta. *Journal of immunology,* 177**,** 1721-8.

HE, X., WOODFORD-THOMAS, T. A., JOHNSON, K. G., SHAH, D. D. & THOMAS, M. L. 2002. Targeting of CD45 protein tyrosine phosphatase activity to lipid microdomains on the T cell surface inhibits TCR signaling. *European journal of immunology,* 32**,** 2578-87.

HOFFMANN, E., DITTRICH-BREIHOLZ, O., HOLTMANN, H. & KRACHT, M. 2002. Multiple control of interleukin-8 gene expression. *Journal of leukocyte biology,* 72**,** 847-55.

HOLDORF, A. D., GREEN, J. M., LEVIN, S. D., DENNY, M. F., STRAUS, D. B., LINK, V., CHANGELIAN, P. S., ALLEN, P. M. & SHAW, A. S. 1999. Proline residues in CD28 and the Src homology (SH)3 domain of Lck are required for T cell costimulation. *J Exp Med,* 190**,** 375-84.

HOLLAND, C. J., RIZKALLAH, P. J., VOLLERS, S., CALVO-CALLE, J. M., MADURA, F., FULLER, A., SEWELL, A. K., STERN, L. J., GODKIN, A. & COLE, D. K. 2012. Minimal conformational plasticity enables TCR cross-reactivity to different MHC class II heterodimers. *Scientific reports,* 2**,** 629.

HOLLER, P. D., CHLEWICKI, L. K. & KRANZ, D. M. 2003. TCRs with high affinity for foreign pMHC show self-reactivity. *Nature immunology,* 4**,** 55-62.

HOLLER, P. D., HOLMAN, P. O., SHUSTA, E. V., O'HERRIN, S., WITTRUP, K. D. & KRANZ, D. M. 2000. In vitro evolution of a T cell receptor with high affinity for peptide/MHC. *Proceedings of the National Academy of Sciences of the United States of America,* 97**,** 5387-92.

HOLLER, P. D. & KRANZ, D. M. 2003. Quantitative analysis of the contribution of TCR/pepMHC affinity and CD8 to T cell activation. *Immunity,* 18**,** 255-64.

HOMBACH, A. A., SCHILDGEN, V., HEUSER, C., FINNERN, R., GILHAM, D. E. & ABKEN, H. 2007. T cell activation by antibody-like immunoreceptors: the position of the binding epitope within the target molecule determines the efficiency of activation of redirected T cells. *Journal of immunology,* 178**,** 4650-7.

HORNSTEIN, I., ALCOVER, A. & KATZAV, S. 2004. Vav proteins, masters of the world of cytoskeleton organization. *Cellular signalling,* 16**,** 1-11.

HOUTMAN, J. C., YAMAGUCHI, H., BARDA-SAAD, M., BRAIMAN, A., BOWDEN, B., APPELLA, E., SCHUCK, P. & SAMELSON, L. E. 2006. Oligomerization of signaling complexes by the multipoint binding of GRB2 to both LAT and SOS1. *Nature structural & molecular biology,* 13**,** 798-805.

HUANG, J., ZARNITSYNA, V. I., LIU, B., EDWARDS, L. J., JIANG, N., EVAVOLD, B. D. & ZHU, C. 2010. The kinetics of two-dimensional TCR and pMHC interactions determine T-cell responsiveness. *Nature,* 464**,** 932-6.

HUGHES, M. S., YU, Y. Y., DUDLEY, M. E., ZHENG, Z., ROBBINS, P. F., LI, Y., WUNDERLICH, J., HAWLEY, R. G., MOAYERI, M., ROSENBERG, S. A. & MORGAN, R. A. 2005. Transfer of a TCR gene derived from a patient with a marked antitumor response conveys highly active T-cell effector functions. *Human gene therapy,* 16**,** 457-72.

HUNDT, M., HARADA, Y., DE GIORGIO, L., TANIMURA, N., ZHANG, W. & ALTMAN, A. 2009. Palmitoylation-dependent plasma membrane transport but lipid raft-independent signaling by linker for activation of T cells. *Journal of immunology,* 183**,** 1685-94.

HUNDT, M., TABATA, H., JEON, M. S., HAYASHI, K., TANAKA, Y., KRISHNA, R., DE GIORGIO, L., LIU, Y. C., FUKATA, M. & ALTMAN, A. 2006. Impaired activation and localization of LAT in anergic T cells as a consequence of a selective palmitoylation defect. *Immunity,* 24**,** 513-22.

HUNIG, T. & DENNEHY, K. 2005. CD28 superagonists: mode of action and therapeutic potential. *Immunology letters,* 100**,** 21-8.

HUPPA, J. B., AXMANN, M., MORTELMAIER, M. A., LILLEMEIER, B. F., NEWELL, E. W., BRAMESHUBER, M., KLEIN, L. O., SCHUTZ, G. J. & DAVIS, M. M. 2010. TCR-peptide-MHC interactions in situ show accelerated kinetics and increased affinity. *Nature,* 463**,** 963-7.

HUSE, M., KLEIN, L. O., GIRVIN, A. T., FARAJ, J. M., LI, Q. J., KUHNS, M. S. & DAVIS, M. M. 2007. Spatial and temporal dynamics of T cell receptor signaling with a photoactivatable agonist. *Immunity,* 27**,** 76-88.

HUSEBY, E. S., WHITE, J., CRAWFORD, F., VASS, T., BECKER, D., PINILLA, C., MARRACK, P. & KAPPLER, J. W. 2005. How the T cell repertoire becomes peptide and MHC specific. *Cell,* 122**,** 247-60.

IKEMIZU, S., GILBERT, R. J., FENNELLY, J. A., COLLINS, A. V., HARLOS, K., JONES, E. Y., STUART, D. I. & DAVIS, S. J. 2000. Structure and dimerization of a soluble form of B7-1. *Immunity,* 12**,** 51-60.

IRVINE, D. J., PURBHOO, M. A., KROGSGAARD, M. & DAVIS, M. M. 2002. Direct observation of ligand recognition by T cells. *Nature,* 419**,** 845-9.

IRVING, B. A. & WEISS, A. 1991. The cytoplasmic domain of the T cell receptor zeta chain is sufficient to couple to receptor-associated signal transduction pathways. *Cell,* 64**,** 891-901.

ISAKOV, N., WANGE, R. L., BURGESS, W. H., WATTS, J. D., AEBERSOLD, R. & SAMELSON, L. E. 1995. ZAP-70 binding specificity to T cell receptor tyrosine-based activation motifs: the tandem SH2 domains of ZAP-70 bind distinct tyrosine-based activation motifs with varying affinity. *The Journal of experimental medicine,* 181**,** 375-80.

ISHIDA, Y., AGATA, Y., SHIBAHARA, K. & HONJO, T. 1992. Induced expression of PD-1, a novel member of the immunoglobulin gene superfamily, upon programmed cell death. *The EMBO journal,* 11**,** 3887-95.

ISHIZUKA, J., STEWART-JONES, G. B., VAN DER MERWE, A., BELL, J. I., MCMICHAEL, A. J. & JONES, E. Y. 2008. The structural dynamics and energetics of an immunodominant T cell receptor are programmed by its Vbeta domain. *Immunity,* 28**,** 171-82.

ITOH, Y. & GERMAIN, R. N. 1997. Single cell analysis reveals regulated hierarchical T cell antigen receptor signaling thresholds and intraclonal heterogeneity for individual cytokine responses of CD4+ T cells. *The Journal of experimental medicine,* 186**,** 757-66.

JACKMAN, R. P., BALAMUTH, F. & BOTTOMLY, K. 2007. CTLA-4 differentially regulates the immunological synapse in CD4 T cell subsets. *J Immunol,* 178**,** 5543-51.

JAIN, N., MIU, B., JIANG, J. K., MCKINSTRY, K. K., PRINCE, A., SWAIN, S. L., GREINER, D. L., THOMAS, C. J., SANDERSON, M. J., BERG, L. J. & KANG, J. 2013. CD28 and ITK signals regulate autoreactive T cell trafficking. *Nature medicine,* 19**,** 1632-7.

JAMES, J. R. & VALE, R. D. 2012. Biophysical mechanism of T-cell receptor triggering in a reconstituted system. *Nature,* 487**,** 64-9.

JAMES, J. R., WHITE, S. S., CLARKE, R. W., JOHANSEN, A. M., DUNNE, P. D., SLEEP, D. L., FITZGERALD, W. J., DAVIS, S. J. & KLENERMAN, D. 2007. Single-molecule level analysis of the subunit composition of the T cell receptor on live T cells. *Proceedings of the National Academy of Sciences of the United States of America,* 104**,** 17662-7.

JAMESON, S. C., CARBONE, F. R. & BEVAN, M. J. 1993. Clone-specific T cell receptor antagonists of major histocompatibility complex class I-restricted cytotoxic T cells. *The Journal of experimental medicine,* 177**,** 1541-50.

JERNE, N. K. 1971. The somatic generation of immune recognition. *European journal of immunology,* 1**,** 1-9.

JOHNSON, K. G., BROMLEY, S. K., DUSTIN, M. L. & THOMAS, M. L. 2000. A supramolecular basis for CD45 tyrosine phosphatase regulation in sustained T cell activation. *Proceedings of the National Academy of Sciences of the United States of America,* 97**,** 10138-43.

JOHNSON, L. A., MORGAN, R. A., DUDLEY, M. E., CASSARD, L., YANG, J. C., HUGHES, M. S., KAMMULA, U. S., ROYAL, R. E., SHERRY, R. M., WUNDERLICH, J. R., LEE, C. C., RESTIFO, N. P., SCHWARZ, S. L., COGDILL, A. P., BISHOP, R. J., KIM, H., BREWER, C. C., RUDY, S. F., VANWAES, C., DAVIS, J. L., MATHUR, A., RIPLEY, R. T., NATHAN, D. A., LAURENCOT, C. M. & ROSENBERG, S. A. 2009. Gene therapy with human and mouse T-cell receptors mediates cancer regression and targets normal tissues expressing cognate antigen. *Blood,* 114**,** 535-46.

JONES, L. L., COLF, L. A., STONE, J. D., GARCIA, K. C. & KRANZ, D. M. 2008. Distinct CDR3 conformations in TCRs determine the level of cross-reactivity

for diverse antigens, but not the docking orientation. *Journal of immunology,* 181**,** 6255-64.

JORDAN, M. S., SMITH, J. E., BURNS, J. C., AUSTIN, J. E., NICHOLS, K. E., ASCHENBRENNER, A. C. & KORETZKY, G. A. 2008. Complementation in trans of altered thymocyte development in mice expressing mutant forms of the adaptor molecule SLP76. *Immunity,* 28**,** 359-69.

JUNE, C. H., LEDBETTER, J. A., GILLESPIE, M. M., LINDSTEN, T. & THOMPSON, C. B. 1987. T-cell proliferation involving the CD28 pathway is associated with cyclosporine-resistant interleukin 2 gene expression. *Molecular and cellular biology,* 7**,** 4472-81.

KAGA, S., RAGG, S., ROGERS, K. A. & OCHI, A. 1998. Stimulation of CD28 with B7-2 promotes focal adhesion-like cell contacts where Rho family small G proteins accumulate in T cells. *Journal of immunology,* 160**,** 24-7.

KAIZUKA, Y., DOUGLASS, A. D., VARMA, R., DUSTIN, M. L. & VALE, R. D. 2007. Mechanisms for segregating T cell receptor and adhesion molecules during immunological synapse formation in Jurkat T cells. *Proc Natl Acad Sci U S A,* 104**,** 20296-301.

KALERGIS, A. M., BOUCHERON, N., DOUCEY, M. A., PALMIERI, E., GOYARTS, E. C., VEGH, Z., LUESCHER, I. F. & NATHENSON, S. G. 2001. Efficient T cell activation requires an optimal dwell-time of interaction between the TCR and the pMHC complex. *Nature immunology,* 2**,** 229-34.

KALOS, M. & JUNE, C. H. 2013. Adoptive T cell transfer for cancer immunotherapy in the era of synthetic biology. *Immunity,* 39**,** 49-60.

KANE, L. P., SHAPIRO, V. S., STOKOE, D. & WEISS, A. 1999. Induction of NF-kappaB by the Akt/PKB kinase. *Current biology : CB,* 9**,** 601-4.

KESSELS, H. W., VAN DEN BOOM, M. D., SPITS, H., HOOIJBERG, E. & SCHUMACHER, T. N. 2000. Changing T cell specificity by retroviral T cell receptor display. *Proceedings of the National Academy of Sciences of the United States of America,* 97**,** 14578-83.

KHOSHNAN, A., TINDELL, C., LAUX, I., BAE, D., BENNETT, B. & NEL, A. E. 2000. The NF-kappa B cascade is important in Bcl-xL expression and for the anti-apoptotic effects of the CD28 receptor in primary human CD4+ lymphocytes. *Journal of immunology,* 165**,** 1743-54.

KIM, H. H., THARAYIL, M. & RUDD, C. E. 1998. Growth factor receptor-bound protein 2 SH2/SH3 domain binding to CD28 and its role in co-signaling. *The Journal of biological chemistry,* 273**,** 296-301.

KIM, S. T., TAKEUCHI, K., SUN, Z. Y., TOUMA, M., CASTRO, C. E., FAHMY, A., LANG, M. J., WAGNER, G. & REINHERZ, E. L. 2009. The alphabeta T cell receptor is an anisotropic mechanosensor. *The Journal of biological chemistry,* 284**,** 31028-37.

KIM, S. T., TOUMA, M., TAKEUCHI, K., SUN, Z. Y., DAVE, V. P., KAPPES, D. J., WAGNER, G. & REINHERZ, E. L. 2010. Distinctive CD3 heterodimeric ectodomain topologies maximize antigen-triggered activation of alpha beta T cell receptors. *Journal of immunology,* 185**,** 2951-9.

KING, C. L., STUPI, R. J., CRAIGHEAD, N., JUNE, C. H. & THYPHRONITIS, G. 1995. CD28 activation promotes Th2 subset differentiation by human CD4+ cells. *European journal of immunology,* 25**,** 587-95.

KJER-NIELSEN, L., CLEMENTS, C. S., PURCELL, A. W., BROOKS, A. G., WHISSTOCK, J. C., BURROWS, S. R., MCCLUSKEY, J. & ROSSJOHN, J. 2003. A structural basis for the selection of dominant alphabeta T cell receptors in antiviral immunity. *Immunity,* 18**,** 53-64.

KOHLER, K., XIONG, S., BRZOSTEK, J., MEHRABI, M., EISSMANN, P., HARRISON, A., CORDOBA, S. P., ODDOS, S., MILOSERDOV, V., GOULD, K., BURROUGHS, N. J., VAN DER MERWE, P. A. & DAVIS, D. M. 2010. Matched sizes of activating and inhibitory receptor/ligand pairs are required

for optimal signal integration by human natural killer cells. *PloS one,* 5**,** e15374.

KONG, K. F., YOKOSUKA, T., CANONIGO-BALANCIO, A. J., ISAKOV, N., SAITO, T. & ALTMAN, A. 2011. A motif in the V3 domain of the kinase PKC-theta determines its localization in the immunological synapse and functions in T cells via association with CD28. *Nature immunology,* 12**,** 1105-12.

KOVALEV, G. I., FRANKLIN, D. S., COFFIELD, V. M., XIONG, Y. & SU, L. 2001. An important role of CDK inhibitor p18(INK4c) in modulating antigen receptor-mediated T cell proliferation. *Journal of immunology,* 167**,** 3285-92.

KRAWCZYK, C., OLIVEIRA-DOS-SANTOS, A., SASAKI, T., GRIFFITHS, E., OHASHI, P. S., SNAPPER, S., ALT, F. & PENNINGER, J. M. 2002. Vav1 controls integrin clustering and MHC/peptide-specific cell adhesion to antigen-presenting cells. *Immunity,* 16**,** 331-43.

KROGSGAARD, M., JUANG, J. & DAVIS, M. M. 2007. A role for "self" in T-cell activation. *Seminars in immunology,* 19**,** 236-44.

KROGSGAARD, M., LI, Q. J., SUMEN, C., HUPPA, J. B., HUSE, M. & DAVIS, M. M. 2005. Agonist/endogenous peptide-MHC heterodimers drive T cell activation and sensitivity. *Nature,* 434**,** 238-43.

KRUMMEL, M. F., SJAASTAD, M. D., WULFING, C. & DAVIS, M. M. 2000. Differential clustering of CD4 and CD3zeta during T cell recognition. *Science,* 289**,** 1349-52.

KUHNS, M. S. & DAVIS, M. M. 2008. The safety on the TCR trigger. *Cell,* 135**,** 594-6.

KUHNS, S. T. & PEASE, L. R. 1998. A region of conformational variability outside the peptide-binding site of a class I MHC molecule. *Journal of immunology,* 161**,** 6745-50.

LADBURY, J. E. 1996. Just add water! The effect of water on the specificity of protein-ligand binding sites and its potential application to drug design. *Chemistry & biology,* 3**,** 973-80.

LADBURY, J. E. 2004. Application of isothermal titration calorimetry in the biological sciences: things are heating up! *BioTechniques,* 37**,** 885-7.

LAFFERTY, K. J. & CUNNINGHAM, A. J. 1975. A new analysis of allogeneic interactions. *The Australian journal of experimental biology and medical science,* 53**,** 27-42.

LEE, J. K., STEWART-JONES, G., DONG, T., HARLOS, K., DI GLERIA, K., DORRELL, L., DOUEK, D. C., VAN DER MERWE, P. A., JONES, E. Y. & MCMICHAEL, A. J. 2004. T cell cross-reactivity and conformational changes during TCR engagement. *The Journal of experimental medicine,* 200**,** 1455-66.

LEE, P. U., CHURCHILL, H. R., DANIELS, M., JAMESON, S. C. & KRANZ, D. M. 2000. Role of 2CT cell receptor residues in the binding of self- and allo-major histocompatibility complexes. *The Journal of experimental medicine,* 191**,** 1355-64.

LENSCHOW, D. J., HEROLD, K. C., RHEE, L., PATEL, B., KOONS, A., QIN, H. Y., FUCHS, E., SINGH, B., THOMPSON, C. B. & BLUESTONE, J. A. 1996a. CD28/B7 regulation of Th1 and Th2 subsets in the development of autoimmune diabetes. *Immunity,* 5**,** 285-93.

LENSCHOW, D. J., WALUNAS, T. L. & BLUESTONE, J. A. 1996b. CD28/B7 system of T cell costimulation. *Annual review of immunology,* 14**,** 233-58.

LETOURNEUR, F. & KLAUSNER, R. D. 1992. Activation of T cells by a tyrosine kinase activation domain in the cytoplasmic tail of CD3 epsilon. *Science,* 255**,** 79-82.

LEUPIN, O., ZARU, R., LAROCHE, T., MULLER, S. & VALITUTTI, S. 2000. Exclusion of CD45 from the T-cell receptor signaling area in antigen-stimulated T lymphocytes. *Current biology : CB,* 10**,** 277-80.

LI, Y., MOYSEY, R., MOLLOY, P. E., VUIDEPOT, A. L., MAHON, T., BASTON, E., DUNN, S., LIDDY, N., JACOB, J., JAKOBSEN, B. K. & BOULTER, J. M. 2005. Directed evolution of human T-cell receptors with picomolar affinities by phage display. *Nature biotechnology,* 23**,** 349-54.

LI, Y., YIN, Y. & MARIUZZA, R. A. 2013. Structural and biophysical insights into the role of CD4 and CD8 in T cell activation. *Frontiers in immunology,* 4**,** 206.

LI, Y. C., CHEN, B. M., WU, P. C., CHENG, T. L., KAO, L. S., TAO, M. H., LIEBER, A. & ROFFLER, S. R. 2010. Cutting Edge: mechanical forces acting on T cells immobilized via the TCR complex can trigger TCR signaling. *Journal of immunology,* 184**,** 5959-63.

LIAO, X. C., FOURNIER, S., KILLEEN, N., WEISS, A., ALLISON, J. P. & LITTMAN, D. R. 1997. Itk negatively regulates induction of T cell proliferation by CD28 costimulation. *The Journal of experimental medicine,* 186**,** 221-8.

LIN, C. H. & HUNIG, T. 2003. Efficient expansion of regulatory T cells in vitro and in vivo with a CD28 superagonist. *European journal of immunology,* 33**,** 626-38.

LIN, J. & WEISS, A. 2003. The tyrosine phosphatase CD148 is excluded from the immunologic synapse and down-regulates prolonged T cell signaling. *The Journal of cell biology,* 162**,** 673-82.

LIN, J., WEISS, A. & FINCO, T. S. 1999. Localization of LAT in glycolipid-enriched microdomains is required for T cell activation. *The Journal of biological chemistry,* 274**,** 28861-4.

LINSLEY, P. S. 2005. New look at an old costimulator. *Nat Immunol,* 6**,** 231-2.

LINSLEY, P. S., BRADY, W., URNES, M., GROSMAIRE, L. S., DAMLE, N. K. & LEDBETTER, J. A. 1991. CTLA-4 is a second receptor for the B cell activation antigen B7. *The Journal of experimental medicine,* 174**,** 561-9.

LINTERMAN, M. A., RIGBY, R. J., WONG, R., SILVA, D., WITHERS, D., ANDERSON, G., VERMA, N. K., BRINK, R., HUTLOFF, A., GOODNOW, C. C. & VINUESA, C. G. 2009. Roquin differentiates the specialized functions of duplicated T cell costimulatory receptor genes CD28 and ICOS. *Immunity,* 30**,** 228-41.

LIU, S. K., FANG, N., KORETZKY, G. A. & MCGLADE, C. J. 1999. The hematopoietic-specific adaptor protein gads functions in T-cell signaling via interactions with the SLP-76 and LAT adaptors. *Current biology : CB,* 9**,** 67-75.

LIU, Y. C., CHEN, Z., BURROWS, S. R., PURCELL, A. W., MCCLUSKEY, J., ROSSJOHN, J. & GRAS, S. 2012. The energetic basis underpinning T-cell receptor recognition of a super-bulged peptide bound to a major histocompatibility complex class I molecule. *The Journal of biological chemistry,* 287**,** 12267-76.

LOHR, J., KNOECHEL, B., JIANG, S., SHARPE, A. H. & ABBAS, A. K. 2003. The inhibitory function of B7 costimulators in T cell responses to foreign and self-antigens. *Nature immunology,* 4**,** 664-9.

LUHDER, F., HUANG, Y., DENNEHY, K. M., GUNTERMANN, C., MULLER, I., WINKLER, E., KERKAU, T., IKEMIZU, S., DAVIS, S. J., HANKE, T. & HUNIG, T. 2003. Topological requirements and signaling properties of T cell-activating, anti-CD28 antibody superagonists. *J Exp Med,* 197**,** 955-66.

MA, Z., SHARP, K. A., JANMEY, P. A. & FINKEL, T. H. 2008. Surface-anchored monomeric agonist pMHCs alone trigger TCR with high sensitivity. *PLoS biology,* 6**,** e43.

MACIAN, F., GARCIA-COZAR, F., IM, S. H., HORTON, H. F., BYRNE, M. C. & RAO, A. 2002. Transcriptional mechanisms underlying lymphocyte tolerance. *Cell,* 109**,** 719-31.

MADDEN, D. R., GARBOCZI, D. N. & WILEY, D. C. 1993. The antigenic identity of peptide-MHC complexes: a comparison of the conformations of five viral peptides presented by HLA-A2. *Cell,* 75**,** 693-708.

MANNING, T. C., SCHLUETER, C. J., BRODNICKI, T. C., PARKE, E. A., SPEIR, J. A., GARCIA, K. C., TEYTON, L., WILSON, I. A. & KRANZ, D. M. 1998. Alanine scanning mutagenesis of an alphabeta T cell receptor: mapping the energy of antigen recognition. *Immunity,* 8**,** 413-25.

MARTINEZ-MARTIN, N., RISUENO, R. M., MORREALE, A., ZALDIVAR, I., FERNANDEZ-ARENAS, E., HERRANZ, F., ORTIZ, A. R. & ALARCON, B. 2009. Cooperativity between T cell receptor complexes revealed by conformational mutants of CD3epsilon. *Science signaling,* 2**,** ra43.

MASON, D. 1998a. A very high level of crossreactivity is an essential feature of the T-cell receptor. *Immunology today,* 19**,** 395-404.

MASON, D. 1998b. A very high level of crossreactivity is an essential feature of the T-cell receptor. *Immunol Today,* 19**,** 395-404.

MATSUI, K., BONIFACE, J. J., STEFFNER, P., REAY, P. A. & DAVIS, M. M. 1994. Kinetics of T-cell receptor binding to peptide/I-Ek complexes: correlation of the dissociation rate with T-cell responsiveness. *Proceedings of the National Academy of Sciences of the United States of America,* 91**,** 12862-6.

MATZINGER, P. 2002. The danger model: a renewed sense of self. *Science,* 296**,** 301-5.

MCKEITHAN, T. W. 1995. Kinetic proofreading in T-cell receptor signal transduction. *Proceedings of the National Academy of Sciences of the United States of America,* 92**,** 5042-6.

MINGUENEAU, M., SANSONI, A., GREGOIRE, C., RONCAGALLI, R., AGUADO, E., WEISS, A., MALISSEN, M. & MALISSEN, B. 2008. The proline-rich sequence of CD3epsilon controls T cell antigen receptor expression on and signaling potency in preselection CD4+CD8+ thymocytes. *Nature immunology,* 9**,** 522-32.

MOLLER, A., DIENZ, O., HEHNER, S. P., DROGE, W. & SCHMITZ, M. L. 2001. Protein kinase C theta cooperates with Vav1 to induce JNK activity in T-cells. *The Journal of biological chemistry,* 276**,** 20022-8.

MORGAN, R. A., CHINNASAMY, N., ABATE-DAGA, D., GROS, A., ROBBINS, P. F., ZHENG, Z., DUDLEY, M. E., FELDMAN, S. A., YANG, J. C., SHERRY, R. M., PHAN, G. Q., HUGHES, M. S., KAMMULA, U. S., MILLER, A. D., HESSMAN, C. J., STEWART, A. A., RESTIFO, N. P., QUEZADO, M. M., ALIMCHANDANI, M., ROSENBERG, A. Z., NATH, A., WANG, T., BIELEKOVA, B., WUEST, S. C., AKULA, N., MCMAHON, F. J., WILDE, S., MOSETTER, B., SCHENDEL, D. J., LAURENCOT, C. M. & ROSENBERG, S. A. 2013. Cancer regression and neurological toxicity following anti-MAGE-A3 TCR gene therapy. *Journal of immunotherapy,* 36**,** 133-51.

MORGAN, R. A., DUDLEY, M. E. & ROSENBERG, S. A. 2010. Adoptive cell therapy: genetic modification to redirect effector cell specificity. *Cancer journal,* 16**,** 336-41.

MORGAN, R. A., DUDLEY, M. E., WUNDERLICH, J. R., HUGHES, M. S., YANG, J. C., SHERRY, R. M., ROYAL, R. E., TOPALIAN, S. L., KAMMULA, U. S., RESTIFO, N. P., ZHENG, Z., NAHVI, A., DE VRIES, C. R., ROGERS-FREEZER, L. J., MAVROUKAKIS, S. A. & ROSENBERG, S. A. 2006. Cancer regression in patients after transfer of genetically engineered lymphocytes. *Science,* 314**,** 126-9.

MUKHOPADHYAY, H., CORDOBA, S. P., MAINI, P. K., VAN DER MERWE, P. A. & DUSHEK, O. 2013. Systems model of T cell receptor proximal signaling reveals emergent ultrasensitivity. *PLoS computational biology,* 9**,** e1003004.

MUNN, D. H., SHARMA, M. D. & MELLOR, A. L. 2004. Ligation of B7-1/B7-2 by human CD4+ T cells triggers indoleamine 2,3-dioxygenase activity in dendritic cells. *Journal of immunology,* 172**,** 4100-10.

MURPHY, K. 2012. Janeway's Immunobiology 8th Edition. *New York: Garland Science*.

NEGISHI, I., MOTOYAMA, N., NAKAYAMA, K., SENJU, S., HATAKEYAMA, S., ZHANG, Q., CHAN, A. C. & LOH, D. Y. 1995. Essential role for ZAP-70 in both positive and negative selection of thymocytes. *Nature,* 376**,** 435-8.

NIKA, K., SOLDANI, C., SALEK, M., PASTER, W., GRAY, A., ETZENSPERGER, R., FUGGER, L., POLZELLA, P., CERUNDOLO, V., DUSHEK, O., HOFER, T., VIOLA, A. & ACUTO, O. 2010. Constitutively active Lck kinase in T cells drives antigen receptor signal transduction. *Immunity,* 32**,** 766-77.

NOLZ, J. C., FERNANDEZ-ZAPICO, M. E. & BILLADEAU, D. D. 2007. TCR/CD28-stimulated actin dynamics are required for NFAT1-mediated transcription of c-rel leading to CD28 response element activation. *J Immunol,* 179**,** 1104-12.

OGAWA, S., WATANABE, M., SAKURAI, Y., INUTAKE, Y., WATANABE, S., TAI, X. & ABE, R. 2013. CD28 signaling in primary CD4(+) T cells: identification of both tyrosine phosphorylation-dependent and phosphorylation-independent pathways. *International immunology,* 25**,** 671-81.

OH-HORA, M. & RAO, A. 2008. Calcium signaling in lymphocytes. *Current opinion in immunology,* 20**,** 250-8.

OKKENHAUG, K. & ROTTAPEL, R. 1998. Grb2 forms an inducible protein complex with CD28 through a Src homology 3 domain-proline interaction. *The Journal of biological chemistry,* 273**,** 21194-202.

ORABONA, C., GROHMANN, U., BELLADONNA, M. L., FALLARINO, F., VACCA, C., BIANCHI, R., BOZZA, S., VOLPI, C., SALOMON, B. L., FIORETTI, M. C., ROMANI, L. & PUCCETTI, P. 2004. CD28 induces immunostimulatory signals in dendritic cells via CD80 and CD86. *Nat Immunol,* 5**,** 1134-42.

P. A. GORER, S. LYMAN & SNELL, G. D. 1948. Studies on the Genetic and Antigenic Basis of Tumour Transplantation. Linkage between a Histocompatibility Gene and 'Fused' in Mice. *Proceedings of the Royal Society B,* 135**,** 449-505.

PAGES, F., RAGUENEAU, M., ROTTAPEL, R., TRUNEH, A., NUNES, J., IMBERT, J. & OLIVE, D. 1994. Binding of phosphatidylinositol-3-OH kinase to CD28 is required for T-cell signalling. *Nature,* 369**,** 327-9.

PALACIOS, E. H. & WEISS, A. 2004. Function of the Src-family kinases, Lck and Fyn, in T-cell development and activation. *Oncogene,* 23**,** 7990-8000.

PALLARDY, M. & HUNIG, T. 2010. Primate testing of TGN1412: right target, wrong cell. *British journal of pharmacology,* 161**,** 509-11.

PANTALEO, G., DEMAREST, J. F., SOUDEYNS, H., GRAZIOSI, C., DENIS, F., ADELSBERGER, J. W., BORROW, P., SAAG, M. S., SHAW, G. M., SEKALY, R. P. & ET AL. 1994. Major expansion of CD8+ T cells with a predominant V beta usage during the primary immune response to HIV. *Nature,* 370**,** 463-7.

PARRY, R. V., CHEMNITZ, J. M., FRAUWIRTH, K. A., LANFRANCO, A. R., BRAUNSTEIN, I., KOBAYASHI, S. V., LINSLEY, P. S., THOMPSON, C. B. & RILEY, J. L. 2005. CTLA-4 and PD-1 receptors inhibit T-cell activation by distinct mechanisms. *Molecular and cellular biology,* 25**,** 9543-53.

PAZ, P. E., WANG, S., CLARKE, H., LU, X., STOKOE, D. & ABO, A. 2001. Mapping the Zap-70 phosphorylation sites on LAT (linker for activation of T cells) required for recruitment and activation of signalling proteins in T cells. *The Biochemical journal,* 356**,** 461-71.

PENNINGER, J. M. & CRABTREE, G. R. 1999. The actin cytoskeleton and lymphocyte activation. *Cell,* 96**,** 9-12.

PIEPENBRINK, K. H., BLEVINS, S. J., SCOTT, D. R. & BAKER, B. M. 2013. The basis for limited specificity and MHC restriction in a T cell receptor interface. *Nature communications,* 4**,** 1948.

PIEPENBRINK, K. H., GLOOR, B. E., ARMSTRONG, K. M. & BAKER, B. M. 2009. Methods for quantifying T cell receptor binding affinities and thermodynamics. *Methods in enzymology,* 466**,** 359-81.

PRASAD, K. V., CAI, Y. C., RAAB, M., DUCKWORTH, B., CANTLEY, L., SHOELSON, S. E. & RUDD, C. E. 1994. T-cell antigen CD28 interacts with the lipid kinase phosphatidylinositol 3-kinase by a cytoplasmic Tyr(P)-Met-Xaa-Met motif. *Proceedings of the National Academy of Sciences of the United States of America,* 91**,** 2834-8.

PRICE, D. A., BRENCHLEY, J. M., RUFF, L. E., BETTS, M. R., HILL, B. J., ROEDERER, M., KOUP, R. A., MIGUELES, S. A., GOSTICK, E., WOOLDRIDGE, L., SEWELL, A. K., CONNORS, M. & DOUEK, D. C. 2005. Avidity for antigen shapes clonal dominance in CD8+ T cell populations specific for persistent DNA viruses. *The Journal of experimental medicine,* 202**,** 1349-61.

PURBHOO, M. A., IRVINE, D. J., HUPPA, J. B. & DAVIS, M. M. 2004. T cell killing does not require the formation of a stable mature immunological synapse. *Nature immunology,* 5**,** 524-30.

QUEZADA, S. A., SIMPSON, T. R., PEGGS, K. S., MERGHOUB, T., VIDER, J., FAN, X., BLASBERG, R., YAGITA, H., MURANSKI, P., ANTONY, P. A., RESTIFO, N. P. & ALLISON, J. P. 2010. Tumor-reactive CD4(+) T cells develop cytotoxic activity and eradicate large established melanoma after transfer into lymphopenic hosts. *The Journal of experimental medicine,* 207**,** 637-50.

QURESHI, O. S., ZHENG, Y., NAKAMURA, K., ATTRIDGE, K., MANZOTTI, C., SCHMIDT, E. M., BAKER, J., JEFFERY, L. E., KAUR, S., BRIGGS, Z., HOU, T. Z., FUTTER, C. E., ANDERSON, G., WALKER, L. S. & SANSOM, D. M. 2011. Trans-endocytosis of CD80 and CD86: a molecular basis for the cell-extrinsic function of CTLA-4. *Science,* 332**,** 600-3.

RAAB, M., CAI, Y. C., BUNNELL, S. C., HEYECK, S. D., BERG, L. J. & RUDD, C. E. 1995. p56Lck and p59Fyn regulate CD28 binding to phosphatidylinositol 3-kinase, growth factor receptor-bound protein GRB-2, and T cell-specific protein-tyrosine kinase ITK: implications for T-cell costimulation. *Proceedings of the National Academy of Sciences of the United States of America,* 92**,** 8891-5.

RACIOPPI, L., MATARESE, G., D'ORO, U., DE PASCALE, M., MASCI, A. M., FONTANA, S. & ZAPPACOSTA, S. 1996. The role of CD4-Lck in T-cell receptor antagonism: evidence for negative signaling. *Proceedings of the National Academy of Sciences of the United States of America,* 93**,** 10360-5.

RAPOPORT, A. P., STADTMAUER, E. A., AQUI, N., BADROS, A., COTTE, J., CHRISLEY, L., VELOSO, E., ZHENG, Z., WESTPHAL, S., MAIR, R., CHI, N., RATTERREE, B., POCHRAN, M. F., NATT, S., HINKLE, J., SICKLES, C., SOHAL, A., RUEHLE, K., LYNCH, C., ZHANG, L., PORTER, D. L., LUGER, S., GUO, C., FANG, H. B., BLACKWELDER, W., HANKEY, K., MANN, D., EDELMAN, R., FRASCH, C., LEVINE, B. L., CROSS, A. & JUNE, C. H. 2005. Restoration of immunity in lymphopenic individuals with cancer by vaccination and adoptive T-cell transfer. *Nature medicine,* 11**,** 1230-7.

REISER, J. B., DARNAULT, C., GREGOIRE, C., MOSSER, T., MAZZA, G., KEARNEY, A., VAN DER MERWE, P. A., FONTECILLA-CAMPS, J. C., HOUSSET, D. & MALISSEN, B. 2003. CDR3 loop flexibility contributes to the degeneracy of TCR recognition. *Nature immunology,* 4**,** 241-7.

ROBBINS, P. F., MORGAN, R. A., FELDMAN, S. A., YANG, J. C., SHERRY, R. M., DUDLEY, M. E., WUNDERLICH, J. R., NAHVI, A. V., HELMAN, L. J., MACKALL, C. L., KAMMULA, U. S., HUGHES, M. S., RESTIFO, N. P., RAFFELD, M., LEE, C. C., LEVY, C. L., LI, Y. F., EL-GAMIL, M., SCHWARZ, S. L., LAURENCOT, C. & ROSENBERG, S. A. 2011. Tumor regression in patients with metastatic synovial cell sarcoma and melanoma using genetically engineered lymphocytes reactive with NY-ESO-1. *Journal of*

clinical oncology : official journal of the American Society of Clinical Oncology, 29**,** 917-24.

ROHATGI, R., NOLLAU, P., HO, H. Y., KIRSCHNER, M. W. & MAYER, B. J. 2001. Nck and phosphatidylinositol 4,5-bisphosphate synergistically activate actin polymerization through the N-WASP-Arp2/3 pathway. *The Journal of biological chemistry,* 276**,** 26448-52.

ROMER, P. S., BERR, S., AVOTA, E., NA, S. Y., BATTAGLIA, M., TEN BERGE, I., EINSELE, H. & HUNIG, T. 2011. Preculture of PBMCs at high cell density increases sensitivity of T-cell responses, revealing cytokine release by CD28 superagonist TGN1412. *Blood,* 118**,** 6772-82.

RUDD, C. E., TAYLOR, A. & SCHNEIDER, H. 2009. CD28 and CTLA-4 coreceptor expression and signal transduction. *Immunol Rev,* 229**,** 12-26.

RUDD, C. E., TREVILLYAN, J. M., DASGUPTA, J. D., WONG, L. L. & SCHLOSSMAN, S. F. 1988. The CD4 receptor is complexed in detergent lysates to a protein-tyrosine kinase (pp58) from human T lymphocytes. *Proceedings of the National Academy of Sciences of the United States of America,* 85**,** 5190-4.

RUDOLPH, M. G., STANFIELD, R. L. & WILSON, I. A. 2006. How TCRs bind MHCs, peptides, and coreceptors. *Annual review of immunology,* 24**,** 419-66.

RULIFSON, I. C., SPERLING, A. I., FIELDS, P. E., FITCH, F. W. & BLUESTONE, J. A. 1997. CD28 costimulation promotes the production of Th2 cytokines. *Journal of immunology,* 158**,** 658-65.

SADELAIN, M., BRENTJENS, R. & RIVIERE, I. 2013. The basic principles of chimeric antigen receptor design. *Cancer discovery,* 3**,** 388-98.

SADRA, A., CINEK, T., ARELLANO, J. L., SHI, J., TRUITT, K. E. & IMBODEN, J. B. 1999. Identification of tyrosine phosphorylation sites in the CD28 cytoplasmic domain and their role in the costimulation of Jurkat T cells. *Journal of immunology,* 162**,** 1966-73.

SALOMON, B., LENSCHOW, D. J., RHEE, L., ASHOURIAN, N., SINGH, B., SHARPE, A. & BLUESTONE, J. A. 2000. B7/CD28 costimulation is essential for the homeostasis of the CD4+CD25+ immunoregulatory T cells that control autoimmune diabetes. *Immunity,* 12**,** 431-40.

SAMI, M., RIZKALLAH, P. J., DUNN, S., MOLLOY, P., MOYSEY, R., VUIDEPOT, A., BASTON, E., TODOROV, P., LI, Y., GAO, F., BOULTER, J. M. & JAKOBSEN, B. K. 2007. Crystal structures of high affinity human T-cell receptors bound to peptide major histocompatibility complex reveal native diagonal binding geometry. *Protein engineering, design & selection : PEDS,* 20**,** 397-403.

SANCHEZ-LOCKHART, M., GRAF, B. & MILLER, J. 2008. Signals and sequences that control CD28 localization to the central region of the immunological synapse. *J Immunol,* 181**,** 7639-48.

SAVIGNAC, M., MELLSTROM, B. & NARANJO, J. R. 2007. Calcium-dependent transcription of cytokine genes in T lymphocytes. *Pflugers Archiv : European journal of physiology,* 454**,** 523-33.

SAVIGNAC, M., PINTADO, B., GUTIERREZ-ADAN, A., PALCZEWSKA, M., MELLSTROM, B. & NARANJO, J. R. 2005. Transcriptional repressor DREAM regulates T-lymphocyte proliferation and cytokine gene expression. *The EMBO journal,* 24**,** 3555-64.

SCHAMEL, W. W., ARECHAGA, I., RISUENO, R. M., VAN SANTEN, H. M., CABEZAS, P., RISCO, C., VALPUESTA, J. M. & ALARCON, B. 2005. Coexistence of multivalent and monovalent TCRs explains high sensitivity and wide range of response. *The Journal of experimental medicine,* 202**,** 493-503.

SCHILHAM, M. W., FUNG-LEUNG, W. P., RAHEMTULLA, A., KUENDIG, T., ZHANG, L., POTTER, J., MILLER, R. G., HENGARTNER, H. & MAK, T. W.

1993. Alloreactive cytotoxic T cells can develop and function in mice lacking both CD4 and CD8. *European journal of immunology,* 23**,** 1299-304.

SCHNEIDER, H. & RUDD, C. E. 2008. CD28 and Grb-2, relative to Gads or Grap, preferentially co-operate with Vav1 in the activation of NFAT/AP-1 transcription. *Biochemical and biophysical research communications,* 369**,** 616-21.

SCHOENBORN, J. R., TAN, Y. X., ZHANG, C., SHOKAT, K. M. & WEISS, A. 2011. Feedback circuits monitor and adjust basal Lck-dependent events in T cell receptor signaling. *Science signaling,* 4**,** ra59.

SCHWEITZER, A. N. & SHARPE, A. H. 1998. Studies using antigen-presenting cells lacking expression of both B7-1 (CD80) and B7-2 (CD86) show distinct requirements for B7 molecules during priming versus restimulation of Th2 but not Th1 cytokine production. *Journal of immunology,* 161**,** 2762-71.

SECRIST, J. P., BURNS, L. A., KARNITZ, L., KORETZKY, G. A. & ABRAHAM, R. T. 1993. Stimulatory effects of the protein tyrosine phosphatase inhibitor, pervanadate, on T-cell activation events. *The Journal of biological chemistry,* 268**,** 5886-93.

SHAHINIAN, A., PFEFFER, K., LEE, K. P., KUNDIG, T. M., KISHIHARA, K., WAKEHAM, A., KAWAI, K., OHASHI, P. S., THOMPSON, C. B. & MAK, T. W. 1993. Differential T cell costimulatory requirements in CD28-deficient mice. *Science,* 261**,** 609-12.

SHERMAN, E., BARR, V., MANLEY, S., PATTERSON, G., BALAGOPALAN, L., AKPAN, I., REGAN, C. K., MERRILL, R. K., SOMMERS, C. L., LIPPINCOTT-SCHWARTZ, J. & SAMELSON, L. E. 2011. Functional nanoscale organization of signaling molecules downstream of the T cell antigen receptor. *Immunity,* 35**,** 705-20.

SIMPSON, T. R., QUEZADA, S. A. & ALLISON, J. P. 2010. Regulation of CD4 T cell activation and effector function by inducible costimulator (ICOS). *Current opinion in immunology,* 22**,** 326-32.

SLOAN-LANCASTER, J., EVAVOLD, B. D. & ALLEN, P. M. 1993. Induction of T-cell anergy by altered T-cell-receptor ligand on live antigen-presenting cells. *Nature,* 363**,** 156-9.

SLOAN-LANCASTER, J., SHAW, A. S., ROTHBARD, J. B. & ALLEN, P. M. 1994. Partial T cell signaling: altered phospho-zeta and lack of zap70 recruitment in APL-induced T cell anergy. *Cell,* 79**,** 913-22.

SMITH-GARVIN, J. E., KORETZKY, G. A. & JORDAN, M. S. 2009. T cell activation. *Annual review of immunology,* 27**,** 591-619.

SOTO, C. M., STONE, J. D., CHERVIN, A. S., ENGELS, B., SCHREIBER, H., ROY, E. J. & KRANZ, D. M. 2013. MHC-class I-restricted CD4 T cells: a nanomolar affinity TCR has improved anti-tumor efficacy in vivo compared to the micromolar wild-type TCR. *Cancer immunology, immunotherapy : CII,* 62**,** 359-69.

SPRINGER, T. A. 1990. Adhesion receptors of the immune system. *Nature,* 346**,** 425-34.

STADINSKI, B. D., TRENH, P., SMITH, R. L., BAUTISTA, B., HUSEBY, P. G., LI, G., STERN, L. J. & HUSEBY, E. S. 2011. A role for differential variable gene pairing in creating T cell receptors specific for unique major histocompatibility ligands. *Immunity,* 35**,** 694-704.

STAMPER, C. C., ZHANG, Y., TOBIN, J. F., ERBE, D. V., IKEMIZU, S., DAVIS, S. J., STAHL, M. L., SEEHRA, J., SOMERS, W. S. & MOSYAK, L. 2001. Crystal structure of the B7-1/CTLA-4 complex that inhibits human immune responses. *Nature,* 410**,** 608-11.

STEFANOVA, I., HEMMER, B., VERGELLI, M., MARTIN, R., BIDDISON, W. E. & GERMAIN, R. N. 2003. TCR ligand discrimination is enforced by competing

ERK positive and SHP-1 negative feedback pathways. *Nature immunology,* 4**,** 248-54.

STONE, J. D., CHERVIN, A. S. & KRANZ, D. M. 2009. T-cell receptor binding affinities and kinetics: impact on T-cell activity and specificity. *Immunology,* 126**,** 165-76.

STONE, J. D. & KRANZ, D. M. 2013. Role of T cell receptor affinity in the efficacy and specificity of adoptive T cell therapies. *Frontiers in immunology,* 4**,** 244.

STOTZ, S. H., BOLLIGER, L., CARBONE, F. R. & PALMER, E. 1999. T cell receptor (TCR) antagonism without a negative signal: evidence from T cell hybridomas expressing two independent TCRs. *The Journal of experimental medicine,* 189**,** 253-64.

SUN, Z. J., KIM, K. S., WAGNER, G. & REINHERZ, E. L. 2001. Mechanisms contributing to T cell receptor signaling and assembly revealed by the solution structure of an ectodomain fragment of the CD3 epsilon gamma heterodimer. *Cell,* 105**,** 913-23.

SZYMCZAK, A. L., WORKMAN, C. J., GIL, D., DILIOGLOU, S., VIGNALI, K. M., PALMER, E. & VIGNALI, D. A. 2005. The CD3epsilon proline-rich sequence, and its interaction with Nck, is not required for T cell development and function. *Journal of immunology,* 175**,** 270-5.

TABARES, P., BERR, S., ROMER, P. S., CHUVPILO, S., MATSKEVICH, A. A., TYRSIN, D., FEDOTOV, Y., EINSELE, H., TONY, H. P. & HUNIG, T. 2014. Human regulatory T cells are selectively activated by low-dose application of the CD28 superagonist TGN1412/TAB08. *Eur J Immunol,* 44**,** 1225-36.

TACKE, M., HANKE, G., HANKE, T. & HUNIG, T. 1997. CD28-mediated induction of proliferation in resting T cells in vitro and in vivo without engagement of the T cell receptor: evidence for functionally distinct forms of CD28. *European journal of immunology,* 27**,** 239-47.

TAI, X., COWAN, M., FEIGENBAUM, L. & SINGER, A. 2005. CD28 costimulation of developing thymocytes induces Foxp3 expression and regulatory T cell differentiation independently of interleukin 2. *Nature immunology,* 6**,** 152-62.

TALPAZ, M., SHAH, N. P., KANTARJIAN, H., DONATO, N., NICOLL, J., PAQUETTE, R., CORTES, J., O'BRIEN, S., NICAISE, C., BLEICKARDT, E., BLACKWOOD-CHIRCHIR, M. A., IYER, V., CHEN, T. T., HUANG, F., DECILLIS, A. P. & SAWYERS, C. L. 2006. Dasatinib in imatinib-resistant Philadelphia chromosome-positive leukemias. *N Engl J Med,* 354**,** 2531-41.

TAN, Y. X., MANZ, B. N., FREEDMAN, T. S., ZHANG, C., SHOKAT, K. M. & WEISS, A. 2014. Inhibition of the kinase Csk in thymocytes reveals a requirement for actin remodeling in the initiation of full TCR signaling. *Nature immunology,* 15**,** 186-94.

TAVANO, R., CONTENTO, R. L., BARANDA, S. J., SOLIGO, M., TUOSTO, L., MANES, S. & VIOLA, A. 2006. CD28 interaction with filamin-A controls lipid raft accumulation at the T-cell immunological synapse. *Nature cell biology,* 8**,** 1270-6.

TEFT, W. A., KIRCHHOF, M. G. & MADRENAS, J. 2006. A molecular perspective of CTLA-4 function. *Annual review of immunology,* 24**,** 65-97.

THERAMAB 2014. TheraMAB LLC. announces initiation of Phase II clinical trial of mAb TABO8 for the treatment of Rheumatoid Arthritis. *[Website:* http://www.theramab.ru/en/news/phase_II%5D.

THOMPSON, C. B. & ALLISON, J. P. 1997. The emerging role of CTLA-4 as an immune attenuator. *Immunity,* 7**,** 445-50.

TIAN, S., MAILE, R., COLLINS, E. J. & FRELINGER, J. A. 2007. CD8+ T cell activation is governed by TCR-peptide/MHC affinity, not dissociation rate. *Journal of immunology,* 179**,** 2952-60.

TIKHONOVA, A. N., VAN LAETHEM, F., HANADA, K., LU, J., POBEZINSKY, L. A., HONG, C., GUINTER, T. I., JEURLING, S. K., BERNHARDT, G., PARK, J.

H., YANG, J. C., SUN, P. D. & SINGER, A. 2012. alphabeta T cell receptors that do not undergo major histocompatibility complex-specific thymic selection possess antibody-like recognition specificities. *Immunity,* 36**,** 79-91.

TIVOL, E. A., BORRIELLO, F., SCHWEITZER, A. N., LYNCH, W. P., BLUESTONE, J. A. & SHARPE, A. H. 1995. Loss of CTLA-4 leads to massive lymphoproliferation and fatal multiorgan tissue destruction, revealing a critical negative regulatory role of CTLA-4. *Immunity,* 3**,** 541-7.

TIVOL, E. A., BOYD, S. D., MCKEON, S., BORRIELLO, F., NICKERSON, P., STROM, T. B. & SHARPE, A. H. 1997. CTLA4Ig prevents lymphoproliferation and fatal multiorgan tissue destruction in CTLA-4-deficient mice. *J Immunol,* 158**,** 5091-4.

TREANOR, B., DEPOIL, D., GONZALEZ-GRANJA, A., BARRAL, P., WEBER, M., DUSHEK, O., BRUCKBAUER, A. & BATISTA, F. D. 2010. The membrane skeleton controls diffusion dynamics and signaling through the B cell receptor. *Immunity,* 32**,** 187-99.

TSENG, S. Y., WAITE, J. C., LIU, M., VARDHANA, S. & DUSTIN, M. L. 2008. T cell-dendritic cell immunological synapses contain TCR-dependent CD28-CD80 clusters that recruit protein kinase C theta. *J Immunol,* 181**,** 4852-63.

TURNER, S. J., DOHERTY, P. C., MCCLUSKEY, J. & ROSSJOHN, J. 2006. Structural determinants of T-cell receptor bias in immunity. *Nature reviews. Immunology,* 6**,** 883-94.

VALITUTTI, S. & LANZAVECCHIA, A. 1997. Serial triggering of TCRs: a basis for the sensitivity and specificity of antigen recognition. *Immunology today,* 18**,** 299-304.

VALITUTTI, S., MULLER, S., CELLA, M., PADOVAN, E. & LANZAVECCHIA, A. 1995. Serial triggering of many T-cell receptors by a few peptide-MHC complexes. *Nature,* 375**,** 148-51.

VAN DER MERWE, P. A. & BARCLAY, A. N. 1996. Analysis of cell-adhesion molecule interactions using surface plasmon resonance. *Current opinion in immunology,* 8**,** 257-61.

VAN DER MERWE, P. A., BODIAN, D. L., DAENKE, S., LINSLEY, P. & DAVIS, S. J. 1997. CD80 (B7-1) binds both CD28 and CTLA-4 with a low affinity and very fast kinetics. *The Journal of experimental medicine,* 185**,** 393-403.

VAN DER MERWE, P. A. & DAVIS, S. J. 2003. Molecular interactions mediating T cell antigen recognition. *Annu Rev Immunol,* 21**,** 659-84.

VAN DER MERWE, P. A. & DUSHEK, O. 2011. Mechanisms for T cell receptor triggering. *Nature reviews. Immunology,* 11**,** 47-55.

VAN LAETHEM, F., SARAFOVA, S. D., PARK, J. H., TAI, X., POBEZINSKY, L., GUINTER, T. I., ADORO, S., ADAMS, A., SHARROW, S. O., FEIGENBAUM, L. & SINGER, A. 2007. Deletion of CD4 and CD8 coreceptors permits generation of alphabetaT cells that recognize antigens independently of the MHC. *Immunity,* 27**,** 735-50.

VAN LAETHEM, F., TIKHONOVA, A. N., POBEZINSKY, L. A., TAI, X., KIMURA, M. Y., LE SAOUT, C., GUINTER, T. I., ADAMS, A., SHARROW, S. O., BERNHARDT, G., FEIGENBAUM, L. & SINGER, A. 2013. Lck availability during thymic selection determines the recognition specificity of the T cell repertoire. *Cell,* 154**,** 1326-41.

VAN LAETHEM, F., TIKHONOVA, A. N. & SINGER, A. 2012. MHC restriction is imposed on a diverse T cell receptor repertoire by CD4 and CD8 co-receptors during thymic selection. *Trends in immunology,* 33**,** 437-41.

VAN OERS, N. S., KILLEEN, N. & WEISS, A. 1994. ZAP-70 is constitutively associated with tyrosine-phosphorylated TCR zeta in murine thymocytes and lymph node T cells. *Immunity,* 1**,** 675-85.

VARMA, R., CAMPI, G., YOKOSUKA, T., SAITO, T. & DUSTIN, M. L. 2006. T cell receptor-proximal signals are sustained in peripheral microclusters and

terminated in the central supramolecular activation cluster. *Immunity,* 25**,** 117-27.

VELU, V., TITANJI, K., ZHU, B., HUSAIN, S., PLADEVEGA, A., LAI, L., VANDERFORD, T. H., CHENNAREDDI, L., SILVESTRI, G., FREEMAN, G. J., AHMED, R. & AMARA, R. R. 2009. Enhancing SIV-specific immunity in vivo by PD-1 blockade. *Nature,* 458**,** 206-10.

VILLALBA, M., COUDRONNIERE, N., DECKERT, M., TEIXEIRO, E., MAS, P. & ALTMAN, A. 2000. A novel functional interaction between Vav and PKCtheta is required for TCR-induced T cell activation. *Immunity,* 12**,** 151-60.

VONDERHEIDE, R. H. 2002. Telomerase as a universal tumor-associated antigen for cancer immunotherapy. *Oncogene,* 21**,** 674-9.

WALKER, L. S. & SANSOM, D. M. 2011. The emerging role of CTLA4 as a cell-extrinsic regulator of T cell responses. *Nature reviews. Immunology,* 11**,** 852-63.

WANG, H., KADLECEK, T. A., AU-YEUNG, B. B., GOODFELLOW, H. E., HSU, L. Y., FREEDMAN, T. S. & WEISS, A. 2010. ZAP-70: an essential kinase in T-cell signaling. *Cold Spring Harbor perspectives in biology,* 2**,** a002279.

WANG, J. H. & REINHERZ, E. L. 2002. Structural basis of T cell recognition of peptides bound to MHC molecules. *Molecular immunology,* 38**,** 1039-49.

WANG, Y., BECKER, D., VASS, T., WHITE, J., MARRACK, P. & KAPPLER, J. W. 2009. A conserved CXXC motif in CD3epsilon is critical for T cell development and TCR signaling. *PLoS biology,* 7**,** e1000253.

WANGE, R. L. 2000. LAT, the linker for activation of T cells: a bridge between T cell-specific and general signaling pathways. *Science's STKE : signal transduction knowledge environment,* 2000**,** re1.

WATERHOUSE, P., PENNINGER, J. M., TIMMS, E., WAKEHAM, A., SHAHINIAN, A., LEE, K. P., THOMPSON, C. B., GRIESSER, H. & MAK, T. W. 1995. Lymphoproliferative disorders with early lethality in mice deficient in Ctla-4. *Science,* 270**,** 985-8.

WELLS, J. A. 1990. Additivity of mutational effects in proteins. *Biochemistry,* 29**,** 8509-17.

WHERRY, E. J. 2011. T cell exhaustion. *Nature immunology,* 12**,** 492-9.

WILD, M. K., CAMBIAGGI, A., BROWN, M. H., DAVIES, E. A., OHNO, H., SAITO, T. & VAN DER MERWE, P. A. 1999. Dependence of T cell antigen recognition on the dimensions of an accessory receptor-ligand complex. *The Journal of experimental medicine,* 190**,** 31-41.

WILLCOX, B. E., GAO, G. F., WYER, J. R., LADBURY, J. E., BELL, J. I., JAKOBSEN, B. K. & VAN DER MERWE, P. A. 1999. TCR binding to peptide-MHC stabilizes a flexible recognition interface. *Immunity,* 10**,** 357-65.

WILLIAMSON, D. J., OWEN, D. M., ROSSY, J., MAGENAU, A., WEHRMANN, M., GOODING, J. J. & GAUS, K. 2011. Pre-existing clusters of the adaptor Lat do not participate in early T cell signaling events. *Nature immunology,* 12**,** 655-62.

WILLS, M. R., CARMICHAEL, A. J., MYNARD, K., JIN, X., WEEKES, M. P., PLACHTER, B. & SISSONS, J. G. 1996. The human cytotoxic T-lymphocyte (CTL) response to cytomegalovirus is dominated by structural protein pp65: frequency, specificity, and T-cell receptor usage of pp65-specific CTL. *Journal of virology,* 70**,** 7569-79.

WOOLDRIDGE, L., EKERUCHE-MAKINDE, J., VAN DEN BERG, H. A., SKOWERA, A., MILES, J. J., TAN, M. P., DOLTON, G., CLEMENT, M., LLEWELLYN-LACEY, S., PRICE, D. A., PEAKMAN, M. & SEWELL, A. K. 2012. A single autoimmune T cell receptor recognizes more than a million different peptides. *The Journal of biological chemistry,* 287**,** 1168-77.

WU, H., KWONG, P. D. & HENDRICKSON, W. A. 1997. Dimeric association and segmental variability in the structure of human CD4. *Nature,* 387**,** 527-30.

WU, L. C., TUOT, D. S., LYONS, D. S., GARCIA, K. C. & DAVIS, M. M. 2002. Two-step binding mechanism for T-cell receptor recognition of peptide MHC. *Nature,* 418**,** 552-6.

WU, Y., BORDE, M., HEISSMEYER, V., FEUERER, M., LAPAN, A. D., STROUD, J. C., BATES, D. L., GUO, L., HAN, A., ZIEGLER, S. F., MATHIS, D., BENOIST, C., CHEN, L. & RAO, A. 2006. FOXP3 controls regulatory T cell function through cooperation with NFAT. *Cell,* 126**,** 375-87.

WULFING, C., RABINOWITZ, J. D., BEESON, C., SJAASTAD, M. D., MCCONNELL, H. M. & DAVIS, M. M. 1997. Kinetics and extent of T cell activation as measured with the calcium signal. *The Journal of experimental medicine,* 185**,** 1815-25.

XU, C., GAGNON, E., CALL, M. E., SCHNELL, J. R., SCHWIETERS, C. D., CARMAN, C. V., CHOU, J. J. & WUCHERPFENNIG, K. W. 2008. Regulation of T cell receptor activation by dynamic membrane binding of the CD3epsilon cytoplasmic tyrosine-based motif. *Cell,* 135**,** 702-13.

XU, X. J. & TANG, Y. M. 2014. Cytokine release syndrome in cancer immunotherapy with chimeric antigen receptor engineered T cells. *Cancer letters,* 343**,** 172-8.

YAMAMOTO, T., HATTORI, M. & YOSHIDA, T. 2007. Induction of T-cell activation or anergy determined by the combination of intensity and duration of T-cell receptor stimulation, and sequential induction in an individual cell. *Immunology,* 121**,** 383-91.

YAMAZAKI, T., AKIBA, H., IWAI, H., MATSUDA, H., AOKI, M., TANNO, Y., SHIN, T., TSUCHIYA, H., PARDOLL, D. M., OKUMURA, K., AZUMA, M. & YAGITA, H. 2002. Expression of programmed death 1 ligands by murine T cells and APC. *Journal of immunology,* 169**,** 5538-45.

YANG, W. C., GHIOTTO, M., BARBARAT, B. & OLIVE, D. 1999. The role of Tec protein-tyrosine kinase in T cell signaling. *The Journal of biological chemistry,* 274**,** 607-17.

YE, Z. S. & BALTIMORE, D. 1994. Binding of Vav to Grb2 through dimerization of Src homology 3 domains. *Proceedings of the National Academy of Sciences of the United States of America,* 91**,** 12629-33.

YIN, Y., WANG, X. X. & MARIUZZA, R. A. 2012. Crystal structure of a complete ternary complex of T-cell receptor, peptide-MHC, and CD4. *Proceedings of the National Academy of Sciences of the United States of America,* 109**,** 5405-10.

YOKOSUKA, T., KOBAYASHI, W., SAKATA-SOGAWA, K., TAKAMATSU, M., HASHIMOTO-TANE, A., DUSTIN, M. L., TOKUNAGA, M. & SAITO, T. 2008. Spatiotemporal regulation of T cell costimulation by TCR-CD28 microclusters and protein kinase C theta translocation. *Immunity,* 29**,** 589-601.

YOKOSUKA, T., KOBAYASHI, W., TAKAMATSU, M., SAKATA-SOGAWA, K., ZENG, H., HASHIMOTO-TANE, A., YAGITA, H., TOKUNAGA, M. & SAITO, T. 2010. Spatiotemporal basis of CTLA-4 costimulatory molecule-mediated negative regulation of T cell activation. *Immunity,* 33**,** 326-39.

YOKOSUKA, T. & SAITO, T. 2009. Dynamic regulation of T-cell costimulation through TCR-CD28 microclusters. *Immunol Rev,* 229**,** 27-40.

YOKOSUKA, T., TAKAMATSU, M., KOBAYASHI-IMANISHI, W., HASHIMOTO-TANE, A., AZUMA, M. & SAITO, T. 2012a. Programmed cell death 1 forms negative costimulatory microclusters that directly inhibit T cell receptor signaling by recruiting phosphatase SHP2. *The Journal of experimental medicine,* 209**,** 1201-17.

YOKOSUKA, T., TAKAMATSU, M., KOBAYASHI-IMANISHI, W., HASHIMOTO-TANE, A., AZUMA, M. & SAITO, T. 2012b. Programmed cell death 1 forms negative costimulatory microclusters that directly inhibit T cell receptor signaling by recruiting phosphatase SHP2. *J Exp Med,* 209**,** 1201-17.

ZEH, H. J., 3RD, PERRY-LALLEY, D., DUDLEY, M. E., ROSENBERG, S. A. & YANG, J. C. 1999. High avidity CTLs for two self-antigens demonstrate superior in vitro and in vivo antitumor efficacy. *Journal of immunology,* 162**,** 989-94.

ZHANG, H. 2010. T cell antigen receptor binding and initial signal transduction. *DPhil Thesis, Sir William Dunn School of Pathology, University of Oxford, UK*.

ZHANG, H., CORDOBA, S. P., DUSHEK, O. & VAN DER MERWE, P. A. 2011. Basic residues in the T-cell receptor zeta cytoplasmic domain mediate membrane association and modulate signaling. *Proceedings of the National Academy of Sciences of the United States of America,* 108**,** 19323-8.

ZHANG, W., SLOAN-LANCASTER, J., KITCHEN, J., TRIBLE, R. P. & SAMELSON, L. E. 1998a. LAT: the ZAP-70 tyrosine kinase substrate that links T cell receptor to cellular activation. *Cell,* 92**,** 83-92.

ZHANG, W., TRIBLE, R. P. & SAMELSON, L. E. 1998b. LAT palmitoylation: its essential role in membrane microdomain targeting and tyrosine phosphorylation during T cell activation. *Immunity,* 9**,** 239-46.

ZHAO, Y., BENNETT, A. D., ZHENG, Z., WANG, Q. J., ROBBINS, P. F., YU, L. Y., LI, Y., MOLLOY, P. E., DUNN, S. M., JAKOBSEN, B. K., ROSENBERG, S. A. & MORGAN, R. A. 2007. High-affinity TCRs generated by phage display provide CD4+ T cells with the ability to recognize and kill tumor cell lines. *Journal of immunology,* 179**,** 5845-54.

ZHONG, S., MALECEK, K., JOHNSON, L. A., YU, Z., VEGA-SAENZ DE MIERA, E., DARVISHIAN, F., MCGARY, K., HUANG, K., BOYER, J., CORSE, E., SHAO, Y., ROSENBERG, S. A., RESTIFO, N. P., OSMAN, I. & KROGSGAARD, M. 2013. T-cell receptor affinity and avidity defines antitumor response and autoimmunity in T-cell immunotherapy. *Proceedings of the National Academy of Sciences of the United States of America,* 110**,** 6973-8.

ZINKERNAGEL, R. M. & DOHERTY, P. C. 1974. Restriction of in vitro T cell-mediated cytotoxicity in lymphocytic choriomeningitis within a syngeneic or semiallogeneic system. *Nature,* 248**,** 701-2.

NATURE PUBLISHING GROUP LICENSE TERMS AND CONDITIONS

Oct 10, 2014

This is a License Agreement between Hong-Sheng Lim ("You") and Nature Publishing Group ("Nature Publishing Group") provided by Copyright Clearance Center ("CCC"). The license consists of your order details, the terms and conditions provided by Nature Publishing Group, and the payment terms and conditions.

All payments must be made in full to CCC. For payment instructions, please see information listed at the bottom of this form.

License Number	3480751487303
License date	Oct 02, 2014
Licensed content publisher	Nature Publishing Group
Licensed content publication	Nature Reviews Immunology
Licensed content title	Mechanisms for T cell receptor triggering
Licensed content author	P. Anton van der Merwe and Omer Dushek
Licensed content date	Jan 1, 2011
Volume number	11
Issue number	1
Type of Use	reuse in a dissertation / thesis
Requestor type	academic/educational
Format	print and electronic
Portion	figures/tables/illustrations
Number of figures/tables/illus	1
High-res required	no
Figures	Figure 1a, 1b, 1c, 1e
Author of this NPG article	no
Your reference number	None
Title of your thesis / dissertat	LIGAND BINDING AND SIGNALLING BY THE T CELL ANTIGEN RECEPTOR AND CD28
Expected completion date	Oct 2014
Estimated size (number of pa	200

Total 0.00 GBP

Terms and Conditions

Terms and Conditions for Permissions

Nature Publishing Group hereby grants you a non-exclusive license to reproduce this material for this purpose, and for no other use,subject to the conditions below:

1. NPG warrants that it has, to the best of its knowledge, the rights to license reuse of this material. However, you should ensure that the material you are requesting is original to Nature Publishing Group and does not carry the copyright of another entity (as credited in the published version). If the credit line on any part of the material you have requested indicates that it was reprinted or adapted by NPG with permission from another source, then you should also seek permission from that source to reuse the material.
2. Permission granted free of charge for material in print is also usually granted for any electronic version of that work, provided that the material is incidental to the work as a whole and that the electronic version is essentially equivalent to, or substitutes for, the print version.Where print permission has been granted for a fee, separate permission must be obtained for any additional, electronic re-use (unless, as in the case of a full paper, this has already been accounted for during your initial request in the calculation of a print run).NB: In all cases, web-based use of full-text articles must be authorized separately through the 'Use on a Web Site' option when requesting permission.
3. Permission granted for a first edition does not apply to second and subsequent editions and for editions in other languages (except for signatories to the STM Permissions Guidelines, or where the first edition permission was granted for free).
4. Nature Publishing Group's permission must be acknowledged next to the figure, table or abstract in print. In electronic form, this acknowledgement must be visible at the same time as the figure/table/abstract, and must be hyperlinked to the journal's homepage.
5.
6.
7. The credit line should read: Reprinted by permission from Macmillan Publishers Ltd: [JOURNAL NAME] (reference citation), copyright (year of publication) For AOP papers, the credit line should read: Reprinted by permission from Macmillan Publishers Ltd: [JOURNAL NAME], advance online publication, day month year (doi: 10.1038/sj.[JOURNAL ACRONYM].XXXXX) **Note: For republication from the *British Journal of Cancer,* the following credit lines apply.** Reprinted by permission from Macmillan Publishers Ltd on behalf of Cancer Research UK: [JOURNAL NAME] (reference citation), copyright (year of publication)For AOP papers, the credit line should read: Reprinted by permission from Macmillan Publishers Ltd on behalf of Cancer Research UK: [JOURNAL NAME], advance online publication, day month year (doi: 10.1038/sj.[JOURNAL ACRONYM].XXXXX)
8. Adaptations of single figures do not require NPG approval. However, the adaptation should be credited as follows: Adapted by permission from Macmillan Publishers Ltd: [JOURNAL NAME] (reference citation), copyright (year of publication) **Note: For adaptation from the *British Journal of Cancer,* the following credit line applies.** Adapted by permission from Macmillan Publishers Ltd on behalf of Cancer Research UK: [JOURNAL NAME] (reference citation), copyright (year of publication)
9. Translations of 401 words up to a whole article require NPG approval. Please visit http://www.macmillanmedicalcommunications.com for more information.Translations of up to a 400 words do not require NPG approval. The translation should be credited as follows: Translated by permission from Macmillan

Publishers Ltd: [JOURNAL NAME] (reference citation), copyright (year of publication). **Note: For translation from the *British Journal of Cancer,* the following credit line applies.** Translated by permission from Macmillan Publishers Ltd on behalf of Cancer Research UK: [JOURNAL NAME] (reference citation), copyright (year of publication)

We are certain that all parties will benefit from this agreement and wish you the best in the use of this material. Thank you.

Special Terms:

Questions? customercare@copyright.com or +1-855-239-3415 (toll free in the US) or +1-978-646-2777.

Gratis licenses (referencing $0 in the Total field) are free. Please retain this printable license for your reference. No payment is required.